NASA CONTRACTOR
REPORT

NASA CR-

LUNAR ORBITER II

Extended-Mission Spacecraft Operations and Subsystem Performance

Prepared by
THE BOEING COMPANY
Seattle, Wash.
for Langley Research Center

NATIONAL AERONAUTICS AND SPACE ADMINISTRATION • WASHINGTON, D. C. • AUGUST 1968

LUNAR ORBITER II

Extended-Mission Spacecraft Operations

and Subsystem Performance

Distribution of this report is provided in the interest of information exchange. Responsibility for the contents resides in the author or organization that prepared it.

Issued by Originator as Document D2-100752-4 (Vol. IV)

Prepared under Contract No. NAS 1-3800 by
THE BOEING COMPANY
Seattle, Wash.

for Langley Research Center

NATIONAL AERONAUTICS AND SPACE ADMINISTRATION

Contents

Contents —Continued

Figures

Figures —Continued

Tables

Abbreviations

AGNQ	Apollo GOSS Navigation Qualification	ODGX	orbit data generation
ASU	acquire Sun	ODPL	orbit determination
BOS	bright-object sensor	OMS	optical-mechanical scanner
CAO	Canopus sensor on	PIM	pitch minus
CAO*	Canopus sensor off	PIP	pitch plus
CDZ	±2.0-degree deadzone	ROM	roll minus
CDZ*	±0.2-degree deadzone	ROP	roll plus
COGL	command generation and programmer simulation program	RTC	real-time command
DACON	data controller	SFOF	Space Flight Operations Facility
DATL	data alarm summary	SLOE	Senior Lunar Orbiter Engineer
DSIF	Deep Space Information Facility	SPA	Stored Program Address
DSN	Deep Space Network	SPAC	Spacecraft Performance Analysis and Command
DSS	Deep Space Station	SPC	stored-program command
EMD	equipment mount deck	TDPX	tracking data validation
FAT	flight acceptance test	TRJL	trajectory program
FPAC	Flight Path Analysis and Control	TSF	Track Synthesizer Frequency
GMT	Greenwich Mean Time	TTY	telemetry
GOSS	Ground Operation Support System	TVC	thrust vector control
IH	inertial hold	TWT	traveling-wave tube
IRU	inertial reference unit	TWTA	traveling-wave-tube amplifier
JPL	Jet Propulsion Laboratory	VCO	voltage controlled oscillator
LRC	Langley Research Center	V/H	velocity-height
MDE	mission-dependent equipment	YAP	yaw plus
MSFN	Manned Space Flight Network	YAM	yaw minus
NASA	National Aeronautics and Space Administration	ΔV	velocity change

1.0 Summary

The Lunar Orbiter II spacecraft was tracked from the start of its extended mission on December 8, 1966 (GMT Day 342) until it was intentionally crashed on the Moon on October 11, 1967 (GMT Day 284). A summary of orbital parameters during the extended mission is shown in Table 1-1. During this period, the primary objective of obtaining selenodetic data was successfully accomplished by ranging, tracking, and monitoring specific spacecraft telemetry channels. Secondary objectives, which included 14 special tests and five experiments in support of future space missions, were generally completed prior to the launch of Lunar Orbiter IV. Following this launch, Lunar Orbiter II was used primarily for Doppler and ranging calibrations. Selenodetic data that could be used in developing a lunar gravitational model that would be more meaningful for Mission III

were obtained by changing the Lunar Orbiter II orbit inclination from 11.9 to 17.5 degrees (similar to that planned for Lunar Orbiter III) at the beginning of the extended mission. Lunar environmental events of significance were proton events indicated by Lunar Orbiter II telemetry on January 30 1967 (GMT Day 030) and on May 25, 1967 (GMT Day 145). Looper radiation increased 39 rads during the first event and 32.5 rads during the second. Seven micrometeoroid hits were recorded during the extended mission.

Special tests were conducted to obtain additional data on performance characteristics of the various subsystems with the spacecraft in unique attitudes and/or environmental configurations. Hopefully, these data would verify acceptable performance of existing systems for

Table 1-1: Orbit Parameter Summary

Event	GMT	Calendar	Perilune (km)	Apolune (km)	Inclination (deg)	Period (min)
Start extended mission	342	Dec. 8, 1966	40	1,863	11.9	209
Inclination change $\Delta V = 100.0$ m/sec Burn time = 61.3 sec	342	Dec. 8, 1966	43	1,884	17.5	210
Phasing for eclipse $\Delta V = 5.5$ m/sec Burn time = 3.2 sec	104	Apr. 14, 1967	68	1,840	16.8	209
Perilune increase $\Delta V = 8.0$ m/sec Burn time = 4.6 sec	178	June 27, 1967	113	1,841	16.5	212
Terminal transfer** $\Delta V = 61.5$ m/sec Burn time = 35.5 sec	284	Oct. 11, 1967	−218*	1,913*	15.2*	197*

*   Predicted values
**   Estimated impact data:
      Time = 284:07:12:54 GMT
      Longitude = 119.13°E
      Latitude = 2.96°N

1

Mission III and assist in the development of design and operational improvements. These tests are summarized below.

- To assist in refinement of operating procedures for multiple spacecraft, a command address test was performed to determine the reaction of a spacecraft which is sent commands with the command address of another spacecraft or commands with a signal strength just below the spacecraft's command threshold.

- Solar panel degradation tests on Day 348 indicated that, as of that day, the degradation was negligible.

- Battery discharge tests were conducted prior to the lunar eclipse of April 24 and the anticipated eclipse of October 18 to improve the battery's performance. By erasing the battery's memory effect, using a deep discharge, the battery's "charge-discharge" characteristics are usually enhanced. As a result of subsequent decisions, the spacecraft was intentionally crashed into the Moon prior to the October 18th eclipse.

- The camera thermal door (CTD) open test was not formally performed since the door had already failed in the open position. From the data available it was concluded that (1) with the door open, photo subsystem temperatures varied with EMD temperatures and (2) moisture would condense on the inner side of the window if the temperature change rate exceeded 7.5 degrees per hour;

- Photo subsystem V/H tests established that image motion compensation (IMC) could be obtained at roll angles up to 53 degrees, pitch angles up to 45 degrees, and Sun angles as high as approximately 98 degrees. A V/H sensor duty cycle test revealed that the present temperature constraint (maximum of 6.6 minutes on, followed by 152 minutes off) is overly conservative.

- Several star tracker tests were conducted to obtain additional information that would be useful during subsequent missions. A star map test measured the relative brightness of stars which had not already been viewed by the tracker. The bright object sensor (BOS) test provided data as to the tracker angles from the sunline where the BOS shutter would open and close. Due to the uniqueness

of the mission IV polar type orbit, a glint mapping test was performed which indicated that Canopus could be tracked under Mission IV lighting conditions.

- The maneuver accuracy test results indicated that both the positive and negative 360-degree maneuvers in the pitch and yaw axes were well within the $\pm 0.3\%$ requirement.

- An IRU turn off-turn on test was conducted after the terminal transfer burn and prior to impact. Test results indicated that the IRU worked properly after turn-on and was capable of controlling the spacecraft's attitude.

Special experiments were performed to obtain scientific and special data, to develop multiple-spacecraft operational procedures, and to support the MSFN. These experiments are summarized below.

- A V/H sensor survey of the eastern and western limb of the Moon was performed with the objective of obtaining data that would permit determination of the lunar radius.

- An ionosphere experiment was performed to obtain data that would assist in analyzing the effects of the Earth's ionosphere on Doppler and ranging data.

- To assist the Mariner-Venus 1967 project, a Doppler ranging calibration experiment was conducted to check out the Mark II ranging system at DSS-14 (Goldstone - Mars).

- The MSFN used Lunar Orbiter II to provide tracking data, training, and experience in tracking a spacecraft at lunar distances. This network used the spacecraft to assist in the generation of special antenna patterns, and in preliminary qualification of the basic real-time computer complex (RTCC) navigational concepts.

- A variety of tests was conducted that concerned the operational control of multiple spacecraft. Rf interference tests verified that an extended-mission spacecraft could be flown and controlled without interfering with the prime (photo mission) spacecraft. It was determined from a blind acquisition and a high static-phase-error test that it was possible to turn on the rf in a spacecraft using "Moon center" antenna pointing predicts.

The following significant events occurred during Lunar Orbiter II's extended mission.

- The ability of the MSFN stations to track a Lunar Orbiter spacecraft, while operating in various rf modes, was verified with Lunar Orbiter II.
- The spacecraft was used extensively along with Lunar Orbiter III to develop multiple-spacecraft control procedures. In general, all of the extended-mission objectives were realized, while one or two other Lunar Orbiter spacecraft were controlled and kept in a safe status.
- The spacecraft was used to assist the DSN in certifying DSS-62 for Mission III support.
- Lunar Orbiter II was used to provide realism during the training period for Mission III.
- A Doppler resolver was used that greatly increased confidence in the received Doppler data.

The spacecraft's subsystems performed satisfactorily with the exception of the TWTA, which failed during the prime mission, and the camera thermal door, which failed due to receipt of a spurious command that caused the door to cycle continuously until it eventually failed. Since solar panel degradation was minimal, there was an adequate power margin which made it possible to fly the spacecraft at 40 to 62 degrees off-Sun to assist in spacecraft thermal control. Due to a higher-than-normal temperature environment, the battery's capacity was reduced approximately 50%. Photo subsystem internal pressure was lost for an unknown reason, but subsequent subsystem operation in the "wind forward" and "read out" mode was successful. This test was conducted just prior to impact of the spacecraft. Operation of the attitude control subsystem at a low storage bottle pressure was also accomplished immediately prior to impact. Proper thruster performance down to a pressure of 70 psia was verified.

A velocity burn was conducted on June 27 in order to raise the orbit's perilune to preclude a premature lunar impact due to orbit decay. The lunar eclipses on April 24, 1967 (GMT Day 114) and October 18, 1967 (GMT Day 291) had considerable impact on the Lunar Orbiter II flight plan. A phasing maneuver was performed so the spacecraft could successfully survive the first eclipse. To preclude the risk of losing spacecraft control due to a marginal nitrogen supply following the second eclipse, the decision was made to impact the spacecraft into the Moon prior to the eclipse.

The Lunar Orbiter II extended mission officially terminated following the terminal transfer maneuver that resulted in the spacecraft's impacting the farside of the Moon on October 11, 1967 (GMT Day 284) at a predicted time of 07:12:54 and at an estimated location of 119.13° E longitude and 2.96° N latitude. The total flight time of 339 days for Lunar Orbiter II represents the longest flight for any of the five Lunar Orbiter spacecraft.

2.0 Introduction

This report covers the spacecraft control and flight path analysis and control operations conducted during the Lunar Orbiter II extended mission and discusses spacecraft performance during these operations. Complete data packages have been prepared for each experiment and special exercise under separate cover and forwarded via the NASA experiment coordinator to the requestor. The highlights of each special exercise and experiment are summarized herein.

Transition from the photographic mission of Lunar Orbiter II to the extended-mission phase was started on Day 342 and completed on Day 343. During this period, the orbit inclination was increased from 11.9 to 17.5 degrees. The remainder of the orbital parameters was essentially unchanged with a perilune of 43 kilometers, apolune of 1884 kilometers, and a period of 210 minutes. All spacecraft systems were operational with the exception of the TWTA, which had failed during the prime mission. The spacecraft was operating in wide deadzone (2.0 degrees) and pitched off the sunline plus 40 degrees for thermal relief.

2.1 SPACECRAFT DESCRIPTION

The 853-pound Lunar Orbiter spacecraft is 6.83 feet high, spans 17.1 feet from the tip of the rotatable high-gain dish antenna to the tip of the low-gain antenna, and measures 12.4 feet across the solar panels. Figure 2-1 shows the spacecraft in the flight configuration with all elements fully deployed (the mylar thermal barrier is not shown). Major components are attached to the largest of three deck structures, which are interconnected by a tubular truss network. Thermal control is maintained by controlling emission of internal energy and absorption of solar energy through the use of a special paint covering the bottom side of the deck structure. The entire spacecraft periphery above the large equipment-mounting deck is covered with a highly reflective aluminum-coated mylar shroud, providing an adiabatic thermal barrier. In addition to its structural functions, the tank deck is designed to withstand radiant energy from the velocity control engine to minimize heat losses. Three-axis stabilization is provided by using the Sun and Canopus as primary angular references, and by a three-axis inertial system when the vehicle is required to operate off celestial references, during maneuvers, or when the Sun and/or Canopus are occulted by the Moon. The spacecraft subsystems are shown in block diagram form in Figure 2-2.

2.2 MISSION OBJECTIVES

The primary objective of the Lunar Orbiter II extended mission was to secure information that could be used to extend the scientific knowledge of the size and shape of the Moon, the properties of its gravitational field, and the lunar environment. Secondary objectives were the conduct of tests to determine the limits of spacecraft capabilities and to develop standard operating procedures, and experiments to provide additional scientific data as well as explore the usages for the Lunar Orbiter subsystems. During the Lunar Orbiter II extended mission the following tests and experiments were included.

- Special tests and experiments to develop operational procedures for multiple-spacecraft operation, including command address and threshold tests to establish the probability of interference between spacecraft;
- Transponder oscillator drift test to establish the transponder best lock frequency as a function of temperature after exposure to space environments;
- Paint coupon and solar panel degradation tests to determine paint and solar panel degradation under space environments;
- Battery deep discharge test to discharge the battery periodically to erase the battery memory effect which will, in turn, extend the life of the battery;
- Camera thermal door open test to determine thermal effects on the photo subsystem;
- V/H sensor tests to: determine the capability of the V/H sensor to track during oblique photography at roll and pitch tilt angles up to 45 degrees, and track at high Sun angles near the terminator; conduct V/H
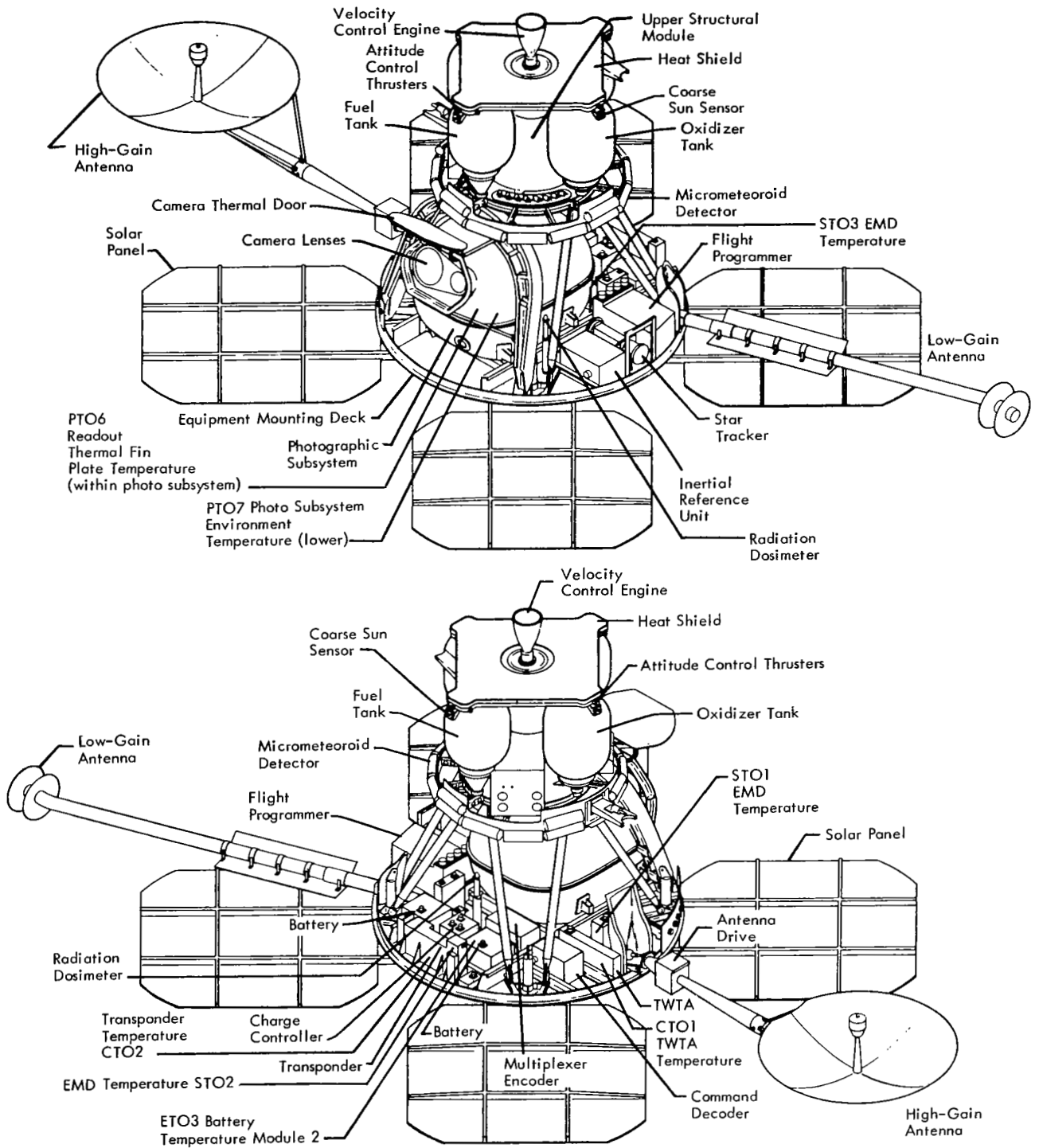
Note: Shown with Thermal Barrier Removed

Figure 2-1: Lunar Orbiter Spacecraft

6
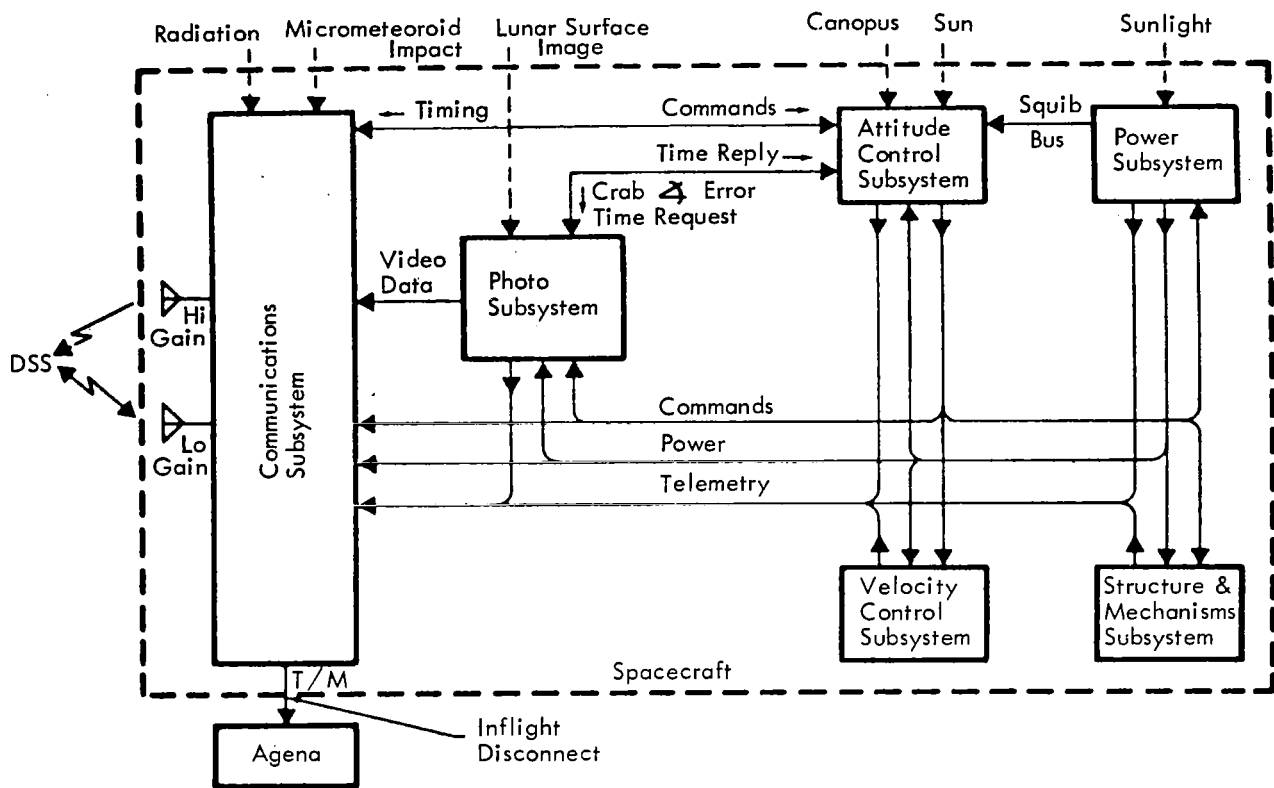
Figure 2-2: Spacecraft Subsystems

surveys of the eastern and western limbs; and determine temperature versus operating time characteristics for the V/H sensor to establish operational constraints;

● Star tracker bright object sensor and glint mapping tests to determine bright object sensor operation and glint characteristics for daylight tracker operating conditions as required for Mission IV. The star tracker was also used to determine the relative tracker output for stars not observed on previous star maps;

● Maneuver accuracy test to determine maneuver accuracies for the pitch and yaw axes;

● IRU turn-off-turn on test to determine IRU operational characteristics during off-on cycles;

● Ionosphere experiment to determine the effects of the Earth's ionosphere on Doppler and ranging data;

● Doppler ranging calibration experiment to aid in the checkout and calibration of the Mark II ranging system at the Goldstone

Mars Station (DSS-14);

● MSFN/Apollo GOSS navigation qualification support to qualify Apollo tracking stations.

Other objectives included impacting the spacecraft on the Moon (nearside if possible) prior to loss of attitude control capability.

2.3 OPERATIONAL ORGANIZATION

The extended mission of Lunar Orbiter II was conducted using a centralized method of control from the Space Flight Operations Facility at Pasadena, California, which was similar to that adopted for the photographic missions. Primary differences between extended- and photographic-mission activities are described in the following paragraphs.

Manning at the SFOF and at the DSS's was at a significantly lower level during the extended mission than during the photographic mission. Manning at the DSS's was reduced by limiting the MDE personnel to the SLOE, Assistant

7

SLOE, and MDE Systems Engineer. During the photographic mission, the additional services of a video engineer and supporting film processing personnel, as well as telemetry operations, were required. Manning at the SFOF was reduced in several areas. The NASA mission advisors were no longer required; however, a small NASA scientific team located at the Langley Research Center was available for selenodetic studies and consultation. The mission director also was no longer required at the SFOF, but was available at Langley for key decisions.

It was possible to safely reduce the size of the SPAC and FPAC teams, while still performing all of the required functions. This was due to shorter track periods such that only one team was required instead of the three teams needed during the photographic mission, cross-training of personnel so that one person could perform several functions, and a generally lower level of operational activity. For those periods when high levels of activity were required, such as in preparation for and during a velocity maneuver, personnel from Seattle were sent to the SFOF to augment the extended-mission team. During long tracking periods, such as MSFN tracks which lasted up to 32 hours in duration, the extended-mission team was augmented by a Seattle-based team.

A list of the manning provided by the contractor at the SFOF for extended-mission tracks is shown below. In addition to these personnel, the Space Flight Operations Director and a reduced (from the photographic mission) complement of JPL personnel (such as Track Chief) and communications personnel were required to support the tracking periods.

- Assistant Space Flight Operations Director
- SPAC
  1) Command Programmer Analyst
  2) Attitude Control Analyst
  3) Power/Thermal Analyst
  4) Communications System Analyst
  5) SPAC Software Analyst
  6) Photo Subsystem Analyst
  7) Command Coordinator
- DACON
     Data Controller
- FPAC
  1) Flight Chief
  2) Orbit Determination Analyst
  3) Guidance Analyst

This team, minus the guidance and photo subsystem analysts, also monitored and controlled the extended mission of Lunar Orbiter II during the primary photographic missions of Lunar Orbiters III, IV, and V.

3.0 Flight Operations

The Lunar Orbiter II extended-mission period — GMT Day 342, 1966, through Day 284, 1967 — spanned many milestones of the Lunar Orbiter project. During a major portion of this period, two other Lunar Orbiter spacecraft were also active. Therefore, the extended-mission flight operations plan underwent several evolutionary changes, enabling extended-mission objectives to be met while several spacecraft were maintained simultaneously in a safe status.

During the first 30 days of the extended mission, the tracking commitment consisted of a daily track of two consecutive orbits to be shared by the active spacecraft. After the first 30 days, the tracking commitment was reduced to three such tracks per week. Beginning in June, 1967, additional tracking commitments were acquired to extend three of these periods per month to approximately 27 hours' duration in support of the Manned Space Flight Network.

Within this framework, an extended-mission flight operations plan was developed which defined the overall activities required during the Lunar Orbiter II extended mission. A more thorough analysis of spacecraft status and extended-mission requirements resulted in preparation of operations directives for each tracking period which defined the support requirements and the sequence of events to be followed.

The primary considerations used in preparing the operations directives included:

● Amount of gaseous nitrogen available;
● Thermal history and temperature trends;
● Electrical power loads and solar array capability at various off-Sun angles versus the thermal history at those angles;
● Past operational constraints of each subsystem versus the desired limits for future missions;
● Noting and reacting to any unusual trends before they became dangerous.

The generally accepted flight operations procedures were intended to:

● Minimize gas usage and maximize spacecraft life;
● Maintain an acceptable thermal-to-power balance;
● Provide maximum safety to all spacecraft;
● Utilize stored-program commands rather than real-time commands whenever possible;
● Maintain the ability to have a controlled lunar impact at the end of useful spacecraft life;
● Monitor each active spacecraft during each scheduled tracking period.

During the initial days of the Lunar Orbiter II extended mission, a velocity maneuver was performed to make the orbit inclination as close as practical to the inclination planned for Mission III. The next 1.5 months were used to gather selenographic data at this new inclination and perform spacecraft tests and experiments in support of Mission III planning, scientific data acquisition, and Manned Space Flight Network tracking.

During this period the spacecraft was also used to assist the DSN in certifying DSS-62 for Mission III support. This certification continued into the early phase of the Mission III cislunar trajectory. In conjunction with the test transponder at DSS-12, the spacecraft was also used during the period to prove the feasibility of multiple spacecraft operation.

The next phase of the extended mission was to use the Lunar Orbiter II spacecraft as a training device to supply realism during training for Mission III.

During the Lunar Orbiter III photographic mission, the Lunar Orbiter II spacecraft was placed in the programmer-controlled extended-mission mode for thermal control and monitored for a few minutes on a daily basis. No tracking data were retained for selenodesy during this period.

When Lunar Orbiter III also entered the

extended-mission phase, experiments and tests to be performed were assigned to whichever spacecraft could best satisfy the requirements; Lunar Orbiter II was used for many of these. In addition, frequent ranging and time correlation periods were assigned in support of the DSN.

On Day 104 a velocity maneuver was performed on the Lunar Orbiter II spacecraft to change the orbit in preparation for the lunar eclipse which occurred on Day 114. This maneuver was to minimize the period that the spacecraft would be without adequate solar power. On Day 110 a battery deep discharge was performed, also in preparation for the lunar eclipse.

Between Days 107 and 111, both Lunar Orbiter II and III spacecraft were used to develop procedures for tracking multiple spacecraft operating in the same radio frequency band. Lunar Orbiter II was used as the passive spacecraft during the sidelobe acquisition test and as the active spacecraft during the many tests used to prove that offset frequencies could be used to prevent interference with the passive spacecraft.

The actual eclipse monitoring occurred during the training period for the Lunar Orbiter IV mission. Lunar Orbiter II was programmed for the extended-mission mode for thermal control between Mission IV training and Mission IV launch. Only a daily " quick- look" monitoring was performed on Lunar Orbiter II during the Lunar Orbiter IV photographic mission.

During quick-look tracking periods the spacecraft was analyzed to determine subsystem performance. Of primary interest was the detection of detrimental spurious commands that may have been received during command transmissions to another spacecraft. When possible, the quick- look tracking periods were scheduled to make possible the observation of predicted events such as sunrise, sunset, and earthset, to evaluate the validity and error magnitudes in the current predicted orbital parameters. This information was used to update the DSS predict information just prior to each tracking period.

After Lunar Orbiter IV had entered the extended-mission phase, very few experiments were performed using Lunar Orbiter II; however, DSN support was provided periodically for Doppler and ranging calibration.

On Day 178 a velocity maneuver was performed to raise the perilune of the Lunar Orbiter II orbit and extend its useful lifetime.

On Day 210, the microwave link between DSS-11 and DSS-12 was verified for command capability using Lunar Orbiter II spacecraft.

During most of the period between Lunar Orbiter IV photo mission and Lunar Orbiter V launch, as well as throughout all of the Lunar Orbiter V photo mission, Lunar Orbiter II was kept in the extended-mission mode for thermal control and monitored on a quick-look basis.

Between Days 272 and 280 preparations, including battery deep discharge tests and phasing maneuver studies, were made to place Lunar Orbiter II in the best possible conditions to survive the lunar eclipse on Day 291. These studies, in conjunction with nitrogen gas usage predictions, which indicated a marginal condition following the eclipse, resulted in the decision to impact the spacecraft on the Moon prior to the eclipse.

The terminal transfer maneuver was performed on Day 284 and several special tests were performed just prior to impact.

3.1 SPACECRAFT CONTROL

The Lunar Orbiter II spacecraft was acquired and tracked by the DSN using such operational techniques and frequency predicts as were employed during the prime mission. After spacecraft acquisition, real-time telemetry readout was obtained at the SFOF via high-speed data line and 60-wpm teletype. The telemetry data were processed in real time by IBM 7044 and 7094 computers and displayed for analysis on 100-wpm teletype machines, X-Y plotters, and bulk printers.

Programmer sequences were generated by the Command Generation and Programmer Simulation Program (COGL), sent to the cognizant DSS, and transmitted to the spacecraft to perform housekeeping functions and to conduct experiments and tests. The stored-programmer routines were supplemented by pre-prepared and manually generated real-time commands as operationally required.

During portions of the Lunar Orbiter II extended mission, Lunar Orbiters III and IV or V were also in the extended-mission phase. These spacecraft were operated by stored-program maps which automatically updated the Sun reference periodically. Whenever Lunar Orbiter II was designated as the primary spacecraft for a tracking pass, the other spacecraft were also tracked for a brief period during each pass to verify the operation of the flight programmer and to monitor the status of the other subsystems. Similarly, when Lunar Orbiter II was the secondary spacecraft, its status was also checked by quick-look monitoring. Spacecraft flight control was maintained using the flight operations guidelines discussed in Section 3.0.

3.1.1 Command Activity

The cruise mode programmer stored sequence consisted of acquiring the Sun reference periodically and pitching 40 to 62 degrees for thermal relief. Pitch values were selected by evaluating gyro drift characteristics and power/thermal requirements for each period of time. As shown in Table 3-1, the cruise program was deviated from so that tests and experiments could be performed.

Real-time commands were used to supplement stored sequences whenever the desired spacecraft activity was not sufficiently predictable to be stored or when a spacecraft reaction had to be evaluated prior to proceeding to the next command. Virtually all activity concerned with star tracking was accomplished by RTC's due to the possibility of glint interfering with the star tracker operation. RTC's were also typically used to overstore discrete programmer locations, to rotate the high-gain antenna, to initiate velocity maneuver sequences, to use

as a backup terminate command for velocity maneuvers, and to orient the spacecraft as dictated by real-time situations.

The communications subsystem, when operating at a received signal strength below the command threshold, can develop bit errors in the address code such that commands addressed to another spacecraft will be accepted and executed. Due to the high probability of more than one bit error occurring, it is likely that the operation code and/or operand of the command message would also be garbled, thus preventing the isolation of the spurious command by the examination of command logs.

With a DSS antenna pointed to the prime photo mission spacecraft, the orbital geometry occasionally resulted in the extended-mission spacecraft acquiring uplink transponder lockon to the signal of a side lobe and therefore operating below the command threshold. As a result, six spurious commands were received during Lunar Orbiter Missions III, IV, and V.

A total of 2,868 stored-program commands (SPC's) and 1,228 real-time commands (RTC's) was executed during the extended mission.

3.1.2 Spacecraft Telemetry

A total of 542.6 hours of telemetry data was processed during 195 tracking passes. Table 3-2 contains a summary of the telemetry data by station and includes a listing of the significant activities accomplished during each pass.

Problems encountered, such as minor communications outages and computer internal restarts, were typical of those experienced during the prime missions. Standard workaround methods, such as processing of telemetry data and use of raw hexidecimal data, were employed to minimize data problems. The communications processor caused the raw telemetry data to lag behind real time, resulting in frequent deletion of data in order to return to real time. This processor, therefore, was not used constantly.

A data and alarm summary (DATL), containing a majority of the telemetry channels for

11

Table 3-1: Programmer Core Map Summary

Map Number	Time Transmitted to Spacecraft Day:Hr:Mn	Purpose	COGL Run Number
57	350:08:00	1. Battery deep discharge test 2. Pitch and yaw maneuver accuracy test 3. Extended mission flight plan (propellant tank heaters on and off each orbit, acquire Sun and pitch plus 40 degrees at approximately 75-hour intervals)	350-01
58	353:08:00	1. Mode I V on and off for MS FN pass 2. Extended mission flight plan	353-01
59	355:11:00	New flight plan (propellant tank heaters on and off each orbit, acquire Sun and pitch plus 50 degrees at approximately 64-hour intervals)	355-01
60	357:06:00	New flight plan (propellant tank heaters on and off each orbit, acquire Sun and pitch plus 50 degrees each 15 orbits at approximately 52 hour intervals)	357-01
61	364:16:15	Flight plan extension	363-01
61 Update	364:17:00	New flight plan (propellant tank heaters on and off each orbit, acquire Sun and pitch plus 50 degrees each 30 orbits)	363-01U
Updated 61 Update	368:17:00	Times of "acquire Sun" in flight plan changed to account for adjusted sunrise/sunset (new O.D.)	368-01 V
61 X	003:20:00	1. New flight plan (propellant tank heaters on and off each orbit, acquire Sun and pitch plus 55 degrees each 15 orbits)	368-02 X
62	009:02:27	2. Film rewind 3. V/H survey experiment (eastern limb)	
62 Update 63	010:22:04 012:05:56	1. Film rewind 2. V/H survey experiment (eastern limb) 3. V/H high Sun angle test	375-01
64	012:20:43	1. V/H survey experiment (eastern limb) 2. V/H high Sun angle test	378-01
65	014:15:25	1. Film rewind 2. V/H roll test	379-01

Table 3-1 (Continued)

Map Number	Time Transmitted to Spacecraft Day:Hr:Mn	Purpose	COGL Run Number
66 67	015:00:50 017:07:25	1. V/H pitch test 2. New flight plan (acquire Sun and pitch + 55 degrees at approximately 88-hour intervals)	379-02
SMP01 SMP02 SMP02UD SMP03 SMP04 SMP05 SMP06 SMP07 SMP08	021:09:00 021:17:35 021:21:14 021:23:35 022:10:51 022:17:15 023:00:38 023:11:15 024:01:10	1. Mission III training	------
69 69 Update	024:12:25 026:22:08	1. V/H survey experiment (western limb) 2. V/H sensor temperature test	389-01.3
70	027:02:00	V/H high roll angle test	391-01.1
71	027:06:45	New flight plan (acquire Sun and pitch plus 50 degrees, wait 59½ hours [15 orbits], repeat. Transponder r.f. exciter redundantly commanded "off" six times during the 60-hour wait period and commanded "on" after 77 days)	392-01
72	044:09:49	New flight plan (same as Map 71, except that pitch plus magnitude was changed to 62 degrees)	407-01
N/A 75	051:03:03 067:23:47	Telemeter memory	N/A
76	068:20:56	Reflects real-time jump commands, and flight plan revision	432-02
77	070:04:04	Star tracker glint mapping test (Mission IV conditions)	435-01
78	070:22:35	Reloads extended mission flight plan (acquire Sun and pitch plus 62 degrees, wait 59 hours, repeat)	436-02
JMP027	073:04:15	Reflects real-time jump command	440-01
79	079:02:52	Film movement (read out)	444-01

Table 3-1 (Continued)

Map Number	Time Transmitted to Spacecraft Day:Hr:Mn	Purpose	COGL Run Number
80	087:15:15	New flight plan (acquire Sun and pitch plus 56 degrees each six orbits)	087-02
81	103:15:40	Preparations for lunar eclipse phasing velocity maneuver	102-01
81 Update	104:05:45	Programmer update for velocity maneuver	104-01
82	105:03:20	Adjust Sun acquisition times for new orbital parameters	105-01
83	110:12:05	Battery deep discharge test	110-01
84	114:05:53	Extend flight plan	113-04.1
85	120:09:40	Extend flight plan for maximum length (last prior to Mission I V)	120-01
86	161:20:46	Flight plan extension	161-01
87	177:07:14	Preparations for perilune increasing velocity maneuver	177-01
87 Update	178:02:39	Programmer update for velocity maneuver	177-02
88	178:13:10	Reloads flight plan (unchanged)	178-01
89	205:07:20	New flight plan (acquire Sun and pitch plus 59 degrees each six orbits)	205-01
SEQ390-394	209:08:35	Telemeter memory prior to Mission V	209-02
90	243:00:31	Extend flight plan	242-03
91	272:14:16	Battery deep discharge test	272-01
92	273:00:13	Battery deep discharge test	272-02
93	275:21:06	New flight plan (acquire Sun and pitch minus 52.5 degrees each 6 orbits)	275-01
94	284:04:30	Terminal descent test sequences	283-03

Table 3-2: Spacecraft Telemetry Summary

Day	Period (GMT)	Deep Space Station	Activities
342	16:10-21:54	12	a. Command address test
342/343	19:04-06:13	41	b. Inclination change
343	05:36-15:27	61	c. Selenodesy
343	12:36-22:27	12	
343	19:37-22:27	41	
344	13:10-14:52	61	Selenodesy
344	13:18-23:00	12	
344	20:12-23:00	41	
346	00:19-06:35	41	Selenodesy
347/348	18:36-00:45	12	Selenodesy
348	05:09-10:50	41	a. Selenodesy
			b. Star tracker bright object sensor test
			c. Paint degradation test
			d. Solar panel degradation test
349	02:19-08:25	41	Selenodesy
350	03:01-09:04	41	Selenodesy
351	03:44-09:43	41	Selenodesy
353	01:37-06:38	12	a. Battery deep discharge test
353	02:25-09:41	41	b. Pitch and yaw maneuver accuracy test
			c. MSFN
			d. Selenodesy
354	05:52-11:50	41	Selenodesy
355	06:35-12:34	41	Selenodesy

Table 3-2 (Continued)

Day	Period (GMT)	Deep Space Station	Activities
356	07:17-13:18	41	a. MS FN b. Selenodesy
357	00:55-06:59	12	a. MS FN b. Selenodesy
361	11:30-19:33	41	a. Selenodesy
361	17:29-19:33		b. DSS-62 Certification
362	07:37-13:48	12	Selenodesy
363	11:50-14:24	12	Selenodesy
363	12:59-21:26	41	
363	19:24-21:27	62	
364	15:38-22:00	41	Selenodesy
003	12:00-19:35	12	Selenodesy
003	14:58-20:47	41	
004/005	18:59-01:23	41	Selenodesy
006/007	19:35-01:56	41	a. MS FN b. Selenodesy
007	13:09-19:29	12	Transponder oscillator drift test
008/009	20:47-04:02	41	Selenodesy
009/010	21:25-03:39	41	Selenodesy
010/011	16:36-00:19	12	a. MS FN b. Selenodesy c. Star map
012	02:16-08:22	41	Selenodesy

16

Table 3-2 (Continued)

Day	Period (GMT)	Deep Space Station	Activities
012/013	19:55-01:58	12	a. V/H survey experiment (eastern limb)
012/013	23:26-05:30	41	b. V/H high Sun angle test
			c. Selenodesy
013/014	20:37-03:37	12	Selenodesy
014	10:43-16:42	62	a. DSS - 62 compatibility test
			b. Selenodesy
014/015	21:18-03:17	12	a. V/H roll test
015	00:51-03:18	41	b. V/H pitch test
			c. Selenodesy
017	02:16-08:16	41	Selenodesy
020/024	22:03-13:09	ALL	a. Mission III training
			b. Selenodesy
026/027	22:07-07:57	62	a. Selenodesy
			b. V/H survey experiment (western limb)
			c. V/H sensor temperature test
027	19:11-19:37	41	a. *
			b. Training in acquisition procedures for rf silent spacecraft
030/031	17:18-03:16	41	a. Selenodesy
030/031	23:05-06:42	62	b. Dual spacecraft tracking training
032	00:57-03:30	62	DSS-62 ranging checkout
032/033	18:27-02:55	41	Selenodesy
033	01:29-03:31	62	
037	19:10-20:06	41	*

Table 3-2 (Continued)

Day	Period (GMT)	Deep Space Station	Activities
040	16:27-17:11	12	*
042	04:22-04:55	41	*
042	18:44-19:22	12	*
042	22:22-22:25	12	*
044	09:41-10:23	41	*
045	20:52-21:20	62	*
048	22:10-22:57	12	*
050/051	23:31-00:02	12	*
051	02:53-03:42	12	*
051	06:24-07:02	12	*
052/053	23:55-00:44	12	*
053	00:30-01:15	12	*
055	01:42-02:11	62	*
056	19:47-20:10	41	*
058	13:51-13:59	12	*
062	15:08-15:24	12	*
065	19:43-20:00	12	*
065	22:59-23:32	41	*
067/068	23:46-00:18	41	*
068	20:50-21:13	12	*
069	03:35-04:00	41	*
070	04:00-06:08	41	*
070	08:00-16:43	62	a. Selenodesy
070	15:23-23:25	12	b. Star tracker glint mapping test c. Star map test

Table 3-2 (Continued)

Day	Period (GMT)	Deep Space Station	Activities
073	04:13-04:45	41	*
075	02:39-02:42	41	*
078	03:01-03:03	12	*
079	02:52-08:59	12	a. Selenodesy
079	06:30-12:22	41	b. Transponder threshold test
081	16:21-16:35	41	*
081	19:58-20:45	62	*
083	10:31-10:45	41	*
085	18:30-18:40	41	*
087	10:57-14:59	12	Selenodesy
087	12:56-19:14	41	
089	09:47-16:10	12	a. Selenodesy
089	13:38-20:00	41	b. MSFN
092	14:14-14:24	12	*
094	04:30-04:46	62	*
095	15:41-15:52	12	*
096/097	23:22-07:10	41	Selenodesy
097	06:25-09:05	62	
098	19:55-20:05	12	*
101	17:40-17:58	12	*
102	18:12-18:30	12	*
103	14:19-20:20	62	a. Selenodesy
103	17:52-23:52	12	b. Star search

Table 3-2 (Continued)

Day	Period (GMT)	Deep Space Station	Activities
104	04:26-10:26	41	a. Star search
104	08:38-13:58	62	b. Lunar eclipse phasing maneuver
105/106	19:46-06:24	12	a. Ionosphere Experiment
106	03:44-08:05	41	b. MS FN
			c. Selenodesy
107	09:41-09:52	41	*
110	10:57-16:59	41	a. Selenodesy
110	14:31-20:44	62	b. Battery deep discharge test
111	04:26-10:44	12	Multiple spacecraft operations experiments
111	07:57-10:58	41	
114	05:45-06:40	12	Lunar Eclipse Monitoring
114	07:54-08:38	12	Lunar Eclipse Monitoring
114	09:14-10:26	12	Lunar Eclipse Monitoring
114	11:00-11:18	41	Lunar Eclipse Monitoring
114	11:40-12:08	41	Lunar Eclipse Monitoring
114	12:43-13:12	41	Lunar Eclipse Monitoring
114	13:35-14:00	41	Lunar Eclipse Monitoring
114	14:25-14:59	41	Lunar Eclipse Monitoring
114	15:15-15:37	41	Lunar Eclipse Monitoring
114	18:42-18:50	41	Lunar Eclipse Monitoring
116	11:41-11:42	12	*
119/120	21:56-02:05	41	Selenodesy
120	01:26-09:51	62	
126	15:48-16:03	62	*

Table 3-2 (Continued)

Day	Period (GMT)	Deep Space Station	Activities
127/128	23:42-00:10	12	*
128/129	23:30-00:05	12	*
129	14:56-15:10	12	*
130	15:05-15:16	12	*
132	02:41-03:00	12	*
133	01:38-01:55	41	*
134	03:30-04:00	41	*
135	20:51-21:00	12	*
137	22:50-23:00	62	*
138	22:50-23:00	12	*
139	23:02-23:19	12	*
141	02:20-02:40	62	*
142	02:34-03:00	62	*
143	01:56-02:12	12	*
144	21:40-21:48	41	*
145	22:34-22:45	41	*
147	15:05-15:17	12	*
149	01:03-01:17	41	*
150	17:47-18:01	12	*
151	17:39-18:00	12	*
152	14:32-14:45	12	*
153	18:09-18:35	41	*
155	14:23-14:35	62	*
156	19:55-20:10	41	*

Table 3-2 (Continued)

Day	Period (GMT)	Deep Space Station	Activities
158	14:19-14:30	12	*
159	23:10-23:21	41	*
161	20:45-20:55	12	*
164	07:00-07:16	41	*
164	19:41-19:50	12	*
165	01:23-01:35	12	*
166/167	21:48-02:30	12	Doppler ranging calibration
169	00:00-00:20	62	*
171	01:30-01:50	12	*
173	19:00-19:10	41	*
176	02:02-07:30	62	a. Doppler ranging calibration experiment
176	05:54-14:53	12	b. Selenodesy
177	04:35-08:00	62	a. Selenodesy
177	07:10-16:40	12	b. Star map test
177	13:27-17:11	41	
178	00:06-09:55	62	a. Selenodesy
178	00:22-01:47	41	b. Orbit adjust (perilune increase) maneuver
178	06:59-14:51	12	
180	14:50-19:40	12	Selenodesy
180/181	14:50-00:33	41	
186	13:56-15:26	62	*
188	15:37-16:20	62	*
192	01:07-01:35	12	*
196	05:07-05:50	12	*

Table 3-2 (Continued)

Day	Period (GMT)	Deep Space Station	Activities
198	02:22-03:00	12	*
202	10:15-23:47	41	Selenodesy
205	04:50-07:33	62	Selenodesy
205	04:50-13:16	12	
209	08:15-09:18	12	*
209	10:14-10:50	12	*
210	11:40-13:01	12	*
215	23:18-23:30	12	*
216	17:30-17:57	62	*
217	22:26-22:46	41	*
219	19:44-20:00	62	*
220	17:08-17:30	12	*
221	18:24-18:35	12	*
223	03:12-03:51	41	*
224	20:51-21:00	62	*
226	01:27-01:46	12	*
226	13:50-14:15	41	*
227	18:31-18:45	62	*
228	13:50-14:00	41	*
230	02:43-03:00	62	*
230	19:43-19:45	41	*
232	21:02-21:07	41	*
233	20:40-21:00	62	*
234	22:06-22:30	41	*

Table 3-2 (Continued)

Day	Period (GMT)	Deep Space Station	Activities
235	22:33-22:43	41	*
236	22:33-22:45	62	*
237	22:27-22:45	41	*
239	17:21-17:40	41	*
240	02:26-02:44	62	*
240	03:00-03:20	62	*
242	02:36-03:12	62	*
242	20:09-20:40	12	*
242	22:16-22:20	41	*
243	00:26-00:40	41	*
244	12:00-12:51	12	*
248	22:21-23:00	12	*
250	13:42-14:20	62	*
253	05:04-05:40	41	*
254	20:20-21:00	62	*
255	15:19-15:28	41	*
256	20:32-21:00	62	*
258	20:20-20:55	62	*
259	00:32-00:52	62	*
261	22:29-23:01	62	*
262	07:28-07:51	12	*
262	11:34-12:10	12	*
264	13:47-14:22	41	*
267	20:23-21:00	41	*

Table 3-2 (Continued)

Day	Period (GMT)	Deep Space Station	Activities
270	16:07-16:26	12	*
272	12:59-15:14	62	a. Selenodesy
272	13:20-22:05	12	b. Battery deep discharge test
272/273	19:41-01:43	41	
274	22:40-23:10	41	*
275	21:03-21:30	12	*
276	23:11-23:23	41	*
277	17:21-17:37	62	*
279	09:36-10:15	41	*
282	10:17-10:20	41	*
282	10:43-10:50	41	*
283	01:59-02:05	12	*
283	05:06-05:15	12	*
284	04:25-07:11	41	a. Terminal transfer maneuver
284	05:21-06:38	12	b. Selenodesy

*Quick-look monitoring — see discussion in Section 3.0, page 10.

each frame, was processed for all tracking passes to provide a permanent record of the telemetry data.

3.2 FLIGHT PATH CONTROL

Flight path control of the spacecraft during the extended mission is the responsibility of the FPAC portion of the flight team. The functions carried out during this period were identical to those during the primary mission, tracking data editing, orbit determination, and guidance maneuver calculations. The processes used to perform these functions are the same as those in the prime mission, except that the quantity of data is less due to the decreased tracking time.

3.2.1 Tracking Data Editing

Tracking data editing is the process of monitoring, analyzing, and judging the quality of the Doppler and range radar tracking data transmitted to the SFOF from the DSN. The Deep Space Stations at Cebreros (Madrid) (DSS-61 and 62), Woomera (DSS-41), and Goldstone Echo (DSS-12) provided the tracking data. Three types of data were provided: continuous count Doppler, ranging units, and antenna pointing angles. The angles were not used because of the small arc traversed by the spacecraft in lunar orbit. The ranging subsystems were changed in 1967 to provide independent

ranging data points on Day 069 at Goldstone, Day 111 at Madrid, and Day 137 at Woomera. Prior to these dates each set of good (not flagged bad) ranging points was equivalent to one independent range data point. Also, a Doppler resolver was incorporated into the tracking data message after June 1967. The resolver data greatly increased the confidence in the received Doppler data. Table 3-3 is a summary of the tracking data.

Computer programs TDPX and ODGX were used to edit and process the tracking data. Tables 3-3 and -4 provide the information used for this editing and processing. Table 3-5 contains a list of master file (tracking data) tapes generated by TDPX; the tapes sent to Langley Research Center and those kept in the JPL tape library are listed.

3.2.2 Orbit Determination

The computer program ODPL was used to calculate the orbit determinations using the tracking data prepared by the editing programs. The program used a fourth-order spherical harmonic expansion of the lunar potential field. NASA provided two sets of coefficients for this model, one on September 4, 1966 and one on November 11, 1966, which were used during the extended mission (see Table 3-6). The latter set of coefficients was used after Day 069 of 1967. The following procedure was used.

- Doppler tracking data (two-way [CC3] and three-way [C3] with data weight of 0.1 cycle per second) were used.
- Range unit residuals were calculated for visual assistance in the determination.
- State vector (and Doppler bias when C3 data were available) was estimated.
- High-order harmonics were estimated to absorb some of the effects of incorrect modeling if there were enough data; i.e. greater than 6.5 hours of C3 and CC3 data.
- True anomaly of spacecraft at epoch was chosen to be as close to 180 degrees (apolune) as possible.

The Keplerian state vectors resulting from the extended-mission orbit determinations are contained in Table 3-7. The tracking data and

statistics used for the orbit determinations are summarized in Table 3-8. Orbit inclination, perilune altitude, and argument of perilune histories are displayed in Figures 3-1, -2 and -3, respectively.

3.2.3 Guidance Maneuvers

During the extended mission four guidance maneuvers, designed to change the orbital inclination, phase the spacecraft's orbit for the April 1967 lunar eclipse, increase the orbital lifetime, and impact the spacecraft on the lunar surface were performed.

3.2.3.1 Inclination Change

The purpose of this maneuver was to increase the orbital inclination of Lunar Orbiter II to a value closer to that which was to be used during Mission III. A maximum velocity change of 100 meters per second was allocated for this maneuver, allowing a 5.6-degree change in inclination. It was hoped that tracking data obtained from this new orbit would aid in the determination of a lunar gravitational model more meaningful for Mission III operational control. The higher orbit inclination was desirable in order to reduce correlations between certain gravitational harmonic coefficients prevalent in low-inclination orbits.

The orbit determination results of OD 5090-5 were used for maneuver design. The state vector was mapped forward to the maneuver time using the LRC 9/4 lunar harmonics. The maneuver design is shown in Table 3-9.

During the maneuver the spacecraft was tracked by DSS-12 and -41. Doppler monitoring was accomplished by DSS-12. Two-way Doppler during the burn is plotted on Figure 3-4 with a Doppler shift of 540 Hz being observed. Both ignition and burn duration were as predicted.

A postmaneuver orbit determination (OD 6002-5) was used to evaluate the maneuver execution. Table 3-7 contains the orbital elements of this postburn OD. A comparison of predicted and actual postburn orbital parameters, which may be seen in Table 3-10, indicates that the burn was executed as designed.

Table 3-3: Tracking Data Summary

Day of Pass	Sta	Type	Doppler				Ranging					*Syn-Freq.
			Start Time	Stop Time	Amount (hrs)	Trans- mitter on Time	Start Time	Stop Time	Amount (hrs)	Sta Delay	Transponder Temp. (°F)	
342	12	CC3	20:00	21:54	1.90	20:00	20:57	21:54	.95	294	N.A.	5610
342/3	41	C3	20:00	21:54	1.90		23:00	23:41	.68	292	N.A.	5570
		C3	05:40	06:12	0.52		02:43	04:02	1.34	292	N.A.	5530
		CC3	22:33	02:07	5.30	22:33						5570
		CC3	02:07	04:53		22:33						5620
343	61	CC3	05:38	09:07	3.30	05:38	05:38	11:55	3.30	290	N.A.	5580
		CC3	09:07	11:55		05:38						5600
		C3	12:08	12:37	0.72							5600
		C3	12:37	14:21								5590
343	12	CC3	12:39	16:08	5:75	12:39	12:39	18:57	4.18	304	78	5610
		CC3	16:08	18:57		12:39						5600
		C3	19:40	22:27	2.78							5620
343	41	CC3	19:38	22:25	2.78	19:38	19:43	22:25	2.14	285	77	5580
344	12	CC3	13:20	16:43	7.66	13:20	14:05	22:28	6.72	299	73	5580
		CC3	16:43	20:13		13:20						5600
		CC3	20:13	22:28		13:20	*Syn freq = 2204xxxx.0					5620

Table 3-3 (Continued)												
Day of Pass	Sta	Type	Doppler			Trans-mitter on Time	Ranging					*Syn freq
			Start Time	Stop Time	Amount (hrs)		Start Time	Stop Time	Amount (hrs)	Sta Delay	Transponder Temp. (°F)	
344	62	C3	13:30	14:52	1.25							5580
344	41	C3	20:15	22:30	2.25							5580
346	41	CC3	01:18	03:50	4.30	01:18	01:18	06:34	4.12	291	71	5600
		CC3	03:50	06:34		01:18						5620
347/8	12	CC3	18:38	22:08	5.25	18:38	18:43	00:40	4.48	295	78	5600
		CC3	22:08	00:43		18:38						5620
348	41	CC3	05:11	08:40	4.14	08:40	05:11	10:38	3.36	283	91	5620
		CC3	08:40	10:08		08:40						5630
348	41	CC3	10:08	10:38		08:40						5600
349	41	CC3	02:21	05:49	5.08	02:21	02:21	08:23	5.08	299	76	5590
		CC3	05:49	08:23		02:21						5610
350	41	CC3	03:03	06:30		03:03	03:03	09:02	4.00	285	79	5590
		CC3	06:30	07:27	4.80	03:03						5610
		CC3	07:27	08:16		03:03						5590
		CC3	08:16	09:02		03:03						5610
351	41	CC3	03:47	07:15	4.85	03:47	03:47	09:43	4.85	398	79	5580

*Syn freq = 2204xxxx.0

28

			Doppler				Ranging					*Syn-
Day of Pass	Sta	Type	Start Time	Stop Time	Amount (hrs)	Trans-mitter on Time	Start Time	Stop Time	Amount (hrs)	Sta Delay	Transponder Temp. (°F)	Freq.
		CC3	07:15	09:43		03:47						5600
353	12	CC3	01:40	04:02	2.36	01:40	01:45	02:20	0.38	299	81	5590
		C3	05:12	06:37	1.30							5600
353	41	C3	02:30	04:02	1.54		05:12	06:43	1.16	286	82	5550
		CC3	05:12	08:42	3.30	05:12						5560
		CC3	08:42	09:40		05:12						5580
354	41	CC3	05:55	09:25	4.80	05:55	05:55	11:50	4.80	295	83	5550
												5580
		CC3	09:25	11:50		05:55						
355	41	CC3	06:39	10:07	4.98	06:39	06:39	12:33	3.88	278	80	5540
		CC3	10:07	12:33		06:39						5570
356	41	CC3	07:18	10:47	4.44	07:18						5540
		CC3	10:47	13:17		07:18						5560
357	12	CC3	00:57	04:26	5.02	00:57						5530
		CC3	04:26	06:58		00:57						5560
362	12	CC3	07:42	11:00		07:42	08:10	13:47	4.98	283	78	5530

*Syn freq = 2204xxxx.0

Table 3-3 (Continued)												
Day of Pass	Sta	Type	Doppler			Trans-mitter on Time	Ranging					*Syn-freq
			Start Time	Stop Time	Amount (hrs)		Start Time	Stop Time	Amount (hrs)	Sta Delay	Transponder Temp. (°F)	
		CC3	11:00	13:47	5.25	07:42						5550
361	41	CC3	11:33	13:58		11:33	14:00	18:54	3.50	284	71	5510
		CC3	13:58	17:27	5.62	11:33						5530
		CC3	17:27	19:20		11:33						5550
363	11	CC3	11:53	14:24	2.52	11:53	12:11	14:24	2.10	3740	66	5560
363	41	C3	13:02	14:23	1.35							5520
		C3	20:42	21:25	0.72							5560
		CC3	15:06	18:35		15:06	15:17	19:39	3.65	053	67	5530
		CC3	18:35	20:26	3.62	15:06						5560
363	62	C3	19:27	20:37	1.15							5530
		CC3	20:45	21:26	0.54							5530
364	41	CC3	15:40	19:08		15:40	17:12	22:00	3.80	278	72	5550
		CC3	19:08	22:00	5.75	15:40						5560
003	12	CC3	12:09	14:25		12:09	12:15	17:15	4.14	299	78	5570
		CC3	14:25	17:16	4.34	12:09						5590
		C3	17:59	19:35	1.66		*Syn freq = 2204xxxx.0					5570

| | | | Doppler | | | Trans- | Ranging | | | | | *Syn- |
Day of Pass	Sta	Type	Start Time	Stop Time	Amount (hrs)	mitter on Time	Start Time	Stop Time	Amount (hrs)	Sta Delay	Transponder Temp. (°F)	Freq.
003	41	C3	15:02	17:15	2.22							5550
		CC3	17:53	20:46	2.86	17:53	18:10	20:27	2.28	272	79	5570
004/5	41	CC3	18:27	21:46	5.80	18:27	19:27	00:50	5.00	271	82	5570
		CC3	21:46	00:50		18:27						5600
005/6	41	CC3	19:02	22:30	5.66	19:02	19:02	01:21	5.64	276	76	5580
		CC3	22:30	01:23		19:02						5600
006/7	41	CC3	19:37	23:05	5.65	19:37						5580
		CC3	23:05	01:57		19:37						5610
008/9	41	CC3	21:13	00:20	4.75	21:13	21:13	22:23	1.18	287	82	5590
		CC3	00:20	03:50		21:13	01:38	02:00	0.36	287	82	5610
		CC3	03:50	04:00		21:13						5630
009/10	41	CC3	21:28	00:56	5.16	21:28	21:28	03:27	5.12	272	66	5590
		CC3	00:56	03:38		21:28						5610
010/11	12	CC3	16:37	18:34	5.78	16:37						5590
		CC3	18:34	22:04		16:37						5610

*Syn freq = 2204xxxx.0

Table 3-3 (Continued)												
			Doppler			Trans-	Ranging					
Day of Pass	Sta	Type	Start Time	Stop Time	Amount (hrs)	mitter on Time	Start Time	Stop Time	Amount (hrs)	Sta Delay	Transponder Temp. (°F)	*Syn-freq
		CC3	22:04	00:18		16:37						5630
012	41	CC3	02:18	05:47	5.06	02:18	02:18	03:15	0.95	278	62	5600
		CC3	05:47	08:22		02:18	07:08	08:22	1.24	278	61	5620
012/3	12	CC3	19:57	23:24	4.20	19:57	20:03	20:39	0.60	313	80	5600
		CC3	23:24	01:57		19:57	23:25	01:57	1.74	313	74	5620
012/3	41	C3	23:32	02:00	1.92							5580
		CC3	03:00	05:30	2.50	03:00	03:16	05:12	1.94	283	68	5600
013/4	12	CC3	20:38	00:07	4.88	20:38	20:38	02:37	4.88	309	73	5590
		CC3	00:07	02:37		20:38						5610
014/5	12	CC3	21:20	00:49	4.55	21:20						5580
		CC3	00:49	03:17		21:20						5610
015	41	C3	00:53	03:17	2.26							5560
017	41	CC3	02:35	05:47	4.40	02:35						5550
		CC3	05:47	08:16		02:35						5560
020/1	12	CC3	22:21	01:34	7.50	22:21	05:19	07:20	2.02	302	N.A.	5520
		CC3	01:34	05:05		22:21	*Syn freq = 2204xxxx.0					5540

32

Table 3-3 (Continued)

Day of Pass	Sta	Type	Doppler			Trans- mitter on Time	Ranging					*Syn- Freq.
			Start Time	Stop Time	Amount (hrs)		Start Time	Stop Time	Amount (hrs)	Sta Delay	Transponder Temp. (°F)	
		CC3	05:05	07:40		22:21						5560
020/1	62	C3	22:32	00:37	1.74							5560
021	41	CC3	08:48	12:00	4.15	08:48	10:00	13:40	2.68	291	N.A.	5530
		CC3	12:00	13:55		08:48						5550
		C3	14:05	14:43	0.64							5550
021	62	C3	13:22	13:53	0.52							5580
021/2	62	CC3	14:05	15:37		14:05						5580
		CC3	15:37	19:12	8.54	14:05						5520
		CC3	19:12	22:38		14:05						5540
		CC3	22:38	01:17		14:05						5550
022	12	CC3	02:14	05:44	5.22	02:14	07:10	08:22	1.16	305	N.A.	5530
			05:44	08:22		02:14						5550
022	41	C3	06:36	08:22	1.76							5580
		CC3	09:17	12:46	5.16	09:17	12:52	15:23	2.52	277	N.A.	5530
		CC3	12:46	15:23		09:17						5550
022/3	62	CC3	16:18	19:48		16:18	17:33	21:49	2.44	306	N.A.	5510

*Syn freq = 2204xxxx.0

			Doppler				Ranging					*Syn-Freq.
Day of Pass	Sta	Type	Start Time	Stop Time	Amount (hrs)	Trans-mitter on Time	Start Time	Stop Time	Amount (hrs)	Sta Delay	Transponder Temp. (°F)	
		CC3	19:48	23:00	7.84	16:18						5530
		CC3	23:00	01:58		16:18						5550
022/3	12	C3	23:20	01:58	2.64							5510
023	12	CC3	02:55	06:23	5.20	02:55						5620
		CC3	06:23	09:00		02:55						5550
023	41	C3	07:39	09:00	1.35							5590
		CC3	09:52	13:24	5.09	09:52						5520
			13:24	16:02		09:52						5540
023	62	C3	15:05	16:02	0.95							5590
023	62	CC3	17:20	20:25	4.95	17:20	18:33	19:03	0.50	290	N.A.	5510
			20:25	23:07		17:20						5530
024	12	CC3	00:05	03:36	7.88	00:05						5510
		CC3	03:36	07:02		00:05						5520
		CC3	07:02	09:38		00:05						5540
024	41	C3	08:43	09:38	0.92							5590
		CC3	10:29	12:00	1.52	10:29						5520

Table 3-3 (Continued)

*Syn freq = 2204xxxx.0

34

Table 3-3 (Continued)												
Day of Pass	Sta	Type	Doppler			Trans-mitter on Time	Ranging					*Syn-Freq.
			Start Time	Stop Time	Amount (hrs)		Start Time	Stop Time	Amount (hrs)	Sta Delay	Transponder Temp. (°F)	
026/7	62	CC3	22:08	01:40		22:08	04:05	04:25	0.35	287	80	5530
		CC3	01:40	05:06	8.12	22:08						5550
		CC3	05:06	07:57		22:08						5560
030	12	CC3	11:54	12:46		11:54						5570
		CC3	12:46	14:15		11:54						5637
		CC3	14:15	14:48	2.36	11:54						5602
		CC3	14:48	15:12		11:54						5622
		CC3	15:12	16:35		11:54						5590
030	41	CC3	20:00	21:07		20:00	23:22	23:36	0.24	279	81	5570
		CC3	21:07	23:38	1.66	20:00						5590
030	41	C3	00:20	01.16	0.90							5530
031	62	C3	23:06	23:43	0.62							5620
031	62	CC3	00:23	03:54	2.96	00:23	00:35	00:42	0.12	N.A.	67	5560
		CC3	03:54	06:11		00:23						5580
032	62	CC3	01:01	03:30	2.42	01:01	01:11	03:23	2.20	271	75	5560
032/3	41	CC3	18:32	21:56	5.75	18:32	19:00	00:43	4.88	285	73	5580

*Syn freq = 2204xxxx.0

| Day of Pass | Sta | Type | Doppler | | | | Ranging | | | | | *Syn-Freq. |
			Start Time	Stop Time	Amount (hrs)	Transmitter on Time	Start Time	Stop Time	Amount (hrs)	Sta Delay	Transponder Temp. (°F)	
		CC3	21:56	00:51		18:32						5600
033	41	C3	01:28	01:30	1.42							5558
		C3	01:30	02:53								5580
033	62	CC3	01:35	03:30	1.88	01:35	01:55	03:22	0.66	271	78	5557
037	41	CC3	19:13	20:06	0.90	19:13						5558
040	12	CC3	16:32	17:09	0.62	16:32						5559
042	41	CC3	04:50	04:55	0.08	04:50						5560
042	12	CC3	18:47	19:20	0.55	18:47						5557
		CC3	22:27	22:50	0.38	22:27						5550
044	41	CC3	09:54	10:23	0.48	09:54						5560
045	62	CC3	20:56	21:20	0.40	20:56						5559
050/1	12	CC3	23:37	00:02	0.42	23:37						5554
051	12	CC3	02:57	03:43	0.75	02:57						5555.8
		CC3	06:26	07:02	0.60	06:26						5546
052	12	CC3	00:06	00:45	0.65	00:06						5551
056	41	CC3	19:48	20:08	0.34	19:48						5557

*Syn freq = 2204xxxx.0

Day of Pass	Sta	Type	Doppler				Ranging					*Syn-Freq.
			Start Time	Stop Time	Amount (hrs)	Trans-mitter on Time	Start Time	Stop Time	Amount (hrs)	Sta Delay	Transponder Temp. (°F)	
070	41	CC3	04:03	06:08	2.08	04:03						5610
070	62	CC3	08:45	10:36		08:45	08:45	11:50	1.92	284	76	5570
		CC3	10:36	14:07	6.10	08:45						5590
		CC3	14:07	16:42		08:45						5610
070	12	C3	15:35	16:42	1.12							5570
		CC3	17:46	23:25	4.66	17:46						5580
079	12	CC3	02:55	05:25	2.50	02:55	03:12	04:53	1.70	306	73	5570
		C3	06:35	08:25	1.84							5580
079	41	CC3	06:24	09:52	5.00	06:24	06:37	08:42	2.08	294	74	5550
		CC3	09:52	12:29		06:24						5570
087	12	CC3	11:08	13:50	2.70	11:08	11:23	13:40	2.28	268	80	5630
		C3	14:32	14:57	0.42							5540
087	41	C3	12:57	13:50	0.88							5650
		CC3	14:57	17:58	3.50	14:57	15:48	19:13	2.76	296	82	5600
		CC3	17:58	19:13		14:57						5620
089	12	CC3	10:05	12:07	4.25	10:05						5610

*Syn freq = 2204xxxx.0

Table 3-3: (Continued)												
Day of Pass	Sta		Doppler				Ranging					*Syn-freq
		Type	Start Time	Stop Time	Amount (hrs)	Trans-mitter on Time	Start Time	Stop Time	Amount (hrs)	Sta Delay	Transponder Temp. (°F)	
		CC3	12:07	15:00		10:05						5630
		C3	15:40	16:08	0.46							5560
089	41	C3	13:38	15:02	1.50							5600
		CC3	15:38	18:28	2.84	15:38						5610
096/7	41	CC3	23:25	02:52	5.26	23:25	23:50	02:02	2.20	291	72	5630
		CC3	02:52	05:32		23:25						5650
097	41	C3	06:25	07:08	0.72							5580
097	62	CC3	06:27	09:03	2.64	06:27	06:31	08:52	0.60	312	80	5610
103	62	CC3	14:23	16:48	2.42	14:23	14:45	16:30	0.32	268	82	5590
		C3	17:53	20:20	2.45							5610
103	12	CC3	17:53	21:23	4.92	17:53	18:02	23:25	3.60	276	84	5570
		CC3	21:23	23:53		17:53						5580
104	41	CC3	04:26	07:57		04:26	05:55	10:20	2.00	288	88	5580
		CC3	07:57	08:17	4.96	04:26						5600
		CC3	08:17	10:25		04:26						5670
104	62	C3	08:40	10:25	1.75		*Syn freq = 2204xxxx.0					5630

38

			Doppler				Ranging					*Syn-freq
Day of Pass	Sta	Type	Start Time	Stop Time	Amount (hrs)	Trans-mitter on Time	Start Time	Stop Time	Amount (hrs)	Sta Delay	Transponder Temp. (°F)	
104	62	CC3	11:41	13:57	2.25	11:41	12:10	13:55	0.35	264	82	5580
105/6	12	CC3	19:47	23:32		19:47	20:00	06:24	6.56	307	80	5570
		CC3	23:32	02:06	7.60	19:47						5580
		CC3	02:06	06:24		19:47						5600
106	41	C3	03:44	05:32	1.52							5640
		C3	05:32	06:24								5580
		CC3	06:25	08:04	1.65	06:25	06:45	07:37	0.86	297	76	5580
110	41	CC3	10:59	14:26	4.98	10:59	10:59	16:58	4.98	N.A.	76	5580
		CC3	14:26	16:58		10:59						5600
110	62	C3	14:33	15:10	0.62							5560
		CC3	18:01	20:22	2.35	18:01	18:15	20:10	1.92	263	76	5570
114	12	CC3	05:48	08:37	1.26	05:48	05:48	08:37	1.26	291	80	5200
		C3	09:51	10:26	0.58							5220
114	41	CC3	11:42	12:42	1.86	11:42	11:42	15:37	1.86	N.A.	80	5180
		CC3	12:42	15:37		11:42						5200
119/20	41	CC3	21:58	01:26	2.92	21:58	21:58	00:43	2.44	289	78	5250

*Syn freq = 2204xxxx.0

Table 3-3: (Continued)												
			Doppler			Trans-mitter on Time	Ranging					*Syn-freq
Day of Pass	Sta	Type	Start Time	Stop Time	Amount (hrs)		Start Time	Stop Time	Amount (hrs)	Sta Delay	Transponder Temp. (°F)	
		CC3	01:26	01:40		21:58						5460
120	41	C3	01:45	02:05	0.34							5460
120	62	CC3	01:45	04:57		01:45	05:05	09:07	3.02	N.A.	79	5220
		CC3	04:57	08:26	6.00	01:45						5230
		CC3	08:26	09:50		01:45						5180
176	62	CC3	02:06	05:35	2.66	02:06						5300
		C3	06:00	07:30	1.50							5300
176	12	CC3	06:00	14:52	7.12	06:00	06:35	14:52	5.14	298	82	5300
177	62	CC3	05:37	08:20	2.72	05:37	05:37	07:05	1.18	288	80	5200
177	12	C3	07:33	08:20	0.78							5200
		CC3	09:05	11:50	2.75	09:05	09:20	10:25	1.08	306	80	5200
177	41	CC3	13:40	15:19	1.68	13:40	14:16	15:19	1.05	285	88	5200
178	41	C3	00:33	01:06	0.55							5200
178	62	CC3	00:34	06:00		00:34						5200
		CC3	06:00	08:42	6.20	00:34						5530
		CC3	08:42	08:50		00:34						5200

*Syn freq = 2204xxxx.0

Table 3-3: (Continued)												
			Doppler				Ranging					
Day of Pass	Sta	Type	Start Time	Stop Time	Amount (hrs)	Trans-mitter on Time	Start Time	Stop Time	Amount (hrs)	Sta Delay	Transponder Temp. (°F)	*Syn-freq
178	12	C3	06:54	08:42	1.50							5490
		C3	08:42	08:50								5200
		CC3	09:05	14:43	5.14	09:05	14:17	14:43	0.42	306	85	5200
180	12	CC3	14:54	17:15	2.32	14:54						5200
		C3	18:26	19:37	1.18							5200
180	41	C3	14:54	17:15	2.32		18:35	21:00	2.20	296	85	5200
180/1	41	CC3	18:24	00:32	4.15	18:24	22:54	00:32	1.64	296	87	5200
205	62	CC3	04:53	06:12	1.25	04:53	05:15	06:13	0.96	281	83	5200
		C3	07:02	07:32	0.50							5200
205	12	C3	04:55	06:12	1.22							5200
		CC3	06:58	13:16	4.52	06:58	11:03	11:46	0.72	291	75	5200
272	62	CC3	13:23	15:14	1.30	13:23	14:47	15:14	0.44	275	N.A.	5300
272	12	C3	13:23	15:14	1.30							5300
		CC3	16:08	18:48	2.68	16:08	16:11	17:50	1.65	N.A.	N.A.	5300
		C3	19:45	22:05	2.34							5300

*Syn freq = 2204xxxx.0

		Doppler					Ranging					*Syn-Freq.
Day of Pass	Sta	Type	Start Time	Stop Time	Amount (hrs)	Trans-mitter on Time	Start Time	Stop Time	Amount (hrs)	Sta Delay	Transponder Temp. (°F)	
272	41	CC3	19:43	22:07	2.40	19:43	19:53	20:33	0.66	301	N.A.	5300
284	12	C3	05:45	06:40	0.92							5300
284	41	CC3	05:46	07:10	1.40	05:46						5300

Table 3-3: (Continued)

*Syn freq = 2204xxxx.0

Table 3-4: Station Timing Synchronization

Time (GMT)	DSS Station	Timing Bias*
315:08:50	62	− 300.
319:04:00	41	−1250.
342:21:50	41	+ 50.
1966		
1967		
039:00:00	62	− 780.
039:00:00	41	+ 350.
125:20:46	41	+ 768.9
126:14:22	62	+ 307.5
126:21:20	41	+ 756.1
127:06:14	41	+ 365.3
127:14:20	62	+ 321.4
129:06:20	41	+ 384.2
129:17:26	62	+ 379.6
130:23:40	41	+ 762.3
131:00:32	41	+ 780.9
156:00:00	41	+ 834.
156:00:01	62	+ 812.0
161:00:01	62	+ 859.0
164:20:48	62	+ 865.0
242:00:00	41	+ 255.3
264:00:00	62	+ 612.4

*Deviation from DSS-12's clock in microseconds.

3.2.3.2 Orbit Phasing Maneuver for April 1967 Lunar Eclipse Passage

Analysis of the orbit of Lunar Orbiter II indicat-ed that the spacecraft would be in total darkness for a period in excess of 4 hours during the lunar eclipse on April 24, 1967. Graphical techniques verified by FPAC user program TRJL were used to determine the sequence of events during eclipse passage which would minimize time spent in total darkness.

To compute a phasing maneuver it was necessary to choose a reference time for use as a targeting parameter in the maneuver design program. Day 114, 10:44 GMT was chosen as the time of apoapsis passage during the eclipse which, if satisfied, would establish the proper phasing for optimum lighting.

Maneuver design was accomplished using orbit determination solution OD 6050-5, as shown in Table 3-7. Using this state vector, the epoch of apoapsis passage (corresponding to the reference epoch) was computed using TRJL. The total timing change of 78 minutes, 21 seconds was required for the spacecraft to arrive at apoapsis at the desired time. The number of orbits between the phasing maneuver and the reference epoch was selected to be 69. An orbital period change of 64.773 seconds was required for the 69 orbits between the selected maneuver time and the reference epoch. It was necessary to change other orbital parameters to satisfy the 5m/sec minimum ΔV constraint on the velocity control subsystem. In this case an increase in perilune altitude was chosen. A total increase of 3.94 kilometers was necessary to raise the ΔV to 5m/sec.

The roll reference for this maneuver was the planet Jupiter which, at the time of the maneuver, had a position in 1950.0 geocentric coordinates of:
    Right Ascension = 128.538 degrees
    Declination   = 19.3305 degrees

The details of the maneuver design may be seen in Table 3-9, and the predicted lighting time history resulting from this maneuver is shown in Figure 3-5.

Monitoring of the phasing maneuver was accomplished using DSS-41. Predicted and actual two-way Doppler are plotted in Figure 3-6. A

43

Table 3-5: Master File Tracking Data Tapes

| Time Interval | | LRC | JPL | Time Interval | | LRC | JPL |
Start Time Day:Hr:Mn	Stop Time Day:Hr:Mn	Tape Number		Start Time Day:Hr:Mn	Stop Time Day:Hr:Mn	Tape Number	
342:20:00	343:14:03	LT 233	10494	003:11:57	011:00:18	LT 247	10494
342:20:00	344:22:30	LT 234	10494	342:20:00	015:03:18		10494
342:20:00	348:00:44	LT 235	10494	342:20:00	017:08:16		7294
342:20:00	348:10:38	LT 236	10494	003:11:57	017:08:16	LT 248	7930
342:20:00	350:09:02	LT 237	10494	020:22:21	027:07:52	LT 249	7930
342:20:00	353:09:40	LT 238	10494	020:22:21	032:23:30	LT 250	7930
342:20:00	355:12:34	LT 239	10494	020:22:21	056:20:09	LT 251	7930
342:20:00	357:06:58	LT 240	10494	020:22:21	087:19:14	LT 252	7930
342:20:00		LT 241	10494	020:22:21	104:09:23	LT 253	7930
342:20:00	003:20:46	LT 242	10494	104:08:50	114:06:37	LT 254	9996,9574
342:20:00	007:01:56	LT 243	10494	104:08:50	120:09:50	LT 255	9996,9574
342:20:00	009:04:00	LT 244	10494	104:08:50	181:00:32	LT 256	9996,9574
342:20:00	364:22:00	LT 245	10494	104:08:50	205:13:16	LT 257	9996,9574
				104:08:50	284:07:11	LT 258	9996,9574

distinct Doppler shift (65 Hz) is noticeable, the parallel lines indicating successful maneuver execution. The bias of 10.5 Hz is induced when forwarding the trajectory 18.5 hours. The state vector used in making the predicts is designated as OD 6050-5.

A series of postmaneuver orbit determinations was used to evaluate the event sequence and lighting conditions during the lunar eclipse. For each OD a series of parameters concerning the eclipse was tabulated. A comparison of predicted and actual postburn orbital parameters may be seen in Table 3-10. Table 3-11 contains the complete results of all postmaneuver OD's. These data show that the maneuver was executed as designed.

Telemetry measurements of solar array current were monitored during the eclipse. This gave an indication of percent sunlight visible to the spacecraft. Figure 3-5 is a plot of predicted lighting time histories and actual telemetry data.

3.2.3.3 Orbital Lifetime Adjust Maneuver

Analysis of the Lunar Orbiter II trajectory indicated that the spacecraft would impact the Moon

Table 3-6: Lunar Harmonic Coefficients

LRC 09/04/66 Moon Model	LRC 11/11/66 Moon Model
u=4902.78	u=4902.58
J20=0.2048E-3	J20=2.07E-4
J30=−0.9049E-4	J30=−0.446E-4
J40=−0.2055E-4	J40=−0.209E-4
C21=−0.1398E-4	C21=0.088E-4
C31=0.2358E-4	C22=0.276E-4
C41=−0.7139E-5	C31=0.435E-4
C22=0.2445E-4	C32=−0.052E-4
C32=0.3840E-5	C33=0.0091E-4
C42=0.2229E-5	C41=−0.051E-4
C33=0.1888E-5	C42=0.028E-4
C43=0.1073E-5	C43=−0.0047E-4
C44=−0.2428E-7	C44=0.00094E-4
S21=−0.6512E-5	S21=−0.411E-4
S22=−0.3747E-5	S22=−0.058E-4
S31=0.1555E-4	S31=0.170E-4
S32=0.1339E-4	S32=0.0187E-4
S33=−0.7343E-6	S33=−0.033E-4
S41=−0.9304E-5	S41=−0.102E-4
S42=0.2928E-5	S42=−0.083E-4
S43=0.6450E-6	S43=−0.026E-4
S44=−0.3438E-6	S44=0.0017E-4

during the month of August 1967, although there was a possibility of impact during the month of July 1967 due to uncertainties in surface elevation and lunar harmonics. The predicted preburn and postburn perilune altitude history may be seen in Figure 3-7. In both cases impact would occur on the farside of the Moon.

A velocity control maneuver was designed such that the minimum perilune altitude, which would occur during the month of October, 1967 (Figure 3-7), would be 20 kilometers above the mean lunar surface (RM = 1,738.09 kilometers). The design would allow for local surface elevation and lunar model uncertainties to guarantee that impact would not occur. The maximum predicted perilune altitude after the maneuver, which would occur about April 1, 1968, would be 130 kilometers. This prediction was based on analysis of past perilune histories from the Lunar Orbiter II photo mission and the extended mission.

The maneuver design was accomplished using the orbit determination results of OD 7005-5, presented in Table 3-6. The state vector was mapped forward to the maneuver time using the LRC 11/11 lunar harmonics. Maneuver design details may be seen in Table 3-9.

Because Canopus was out of view of the star tracker it was necessary to use another star as a roll reference for the maneuver. The star Alpha-Eri (Achernar) was selected. It had the following 1950.0 geocentric position:

Right ascension =   23.95 degrees
Declination   = −57.48 degrees

During the maneuver the spacecraft was tracked with DSS-12 and -62. Doppler monitoring was accomplished using DSS-62. Predicted and actual two-way Doppler are plotted in Figure 3-8, and it may be seen that a Doppler shift of 105 Hz was observed during the burn. Also, a comparison of the predicted and actual Doppler indicates a slight overburn based on preburn calculation (0.2 seconds), which caused the crossover of the two curves at burn termination.

Table 3-7: Orbital Elements (Selenographic, True of Date)

OD No.	Epoch (GMT) Day:Hr:Mn:Sc	Semi-major axis a(km)	Eccentricity e	Argument of Perilune ω (deg)	Long. of Asc. Node Ω (deg)	Inclination i (deg)	Time from Periapsis Tp (sec)
6000-5	342:20:37:30.796	2701.0	0.3408	---	---	---	---
6002-5	342:20:37:30.796	2701.64	0.340855	174.984	327.063	17.5959	−5119.39
6004-5	342:20:37:30.796	2701.62	0.340832	175.001	327.048	17.5941	−5119.41
6006-5	344:13:15:00	2701.39	0.337513	176.707	303.892	17.6575	2539.89
6008-5	346:01:15:00	2701.0	0.3357	---	---	---	6160.
6010-5	347:18:35:00	2701.6	0.33495	179.	260.	17.7	3786.5
6012-5	347:18:35:00	2701.49	0.335063	178.401	260.564	17.5802	3785.45
6014-5	349:02:15:00	2701.71	0.33546	180.	242.	17.6	4405.
6016-5	350:03:00:00	2701.6	0.33631	---	---	---	5315.
6017-5	351:03:45:00	2701.6	0.33729	---	---	---	6220.
6018-5	353:01:40:00	2701.54	0.338746	181.909	188.521	17.6060	−4878.66
6019-5	354:05:55:00	2701.55	0.339032	---	---	---	−3982.
6020-5	355:06:35:00	2701.6	0.33852	---	---	---	−3384.
6021-5	356:07:15:00	2701.7	0.33772	---	---	---	−2784.
6022-5	356:07:15:00	2701.7	0.33771	184.	145.	17.6	−2784.2
6023-5	357:00:50:00	2701.8	0.33703	---	---	---	−2482.
6024-5	357:00:50:00	2701.7	0.33702	184.	136.	17.7	−2482.
6025-5	361:12:00:00	2701.4	0.33561	184.	78.	17.3	5345.
6026-5	362:08:40:00	2701.1	0.33610	188.	63.	17.4	4154.
6027-5	363:13:00:00	2701.6	0.33782	---	---	---	5362.
6028-5	364:16:15:00	2702.	0.3400	---	---	---	2660.
6029-5	003:12:10:00	2701.89	0.342197	194.937	338.420	17.6977	5920.10
6030-5	004:18:55:00	2701.4	0.34078	196.	321.	17.7	3200.
6031-5	005:19:30:00	2701.4	0.33906	198.	307.	17.7	3491.
6032-5	006:20:00:00	2701.5	0.33719	199.	293.	17.7	3486.

Table 3-7 (Continued)

OD No.	Epoch (GMT) Day:Hr:Mn:Sc	Semi-major axis a(km)	Eccentricity e	Argument of Perilune ω (deg)	Long. of Asc. Node Ω (deg)	Inclination i (deg)	Time from Periapsis Tp (sec)
6033-5	008:21:10:00	2701.5	0.33408	203.	263.	17.7	4087.
6034-5	009:21:25:00	2701.8	0.33319	201.	252.	17.4	3193.
6035-5	010:16:35:00	2701.5	0.33302	201.	241.	17.3	−3400.
6036-5	012:02:15:00	2701.8	0.33334	---	---	---	4404.
6037-5	012:19:50:00	2701.78	0.333796	205.321	208.951	18.42	4704.58
6038-5	013:20:40:00	2701.8	0.33474	204.	197.	17.7	5904.
6039-5	014:21:25:00	2701.7	0.33575	205.	183.	17.6	−5801.
6040-5	017:02:35:00	2701.6	0.33660	206.	153.	17.5	−3419.
6043-5	030:23:20:00	2701.22	0.341440	217.910	324.496	17.6730	−2545.94
6045-5	070:10:35:00	2701.89	0.332706	255.496	144.105	17.5070	5333.20
6046-5	079:04:00:00	2701.63	0.331878	262.794	25.207	17.2879	3124.59
6047-5	087:11:40:00	2701.82	0.340492	272.101	270.082	17.2350	3636.53
6048-5	089:10:05:00	2701.95	0.338549	275.610	242.740	17.3899	−5712.96
6049-5	096:23:25:00	2701.88	0.329816	281.640	140.203	17.3472	4425.67
6050-5	103:14:25:00	2702.03	0.332982	286.855	50.304	17.0786	−2875.08
7000-5	104:09:15:00	2692.	0.3290	287.	40.	17.	1913.
7001-5	105:21:00:00	2692.29	0.328328	289.171	19.024	17.2334	5244.50
7002-5	110:12:00:00	2692.7	0.32798	292.	316.	17.	3701.
7003-5	119:22:40:00	2692.13	0.328290	305.012	185.451	17.3834	4755.17
7004-5	176:02:00:00	2692.00	0.331754	354.286	141.008	16.9976	3446.67
7005-5	177:05:30:00	2692.73	0.330333	355.937	124.712	16.6515	2161.72
8000-5	178:07:05:00	2715.2	0.31811	357.	110.	16.5	−6098.
8001-5	180:14:50:00	2715.99	0.317854	358.321	78.103	16.3929	4153.28
8002-5	205:04:50:00	2715.53	0.323986	18.494	103.848	16.1341	−5075.13
8003-5	272:14:45:00	2715.31	0.334655	67.708	266.840	15.5850	4466.20

47

Table 3-8: Orbit Determination Data Summary

OD	Station	Data Type	Start Time (GMT) Day:Hr:Mn	End Time (GMT) Day:Hr:Mn	Number of Points	Standard Deviation
6000-5	41	C3	342:20:38	342:21:53	70	.0575
	12	RU	342:20:57	342:21:54	21	9.23
	12	CC3	342:20:38	342:21:53	71	.0598
6002-5	12	CC3	342:20:38	342:21:40	57	.0734
	41	C3	342:20:38	343:06:11	91	.0982
	41	CC3	342:22:33	343:04:40	280	.0876
	61	CC3	343:05:38	343:11:16	236	.0862
6004-5	12	CC3	342:20:38	343:14:01	123	.103
	41	C3	342:20:38	343:06:11	91	.131
	41	CC3	342:22:33	343:04:40	280	.104
	61	CC3	343:05:38	343:11:40	257	.0842
	61	C3	343:12:52	343:14:01	61	.0339
6006-5	12	CC3	344:13:23	344:22:27	400	.0386
	61	C3	344:13:32	344:14:51	66	.0210
	41	C3	344:20:16	344:22:29	121	.0425
6008-5	41	CC3	346:01:18	346:06:10	198	.127
6010-5	12	CC3	347:18:38	348:00:10	233	.168
6012-5	12	CC3	347:18:38	348:00:10	233	.0511
	41	CC3	348:05:11	348:10:37	177	.0670
6014-5	41	RU	349:02:23	349:08:24	69	248.
	41	CC3	349:02:21	349:08:23	208	.761
6016-5	41	CC3	350:03:03	350:09:01	190	.601
6017-5	41	CC3	351:03:47	351:09:42	179	.411

Table 3-8 (Continued)

OD	Station	Data Type	Start Time (GMT) Day:Hr:Mn	End Time (GMT) Day:Hr:Mn	Number of Points	Standard Deviation
6018-5	12	CC3	353:01:40	353:04:01	101	.0248
	12	C3	353:05:13	353:06:08	49	.0699
	41	C3	353:02:32	353:04:01	44	.0529
	41	CC3	353:05:12	353:19:38	153	.0437
6019-5	41	CC3	354:05:57	354:11:47	138	.896
6020-5	41	CC3	355:06:38	355:12:33	197	.231
6021-5	41	CC3	356:07:19	356:13:17	136	.720
6022-5	41	CC3	356:07:19	356:13:17	192	.929
6023-5	12	CC3	357:00:57	357:06:54	210	1.20
6024-5	12	CC3	357:00:57	357:06:54	292	1.33
6025-5	41	CC3	361:12:04	361:19:19	289	.867
6026-5	12	CC3	362:08:40	362:13:46	248	.610
6027-5	11	CC3	363:13:00	363:14:23	83	1.14
	41	C3	363:13:02	363:14:23	81	1.61
	41	CC3	363:15:20	363:20:26	249	1.52
6028-5	41	CC3	364:16:15	364:21:59	295	.950
6029-5	12	CC3	003:12:10	003:17:09	235	.0625
	12	C3	003:17:55	003:19:33	98	.0958
	41	C3	003:15:02	003:17:06	116	.132
	41	CC3	003:17:54	003:20:39	151	.0744
6030-5	41	CC3	004:18:55	005:00:49	229	.545
6031-5	41	CC3	005:19:30	006:01:22	289	.273
6032-5	41	CC3	006:20:00	007:01:55	296	.156
6033-5	41	CC3	008:21:13	009:03:59	262	.352

Table 3-8 (Continued)

OD	Station	Data Type	Start Time (GMT) Day:Hr:Mn	End Time (GMT) Day:Hr:Mn	Number of Points	Standard Deviation
6034-5	41	CC3	009:21:28	010:03:37	305	.715
6035-5	12	CC3	010:16:37	011:00:17	333	1.44
6036-5	41	CC3	012:02:18	012:08:19	274	.856
6037-5	12	CC3	012:19:57	013:01:56	154	.0734
	41	C3	012:23:32	013:01:57	67	.131
	41	CC3	013:03:00	013:05:28	99	.0608
6038-5	12	CC3	013:20:40	014:02:35	290	.100
6039-5	12	CC3	014:21:25	015:03:16	260	.151
	41	C3	015:00:53	015:03:17	133	.146
6040-5	41	CC3	017:02:35	017:08:15	255	.894
6043-5	41	CC3	030:23:20	030:23:37	18	.411
	41	C3	031:00:27	031:01:15	27	.617
	62	C3	030:23:20	030:23:43	22	.669
	62	CC3	031:00:26	031:05:59	144	.653
6045-5	62	CC3	070:10:38	070:16:41	276	.215
	12	C3	070:15:36	070:16:41	64	.339
	12	CC3	070:17:45	070:20:09	144	.216
6046-5	12	CC3	079:04:00	079:05:25	82	.0539
	12	C3	079:07:35	079:08:23	35	.0680
	41	CC3	079:06:23	079:12:28	239	.171
6047-5	12	CC3	087:11:40	087:13:51	127	.111
	12	C3	087:14:33	087:14:57	25	.228
	41	C3	087:12:59	087:13:51	44	.237
	41	CC3	087:14:31	087:19:13	234	.211

Table 3-8 (Continued)

OD	Station	Data Type	Start Time (GMT) Day:Hr:Mn	End Time (GMT) Day:Hr:Mn	Number of Points	Standard Deviation
6048-5	12	CC3	089:10:06	089:14:58	249	.177
	12	C3	089:15:41	089:16:08	28	.134
	41	C3	089:13:39	089:15:01	78	.206
	41	CC3	089:15:40	089:18:26	150	.135
6049-5	41	CC3	096:23:26	097:05:32	278	.207
	41	C3	097:06:30	097:07:08	39	.132
	62	CC3	097:06:27	097:09:03	141	.225
6050-5	62	CC3	103:14:25	103:16:47	123	.131
	62	C3	103:17:54	103:20:19	141	.144
	12	CC3	103:17:54	103:23:51	292	.155
7000-5	41	CC3	104:09:15	104:10:24	69	.552
	62	C3	104:09:15	104:10:24	65	.332
	62	CC3	104:11:43	104:13:56	127	.389
7001-5	12	CC3	105:21:00	106:06:24	313	.209
	41	C3	106:03:44	106:06:23	90	.244
	41	CC3	106:06:27	106:08:03	96	.142
7002-5	41	CC3	110:12:00	110:16:57	219	.117
	62	C3	110:14:33	110:15:09	25	.194
	62	CC3	110:18:02	110:20:21	117	.0911
7003-5	41	CC3	119:22:40	120:01:39	127	.0861
	62	CC3	120:01:46	120:09:49	363	.0914
7004-5	62	CC3	176:02:06	176:05:43	128	.138
	62	C3	176:06:13	176:07:28	71	.0434
	12	CC3	176:06:13	176:14:53	413	.123

Table 3-8 (Continued)

OD	Station	Data Type	Start Time (GMT) Day:Hr:Mn	End Time (GMT) Day:Hr:Mn	Number of Points	Standard Deviation
7005-5	62	CC3	177:05:37	177:07:58	103	.0140
	12	C3	177:07:34	177:07:58	23	.0160
	12	CC3	177:09:12	177:11:39	155	.0229
	41	CC3	177:13:41	177:14:58	70	.0256
8000-5	62	CC3	178:07:05	178:08:48	66	.0482
	12	C3	178:07:05	178:08:48	76	.0400
	12	CC3	178:09:37	178:14:12	243	.0441
8001-5	12	CC3	180:14:55	180:17:23	112	.0362
	12	C3	180:18:26	180:19:37	68	.0413
	41	C3	180:14:53	180:17:14	106	.0421
	41	CC3	180:18:25	181:00:24	230	.0359
8002-5	62	CC3	205:04:55	205:05:58	60	.0303
	62	C3	205:07:03	205:07:31	22	.0239
	12	C3	205:04:55	205:06:00	56	.0353
	12	CC3	205:06:58	205:13:04	238	.0247
8003-5	62	CC3	272:14:47	272:15:13	27	.0098
	12	C3	272:14:48	272:22:04	150	.0936
	12	CC3	272:16:08	272:18:43	149	.0951
	41	CC3	272:19:43	273:01:43	183	.0897
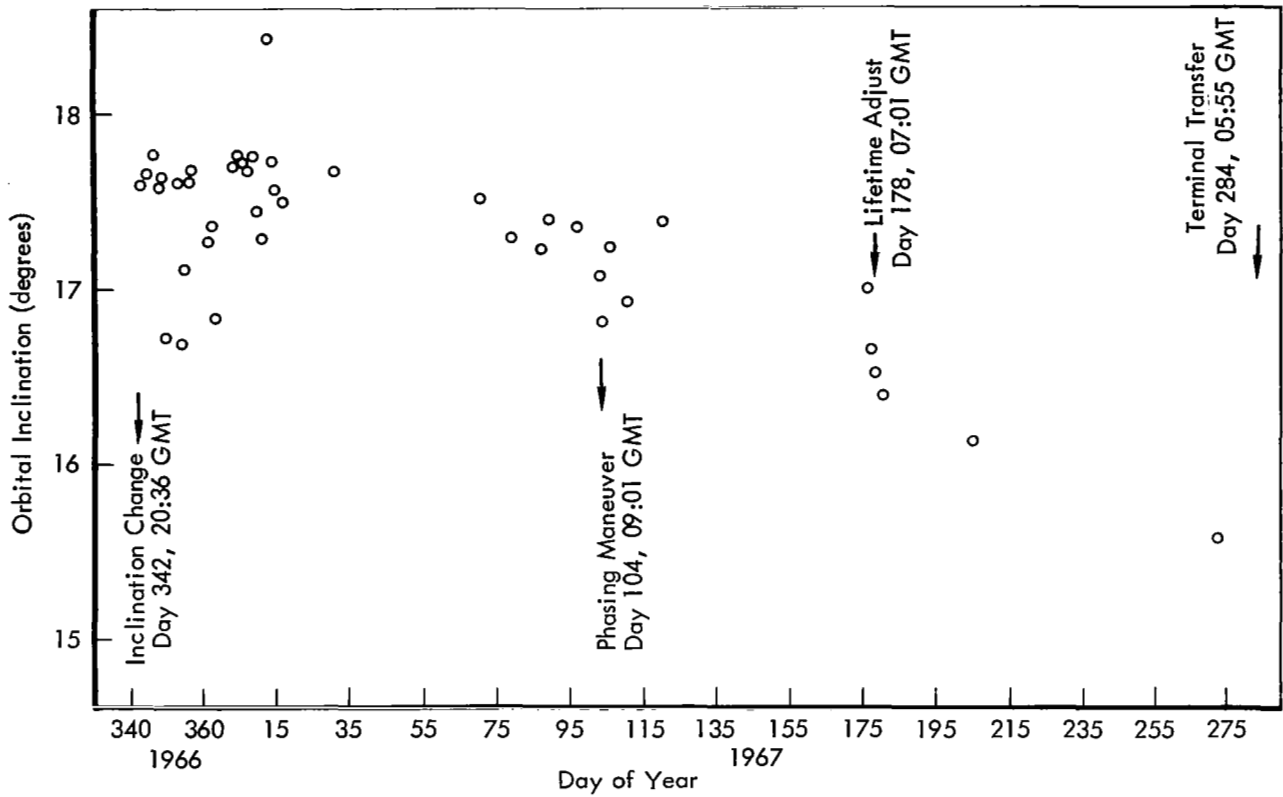
Figure 3-1: Orbit Inclination History
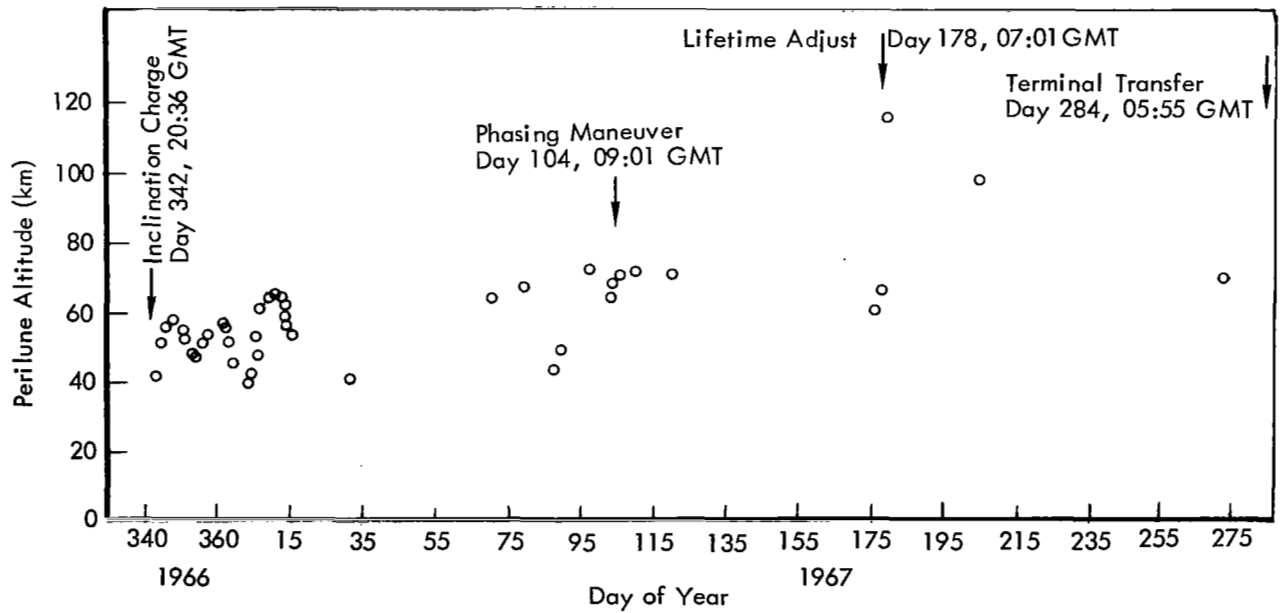
Figure 3-2: Orbit Perilune Altitude History

53
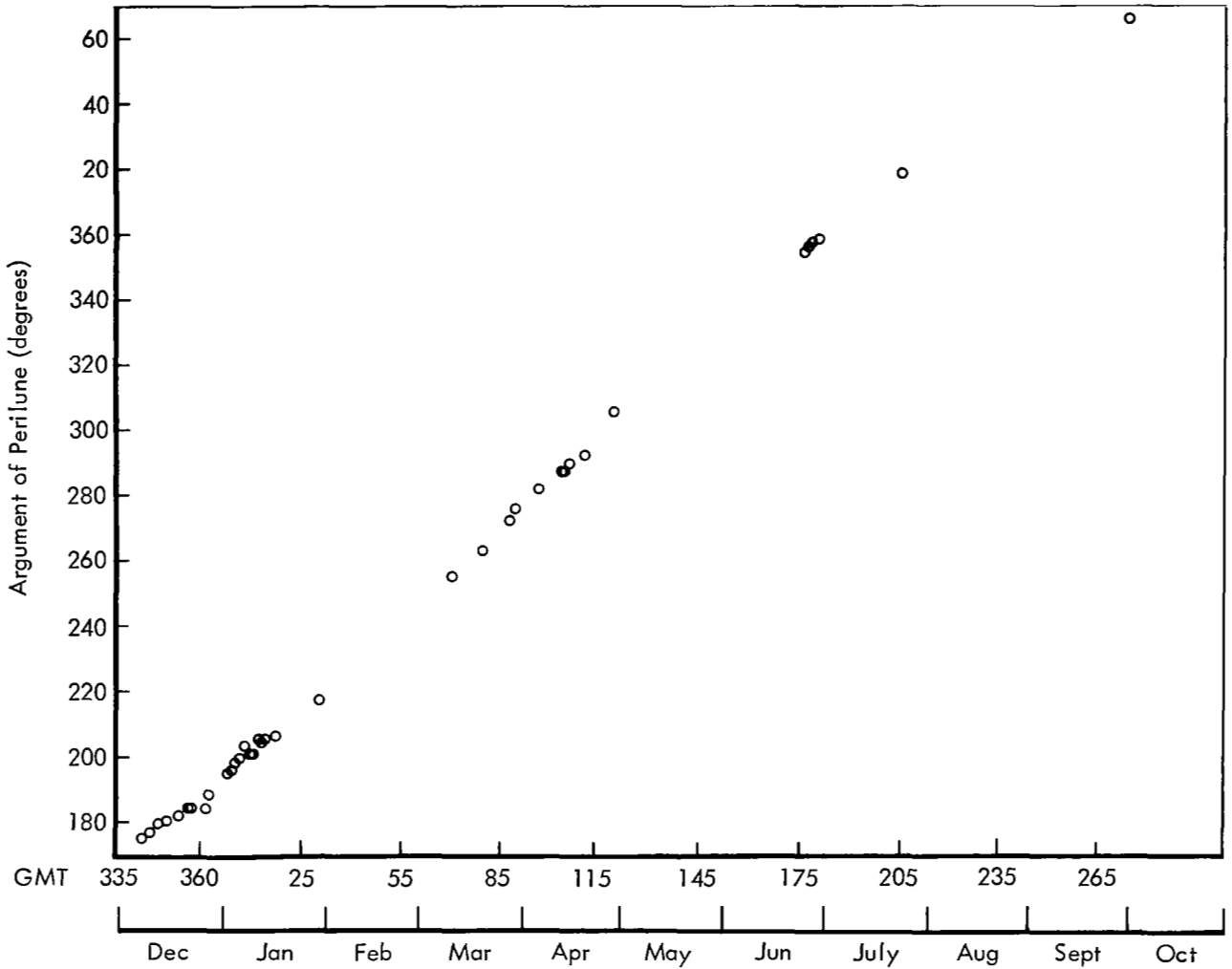
Figure 3-3: Argument of Perilune History

The slight bias in the preburn predicted and actual Doppler data (1.8 Hz) is caused by the epoch forwarding of the OD state vector (OD 7005-5) to the burn time, a period of 26 hours.

A postmaneuver orbit determination (OD 8000-5) was used to evaluate the maneuver execution. Table 3-10 contains a comparison of orbital elements between the preburn prediction and the postburn OD. All indications are that the maneuver was performed as commanded.

3.2.3.4 Terminal Transfer

It was desired to impact Lunar Orbiter II in the Apollo landing zone to provide useful tracking data of a lunar nearside impact, and possibly to allow examination of the crash site

by an Apollo astronaut at a later date. However, lunar impact was possible only by means of a velocity maneuver at or near apolune. The dual requirement of an impact in the Apollo zone and a velocity maneuver at apolune was only possible when perilune occurred over the lunar nearside. This condition did not exist on Day 284, the day selected for the terminal transfer; thus, a nearside impact was not possible. Consideration was given to delaying the terminal transfer until after Day 291, at which time an Apollo-zone impact could have been accomplished, but this option was not exercised because calculations indicated that nitrogen gas for attitude control would have been marginal by that time.

54

Table 3-9: Maneuver Design

Requirements	Inclination Change	Phasing for Eclipse	Lifetime Adjustment	Terminal Transfer
Δ V m/sec	99.9	5.486	7.98	41* 10**
Attitude (deg)				
Roll (sunline)	+17.00	+89.94	+10.82	0
Yaw	−72.5	0	0	0
Pitch	0	+88.30	−74.69	180
Ignition time (GMT)	342:20:36:28.7	104:09:01:15.3	178:07:00:45.33	284:05:55:00
True anomaly (deg)	194.8	60.0	180.0	−178.0
OD used	5090-5	6050-5	7005-5	8003-5
Spacecraft constants				
Thrust (lb)	100.1	104.0	103.5	102.3* 18**
Initial weight (lb)	612.8	587.5	583.3	582.1 573.3
Weight flow rate (lb/sec)	0.363	0.377	0.375	0.3706 0.11
Average acceleration (m/sec^2)	1.63	1.74	1.736	1.736 0.305
Burn duration (sec)	61.3	3.2	4.64	23.7 30

Orbit Elements	Before	After	Before	After	Before	After	Before	After
a (km)	2,689.31	2,701.25	2,702.01	2,692.74	2,692.11	2,715.01	2,715.42	2,585.55
e	0.338876	0.340361	0.332715	0.328954	0.329451	0.318238	0.344359	0.412054
ω (deg)	183.25	175.23	287.51	287.74	356.76	356.77	78.12	76.57
Ω (deg)	321.25	326.07	39.76	39.76	109.96	109.96	107.97	109.09
i (deg)	11.91	17.50	17.062	17.062	16.568	16.567	15.11	15.17
T (min)	208.58	209.97	210.06	208.98	208.91	211.58	211.63	196.63
h_a (km)	1,862.57	1,882.56	1,862.91	1,840.44	1,840.94	1,840.93	1,912.41	1,912.84
h_p (km)	39.88	43.76	64.919	68.863	67.10	112.90	42.25	−217.93

*   First segment
**   Second segment

Orbit geometry is shown in Figure 3-9. A sunline burn was chosen to eliminate the need for a roll reference. Tracking data for approximately half an orbit were obtained after the maneuver.

Maneuver design was accomplished using the orbit determination results of OD 8003-5, presented in Table 3-7. The solved-for state vector was mapped forward to the maneuver time using the LRC 11/11 lunar harmonics. The burn was simulated with two segments, the first being a normal burn and the second simulating fuel expulsion after depletion of the oxidizer. Maneuver design details may be seen in Table 3-9.

During the maneuver the spacecraft was tracked by DSS-12 and -41. Doppler monitoring was accomplished using DSS-41. Predicted and actual two-way Doppler are plotted in Figure 3-10, with a Doppler shift of 192 Hz observed during the burn. A comparison of the predicted and actual Doppler indicates that a significantly greater amount of ΔV was available in the spacecraft than was considered in the maneuver design.

The initial bias in the preburn predicted and
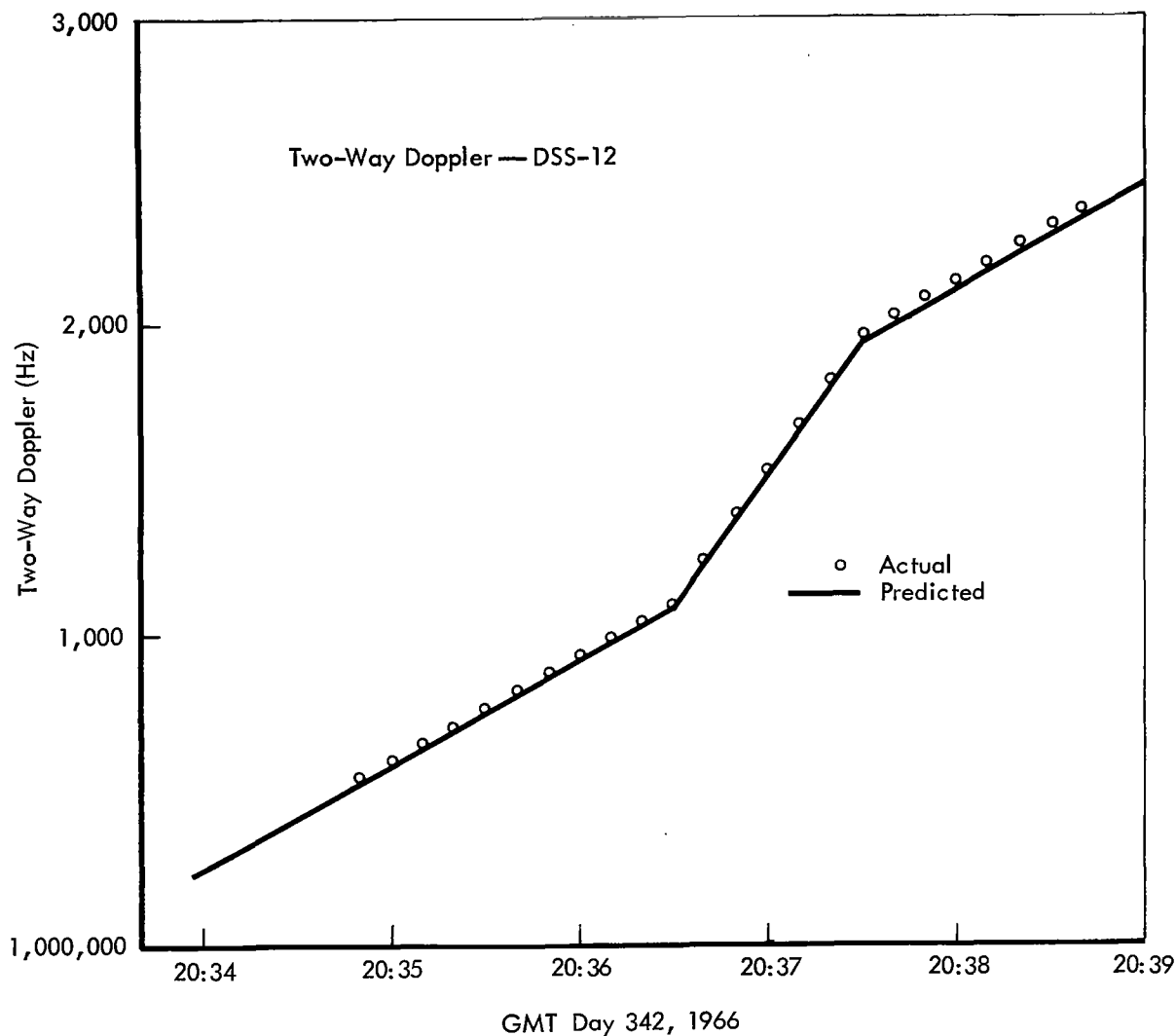
Figure 3-4: Inclination Change Maneuver

actual Doppler data (252 Hz) is caused by the epoch forwarding of the OD state vector (OD 8003-5) to the burn time, a period of 11 days, 15 hours.

From an investigation of the actual Doppler plot in Figure 3-10, it was possible to compute the burn duration and velocity change. The Doppler shift of 192 Hz corresponds to a velocity change of approximately 70 meters per second. A burn time of 36.0 seconds at full thrust is indicated, followed by 17.5 seconds at a greatly reduced thrust level. The change in slope of the Doppler data plot after oxidizer runout reflects this reduction in thrust level.

A postburn analysis of the tracking data prior to impact was accomplished using Doppler data from Stations 12 and 41. Three separate determinations of impact point were completed, using a spherical Moon model, and lunar models LRC 11/11 and LRC 7/28 B. The mean values resulting from these determinations are listed below.

	Preburn Predicted Values	Postburn Mean Values
Impact time	284:07:20:15.1	284:07:12:54
Longitude	134.64°E	119.13°E
Latitude	6.91°N	2.96°N

56

Table 3-10: Comparison of Predicted Versus Actual Postmaneuver Orbital Elements

Orbit Elements	Inclination Change		Phasing for Eclipse		Lifetime Adjustment		Terminal Transfer	
	Predicted	Actual	Predicted	Actual	Predicted	Actual	Predicted	Actual
OD used	5090-5	6002-5	6050-5	7005-5	7005-5	8000-5	8003-5	
Semi-major axis -a (km)	2,701.25	2,701.64	2,692.74	2,692.42	2,715.01	2,715.24	2,585.55	
Eccentricity-e	0.340361	0.340855	0.328954	0.329058	0.318238	0.318144	0.412054	
Argument of Perilune- ω (deg)	175.23	174.98	287.74	286.89	356.76	356.65	76.57	
Longitude of the ascending node- Ω (deg)	326.07	327.063	39.758	40.447	109.956	110.089	109.09	
Inclination-i (deg)	17.50	17.596	17.062	16.817	16.567	16.529	15.17	
Period-T (min)	209.97	210.01	208.98	208.94	211.58	211.61	196.63	
Apolune Altitude-h_a (km)	1,882.56	1,884.42	1,840.44	1,840.30	1,840.93	1,840.91	1,912.84	
Perilune Altitude-h_p (km)	43.76	42.68	68.86	68.37	112.90	113.39	−217.93	
Impact Data								
Time of impact (GMT)							284:07:20:15.1	(Mean values) 284:07:12:54
Longitude (deg)							134.64°E	119.13°E
Latitude (deg)							6.91°N	2.96°N
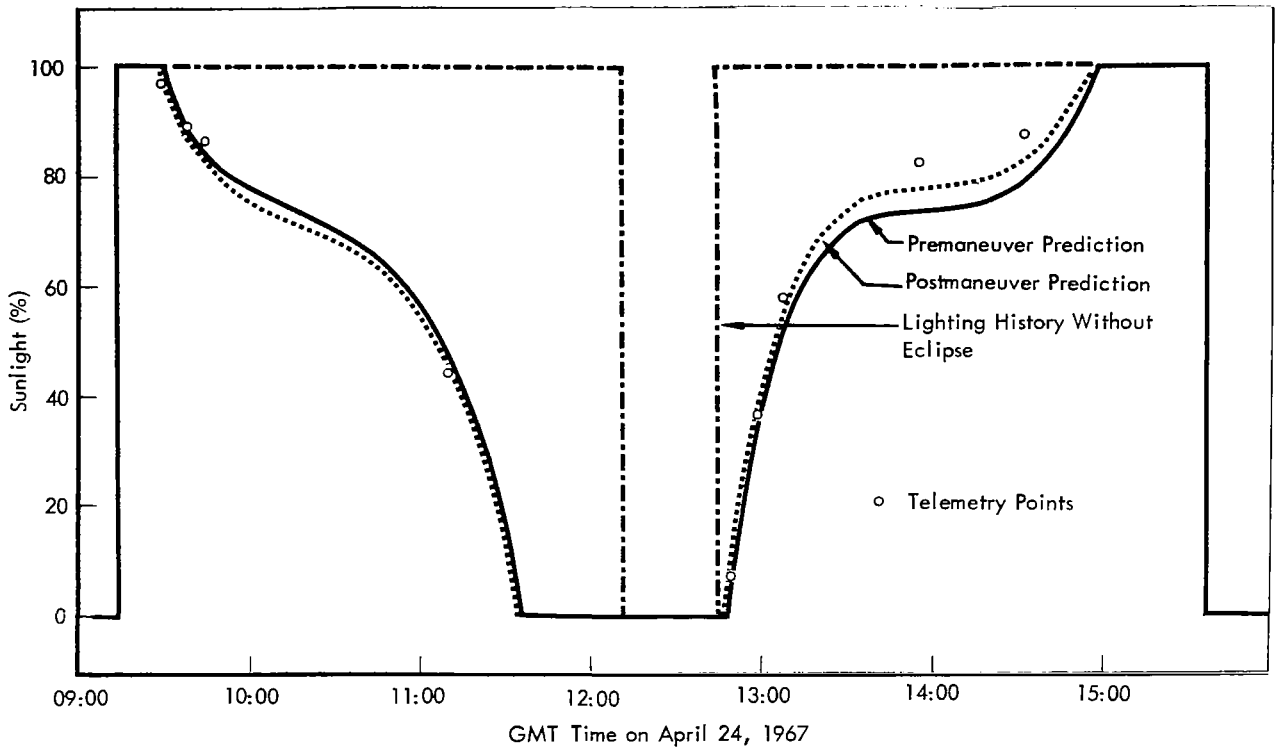
Figure 3-5: Lighting Characteristics Related to the April 24, 1967 Lunar Eclipse
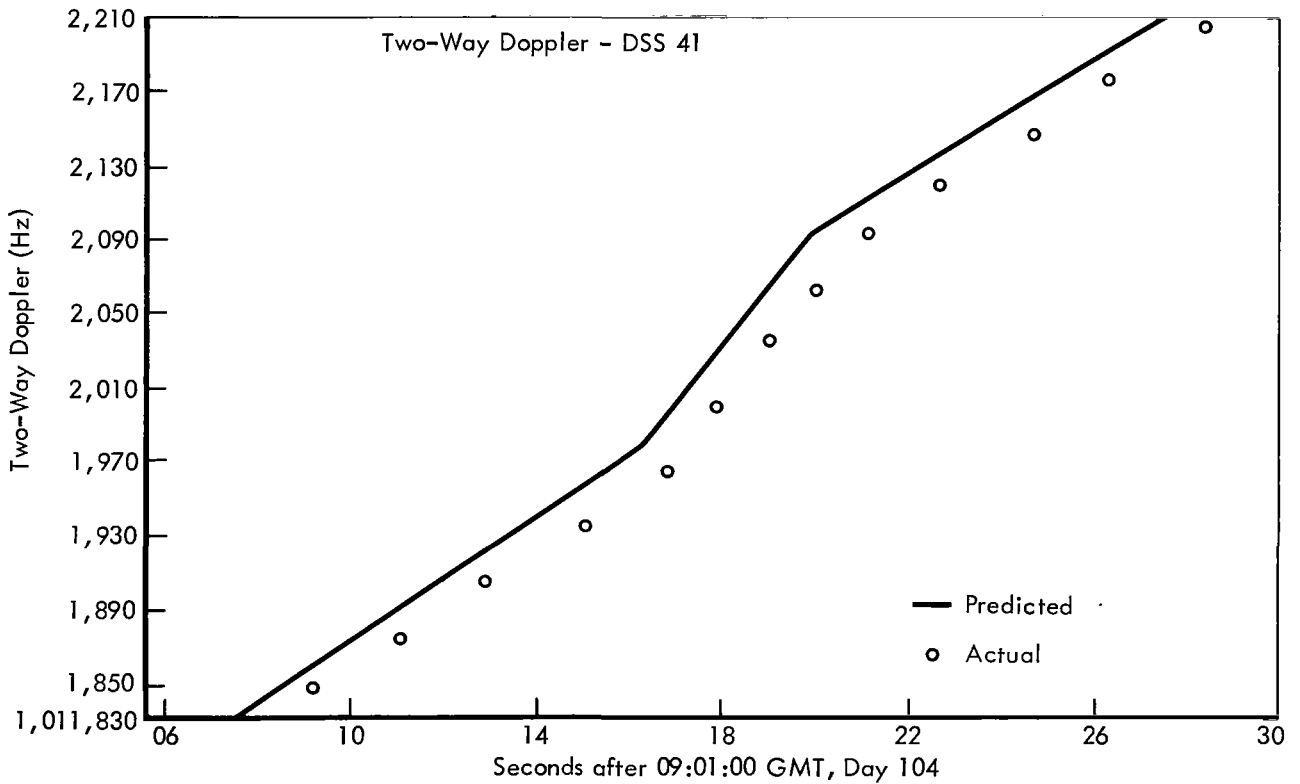
Figure 3-6: Phasing Maneuver

58

The great difference between the preburn predicted impact point and the postburn impact point (calculated utilizing tracking data prior to impact) was primarily due to the significantly greater amount of ΔV imparted to the spacecraft as well as the relatively long 11-day epoch forwarding of the state vector.

Table 3-11: Postmaneuver Orbit Determination Data

OD Number	OD Data Arc Length	OD Epoch Time Before Eclipse*	Orbital Period (sec)	Time of Apoapsis Passage (GMT)	Time in Total Darkness (min)	Time Below 30% Sunlight (min)	Time of Entering Umbra (GMT)	Time of Exiting Umbra (GMT)
Maneuver design			12538.9	Day 114 10:44:00	72	95	Day 114 11:36	Day 114 12:48
7000-5	4:41	10:02:52	12536.7	10:45:22	70	95	11:37	12:47
7001-5	11:03	8:15:07	12535.7	10:44:31	70	95	11:36	12:46
7002-5	8:21	4:00:07	12538.4	10:45:02	69	95	11:38	12:47

*Referred to center of eclipse Day 114, 12:07 GMT
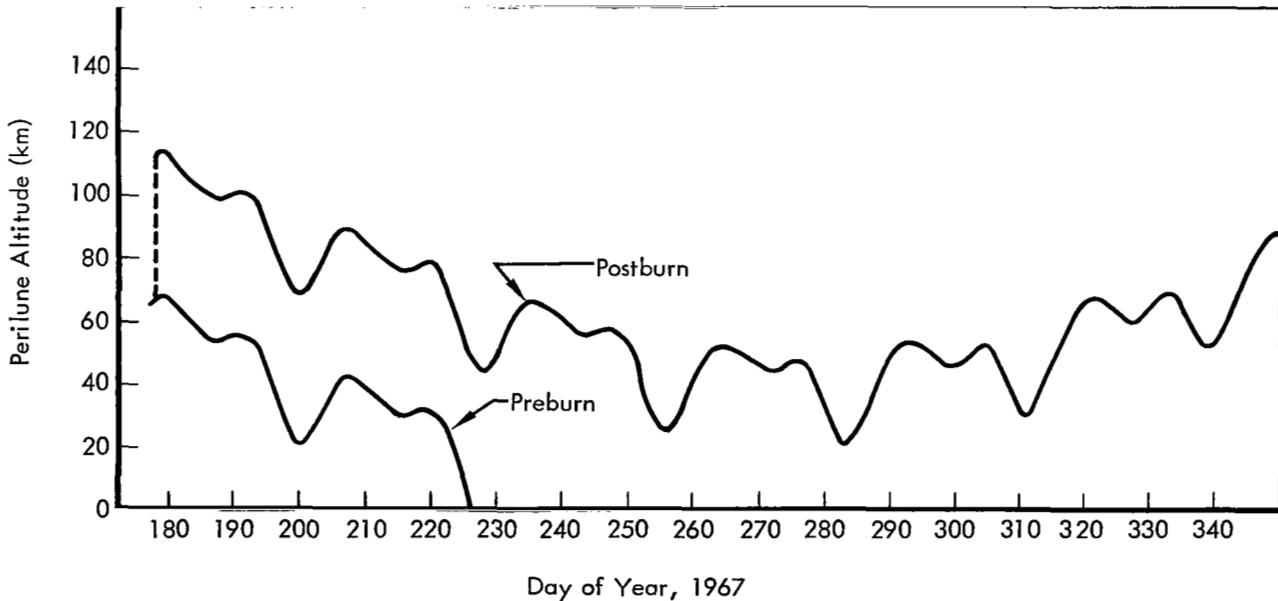
Figure 3-7: Lifetime Adjustment Maneuver — Predicted Perilune Altitudes

59
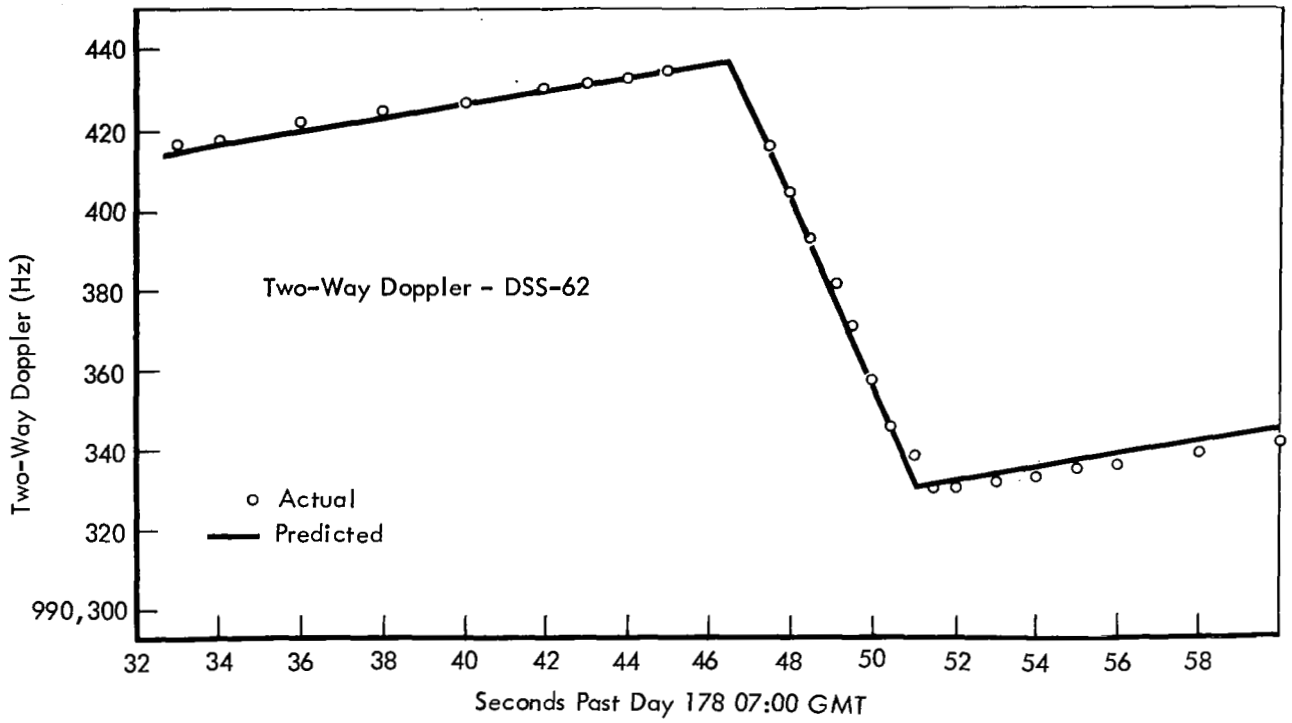
Figure 3-8: Orbital Lifetime Perilune Adjustment Maneuver
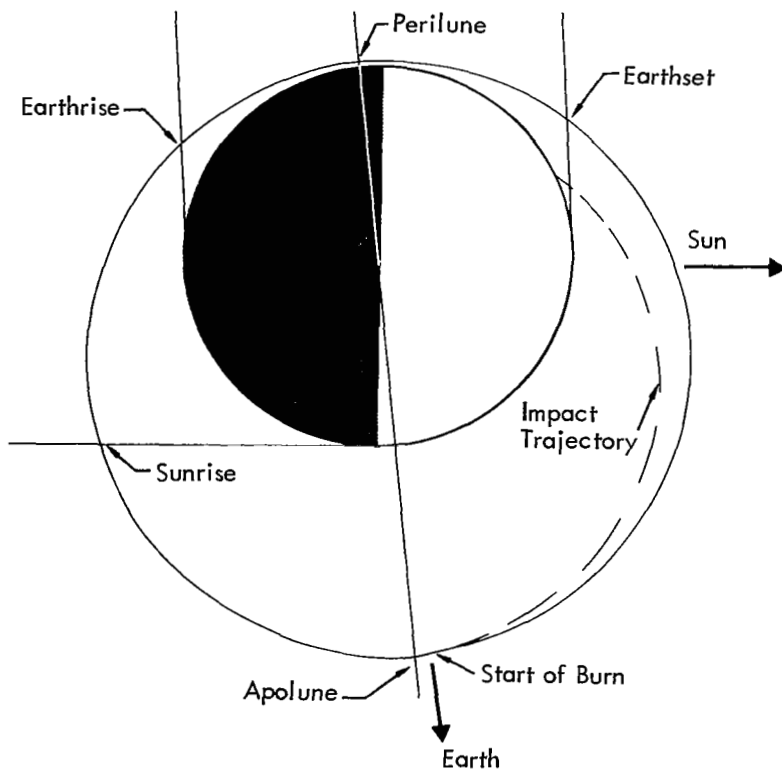
Figure 3-9: Orbit Geometry for Terminal Transfer Maneuver
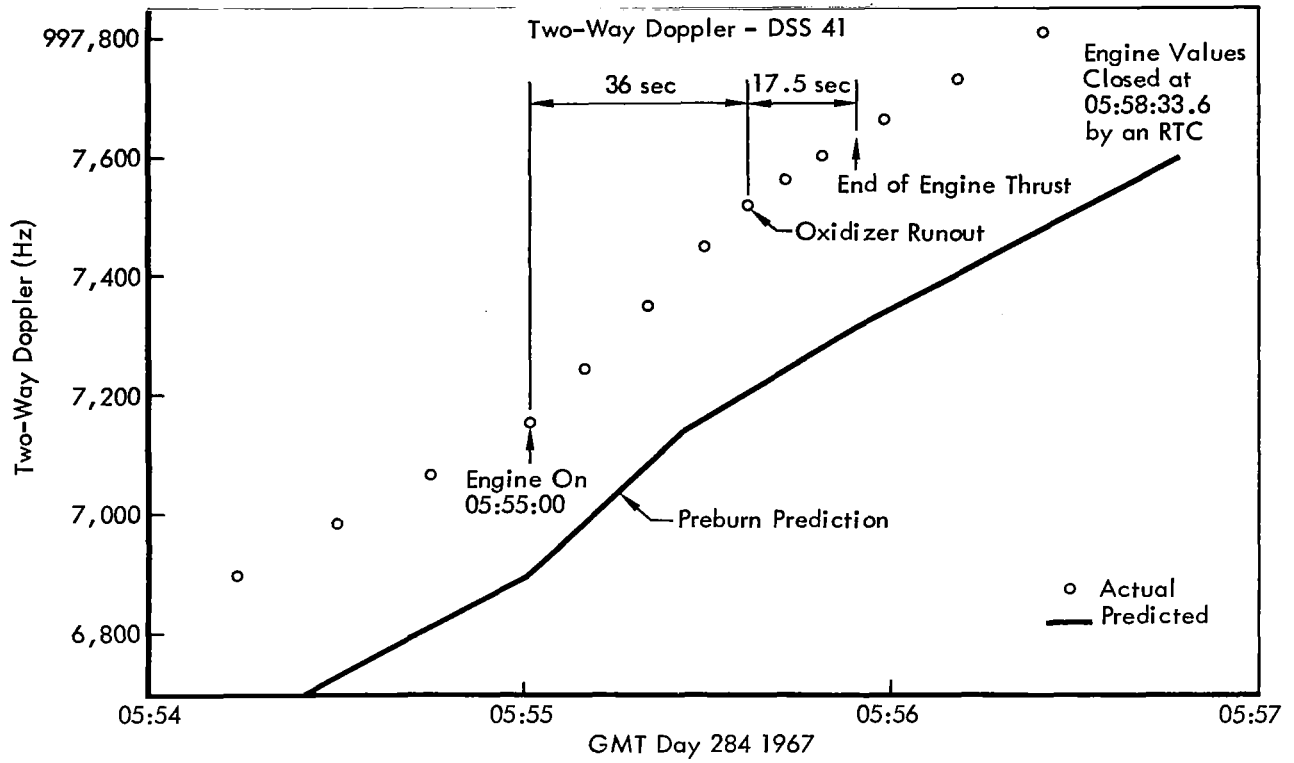
Figure 3-10: Terminal Transfer Maneuver

4.0 Flight Data

4.1 ENVIRONMENTAL DATA
A prime objective of the extended mission was to collect data in flight about the lunar environment. The spacecraft telemetry was monitored during each tracking period to determine if there had been any increase in radiation flux or micrometeoroid activity. Frequently, the increases were not recorded during a tracking pass; therefore, the exact location or time of the activity is not known.

4.1.1 Radiation
Table 4-1 shows radiation data collected during the extended mission. Scintillation counter DF04, located near the film cassette, had recorded 1.75 rads and DF05, located near the film looper, had recorded 1.0 rad at the beginning of the extended mission. Figure 4-1 shows the trend of the increase in radiation.

4.1.2 Micrometeoroid Hits
The spacecraft sustained a total of ten micrometeoroid hits, seven of which occurred during the extended-mission phase. Again, only the periods between which the hits were recorded can be reported. A summary of the hits, as well as the approximate orbit parameters and type of flight plan in use at the time of each hit, may be seen in Table 4-2. At the time of each hit, the spacecraft's roll position was not known since it was not being monitored, the yaw position was approximately 0 degrees, and the pitch position was generally between approximately 45 degrees and the appropriate pitch-off angle of 55, 56, or 59 degrees. However, if the hit happened to occur shortly after the spacecraft acquired the Sun, the pitch angle would be approximately 0 degrees. After each pitch-off maneuver, the spacecraft would slowly drift back to an off-Sun angle of approximately 45 degrees.

4.2 SPECIAL EXPERIMENTS
The type of experiments and tests conducted with Lunar Orbiter II during the extended mission include the following:
- Experiments to obtain scientific data;
- Experiments to obtain special data;
- Experiments for developing operational procedures;
- Tests to obtain engineering data on spacecraft subsystems.

The three different types of experiments described above are discussed in this section. Tests for engineering data, as well as discussions on the performance of spacecraft subsystems during any particular test or experiment, are discussed in Section 5.

The V/H survey of the eastern and western limb to determine the lunar radius is an example of an experiment to obtain scientific data. Use of Lunar Orbiter II to aid in the checkout and calibration of the Mark II Doppler-ranging system at the Goldstone Mars Station (DSS-14) for the Mariner Venus 1967 project is typical of an experiment to obtain special data. For both the scientific data and special data experiments, data analysis is the responsibility of the requesting agency. Information in this section is limited to the purpose of the experiment and the type of data collected.

The third type of experiment listed is concerned mainly with the development of operational procedures to enable multiple-spacecraft operation.

4.2.1 V/H Survey - Eastern and Western Limb Experiment
The purpose of this experiment was to determine the lunar radius using the V/H sensor and to compare the data with that obtained during Earth-based operations. The experiment consisted of pointing the camera axis at the Moon and obtaining V/H sensor data at passage over the Moon's eastern and western limbs. Data for the eastern limb was obtained on Day 012 and for the western limb on Day 027.

The V/H sensor was commanded "on" approximately 2 minutes prior to passage over the eastern limb, and "off" approximately 4 minutes after passage to comply with photo subsystem constraints. The V/H sensor was commanded

Table 4-1: Radiation Data

Tracking Period Day GMT	Casette Radiation D F04 (Rad)	Looper Radiation D F05 (Rad)	Tracking Period Day GMT	Casette Radiation D F04 (Rad)	Looper Radiation D F05 (Rad)
342/343	1.75	1.0	030/031	13.25	41.5
344	----	----	032	13.50	44.0
346	1.75	1.0	032/033	13.75	45.5
347	1.75	1.0	037	14.5	53.0
348	2.0	1.0	040	14.5	53.5
349	2.0	1.0	042	14.75	54.0
350	2.0	1.0	042	14.75	54.0
351	2.0	1.0	042	14.75	54.0
353	2.0	1.0	044	14.75	54.0
354	2.0	1.0	045	14.75	54.5
355	2.0	1.5	048	14.75	54.5
356	2.0	1.5	050/051	15.0	54.5
357	2.25	1.5	051	15.0	54.5
361	2.25	1.5	051	15.0	54.5
362	2.25	1.5	052	15.0	54.5
363	2.25	1.5	053	15.0	54.5
364	2.25	1.5	055	15.0	54.5
003	2.5	1.5	056	15.0	54.5
004/005	2.5	1.5	058	15.0	54.5
005/006	2.5	1.5	062	15.25	55.0
006/007	2.5	1.5	065	15.25	55.0
007	2.5	2.0	065	15.25	55.0
008/009	2.5	2.0	067/068	15.5	55.0
009/010	2.75	2.0	068	15.5	55.0
010/011	2.75	2.0	069	15.5	55.0
012	2.75	2.0	070	15.5	55.0
012/013	2.75	2.0	070	15.5	55.0
013/014	2.75	2.0	073	15.5	55.0
014	----	----	075	----	----
014/015	2.75	2.0	078	15.75	56.5
017	2.75	2.0	079	16.0	56.5
020/024	----	----	081	16.0	56.5
026/027	3.0	2.5	081	16.0	56.5
027	----	----	083	17.0	56.5

Table 4-1 (Continued)

Tracking Period Day GMT	Casette Radiation DF04 (Rad)	Looper Radiation DF05 (Rad)	Tracking Period Day GMT	Casette Radiation DF04 (Rad)	Looper Radiation DF05 (Rad)
085	17.0	56.5	143	18.75	58.5
087	17.0	56.5	144	18.75	58.5
089	17.25	56.5	145	19.0	91.0
092	17.25	57.0	147	19.0	92.0
094	17.25	57.0	149	19.5	96.0
095	17.25	57.0	150	19.5	96.0
096/097	17.5	57.0	151	19.75	97.0
098	17.5	57.0	152	19.75	97.0
101	17.5	57.0	153	19.75	97.0
102	17.5	57.0	155	19.75	97.0
103	17.5	57.0	156	19.75	97.0
104	17.5	57.0	158	20.0	98.0
105/106	17.75	57.0	159	20.0	98.0
107	17.75	57.5	161	20.0	98.5
110	----	----	164	20.0	98.5
111	17.75	57.5	164	20.0	98.5
114	17.75	57.5	165	20.0	98.5
(9 Tracks)	Same	Same	166/167	20.25	98.5
116	18.0	57.5	169	20.25	99.0
119/120	18.0	58.0	171	20.25	99.0
126	18.25	58.0	173	20.5	99.0
127/128	18.25	58.0	176	20.5	99.0
128/129	18.25	58.0	177	20.5	99.5
129	18.25	58.0	178	20.5	99.5
130	18.25	58.0	180/181	20.5	99.5
132	18.25	58.5	186	20.75	99.5
133	18.5	58.5	188	20.75	100.0
134	18.5	58.5	192	21.0	100.0
135	18.5	58.5	196	21.0	100.0
137	18.5	58.5	198	21.0	100.5
138	----	----	202	21.25	100.5
139	18.75	58.5	205	21.25	100.5
141	18.75	58.5	209	21.5	101.0
142	18.75	58.5	209	21.5	101.0

Table 4-1 (Continued)

Tracking Period Day GMT	Casette Radiation D F04 (Rad)	Looper Radiation D F05 (Rad)	Tracking Period Day GMT	Casette Radiation D F04 (Rad)	Looper Radiation D F05 (Rad)
210	----	----	262	22.75	103.5
215	21.5	101.0	262	22.75	103.5
216	21.5	101.0	264	23.0	104.0
217	21.5	101.0	267	23.0	104.0
219	----	----	270	23.0	104.0
220	21.75	101.5	272/273	23.0	104.5
221	21.75	101.5	274	23.25	104.5
223	21.75	101.5	275	23.25	104.5
224	21.75	101.5	276	23.25	104.5
226	21.75	101.5	277	23.25	104.5
226	21.75	101.5	279	23.25	104.5
227	21.75	101.5	282	23.5	105.0
228	21.75	101.5	282	23.5	105.0
230	22.0	102.0	283	23.5	105.0
230	22.0	102.0	283	23.5	105.0
232	22.0	102.0	284	23.5	105.0
233	22.0	102.0			
234	22.0	102.0			
235	22.0	102.0			
236	22.0	102.0			
237	22.25	102.0			
239	22.25	102.5			
242	22.25	102.5			
243	22.25	102.5			
244	22.25	102.5			
248	22.5	103.0			
250	22.5	103.0			
253	22.5	103.0			
254	22.5	103.0			
255	22.75	103.0			
256	22.75	103.5			
258	22.75	103.5			
259	22.75	103.5			
261	22.75	103.5			
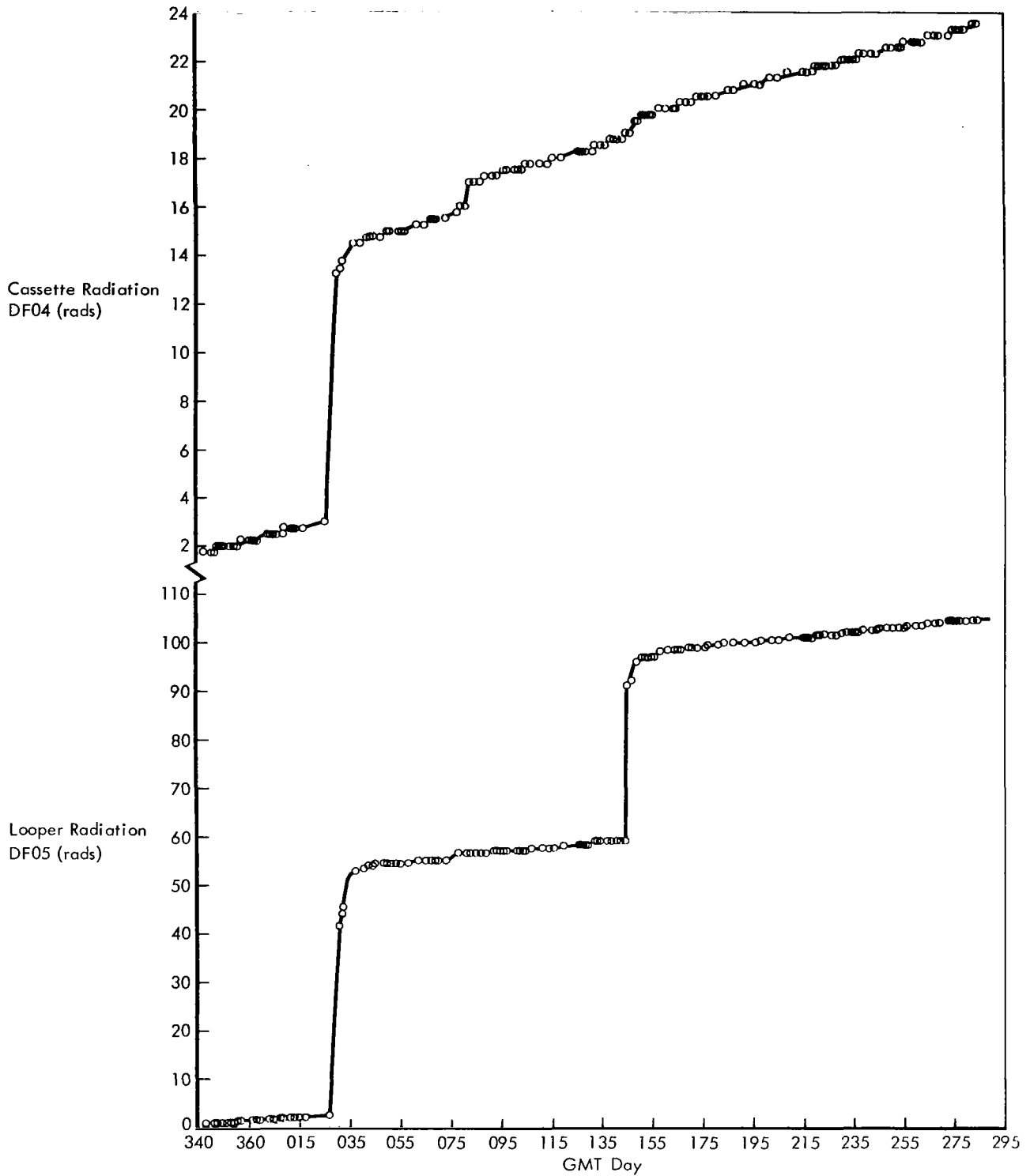
Figure 4-1: Radiation Dosage Measurement, Looper and Cassette

Table 4-2: Micrometeoroid Hit History

Micrometeoroid Detector Number	Hit Recorded Between GMT Times		Approximate Orbital Parameters at Times of Hit				Flight Plan*
	Day:Hr:Min.	Day:Hr: Min.	Perilune (km)	Apolune (km)	Inclination (deg)	Period (min)	
18	006:19:35	006:19:41	53	1,967	17.7	210	A
19	114:18:50	116:11:41	71	1,838	16.9	209	B
06	159:23:21	161:20:45	61	1,841	17.0	209	B
02	169:00:20	171:01:30	60	1,847	16.7	209	B
01	205:13:16	209:08:15	98	1,857	16.1	212	C
15	256:21:00	258:20:20	75	1,880	15.7	212	C
11	264:14:22	267:20:23	69	1,886	15.6	212	C

* Flight plan at time of hit:
  A - Acuire Sun and pitch +55 degrees each 15 orbits.
  B - Acquire Sun and pitch +56 degrees each 6 orbits.
  C - Acquire Sun and pitch +59 degrees each 6 orbits.

"on" approximately 2 minutes prior to passage over the western limb and "off" 11.2 minutes after passage. The V/H sensor temperature test was conducted concurrently with the western limb survey (see Section 5.3.9). The various parameters during the passage over the limbs are as follows:

Orbit 432 — Parameters:
- Time of passage over eastern limb = Day 012, 22:13:00 GMT
- All data apply to this point in time
- Total V/H "on" time = 6.0 minutes
- Single-frame advance 4.0 minutes after V/H "on"
- Longitude = 90 degrees
- Latitude = 15.6 degrees
- Altitude = 167.5 kilometers
- Altitude Rate - +0.293 km/sec
- True Anomaly = +38.1 degrees
- Time from periapsis = +654.8 seconds
- V/H Ratio = 0.0108 milliradians/sec
- Sun Angle = 68.7 degrees
- Sun Azimuth = 85.4 degrees

Orbit 530 — Parameters:
- Time of passage over western limb = Day 027, 01:43:21 GMT
- All data apply to this point in time
- Sun Angle = 76.5 degrees
- V/H Ratio = 11.45 milliradians/sec

- Altitude = 157.8 kilometers
- True Anomaly = 38.6 degrees
- Longitude = 90 degrees
- Latitude = −16.65 degrees
- V/H "on" time = 13.2 minutes

The V/H ratio for both the eastern and western limb survey agreed very closely with that predicted, indicating successful execution of the experiment (see Figures 4-2 and 4-3). Data obtained during this experiment were forwarded to the NASA experiment coordinator for distribution and analysis.

4.2.2 Ionosphere Effects Experiments

The purpose of this JPL experiment was to determine the effect of the Earth's ionosphere on the Doppler and ranging data obtained from the spacecraft. The experiment, when completed, will consist of a total of eight horizon-to-horizon passes of two-way Doppler and ranging data. The Lunar Orbiter II spacecraft was used for two of these passes as follows:

GMT Day	GMT
105/106	19:46-06:24
176	05:54-14:53

DSS-12 collected ranging data throughout each of these passes. Data were forwarded to JPL for analysis and reporting.
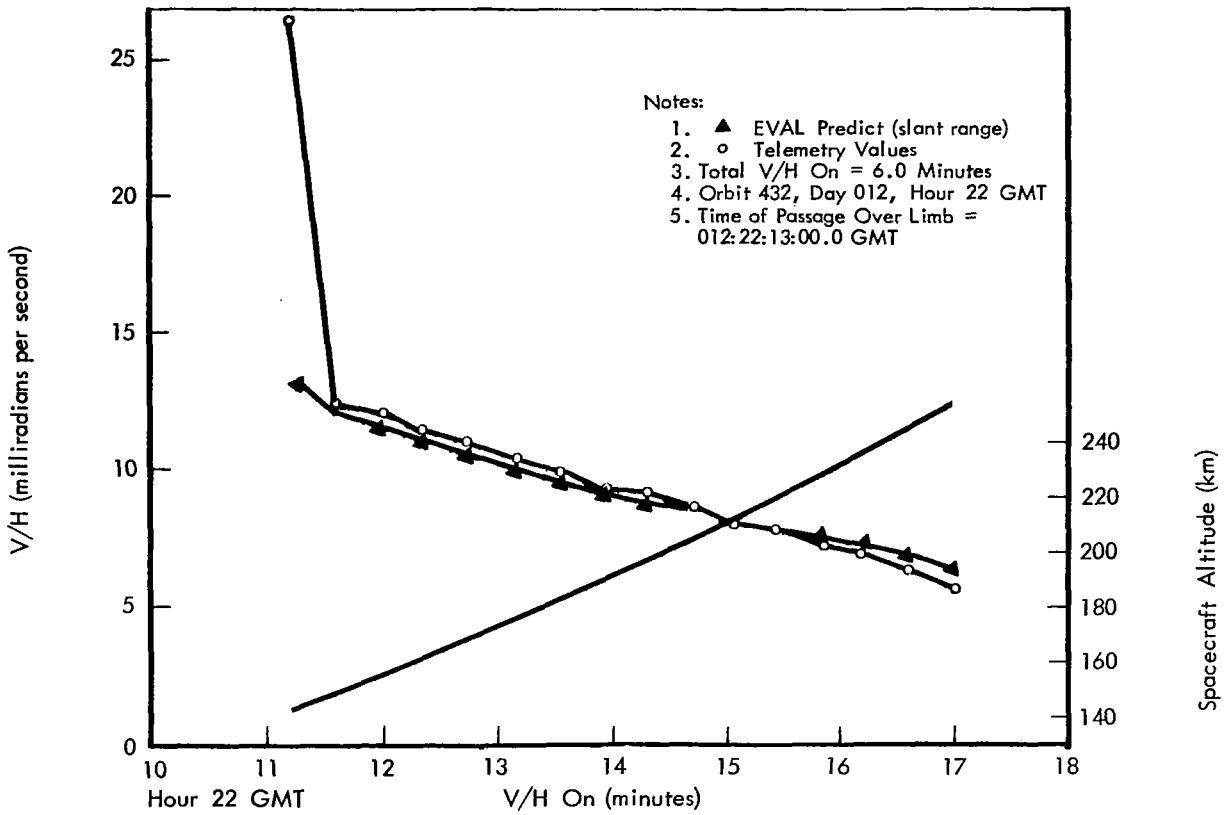
Figure 4-2: V/H Ratio During Flight over Eastern Limb

Notes:
1. ▲ EVAL Predict (slant range)
2. o Telemetry Values
3. Total V/H On = 6.0 Minutes
4. Orbit 432, Day 012, Hour 22 GMT
5. Time of Passage Over Limb = 012:22:13:00.0 GMT
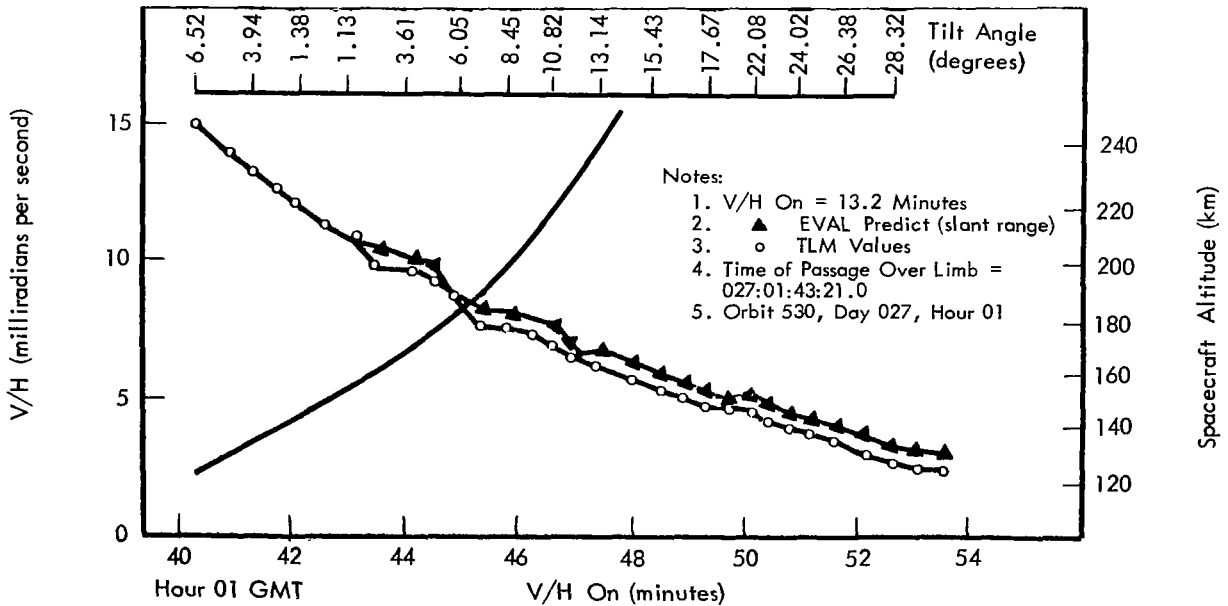
Figure 4-3: V/H Ratio During Flight over Western Limb

Notes:
1. V/H On = 13.2 Minutes
2. ▲ EVAL Predict (slant range)
3. o TLM Values
4. Time of Passage Over Limb = 027:01:43:21.0
5. Orbit 530, Day 027, Hour 01

4.2.3 Doppler-Ranging Calibration Experiment

The Lunar Orbiter II spacecraft was used to aid in checkout and calibration of the Mark II ranging system at the Goldstone Mars Station (DSS-14) for the Mariner Venus 1967 project. The test, on Day 166/167 between 21:48 and 02:30 GMT, was conducted in accordance with JPL Memorandum 312.1-187-JPB, May 18, 1967, and consisted of maintaining the spacecraft in two-way lock while ranging data were acquired. Telemetry data from the spacecraft were received by DSS-14 and transmitted to DSS-12 MDE via the Goldstone microwave system. Data were forwarded to JPL for analysis and reporting.

4.2.4 MSFN Apollo GOSS Navigation Qualification Support

The purpose of the exercise was to assist the Manned Space Flight Network (MSFN) in the qualification of their tracking systems for use during the Apollo mission. The MSFN activities for which the Lunar Orbiter II spacecraft was used included:

1) Actively tracking the spacecraft at lunar distances using the MSFN Unified S-Band (USB) tracking systems.
2) Transmitting tracking data to the Manned Spacecraft Center (MSC), Houston, Texas.
3) The generation of antenna patterns to determine the optimum focus position of the hyperbolic subreflectors.
4) Preliminary qualification of the basic Real-Time Computer Complex (RTCC) navigational concepts.

Table 4-3 is a summary of the tracking periods during which the Lunar Orbiter II spacecraft was used in support of Phase A of the MSFN/AGNQ program as defined in the Operational Interface Agreement and EPD 258 Volume II.

4.2.5 Multiple Spacecraft Operations Experiments

Tests were conducted prior to Mission III and between Photographic Missions III and IV to aid in the development of operations procedures for flying two or more spacecraft simultaneously. The tests conducted prior to Mission III were conducted on Days 025 and 030. They were divided into three categories; rf interference,

Table 4-3: MSFN/AGNQ Tracking Summary

Day	Total Tracking Time (GMT)	MSFN Three-Way Tracking (GMT)
356/357	07:17-06:59	07:25-06:59
006/007	19:35-01:57	19:41-01:56
010/011	16:15-00:19	16:30-00:19
020/021	22:03-04:09	22:16-04:09
089	09:47-20:00	11:00-20:00
105/106	19:02-08:05	19:47-08:05

blind acquisition, and high-transponder static-phase error (SPE) during command transmission, and are discussed below under 4.2.5.1. The tests conducted between Photographic Missions III and IV were conducted on Day 111, and are discussed in 4.2.5.2.

4.2.5.1 Experiments Conducted on Days 025 and 030

Rf Interference — These tests were conducted on Days 025 and 030. The test transponder at DSS-12 was used to simulate a second transponder. It was determined from the tests that:

1) Two transponders in Modulation Mode III and at equal signal strengths could be acquired on two receivers, and that telemetry-lock could be maintained as long as the frequency separation between the two carriers was other than 60 KHz, 30 KHz, and 0 Hz ± 100 Hz.
2) When the carrier frequency of a spacecraft in two-way lock and transmitting in Modulation Mode III was swept across the carrier frequency of the other spacecraft in Modulation Mode III, both receivers were apt to acquire both spacecraft, and telemetry interference resulted. This "stealing" occurred when the receivers had bandwidths of 152 Hz. The receivers tended to lock up on the strongest signal when the two spacecraft frequencies were close. When both receivers had a band width of 12 Hz, "stealing" did not occur because the receiver operators were

able to "walk-through" the point of interference. Interference could also be avoided by tuning the exciter to control the frequency of the spacecraft which was in two-way lock.

3) When carrier frequencies of two spacecraft in Modulation Mode III were separated by approximately 30 KHz, the first-order sideband of each spacecraft interfered with the carrier of the other spacecraft and significant bit errors resulted. The receiver was apt to drop lock on one spacecraft and acquire the sideband of the other. The receiver operator could anticipate this situation upon hearing heterodyning in his headphones and avoid it by tuning the exciter appropriately to avoid the 30 KHz separation.

4) When carrier frequencies of two spacecraft in Modulation Mode III were separated by 60 KHz, interference again developed and noisy telemetry could be seen. The bit synchronizer and decommutator did not drop lock and no bit errors were counted. Receivers maintained lock on the separate spacecraft. It is probable that second-order sidebands were interfering with the carriers. A beat was easily recognized by the receiver operator, and he could avoid a 60 KHz separation by appropriate tuning of the two-way-lock spacecraft.

5) When the carrier frequency of a spacecraft transmitting in Modulation Mode II and a received signal level of −98 dbm to −110 dbm was swept across the carrier frequency of a spacecraft transmitting in Modulation Mode III and a received signal level of −139 dbm, no interference of either video or Mode II telemetry was observed.

Blind Acquisition — The test plan called for the DSS to acquire the spacecraft one-way with the antenna pointed at the center of the Moon. The receiver was unable to acquire the spacecraft one-way since the spacecraft was at one side of the Moon and apparently outside the 0.3-degree beam width of the antenna. It was then decided to do an uplink search with the transmitter on at 2 kw, transmit a command, maintain the "enable" tone and then search for the spacecraft while maintaining the "enable" tone. The results were as follows: The antenna was pointed at the center of the Moon and the transmitter was turned on at 2 kw. An uplink search was conducted by tuning the exciter from +200 Hz to −200 Hz and back to center frequency at a rate of about 1 Hz per second. When the center frequency was reached, command was transmitted in the "emergency execute" mode so that extraneous receiver register updates during downlink acquisition would not remove the "enable" tone. The antenna then searched for the spacecraft until a downlink lock was obtained on the receiver. Telemetry then received from the spacecraft verified that the command that was transmitted had been correctly received.

It was concluded that "Moon Center" predicts could be used successfully to turn on the transmitter of rf silent spacecraft. This technique, however, could result in acquiring the spacecraft uplink at a higher-value SPE than previously accepted for transmitting commands. For this reason the following test was conducted.

High SPE — The spacecraft was acquired in two-way lock with transmitter power at 500 watts. Power was reduced to approximately 250 watts so that the spacecraft's received signal level indicated −93 dbm (Telemetry Measurement CE08). The exciter was then tuned at 150-Hz increments, and a command transmitted after each tuning increment. Maximum possible tuning dispersion was reached on both sides of the center frequency. Spacecraft SPE exceeded the indicated limits of −15.776 and +17.544 degrees maximum. Command verification was obtained at all SPE variations, with zero errors. It was then concluded that SPE variations beyond the limits specified above would not affect command transmissions.

From these tests it was concluded that an extended-mission spacecraft could be flown without interfering with the photo-mission spacecraft.

4.2.5.2 Experiments Conducted on Day 111 — These tests, summarized below, were conducted at a time when Lunar Orbiters II and III were both in lunar orbit.

Inadvertent Second-Spacecraft Acquisition — The purpose of this test was to verify that uplink on a Lunar Orbiter spacecraft would not be acquired when a DSS is tracking another Lunar Orbiter spacecraft two-way at track synthesizer frequency (TSF) plus 420 Hz (exciter VCO). DSS-41 acquired Lunar Orbiter II two-way prior to earthrise of Lunar Orbiter III and tuned the exciter VCO to TSF plus 420 Hz. DSS-62 acquired Lunar Orbiter III one-way at earthrise. The two stations tracked both spacecraft until Lunar Orbiter II occulted. DSS-62 did not observe any attempt of DSS-41 to acquire the Lunar Orbiter III uplink. It was concluded from this test that a Lunar Orbiter spacecraft can be flown at an offset frequency without acquiring the uplink on a second Lunar Orbiter if the TSF offset frequency is judiciously selected, based on the current orbital geometry. Based on this test, the following tests were performed to refine the procedures to be used when flying at an offset frequency.

Ranging at TSF Plus 420 Hz — DSS-12 successfully ranged for approximately 10 minutes.

Handover at An Offset Frequency and A Transmitter Power of 10 kw — DSS-12 successfully handed over to DSS-41 per standard procedures, except that both stations were tuned to the offset frequency.

Handover with Both Stations at An Offset Frequency and Using Different Transmitter Powers — The incoming station's (DSS-41) transmitter was set at 10 kw and the outgoing station's transmitter was set at 1 kw. The handover was at the offset frequency and was successful.

Handover at A Transmitter Power of 10 watts and An Offset Frequency — The stations' transmitters were set at 10 watts. The outgoing station lost uplink lock repeatedly while tuning to the offset transfer frequency and the handover was unsuccessful.

Determine If Uplink Lock on a Second Lunar Orbiter Spacecraft Can Be Broken by Decreasing the DSS Transmitter Power to 10 watts — DSS-12 simultaneously acquired the uplink on both Lunar Orbiters II and III while DSS-41 acquired Lunar Orbiter III three-way. The DSS-12 antenna was pointed to Lunar Orbiter II. DSS-12 decreased its transmitter power to 10 watts but did not drop the uplink in the second spacecraft.

5.0 Spacecraft Subsystem Performance

5.1 SUMMARY

Performance of each spacecraft subsystem during the Lunar Orbiter extended mission is summarized herein. At the time of the last communications with the spacecraft, 339 days after launch, all subsystems were operating normally, and the primary photo mission and all special tests in support of other missions were complete. Detailed descriptions of performance and operation of each subsystem are presented in Section 5.2. The tests performed during the extended mission are presented in Section 5.3.

5.2. SUBSYSTEM PERFORMANCE

5.2.1 Attitude Control Subsystem

The attitude control subsystem consists of an inertial reference unit, a control assembly unit, a star tracker unit, a switching unit, and a sun sensor unit. The inertial reference unit is a three-axis strap-down gyro system with an accelerometer for differential velocity derivation. The inertial reference outputs consist of angular rates and positions about each of the three orthogonal spacecraft axes and spacecraft velocity changes in line with the X axis of the spacecraft. The control assembly unit consists of a memory that can be programmed, a clock oscillator, appropriate logic, input-output circuitry, and a power supply. In addition, the closed-loop electronics are housed in, and are part of, the control assembly. The primary purpose of the control assembly is to command the spacecraft either from memory or in real time, and through the flight-control logic and closed-loop electronics to control the operation of the position thrusters and the engine pointing angle. The star tracker unit contains a photo multiplier tube for sensing Canopus and a bright-object sensor, and associated Sun shutter to protect the photo multiplier tube, input-output circuitry, and associated electronics. The purpose of this tracker is to furnish spatial roll axis reference. The sun sensors are silicon solar cells located on the spacecraft to provide a spatial yaw and pitch axis reference. The switching assembly contains the high-power switching circuitry and is controlled by the control assembly (refer to Figure 5-1 for a block diagram

of the subsystem). Functionally, the attitude control subsystem maintains control of the attitude of the spacecraft with respect to inertial and celestial references. Control with respect to celestial references (celestial hold) is accomplished using sun sensors in the pitch and yaw axes and a Canopus tracker in the roll axes for position reference. Rate damping is provided by a single-axis floated gyro in the rate mode on each axis. Control of the spacecraft with respect to inertial reference (inertial hold) is by means of the gyros in the rate integrating mode for all three axes. Lead lag networks on the output of the gyros are used for rate damping. Maneuvers are performed with the gyros in the rate mode. Integration of rate mode output is used to measure and control maneuver angles. Control torques are generated by nitrogen thrusters located on the engine mount deck. Control of the pitch and yaw attitude during engine burns is by means of actuators which vector the engine in response to rate integrating mode output signals from the gyros.

A summary of significant extended-mission events for this subsystem is given in Table 5-1 in chronological order.

The spacecraft performed 452 maneuvers, 292 sun acquisitions, 21 acquire Canopus and 1 acquire Canopus plus. A breakdown of these maneuvers appears in Table 5-2 following.

5.2.1.1 Inertial Reference Unit

The inertial reference unit's performance was nominal, with the exception of anomalies occurring on Days 023, 070, 081, 110, 147, 152, 156, and 254. A discussion of these anomalies is contained in *Roll Anomalies* at the end of this section. Gyro drift remained relatively constant throughout the extended mission. Figures 5-2 and -3 show the values of gyro drift versus time that were measured during the Lunar Orbiter II extended mission. Mission I drifts are included as a comparison. Roll drift was large, reaching the specification limit of 0.5 degree per hour. After Day 059 no further roll drift tests were attempted because of the roll problem (see *Roll Anomalies* below). There is no reason to believe that any significant change to the gyro

Programmer Functions

Closed-Loop Electronics

Velocity Mode Select

Deadband Change

Slew Plus

+1/2°/sec
−1/2°/sec

Slew Minus

Two-Step Gain
K = 1 or 10

Switching Amplifier

One-Shot

Valve Driver

Plus Jet

One-Shot

Valve Driver

Minus Jet

Thrust Vector Control Electronics

Thrust Vector Control Actuator (Pitch & Yaw)

Spacecraft Dynamics

$\dfrac{1}{4}\dfrac{(4S+1)}{(0.1S+1)}$

Position
4 v/o

Rate
4 v/o/sec

Inertial Reference Unit

Rate

Rate

Fine Sun Sensor *

Gyro Mode Select

Sun Sensor Select

Switch Yaw Control

Coarse Sun Sensor *

Photo Subsystem V/H Crab Angle **

Sun Occulted

Solar Detector

*Sun Sensor Replaced by Star Tracker in Roll
**Yaw Only

Figure 5-1: Attitude Control Subsystem Functional Block Diagram

drift occurred over the spacecraft life. Maneuvers based on the + 0.5-degree per hour drift were nominal. Pitch drift appears to be somewhat cyclic but is extremely low. Although no pitch or yaw drift tests were attempted after Day 059 because of thermal problems while on-Sun, pitch drift was derived by maneuvers from off-Sun to on-Sun. Averaging the short times the spacecraft was on-Sun indicates that pitch and yaw drift rates did not deviate significantly from those already recorded. Table 5-3 shows the drift rates and change of drift per day for prelaunch and flight in the inertial hold mode. Long-term drift for all gyros appears to be low and stable, and short-term drift is normal except for the roll axis malfunction.

Table 5-1: Significant Mission Events

GMT Day:Hr:Min	Event
341:17:34 (1966)	Star map
342:13:00	Nitrogen isolation squib fired
342:20:37	|Δ'V 328.1 ft/sec change of velocity to change orbit inclination
348:00:06 to 348:10:00	Paint degradation test - solar panel degradation test, Bright object sensor test
353:03:20 to 353:07:30	Battery deep discharge test, pitch and yaw maneuver accuracy test, pitch and yaw drift test
356:07:30 to 010:20:20 (1967)	Maintain off-Sun attitude pitched plus approximately 50 degrees
010:20:30	Star map, Canopus identified but not tracked
012:21:24	Roll to Canopus, Canopus tracked
012:22:00 to 015:02:48	V/H experiments
015:02:48 to 021:14:34	Maintain off-Sun attitude pitched plus approximately 50 degrees
021:15:44	Star map for Mission III training
021:15:44 to 024:13:00	Lunar Orbiter II used for Mission III training, roll gyro hangup observed, star map to relocate Canopus
027:00:30	V/H Experiment
027:06:00 to 070:11:40	Maintain off-Sun attitude pitched plus approximately 60 degrees
070:12:12	Star map, Canopus identified and tracked
070:15:00 to 070:23:14	Canopus tracker glint test
070:23:14 to 087:18:30	Maintain off-Sun attitude pitched plus approximately 60 degrees
087:18:30 to 103:18:00	Maintain off-Sun attitude pitched plus approximately 55 degrees, update period changed from 60 hours to 21 hours because of periodic roll gyro hangups

Table 5-1 (Continued)

GMT Day:Hr:Min	Event
103:18:25	Star map, Vega (α Lyr) identified and tracked
104:04:50	Roll to Jupiter, difficulty in tracking Vega made Jupiter a preferable reference
104:09:01	Δ V - 18 ft/sec change in velocity for orbit phasing prior to lunar eclipse
110:18:50	Roll gyro hangup observed
114:09:30	Lunar eclipse
114:16:00 to 177:15:00	Maintain off-Sun attitude pitched plus approximately 55 degrees
177:15:07	Star map, Achernar (α Eri) identified and tracked
178:07:01	Δ V 26.2 ft/sec change in velocity to raise the perilune altitude
178:07:01 to 272:13:00	Maintain off-Sun attitude pitched plus approximately 55 degrees
272:20:45	Battery deep discharge test
276:01:07 to 284:05:30	Maintain off-Sun attitude pitched minus approximately 52 degrees
284:05:55	Δ V 258 ft/sec - sunline burn to impact
284:06:24	All axes to rate mode - acquire Sun with sun sensors off, acquire Canopus with tracker off and CRS on, turn IRU off
284:06:38	IRU on
284:05:50 to 284:07:11	29 conseuctive roll maneuvers to decrease nitrogen supply
284:07:11	Occultation - spacecraft impact was on farside of Moon.

Table 5-2: Extended-Mission Maneuver Summary

	0.2-degree Deadband		2.0-degree Deadband	
	Number	Typical Rate	Number	Typical Rate
Roll	83	0.55 ± 0.05 deg/sec	8	0.044 deg/sec
Pitch	50	0.55 ± 0.05 deg/sec	280	0.048 deg/sec
Yaw	27	0.55 ± 0.05 deg/sec	4	0.043 deg/sec
ASU	24		268	
ACA	26		1	
ACP	1		0	
CDZ*	--		18	
CDZ	18		--	
V	--		4	

Limit cycle was normal both in the rate and inertial hold modes. Rates averaged between 21 degrees per hour and 2.0 degrees per hour for typical orbits; however, sunrise and sunset disturbance increased the rate up to 45 degrees per hour. Except for the disturbances, the average rate was below the design goal of 9 degrees per hour and considerably below the mission requirement of 36 degrees per hour (to reduce smear on pictures). Figure 5-4 shows a typical limit cycle during an orbit, with the attitude control in the 2.0-degree deadband and the inertial hold mode.

The predominant preference for one switching line, as seen for the pitch position, is a reflection of solar pressure due to the spacecraft's pitch off the sunline. Spacecraft rates are well within design tolerances, being less than 0.005 degree per second. Correct operation of the reaction control switching amplifiers and thruster amplifiers at the plus and minus 2-degree deadband limits is evident from the figure.

Deadband limits for the 0.2-degree and 2.0-degree deadbands are shown in Table 5-4. It is evident that the deadband was generally within specification during the extended mission.

Operation of the attitude control in the maneuver mode was normal. Maneuver rates and accuracies were within design tolerances. Table 5-5 consists of a maneuver rate summary. The specification was +0.55 deg/sec ± 0.1 deg/sec for the 0.2-degree deadband. The wide deadband was not specified.

Table 5-6 shows the maneuver accuracies achieved. The maneuvers all fall within the design tolerance range, ± 0.3%.

Figures 5-5 and 5-6 show the roll, pitch, and yaw wheel currents (Telemetry Points AE01, AE02, and AE03, respectively), gyro temperature (Telemetry Point AT02), and deck temperature (Telemetry Point STO3) versus time for the start and end of the extended mission. The spacecraft was constrained to an off-Sun attitude of 50 to 60 degrees due to excessive heating when on-Sun. The deck temperature and gyro temperature show the results of this heating. Gyro temperature is a pseudo-temperature output signal derived from the addition of error
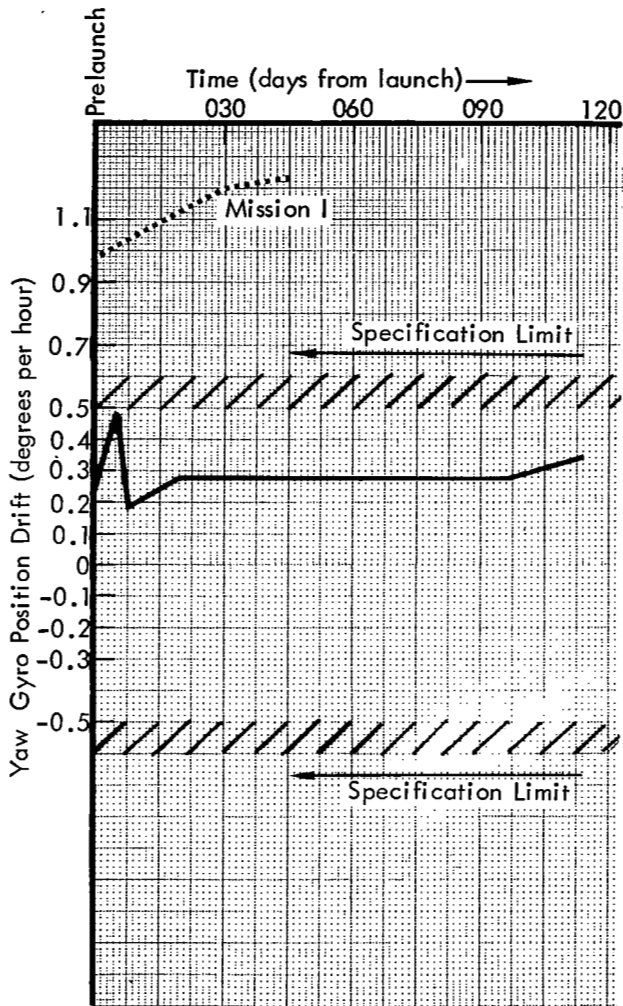
Figure 5-2: Gyro Drift — Yaw
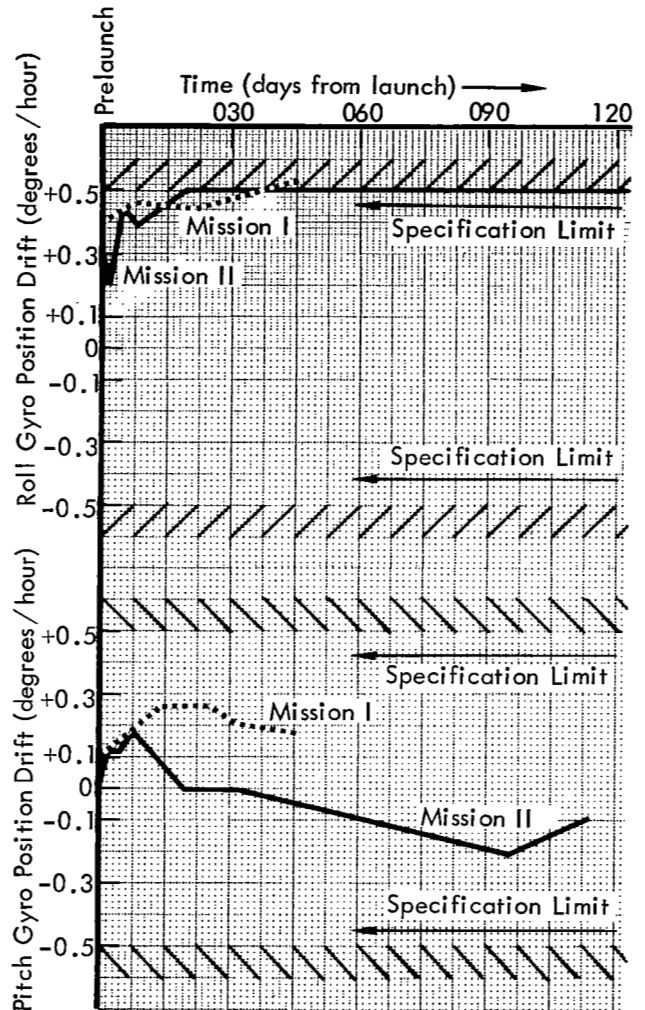
Figure 5-3: Gyro Drift — Pitch and Roll

Table 5-3: Drift Rates

	Prelaunch Data * Averaged		Flight Data Averaged	
	Drift deg/hr	Change deg/day	Drift deg/hr	Change deg/day
Roll	−0.15	−0.011	+0.5	−0.0018
Pitch	+0.075	+0.019	−0.04	−0.0013
Yaw	−0.12	+0.018	+0.3	+0.005

* Ground test results are opposite in sign to those of flight data due to method of testing.
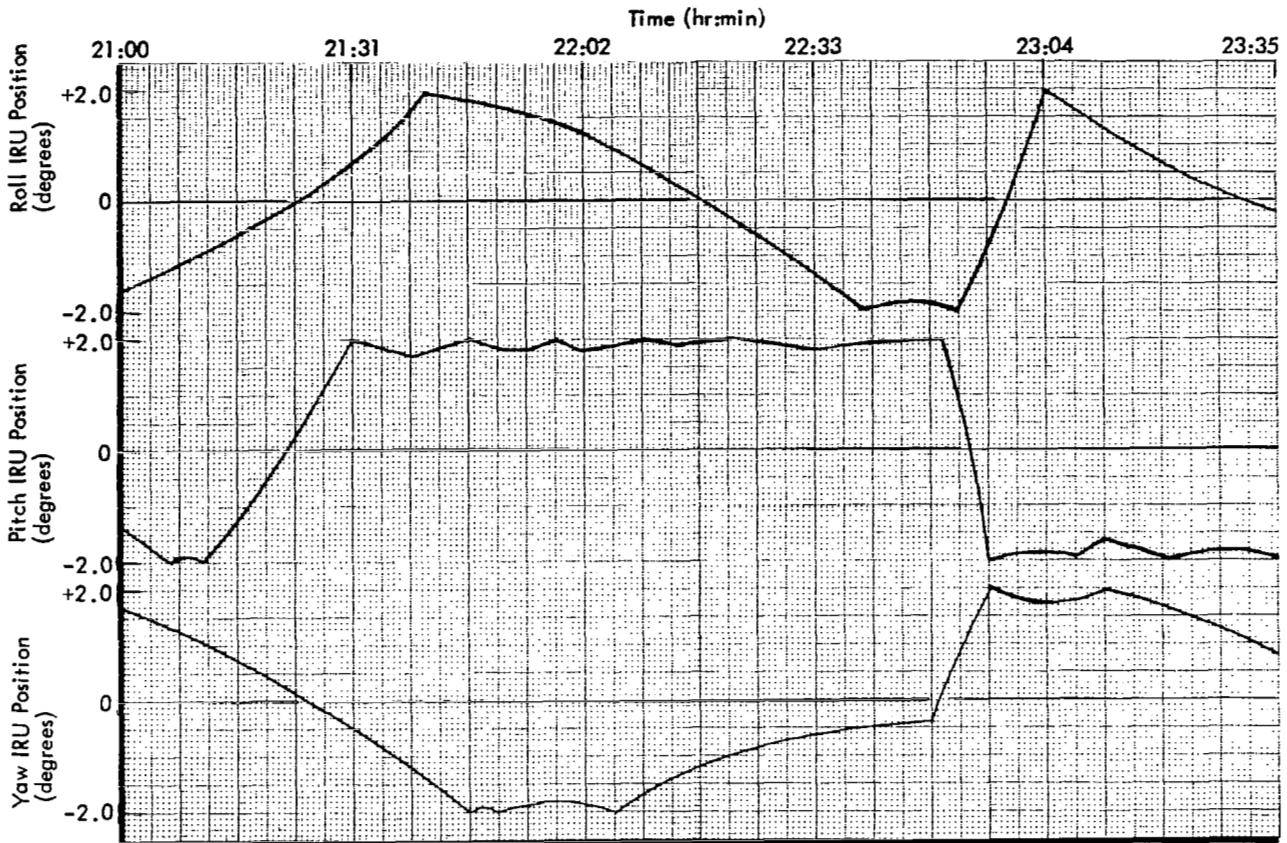
Figure 5-4: IRU Position Versus Time

signals in the roll, pitch, and yaw gyro heater control circuits and is somewhat dependent on spacecraft bus voltage. The temperature control circuits are used to stabilize the viscosity and density of the gyro flotation fluid. The measurement is expressed in percent of full scale, with 0 to 100% corresponding to the telemetry range of 0 to 5 volts. The approximate indicated IRU temperature range was 142.5 to 147.5°F. IRU temperature control was normal, and followed the deck temperature. No temperature oscillations were observed, indicating that the IRU temperature was never saturated. The wheel currents were stable and reasonably constant, except for the normal fluctuation with temperature. No changes in wheel current that would indicate gyro problems are apparent. Initial and final values of wheel currents over the extended mission were: roll, 85.1-84.1 ma;

pitch, 89.4-87.8 ma; yaw, 92.6-91.0 ma. A slight decrease in wheel current with time is to be expected, since the motor-bearing preload relaxes and less torque is required to maintain synchronous speed in the gyro. Accelerometer performance was normal; tracking data and orbit determinations showed that the accelerometer performed as programmed within the resolution of the tracking data. Table 5-7 shows desired and achieved trajectories for three extended-mission orbital changes.

Roll Anomalies — The anomalies in the roll axis appear to be from two sources. One seems to be roll gimbal hangup; the other (Day 070) seems to be in the deadband limit circuitry or in the telemetry of the roll position error. The anomaly on Day 070 is reported in 5.2.1.3 *Closed-Loop Electronics*. A summary of the

Table 5-4: Deadband Limit Performance

Position Error	Deadband Limits (deg)			
Channel Designation	Narrow Deadband		Wide Deadband	
	Plus	Minus	Plus	Minus
Attitude control specification	0.18 ± 0.03	0.18 ± 0.03	2.0 ± 0.3	2.0 ± 0.3
Roll position (AG01)	0.18 ± 0.01	0.17 ± 0.01	1.95 ± 0.04	1.98 ± 0.02
Pitch position (AG02)	0.19 ± 0.04	0.18 ± 0.02	1.95 ± 0.05	1.97 ± 0.02
Yaw position (AG03)	0.17 ± 0.01	0.17 ± 0.02	1.94 ± 0.02	1.96 ± 0.04

problems encountered follows.

Day 023 — Yaw sensor showed an apparently uncommanded angle of 35 degrees. Roll was 24 degrees away from the zero reference and the pitch angle was approximately 5 degrees less than expected.

Day 070 — During a 360-degree pitch maneuver the roll gyro position exceeded the deadband limits of ± 0.2 degree.

Day 081 — Yaw sun sensor saturated. Pitch sun sensor reads −15 degrees. Sunline indicates X axis was 63 degrees from the Sun.

Day 087 — Roll gyro position output fixed at +1.978/1.954 degrees for 2 hours.

Day 110 — Roll gyro position output fixed at +1.8 degrees, drifting at a rate of approximately 40 degrees per hour.

Day 147 — Yaw sun sensor reads +13 degrees, pitch sun sensor reads +28 degrees. Gyro data normal.

Day 152 — Yaw sun sensor reads +10 degrees, pitch sun sensor reads +28 degrees. Gyro data normal.

Day 186 — Yaw sun sensor reads −11 degrees, pitch sun sensor reads +28 degrees. Gyro data normal.

Day 254 — Yaw sun sensor reads −26 degrees, pitch −26 degrees. Gyro data normal.

Table 5-5: Maneuver Rate Summary

Axis	Number Completed	0.2 Deadband		Number Completed	2.0 Deadband	
		Plus	Minus		Plus	Minus
Roll	83	0.486 to 0.503	0.484 to 0.498	8	0.047 to 0.058	0.040 to 0.052
Pitch	50	0.494 to 0.521	0.494 to 0.521	280	0.048 to 0.067	0.045 to 0.540
Yaw	27	0.487 to 0.512	0.494 to 0.512	4	--- ---	0.040 to 0.052

GMT Day 353, 1966

AE01
Roll Wheel Current
(milliamps)
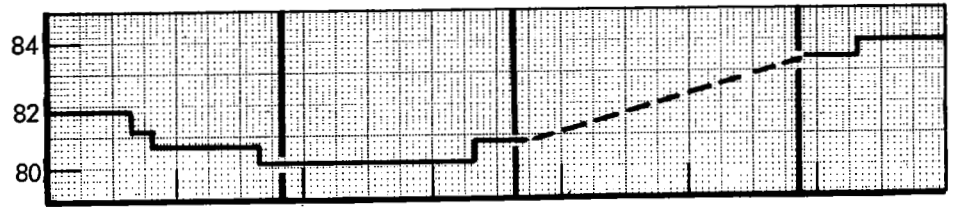
AE02
Pitch Wheel Current
(milliamps)
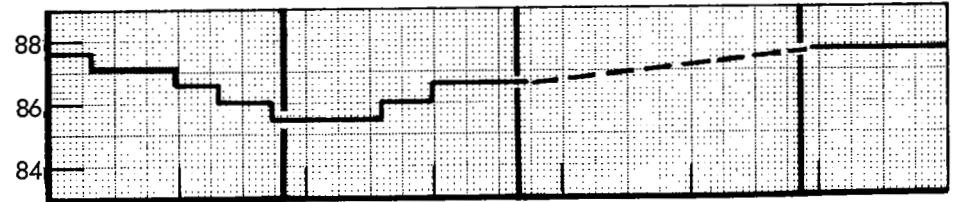
AE03
Yaw Wheel Current
(milliamps)
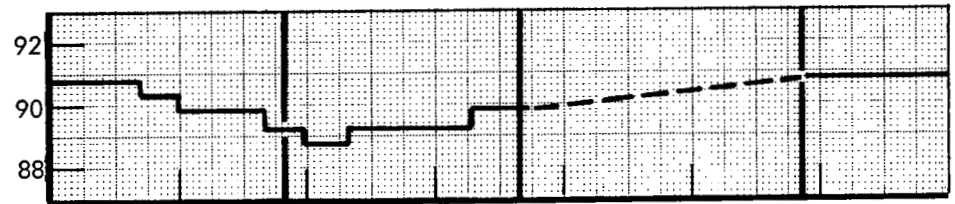
AT02
Gyro Temperature
(percent)
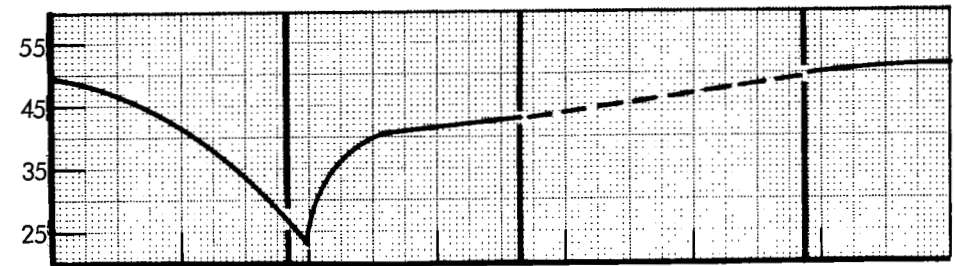
ST03
Equipment Mounting
Deck Temperature
(degrees Fahrenheit)

Time

Figure 5-5: Gyro Wheel Currents (Roll, Pitch and Yaw) on Day 353, 1966

81
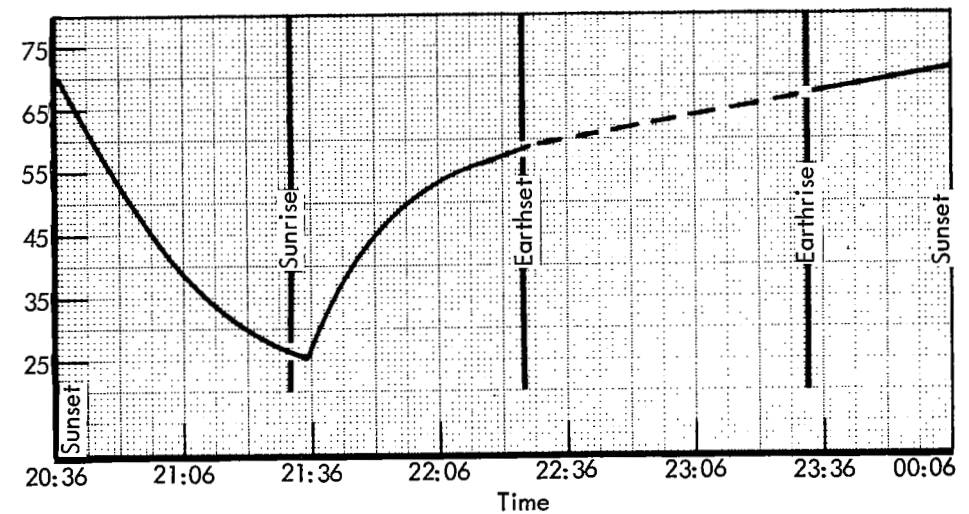
Figure 5-6: Gyro Wheel Currents (Roll, Pitch and Yaw) on Day 272, 1967

Table 5-6: Maneuver Accuracy Summary

Maneuver	Actual Mag. (deg)	Maneuver Error (deg)	Percent Error
Roll plus 360 deg	359.52	−0.478	−0.133
Pitch plus 360 deg	359.949	−0.051	−0.014
Yaw plus 360 deg	360.361	−1.361	+0.10

No minus maneuvers were attempted in order to save attitude control gas.

Table 5-7: Velocity Maneuver Summary

Orbit Change Date	Orbit Altitude	Desired Trajectory (km)	Actual Trajectory (km)
342	h_p	43.76	42.68
	h_a	1,882.56	1,884.42
104	h_p	68.86	68.37
	h_a	1,840.44	1,840.30
178	h_p	112.9	113.39
	h_a	1,840.93	1,840.91

Observations on Day 023 — On Day 023, between 00:00 and 05:00 GMT, the telemetry output of the yaw sun sensor amplifier indicated an apparently uncommanded yaw angle attitude change of about −18 degrees at a time when the spacecraft was pitched off the Sun at an angle of 48 degrees for thermal control. A +25-degree yaw corrective maneuver was performed at 05:20 GMT to correct this condition. However, the spacecraft's attitude was not corrected as expected, since the yaw angle indicated by the sun sensor was an apparent yaw error caused by an uncommanded roll axis maneuver. This roll maneuver shifted the yaw sun sensor eye to a position relative to the sunline so that a yaw error was indicated. Figure 5-7 shows the yaw sun sensor output as a function of time through-

out this period (Note: The actual yaw position as a function of yaw sun sensor output is approximately two times the indicated sun sensor angle due to the reduction in yaw sun sensor output resulting from the pitch angle off-Sun). Figure 5-8 shows the apparent pitch angle versus time, where the pitch angle (actually the +X axis of the spacecraft) was deduced from solar array current data. The apparent pitch angle is steady until 05:20 GMT, when it decreases by approximately 2.5 degrees. This is due to the +25-degree yaw maneuver which reorients the X axis in relation to the sunline.
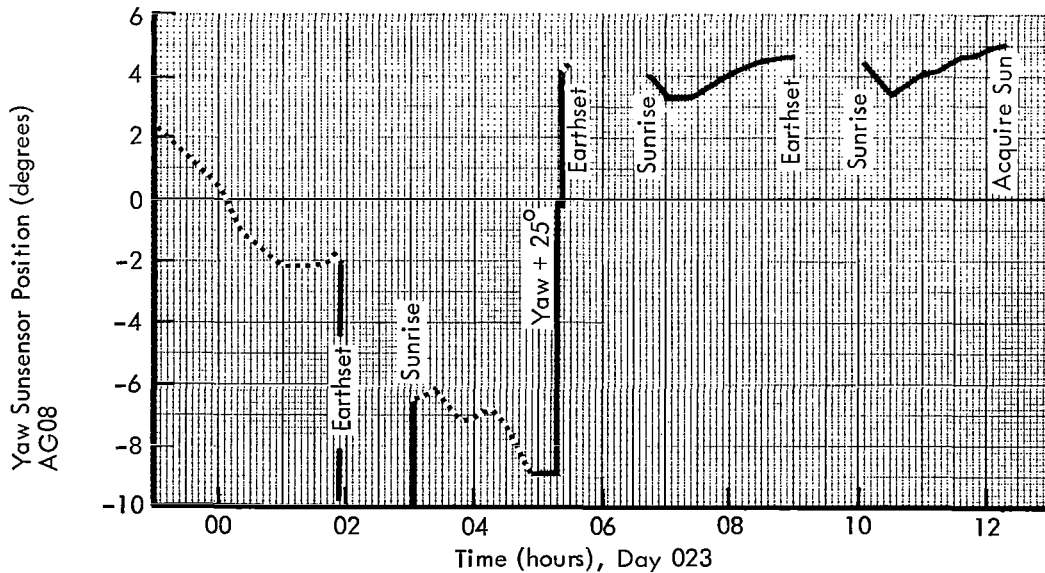
Figure 5-7: Yaw Sun Sensor Position
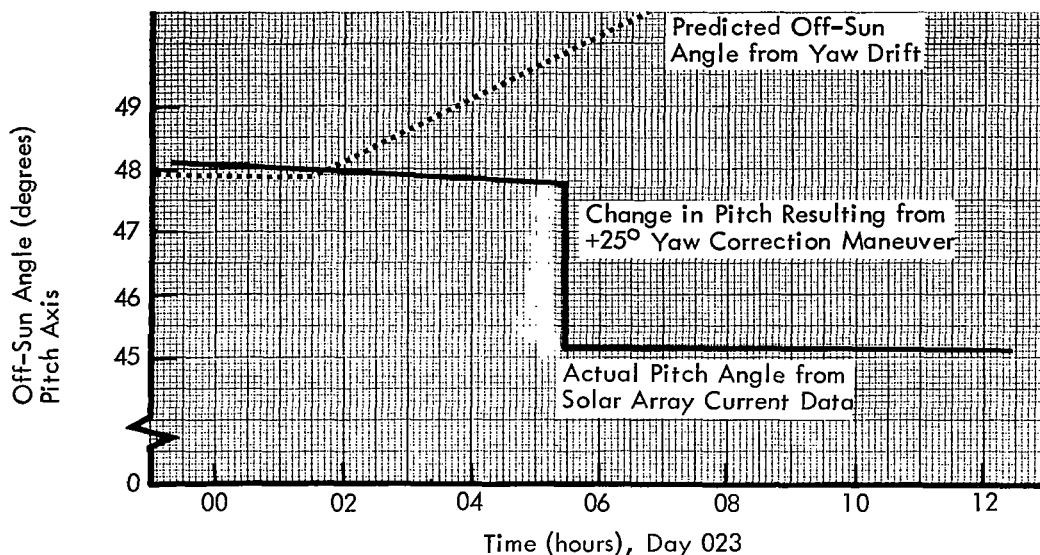
Figure 5-8: Off-Sun Angle — Pitch Axis

On Day 023, during the same 12-hour period that the yaw attitude change occurred, the star Canopus was lost from the tracker's field of view. To relocate Canopus, a star-mapping maneuver was performed at 13:27 GMT, resulting in Canopus acquisition at a roll angle of +24 degrees away from the IRU's zero-degree roll error position.

At the time, two possible explanations for the phenomenon were advanced. These were:
- That the yaw gyro developed a drift rate of −3.4 degrees per hour, or the yaw gyro gimbal was sticking;
- That the roll gyro gimbal was sticking, or a roll gyro drift rate of +4 degrees per hour occurred.

If the yaw gyro had caused the problem, the off-Sun angle would have increased, as shown by the dashed line of Figure 5-8, but this was contradictory to the solar panel current data, since when the yaw maneuver was completed, the off-Sun pitch angle should have been about 48.5 degrees, but was actually only 45 degrees. Also, the assumption of an error in the yaw axis would not completely explain the subsequent +24-degree roll error.

If the roll gyro had caused the problem, the spacecraft could have rolled without the off-Sun

pitch angle having changed. This agrees with the solar panel current data. If the spacecraft had changed roll attitude by +22 degrees between 00:00 and 05:20 GMT, the apparent yaw error from the sun sensors would be −17 degrees (almost equal to the − 18 - degree error actually measured). This yaw error would result from roll coupling the 40-degree pitch error into the yaw axis. When the yaw position error reached −18 degrees after a roll of +22 degrees, the spacecraft would actually be nearer the Sun with an approximate pitch angle of +45 degrees. This also agrees with the solar array current data.

Furthermore, the roll of +22 degrees correlates with the +24 degree roll error determined from star mapping, and the telemetry data for the roll axis position error shown in Figure 5-9 indicates that the roll gyro has a steady state error output of approximately 1.7 degrees during the time period in which the error could have occurred. This is not a normal limit cycle for roll, as can be seen in Figure 5-4, since roll does not show any particular tendency to stay on either switching line. Assuming the spacecraft drifted in roll at the rate shown in Figure 5-9 of about 0.06 degree per minute from GMT 00:00 until GMT 01:20, a drift of about +5 degrees in roll would occur. This would cause an apparent yaw sun sensor error of approximately 2 degrees. Figure 5-7 indicates the yaw sun

84
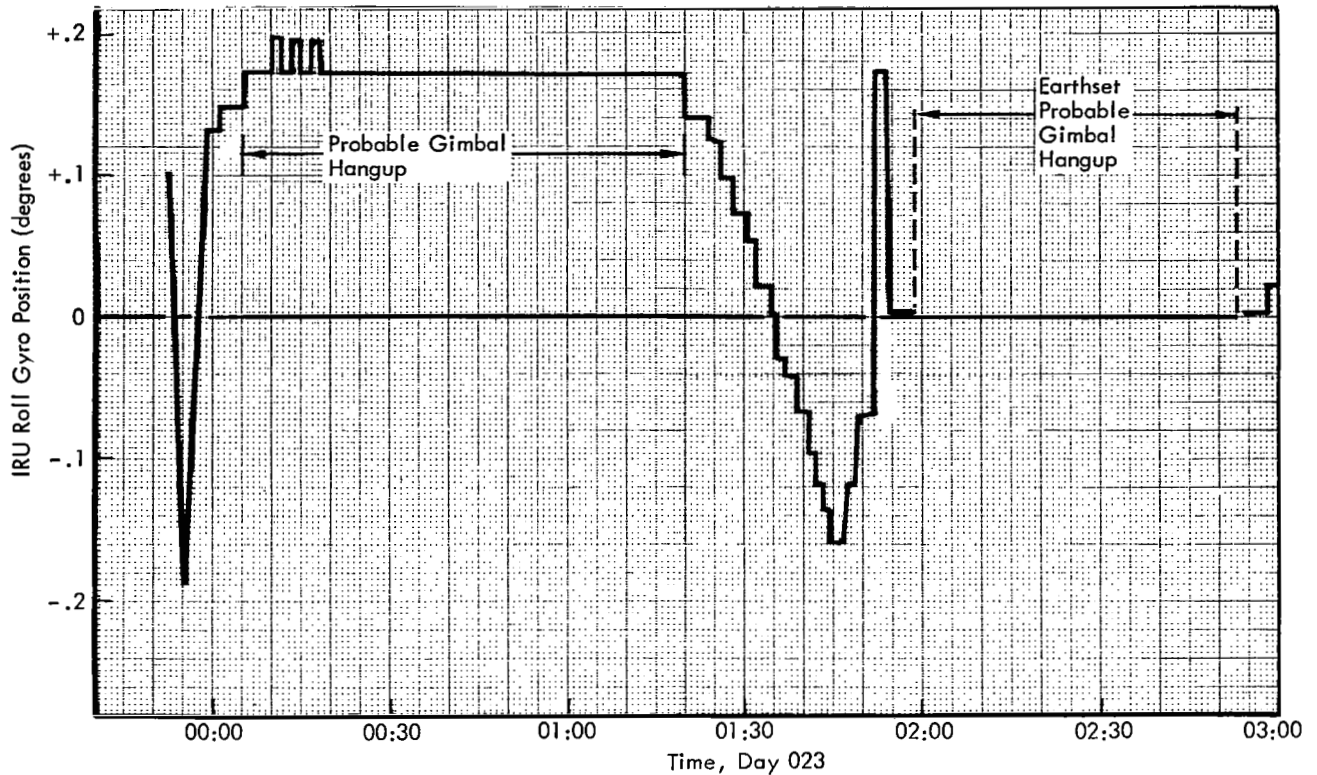
Figure 5-9: Roll Gyro Position Error

sensor angle actually changed by this amount during this period.

It is concluded, therefore, that the roll gyro suffered a malfunction that caused it to produce a steady state error. The most likely cause of this type of malfunction is a gimbal hangup. A gimbal hangup within the deadzone would permit the spacecraft to drift beyond the roll axis deadzone without an error signal being produced which would normally fire the roll axis thrusters.

Observations on Day 081 — On Day 081 the spacecraft was tracked from 16:25:41 to 16:35:19 GMT and from 20:28:22 to 20:44:53 GMT. During the first time period it was noted that pitch position (AGO7C) was −15.7 degrees and the yaw position (AGO8C) was saturated at +30.0 degrees. The gyros appeared to be operating normally. The true angle between the sunline and X axis was 63 degrees, based on solar array current which was about 5 amperes. From these data it is concluded that the net result

of spacecraft motion since the last plus 62-degree pitch off the sunline on Day 080 at 15:41: 25 GMT was equivalent to rolling minus 105 degrees without appreciable motion of the X axis from its original position. The most plausible explanation for this is that a roll gyro gimbal hangup occurred. To eliminate the possibility of a catastrophic failure, the spacecraft programmer was revised to reacquire the Sun and pitch plus 56 degrees every 21 hours. This kept the total Sun angle between 50 and 62 degrees for any roll attitude that might occur as a result of a roll gyro hangup. Since the worst case would be a plus or minus 90-degree roll (this aligns the yaw gyro in pitch plane), this revised program kept the spacecraft in a safe attitude with respect to the Sun.

Observations on Day 110 — On Day 110 the roll gyro was observed to hang up again. Figure 5-10 is a plot of position data versus time. The roll gyro position error reached a steady state output at GMT 18:42 and continued a steady state output into earthset at 20:21. During this

85
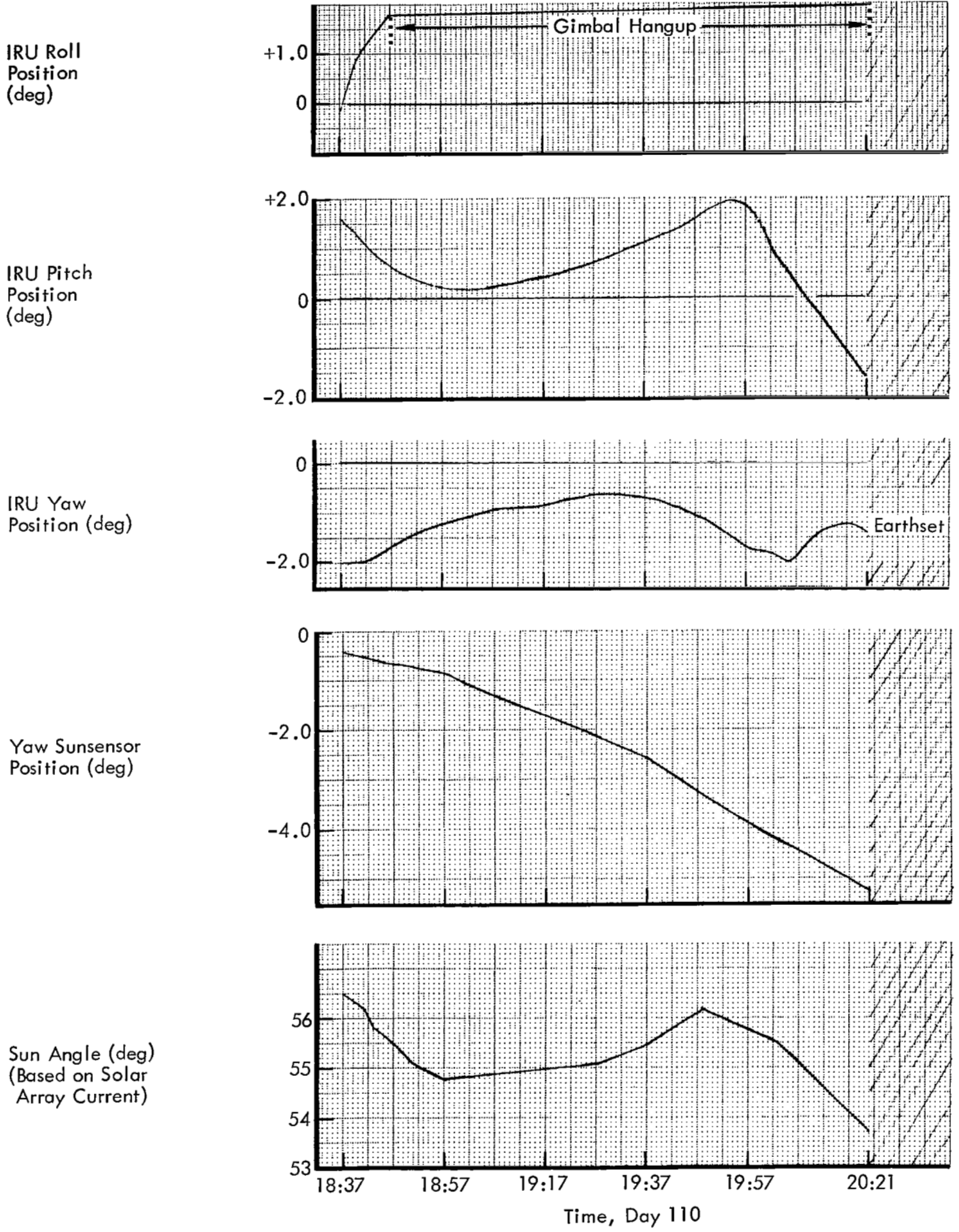
Figure 5-10 Position Data During Roll Gimbal Hangup

period the yaw sun sensor position output changed, from about 0 to −4.7 degrees. This is the result of the yaw sun sensor's changing its relationship to the sunline. The X axis spatial position in relation to the Sun, which can be determined by solar array current, shows no change except for the expected deviations caused by the pitch gyro. It is concluded that the roll gyro gimbal hung up, thereby causing the change in sun sensor output on the yaw axis.

Other observations — The events that occurred on Days 087, 147, 152, 186, and 254 were also apparently caused by the suspected intermittent failure of the roll gyro gimbal. However, the pitch off-Sun program that was used prevented any degradation to the mission. Thus, although the roll gyro gimbal hangup constitutes an intermittent failure in the attitude control sub-system and does present operational difficulties, it did not prevent the spacecraft's accomplishing any of the mission objectives.

5.2.1.2 Star Tracker

The star tracker continued to operate satisfactorily throughout the extended mission. The tracker was cycled on and off 67 times and accumulated an operating time of 19.6 hours. The total operating time, including the photographic mission, was 162.5 hours, which included 252 on-off cycles. Canopus was not observed after Day 081, 1967 and went out of the yaw field of view on Day 098, 1967. The tracker was last used on Day 178. At that time it did not show any serious degradation of star map sensitivity.

Figure 5-11 shows the range of star tracker voltages observed during the extended mission; Figure 5-12 shows maximum and minimum star tracker sensitivity in relation to the total cumulative operating time during this same period. Both figures are normalized to Canopus for celestial objects other than Canopus so as to give a time picture of star tracker output versus time. The figures indicate that star map data became stabilized near 2.95 volts for Canopus during the extended mission. There was little degradation with time, primarily due to the policy of keeping the tracker in an off condition to prevent light from fatiguing the photo-multi-

*Star other than Canopus
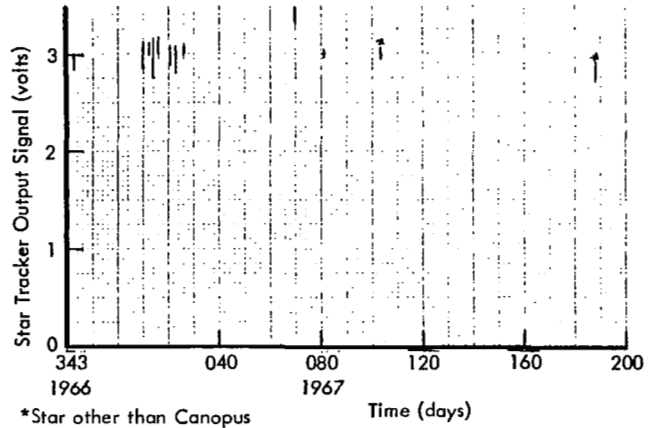
**Figure 5-11:
Star Tracker Output Signal Characteristics**

*Time tracker "on" but could not acquire star
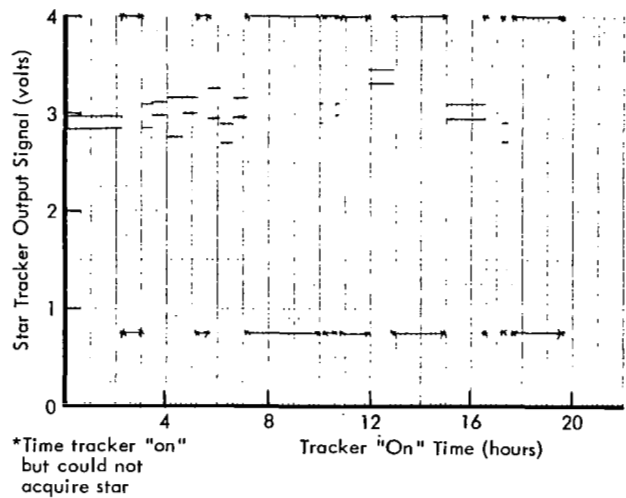
**Figure 5-12:
Extended-Mission Total Tracker "On" Time**

plier tube. It is concluded that the tracker operated properly during the period that it was used, and that mission operations were not compromised by the tracker's performance. .

5.2.1.3 Closed-Loop Electronics

The closed-loop electronics operated correctly throughout the extended mission, except for the anomaly noted on Day 070 which is discussed herein. The minimum impulse circuit, or "one shot," appeared to be operating between 11 and 14 milliseconds (11 milliseconds is considered nominal). During limit cycle operation, the minimum impulse circuit allowed approximate single pulses 70, 50, and 20% of the time in the roll, pitch, and yaw axes, respectively, in

87

the 2.0- and 0.2-degree deadbands in both the inertial hold and rate modes of operation. The compensation networks for the thrust vector control circuitry and the inertial hold circuitry performed correctly.

During a 360-degree pitch maneuver on Day 070 the yaw gyro position held within the ±0.2-degree limits while the roll gyro position exceeded the deadband limits of ±0.2 degree, as may be seen in Figure 5-13. This anomaly was first thought to be a roll gimbal hang up similar to that which occurred on Day 023. However, further analysis indicated it to be some type of failure concerned with the solid state switches in the closed-loop portion of the roll axis. A time history of data during the 360-degree pitch maneuver is shown in Figures 5-13 and -14. An analysis of these data appears below.

- Excursions of the roll position beyond −0.2 degree were not strictly a loss of control, but rather a shifting of the control points or deadband limits. The roll position plot indicates a form of limit cycle behavior, but with a shifting and unstable negative limit.
- Excursions of the roll position beyond −0.2 degree were coincident with a high tracker-error signal and a star tracker voltage large enough to produce a Canopus presence signal.
- The Canopus presence signal is coincident with the roll excursions.
- Excursions of roll position beyond −0.2 degree were coincident with a depressed bus voltage resulting from the off-Sun angle during the pitch maneuver.
- The large changes in roll position are roughly coincident with abrupt changes in star map signal and tracker position output. However, the roll variation is not large enough to be the probable cause of tracker output variations.
- An examination of all telemetry information at this time discloses no anomalies in the telemetry system. Further, the roll axis was in the in the inertial hold mode and no commands were present to shift it to the rate mode.

A further clue to the nature of this anomaly is in the consistently observed attitude disturbances resulting from electrical coupling during tracker turn-on transients. These disturbances demonstrate that tracker transients will couple into the closed-loop electronics, although in theory the tracker is isolated by the solid state switches which control the ACS mode. Because of this fact, and the six relationships outlined above, it is felt that the most probable cause of this anomaly was partial coupling of the tracker position output signal into the roll axis control circuitry, with a resulting shift in the deadband limits. The coupling was much more pronounced during abrupt changes in tracker output and was possibly aggravated by the low bus voltage condition. The apparently abnormal behavior of the roll axis control circuitry was probably a proper reaction to a combination of unusual spacecraft conditions which were experienced on this one occasion. The apparent anomaly conditions described did not repeat themselves and did not cause any problems in mission operations or in the mission itself.

5.2.1.4 Sun Sensors

The sun sensors provided an accurate celestial reference throughout the extended mission. Operation was normal and no anomalies were noted. Since approximately 90% of the extended mission was accomplished with the spacecraft pitched off-Sun at 36 to 62 degrees, the capability of selecting either fine or coarse, or fine and coarse sun sensors provided the needed versatility for the off-Sun operation. The minus-pitch sun sensor had a hard limit at 26.8 degrees; the plus-pitch sensor had a soft limit at 26.8 degrees. The expected limit is 25 degrees ±3.75 degrees. The reduction in the yaw sun sensor output for a pitch angle of 30 degrees was actually −23%, whereas the predicted change was only −14%. However, this reduction in output compares with that of Mission I, which was −25%. Moonlight, as in Mission I, was seen to affect the coarse eyes during certain portions of the mission. At these times, when both sunlight and moonlight were entering the tracker, the moonlight caused a slight shift in apparent Sun position. Operation of the spacecraft in the celestial hold limit cycle resulted in the performance figures listed in Table 5-8.

There was little or no degradation in the sun sensors' outputs throughout the extended mission and almost no null shifts. Table 5-9 shows the sun sensor null readings for ground test, start of mission, and end of mission.
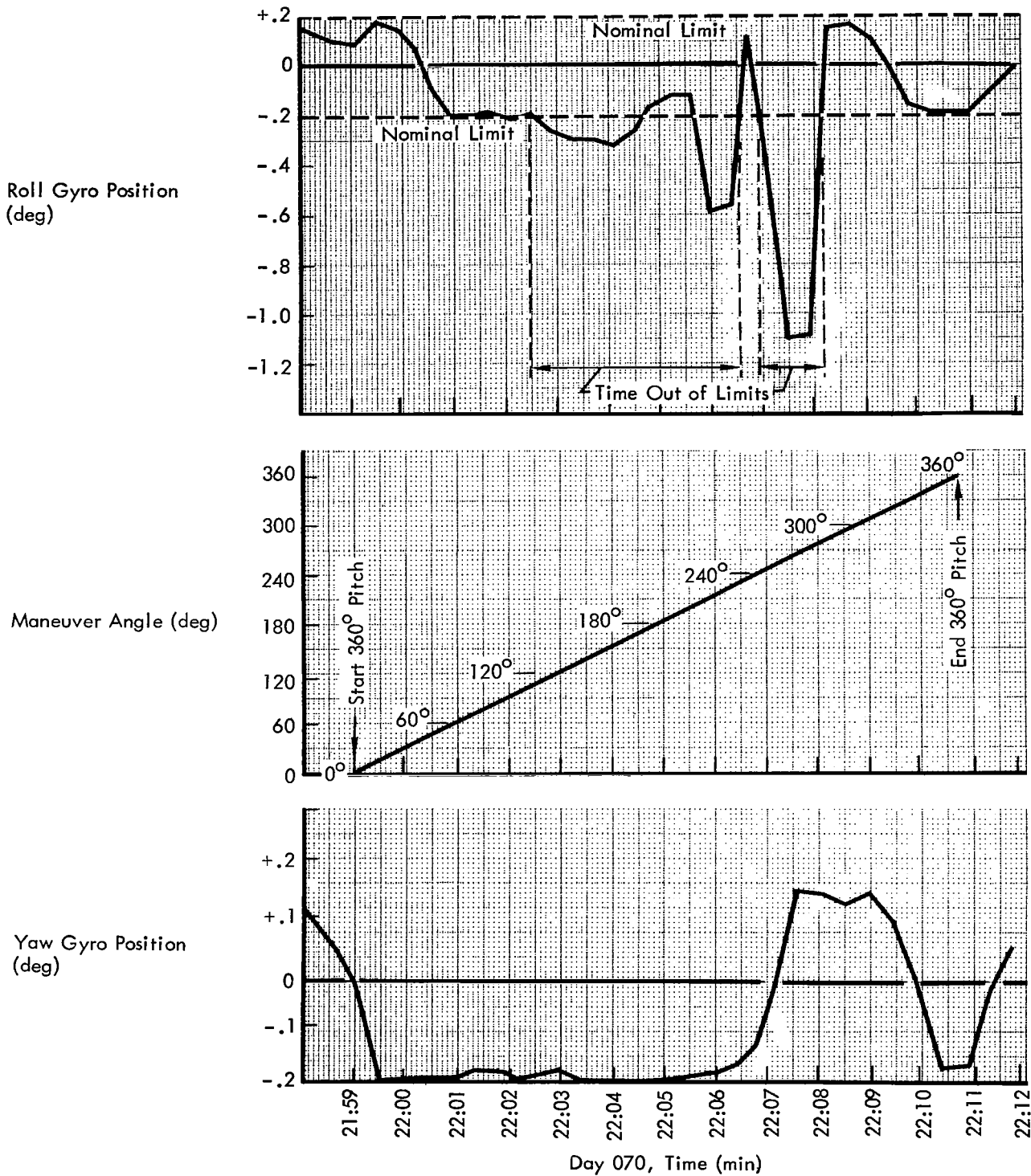
Figure 5-13: Roll and Yaw Gyro Position During 360-Degree Pitch Maneuver

89
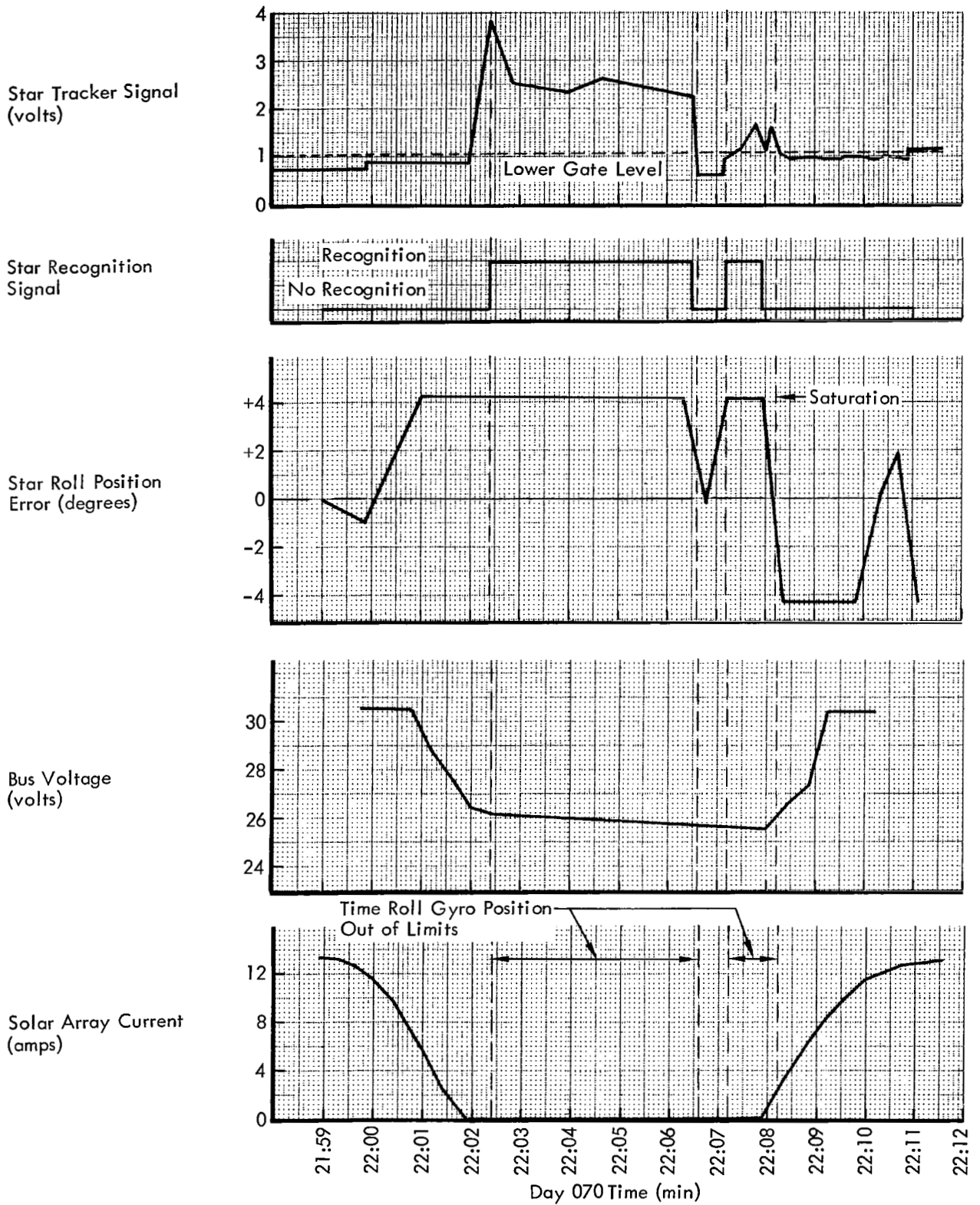
Figure 5-14: Star Tracker and Solar Array Data During 360-Degree Pitch Maneuver

90

Table 5-8: Deadband Performance

Axis	0.2 Deadband			2.0 Deadband		
	Design	+ Edge	− Edge	Design	+ Edge	− Edge
Pitch	±0.18 ±0.02	0.21 ±0.01	0.11 ±0.04	2.0 ±0.3	1.64 ±0.02	1.60 ±0.02
Yaw	±0.18 ±0.03	0.18 ±0.02	0.07 ±0.01	2.0 ±0.3	1.68 ±0.02	1.53 ±0.02

Table 5-9: Null Characteristics*

Time of Evaluation	Fine Pitch Sensors (deg)	Fine Yaw Sensors (deg)
Ground test	+ 0.002 to + 0.100	−0.034 to + 0.061
Start of extended mission	+ 0.051	+ 0.061
End of extended mission	---	----

	Coarse Pitch Sensors (deg)	Coarse Yaw Sensors (deg)
Ground test	−0.053 to 0.537	+ 0.126 to 0.690
Start of extended mission	+ 0.24	+ 0.41 to + 0.69
End of extended mission	+ 0.102	+ 0.48

* Measurements taken during Sun occultation

5.2.1.5 Control Assembly

During the extended mission the control assembly responded correctly to every received and stored program command. Its flawless operation contributed greatly to the success of the extended mission. A total of 4,096 commands was transmitted and executed during the extended mission; of these, 1,228 were real-time commands and 2,868 were stored-program commands.

Including the photographic mission, 8,958 commands were transmitted and executed, and a total of approximately 23,700 commands, including repetitive sequences, was executed. The programmer cycled approximately 3 billion times and accumulated some 300 million clock incrementations while directing spacecraft operations. The total clock drift as of Day 284 was plus 5.69 seconds for a slope of 0.7 milliseconds per hour, well within the design tolerance of 3.4 milliseconds per hour.

5.2.1.6 Switching Assembly

Switching assembly performance throughout the extended mission was normal. Tank heaters were switched properly and four velocity commands were executed correctly. No anomalies

were observed in the spacecraft telemetry data that would indicate a switching assembly problem.

5.2.2 Communications Subsystem

The communications subsystem consists of the equipment which: (1) receives information from the ground via an rf link and converts this information to a form suitable for use by the spacecraft; (2) receives telemetry and video information from the spacecraft, converts this information to modulation on an rf carrier and transmits this modulated rf carrier to the ground; (3) receives ranging information from the ground via rf link, modulates this information on an rf carrier and retransmits this to the ground for use in range determination; and (4) establishes a specific ratio between the received rf frequency from the ground and the spacecraft transmitted frequency for accurate determination of the spacecraft velocity using Doppler information.

The communications subsystem as described herein consists of the following equipment.

- Transponder
- Traveling-wave-tube amplifier (TWTA)
- Low-gain antenna
- High-gain antenna
- High-gain antenna position controller
- Modulation selector
- Command decoder
- Multiplexer encoder
- Scintillation counter
- Logic circuitry
- Signal conditioners (2)
- Micrometeoroid detectors

Refer to Figure 5-15 for a functional schematic.

The communications subsystem operated nominally throughout the extended mission while performing the following functions.
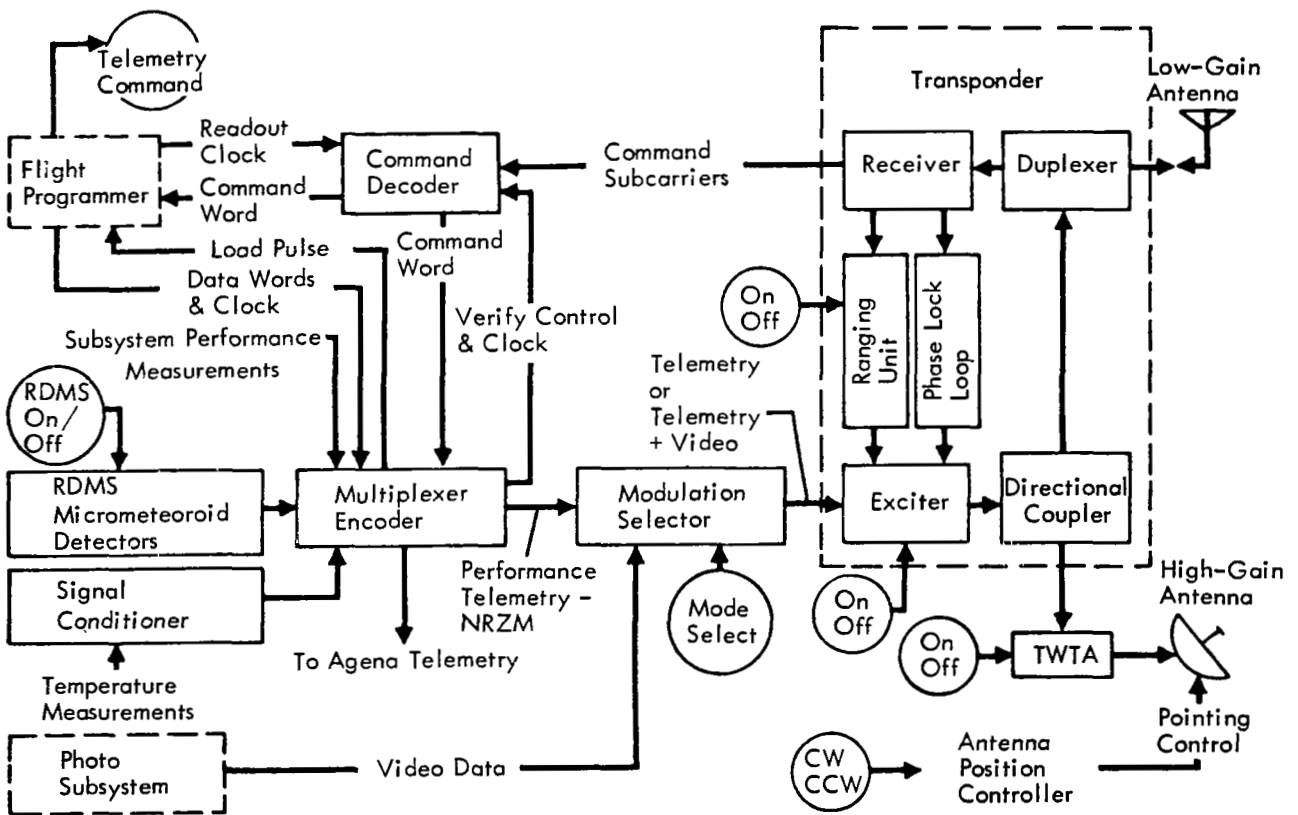
Figure 5-15: Communications Subsystem Block Diagram

Command Capability — The command loop received, verified, and executed 4,096 commands without error. The redundant-command register of the command decoder was never used. During Mission II tracking periods, the communications subsystem responded to all operational commands as directed. However, during the photographic missions of Lunar Orbiters III and IV, several unintentional commands were received by the programmer. These commands resulted from having the Mission II (Spacecraft 5) transponder in uplink lock under weak uplink signal conditions. The following spurious commands were received and executed by Lunar Orbiter II's flight programmer.

Lunar Orbiter III

- An RTC maneuver of 1.9 degrees.
- An RTC SPA command and three SPC commands.
- An RTC JMP command.
- An RTC "camera thermal door open" command (resulting in eventual failure of the camera thermal door in the "open" position).

Lunar Orbiter IV

None

Lunar Orbiter V

- A command that caused the flight programmer to indicate a parity error. No command was performed.
- An SPC time word was stored in Fixed Memory Address Location 005. This was subsequently overstored with an SPC JMP 005.

The reduction in the number of spurious commands received after Lunar Orbiter III's prime mission is largely due to the development of greatly improved multiple-spacecraft operational tracking procedures.

Blind Acquisition — During Mission III, the transponder rf exciter in Spacecraft 5 (Mission II) was turned off to prevent possible interference with the prime mission. Approximately 25 blind acquisitions were performed. Although in some cases more than one attempt was required, rf turn-on was always achieved.

Spacecraft Performance Information — Telemetry data from all spacecraft subsystem transducers were compiled and transmitted with the desired accuracy.

Lunar Environment Information — As a primary objective of the extended mission, radiation and micrometeoroid data were provided by the communications subsystem throughout the extended mission.

Selenodetic Information — Coherent Doppler data with one and two tracking stations, as well as ranging data, were successfully provided throughout the extended mission. Time correlation between tracking stations was accomplished using the ranging system.

5.2.2.1 Transponder

The transponder operated satisfactorily during the extended mission. Telemetry indication of transponder rf power output (CE10) variations with transponder temperature (CT02) and equipment mounting deck temperature (ST02) are shown in Figures 5-16 and 5-17, respectively. The decrease in power output with increasing temperature is normal. The change in slope of transponder thermal characteristics from the flight acceptance test (FAT) data, as shown in Figure 5-16, may be due to a shift in the characteristics of the temperature on power output transducers. The effect on ground-received signal strength would be barely discernible (0.2 decibels), since actual rf power output variation is only about one-third of that indicated by telemetry due to the sensitivity of the transponder power output signal samplers to temperature variations. No problems with ground-received signal strength were encountered during the extended mission. Figure 5-18 portrays typical transponder rf power output versus transponder temperature during the extended mission.

AGC Telemetry Anomaly — It has been observed that at strong signal levels (−70 dbm to −100 dbm), transponder AGC (CE08) indicated a best-case input strength approximately 8 to 12 decibels too high. From prelaunch field experience with Spacecraft 6 on the same problem, it was found that the actual AGC

93
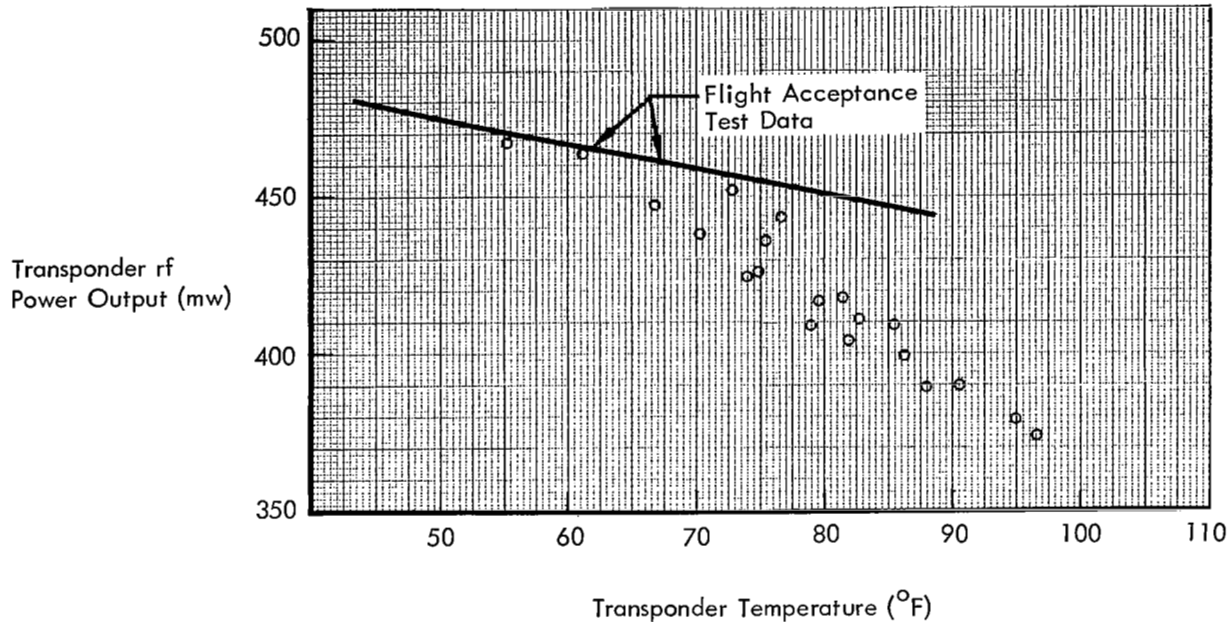
Figure 5-16: Effects of Temperature on rf Power Output
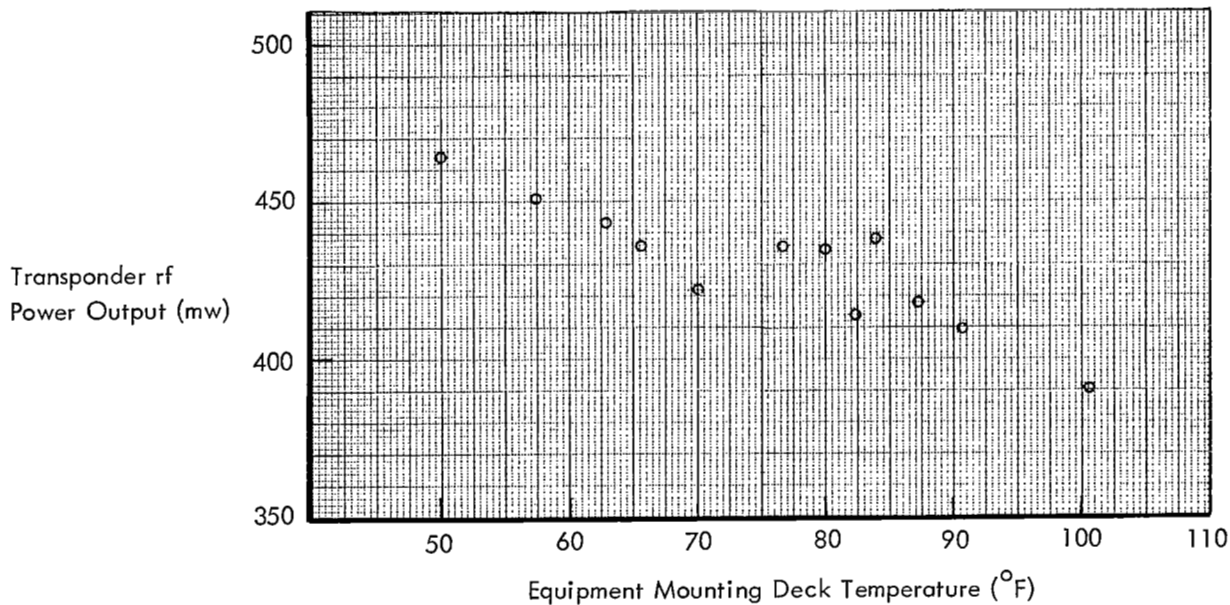
Figure 5-17: Effect of EMD Temperature on rf Power Output

94
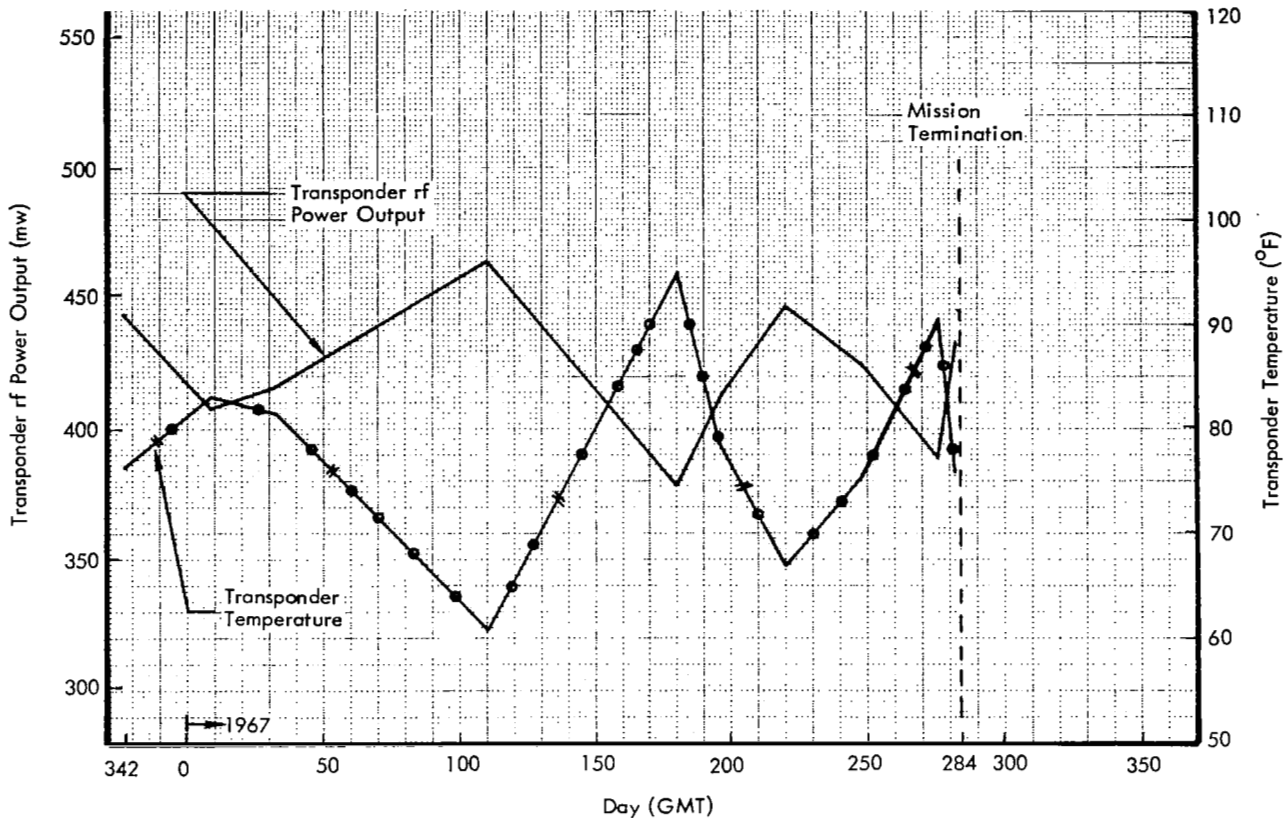
Figure 5-18: Typical Transponder rf Power Output Versus Transponder Temperature

voltage controlling the receiver gain was correct, and that the apparent variation was associated with the AGC telemetry signal conditioning circuitry. With the exception of resistor values in the input and voltage level shift circuits, the AGC telemetry signal conditioning is identical with the static phase error (SPE) telemetry conditioning circuitry. However, no problem has been encountered with SPE telemetry from any of the Lunar Orbiter spacecraft.

On Day 079 a check was made of the transponder threshold sensitivity and command threshold. These levels were determined to be −140 and −123 dbm, respectively, and are within acceptable limits. A review of the SPE and AGC telemetry conditioning circuitry by the equipment supplier indicates that 1% deposited film resistors were used in the input and voltage level shift networks of the SPE telemetry conditioning circuitry. Carbon composition resistors were used for portions of similar networks in the AGC telemetry circuitry. Due

to the nonlinear characteristics of the AGC telemetry curve, a 3% change in the composition resistors would reflect an 8-decibel change in input signal level for strong signals and approximately 1 decibel at threshold. Therefore, the anomaly encountered in AGC telemetry at strong signal levels is attributable to aging effects on the composition resistors used in the AGC telemetry conditioning networks.

During the course of the extended mission, it was demonstrated that commands could be transmitted without error beyond the spacecraft upper and lower telemetry static phase error limits of +17.544 and −15.776 degrees, respectively.

At the end of the extended mission on Day 284, the transponder had operated successfully over a period of 339 days, with no significant change in characteristics other than the telemetry indications of uplink AGC during strong signal conditions.

95

5.2.2.2 Command Decoder

The command decoder performed satisfactorily throughout the extended mission. A special test was performed on Day 342 (see Section 5.3.1) to determine command threshold. This level was determined to be -123 dbm, the nominal link analysis value. There were no errors in any of the verified words that were executed into the flight programmer.

5.2.2.3 Modulation Selector

Except for the frequency of the subcarrier oscillator, the modulation selector operation was satisfactory. The performance telemetry subcarrier oscillator operated approximately 5 to 20 cps higher in frequency than the specification limit of 30,090 cps. Mission operation was not affected by this anomaly since the ground station 30 kc demodulator had more than sufficient tuning range. The performance telemetry subcarrier frequency was measured on all subsequent spacecraft prior to launch and all frequencies measured were well within the specification requirements.

5.2.2.4 Radiation

The RDMS continued to function normally during the Lunar Orbiter II extended mission. Dosimeter 1 (DF04), located near the film cassette, had a sensitivity of 0.25 rad per count with a capacity of 0 to 255 counts. Dosimeter 2 (DF05), located near the camera looper, had a sensitivity of 0.5 rad per count and a similar capacity of 0 to 255 counts. Dosimeter 1 had recorded 1.75 rads at the beginning of the extended mission and increased to 23.5 rads by the end of the mission. Dosimeter 2 had recorded 1.0 rad at the beginning, and increased to 105.0 by the end of the mission. More detailed radiation information is presented in Section 4.1.1.

5.2.2.5 Micrometeoroid Hits

At the initiation of this extended mission, hits had already been sustained on Detectors 4, 5, and 13. Additional hits were later recorded on Dectors 01, 02, 06, 11, 15, 18, and 19. Additional information regarding the orbit parameters, spacecraft attitude, and the time of these hits is presented in Section 4.1.2.

5.2.2.6 Traveling-Wave-Tube Amplifier

On Day 284 the TWTA was commanded "on" prior to lunar impact, but did not respond to the command. It had not been commanded "on" since its failure on Orbit 179 during the prime mission.

5.2.2.7 High-Gain-Antenna Position Controller

The antenna position controller rotated the high-gain antenna in either direction as commanded for the duration of Mission II.

5.2.3 Electrical Power Subsystem

The electrical power subsystem is the sole source of all the electrical power used by the spacecraft as it performs all phases of its space mission. Radiant solar energy is collected by 2,714 N-on-P solar cells mounted on each of four solar panels and is converted into electrical energy. This energy supplies all spacecraft loads, power subsystem losses, and charge current to the nickel-cadmium battery. The shunt regulator dissipates excessive electrical energy in power dissipating elements mounted external to the spacecraft heat shield. The shunt regulator dissipates excessive electrical energy in power dissipating elements mounted external to the spacecraft heat shield. The shunt regulator also limits the bus voltage to less than 31 volts. A charge controller protects the battery from overvoltage and overtemperature conditions by regulating the charging current. The 12-ampere-hour battery provides electrical power to the spacecraft loads during periods of Sun occultation.

5.2.3.1 Solar Array Performance

The solar array operated normally throughout the extended mission. Sufficient power was provided to maintain a constant bus voltage of 30.56 volts when in the sunlight. Solar panel degradation was minimal. Total solar panel output power at the start of Mission II was 13.4 amperes at 30.56 volts. The output power then varied with time as a function of solar cell degradation and the changing solar constant. Figure 5-46 shown in Section 5.33,"Solar Panel Degradation Test," shows the changing solar panel output. This curve shows that by mid-July

1967, following approximately 8 months in orbit, the solar panels degraded less than 5%. By the end of the extended mission following 339 days of space exposure, the degradation was 5.5%. This low rate of degradation permitted the spacecraft to be operated at large off-Sun angles late in the mission to enhance the spacecraft thermal conditions.

5.2.3.2 *Battery Performance*
Battery performance was normal throughout the primary and extended missions. Adequate electrical power was provided to the spacecraft during all maneuvers and Sun occult periods. However, the battery temperatures were higher than desired. The temperatures plotted in Figure 5-19 reflect the end-of-discharge temperatures. A few of the higher temperatures reached during battery charge periods are given in Table 5-10.

Operation of the battery at these relatively high temperatures for 1 year contributed significantly to battery degradation. The last deep-discharge tests performed on GMT Days 272 and 273 showed that the battery capacity after 2,210 cycles was between 5 and 6 ampere-hours at approximately the 3-hour rate of discharge. For further details on deep-discharge tests, see Section 5.3.4.

5.2.3.3 *Shunt Regulator Performance*
On GMT Day 267, the shunt regulator started performing abnormally. The shunt regulator drew current when the bus voltage was below 30.0 volts. This occurred during periods of
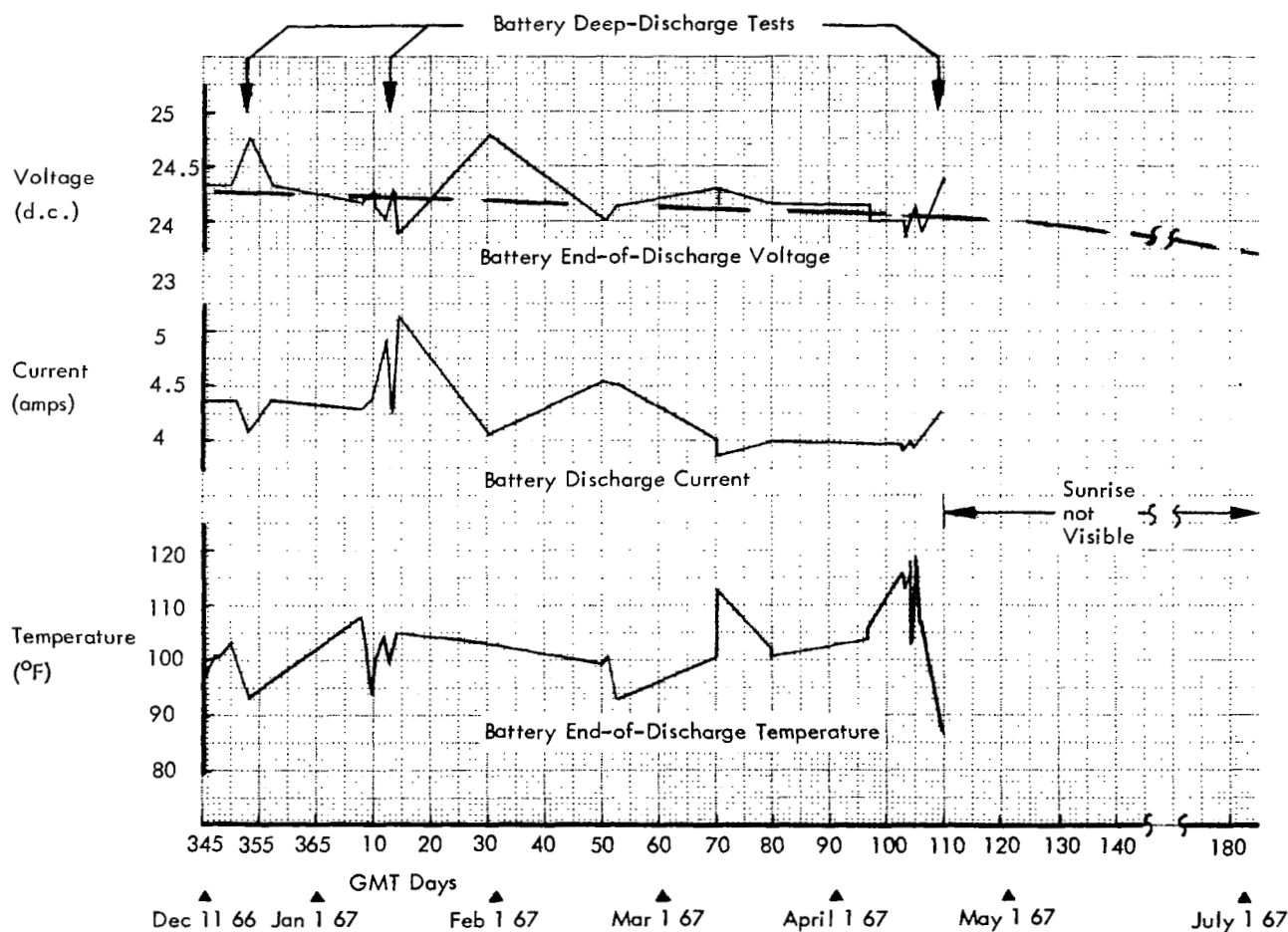
Figure 5-19: Battery Performance Characteristics

97

Table 5-10: Battery Temperature Data

GMT Day	Battery Temperature
348	127.7°F
012	109.0°F
027	109.4°F
105	108.0°F
120	118.1°F
202	123.8°F
205 6th hour	119.5°F
205 9th hour	119.8°F
205 13th hour	126.1°F
250	102.3°F
256	119.8°F
261	111.8°F
267	109.7°F
276	108.3°F

both battery charge and discharge while the spacecraft's solar array was pitched off to large solar array off-Sun angles where no current should have been shunted. The shunted currents under these conditions ranged from 0.13 to 1.25 ampere. No consistent pattern was evident. This abnormal shunt current did not affect the quality of the power supplied to the spacecraft. Insufficient information is available from the telemetry data to develop an explanation for this phenomenon. The characteristics do not parallel the failure mode experienced earlier on the Lunar Orbiter I power transistor assembly.

5.2.3.4 Charge Controller Performance
The charge controller performed properly throughout the primary and extended mission. The charge rate, which is a function of battery

temperature and voltage, was controlled to the proper level at all times. No charge controller anomalies were observed.

5.2.4 Photo Subsystem
The photo subsystem is housed in a pressurized thermally controlled container. The subsystem includes the camera, lens, film, film handling mechanisms, film processor, readout equipment, and environmental controls. The subsystem is designed to expose, develop, and read out images for transmission to Earth via the communications subsystem. Subsystem component relationships are shown in Figure 5-20.

Status of the various component elements during the extended mission follows.
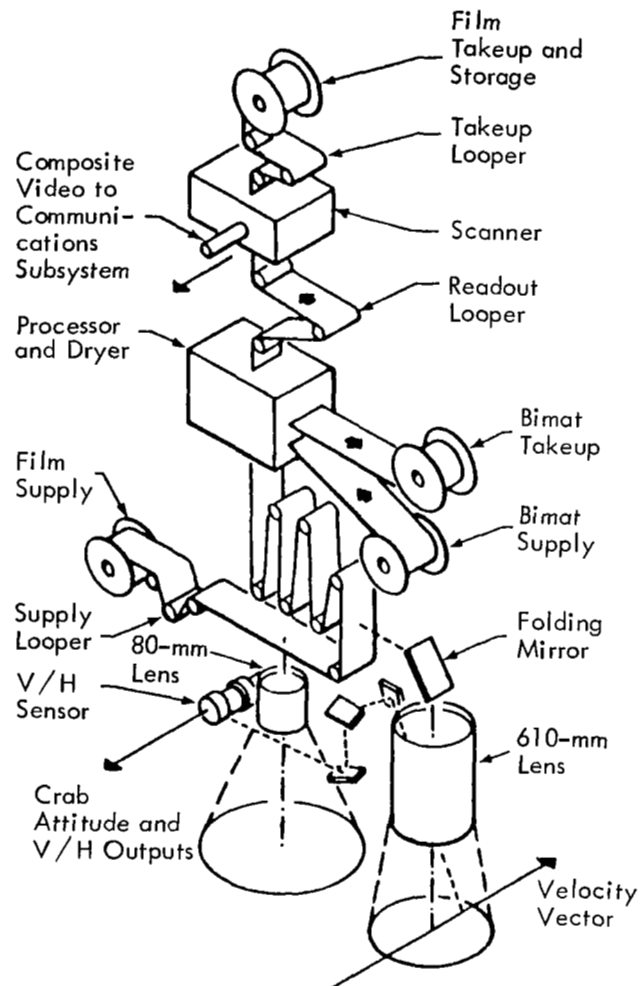
Figure 5-20: Photo Subsystem

98

5.2.4.1 Camera And Lens

No photography was possible during the extended mission because film and Bimat were exhausted on Day 330. During the latter stages of the regular mission, after failure of the TWTA, the readout mode was continued until the splice was wound back on the supply reel to an index of −23.00.

On Days 012, 013, and 027, V/H sensor exercises were conducted, as reported in Section 5.3. During the premission Lunar Orbiter III training session, Lunar Orbiter II was used extensively as a live training aid. Table 5-11 provides a list of the command activity involving the photo subsystem during the training period. Photo subsystem response to all commands was normal.

On Day 103, the shutter speed was reset from 1/100 to 1/25 second to facilitate detection of inadvertent logic changes. The indicated response to the two required "shutter speed change" commands was normal.

5.2.4.2 Film Processor

There was no processing activity during the extended mission since processing was terminated at the time of Bimat cut on Day 330.

5.2.4.3 Film Handling

During the first few hours of the extended mission, rewinding of the film was continued to a readout index of −23.00, at which point the splice between flight film and leader was safely under several wraps on the supply spool. Based on calculations from preflight threadup data and photo subsystem dimensions, 4.37 frames of Goldstone leader were then on the supply spool. With a supply spool circumference of 1.41 frames, the splice was covered by 4.37 minus 1.41 frames, or 2.96 frames. Thus, the splice would be on the outside wrap of the spool and would be subjected to increasing tension for film advances from 2.96 to 4.37 frames, with the splice being under maximum tension for advances equal to, or greater than, the latter amount.

During the V/H experiments on Days 013 through 015, 2.85 frames of film were advanced to observe the constraint that the V/H sensor should not be operated for longer than 4 minutes without advancing one frame through the platen. At this point, the splice was within 1.52 frame of being off the supply spool.

The training activity for Mission III on Days 021 through 024 resulted in 3.65 additional frames being rewound onto the supply reel. At this point the splice was covered by 3.76 frames, with a total of 5.17 frames of leader on the supply reel.

On Day 027 during the V/H sensor temperature exercise, four frames were advanced resulting in 1.17 frames of leader remaining on the supply reel. The splice was thus on the outside wrap of the spool and was subject to increasing tension with further film advances.

On Day 070 to evaluate photo subsystem performance after the camera thermal door failure, one frame was advanced. At this point the splice was within 0.17 frame of being completely off the supply spool and under full tension. To relieve the tension on the splice, 3.89 frames were rewound on Day 079. The splice was then covered by 2.65 frames of leader and remained in that condition until Day 284.

5.2.4.4 Readout Equipment

Operation of the readout section of the P/S appeared normal during the extended mission. Since the TWTA had ceased operation during the regular mission, no examination of video output was possible. However, all telemetry indications of readout parameters were normal during the extended-mission readout sequence, including the final preimpact sequence reported in Section 5.2.4.5.

5.2.4.5 Environmental Controls

Telemetry data showed that, at some time after Day 244, the photo subsystem internal pressure and the photo subsystem nitrogen makeup bottle pressure both began to decrease rather rapidly, reaching essentially 0 psi by Day 253. Both had been constant throughout the primary and extended missions, except for temperature-induced variations. It is assumed that the loss of pressure was caused either by a small micrometeoroid puncture of the photo subsystem shell, or by a small crack having opened in a weld seam or around the window, probably due to thermal cycling.

Table 5-11: Photo Subsystem Command Sequence During Training

Time—GMT Day:Hr:Min	Event	Time—GMT Day:Hr:Min	Event
021:19:46	Simulated Photo Site T-1	023:14:35	R/O drive on
021:23:16	Simulated Photo Site T-2	023:15:42	R/O drive off
022:02:41	Simulated Photo Site T-3	023:17:55	R/O electronics on
022:06:10	Simulated Photo Site T-4	023:17:55	R/O drive on
022:09:39	Simulated Photo Site T-5	023:18:01	R/O drive on
022:13:16	Simulated Photo Site T-6	023:19:14	R/O drive off
022:16:43	Simulated Photo Site T-7	023:21:00	R/O electronics on
022:23:46	Simulated Photo Site T-8	023:21:01	R/O drive on
023:03:30	R/O electronics on	023:21:04	R/O drive on
023:03:30	R/O drive on	023:22:44	R/O drive off
023:03:32	R/O drive on	024:00:30	R/O electronics on
023:05:09	R/O drive off	024:00:34	R/O drive on
023:06:54	R/O electronics on	024:00:39	R/O drive on
023:06:55	R/O drive on	024:02:17	R/O drive off
023:07:03	R/O drive on	024:04:00	R/O electronics on
023:08:40	R/O drive off	024:04:04	R/O drive on
023:10:21	R/O electronics on	024:04:09	R/O drive on
023:10:22	R/O drive on	024:05:47	R/O drive off
023:10:24	R/O drive on	024:08:09	R/O electronics on
023:12:12	R/O drive off	024:08:11	R/O drive on
023:12:15	R/O drive on	024:08:16	R/O drive on
023:14:32	R/O electronics on	024:08:48	R/O drive off
023:14:33	R/O drive on		
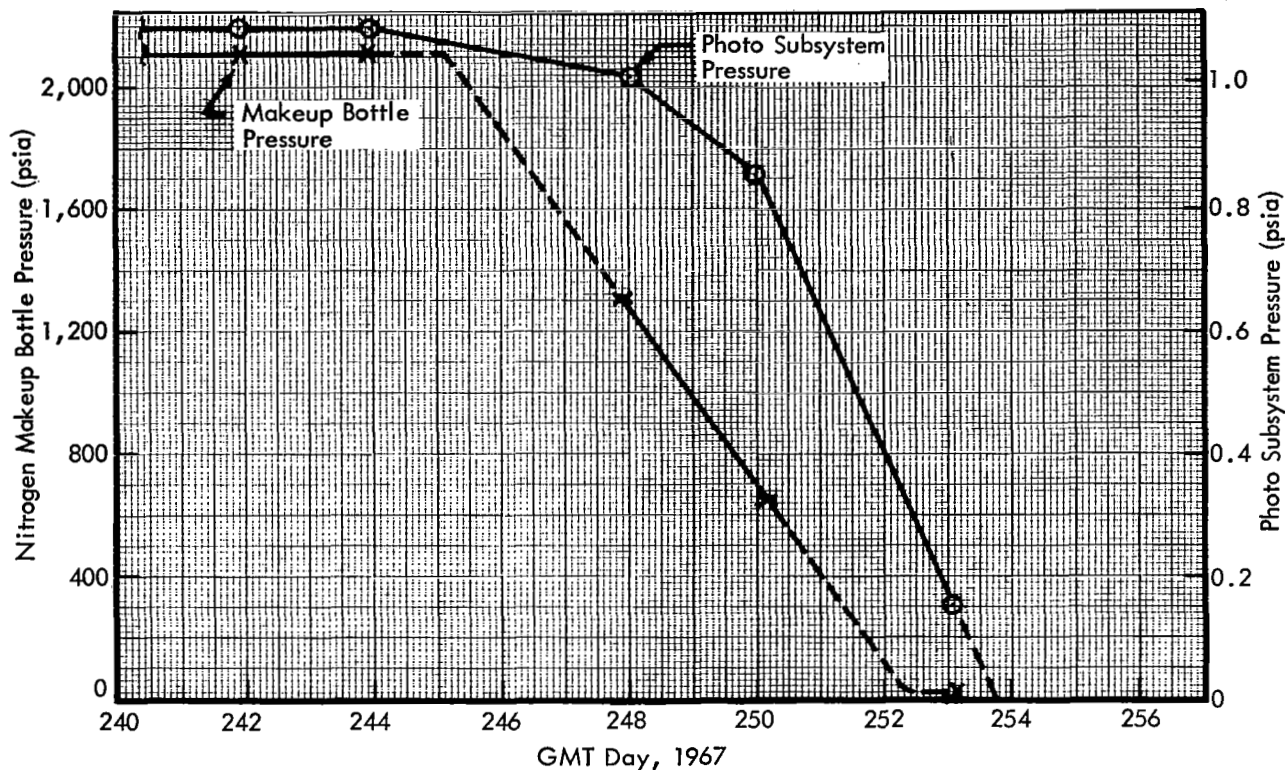
Figure 5-21: Photo Subsystem Pressure Loss

Figure 5-21 shows the photo subsystem pressure changes as revealed by the limited telemetry data that are available. Analysis of these data in conjunction with the characteristics of the nitrogen and humidity controls of the photo subsystem revealed that the area of the leak was probably between 0.76×10^{-4} in.^{2} and 4.5×10^{-4} in.^{2}.

On Day 284, shortly after completion of the final burn, the photo subsystem was activated in an attempt to determine whether the photo subsystem could operate in a very-low-pressure environment. At this time, both the photo subsystem pressure and N_2 bottle pressure were zero psia as indicated by telemetry. The photo subsystem logic was set to a known state while the photo subsystem was in the solar eclipse mode. A short (11.5 minutes) Goldstone leader readout sequence was commanded, followed by two 16-frame camera sequences. The command sequence is shown in Table 5-12.

Telemetry indications of readout voltages appeared normal. However, the readout rate, as indicated by the increase in Readout Looper Contents (PB03), was only 0.218 inch per minute rather than the normal 0.272 inch per minute. This reduced rate of movement may be due to either or both of the following two causes.

1) Since there had been no film movement in the photo subsystem for 105 days (since Day 079), some film-set would have developed, even in the extremely flexible estar leader material. This would have been most pronounced around the small-diameter rollers of the takeup looper, optical mechanical scanner, and readout looper. The consequence of this could have been that the OMS was not able to move the film in full 0.10-inch advances for each scan.

2) The OMS drive motor or the film takeup motor may have been rendered only partially operational by the low pressure, thus not pulling film through the OMS

101

Table 5-12: Photo Subsystem Command Sequence for Low-Pressure Environment

Time — GMT Day:Hr:Min:Sec	Event	Comments
		Camera Reset Logic Sequence
284:06:05:23.7	Solar eclipse on	Command not verified because "S.E. Off" (below) occurred within T/M frame
284:06:05:23.8	Cut Bimat	Command verified
06:05:23.9	Fast 16	PC03 to 7, command verified
06:05:24.0	Camera on	Command verified
06:05:24.1	V/H sensor off	Command verified
		R/O Sequence
284:06:05:27.5	Solar eclipse off	See "S.E. On" above
06:05:27.6	R/O electronics on	Command verified
06:09:18.3	R/O drive on	Command verified
06:10:22.6	R/O drive on	Command verified
06:11:00.0	Photo video gain increase	Command verified R/O progressed normally, P B03 increased from 2.84 to 5.57 inches.
284:06:20:37.3	R/O drive off	Command verified-R/O electronics remained on
284:06:21:28.7	R/O drive on	Command verified
06:22:43.6	R/O electronics off	P B03 remained at 5.34
		Camera Sequence
284:06:22:20.1	Camera on	Command verified
284:06:23:11.5	Camera on	Command verified
06:23:52.7		Maximum P B02 = 244.56
284:06:28:06.1		P B03 returned to 2.84

No further photo subsystem action prior to impact.

at the proper rate, or releasing it into the takeup looper in a normal manner.

Film advance during the "camera-on" (wind forward) sequence appeared normal. Figure 5-22 shows a plot of both camera storage looper and takeup reel contents. It may be seen that the second 16-frame advance filled the camera looper, which would then terminate the camera sequence before its completion. Approximately 25 frames were advanced rather than the commanded 32 frames.

During the camera-on sequence the takeup contents increased at approximately 0.77 inch per second rather than at the expected 1.0 to 1.25 inch-per-second rate. This lower rate may

be due to the same reasons mentioned above in connection with the reduced readout rate.

5.2.5 Structure and Mechanisms

The structure and mechanisms subsystem consists of the support structure, thermal control coatings, thermal barrier, engine deck heat shield, solar panel and antenna deployment mechanisms, camera thermal door, rocket engine gimbal, bipropellant tank heaters, and the interconnecting electrical wiring.

With the exception of the camera thermal door (CTD) and the rocket engine gimbal, this subsystem is in a passive state during the extended mission. Only the thermal control coating and the CTD performance are discussed, since the
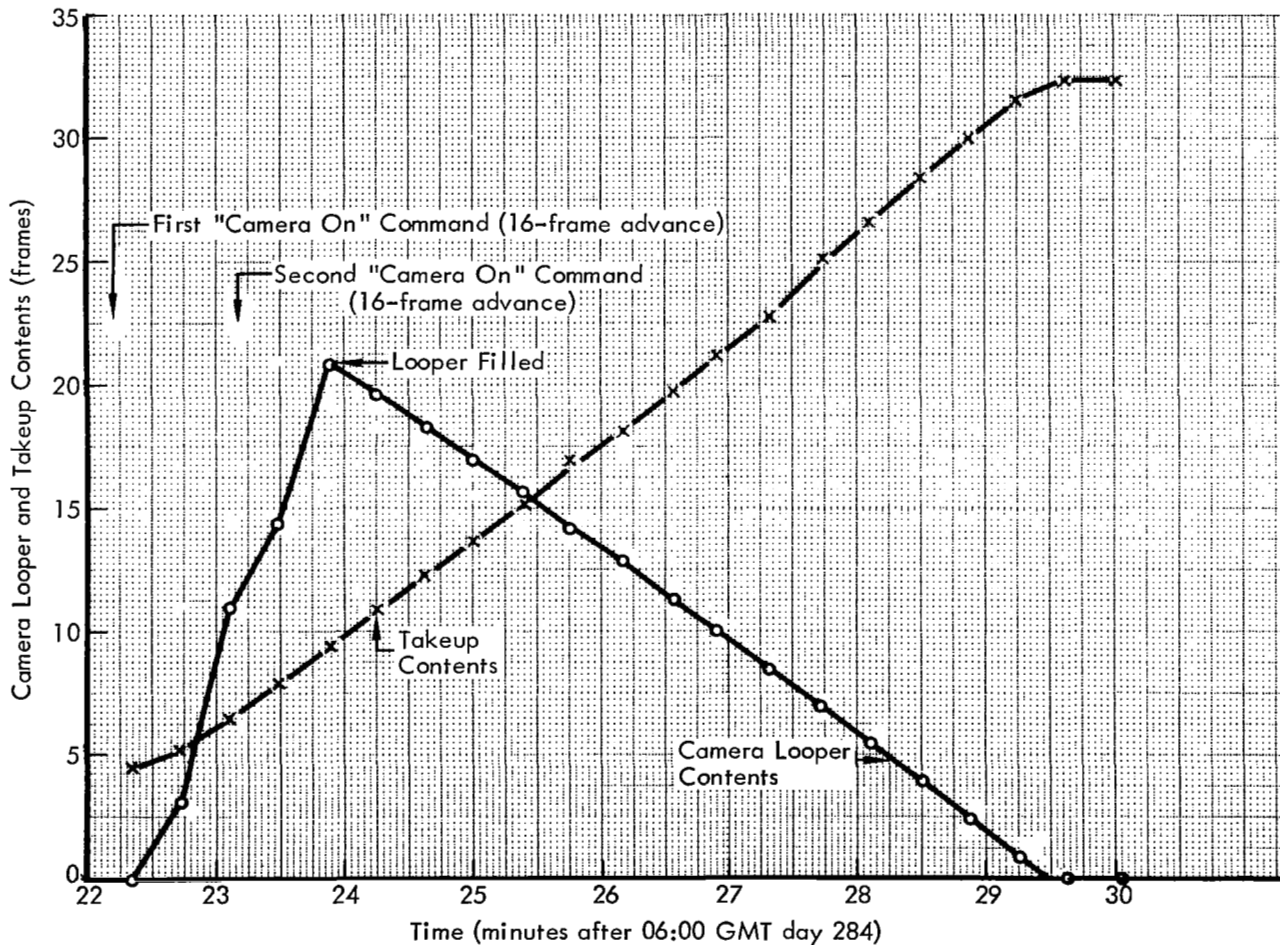
Figure 5-22: Camera Looper and Take-up Reel Contents

103

remainder of the subsystem performed as anticipated.

5.2.5.1 Equipment-Mount Deck Thermal Control Coating

The Mission I EMD thermal control coating (B1056) degraded at a higher rate than anticipated, requiring that the spacecraft be operated off-Sun to maintain proper thermal control. Since the increased solar intensity for Mission II would result in temperatures approximately 6°F higher, it was apparent that the mission should be altered to fly off-Sun and/or the EMD thermal coating should be improved. It was decided to overcoat the EMD for Mission II with 2 mils of S13G paint, based on 350 equivalent Sun hours of testing by Hughes Aircraft Company on a coupon of S13G over B1056. The Hughes test data indicated that approximately 10°F improvement in EMD temperatures could be expected with the S13G overcoat. In addition, Mission II would be flown off-Sun, except during picture taking, in order to retard the thermal coating degradation.

The coating S13G over B1056 resulted in an initial thermal improvement of approximately 9°F over that of Mission I. However, by the end of the photographic mission the degradation of the S13G over B1056 was approaching that of the Mission I coating and required that the spacecraft be oriented approximately 50 degrees off-Sun for thermal control. Figures 5-23 through 5-26 show the EMD temperatures and the approximate spacecraft angle off-Sun for reference. The extent to which the thermal coating has been degraded cannot be determined because the spacecraft attitude was not constant for a sufficient period of time to allow the EMD temperature to stabilize during the tracking period.

The spacecraft was instrumented with a paint coupon assembly to provide flight data on thermal control coatings by measuring the temperature of the individual coupons.

The following paint coupons were installed on the spacecraft.

Paint Coupon	Telemetry Measurement Identification
B1056	ST06
Second surface mirror over B1056	ST07
B1059 over B1056	ST08
S13G over B1056	ST09

The coupon assembly design permitted reflected and/or radiated thermal energy to "view" the bare aluminum edge of the coupons. The combined effect of direct solar energy and radiated energy (from sources such as the back of solar panels) resulted in elevated coupon temperatures. This masked the characteristics of the individual coupons and, therefore, did not allow meaningful thermal degradation data to be obtained from the coupons' telemetry.

5.2.5.2 Camera Thermal Door

Between the tracking periods of GMT Day 048 and 050, 1967, the programmer memory was scrambled, presumably by erroneous receipt of commands transmitted to Lunar Orbiter III. One of the adverse results of this condition was the "CTD open control" activation, opening the camera thermal door. When the change in the programmer memory was observed and corrected, the fact that the CTD open control had been activated was not detected even though the CTD was fully open, as indicated by the "1" state of telemetry measurement PC18. This left the CTD motor being continuously pulsed in the open direction and driving against the open stop. On GMT Day 068, 1967, the CTD open condition was detected and a "CTD control off" command was executed. Since this and subsequent attempts to close the door were unsuccessful, it is reasonable to assume that the 18 days of continuous pulsing resulted in failure of the CTD motor.

5.2.6 Velocity and Reaction Control Subsystem

The velocity control subsystem consists of the propellant pressurization equipment, the pro-
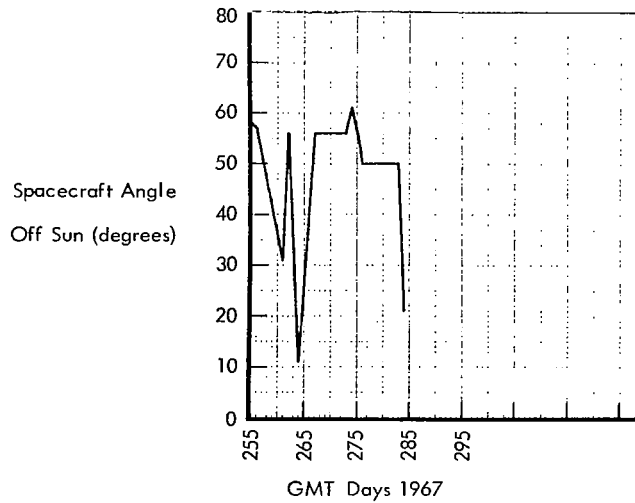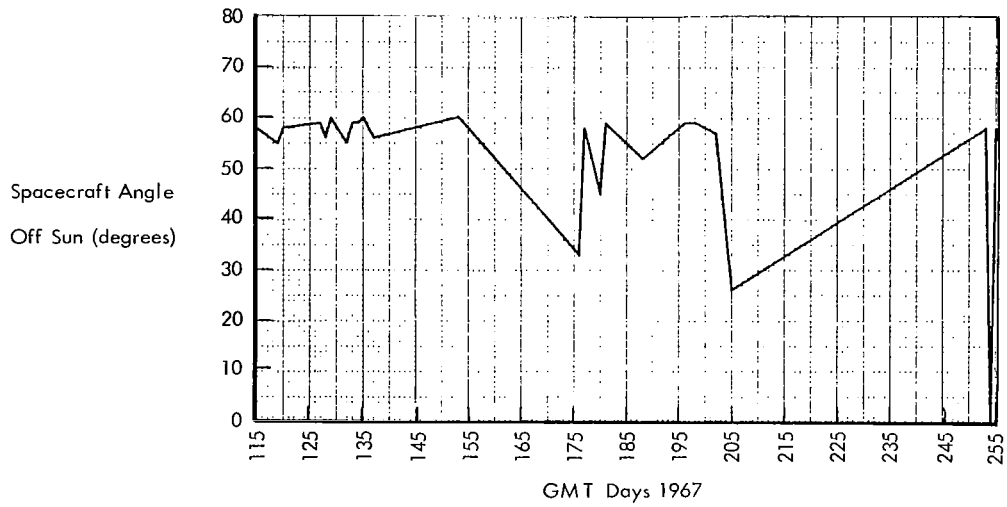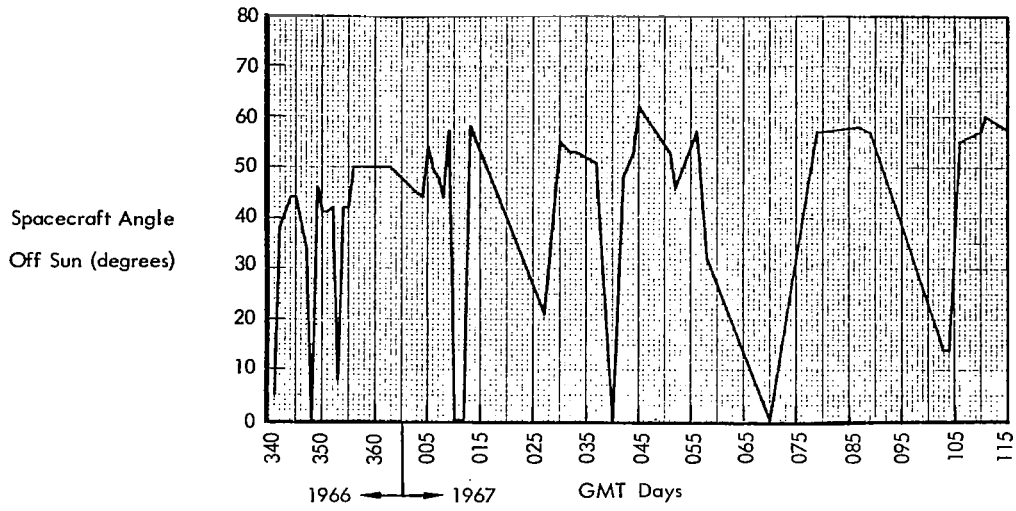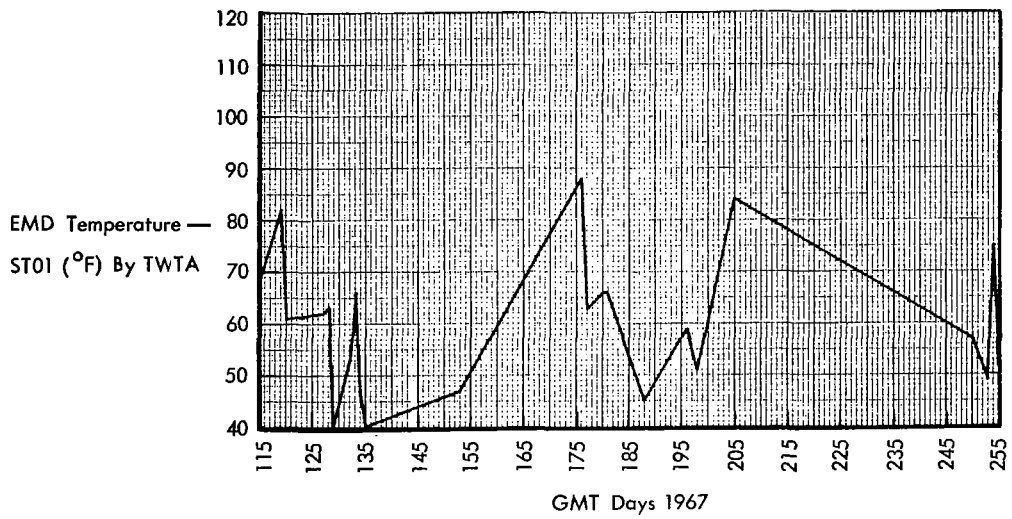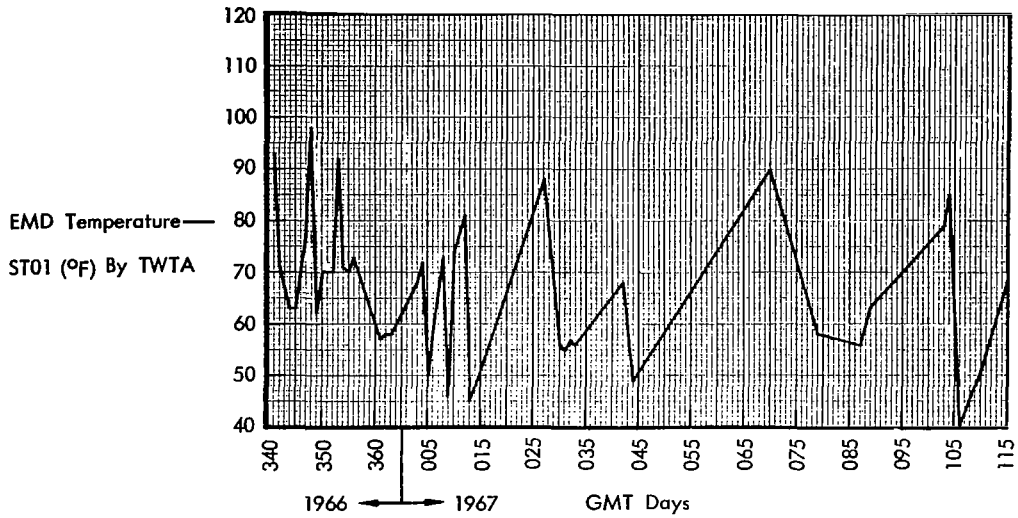
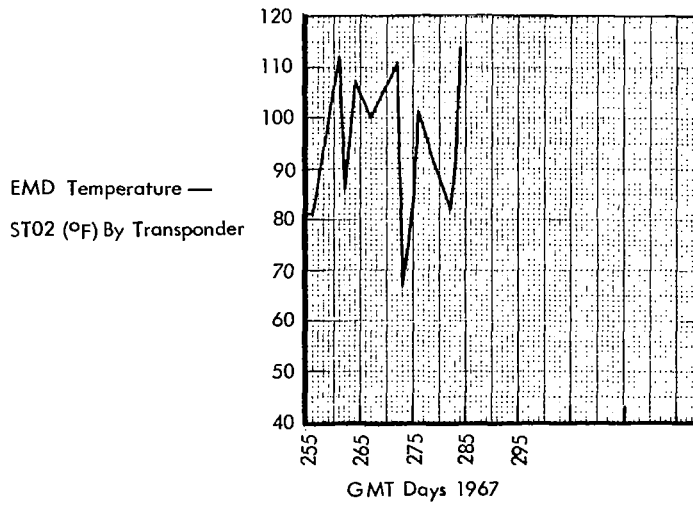**Figure 5-23: Spacecraft Angle Off-Sun History**
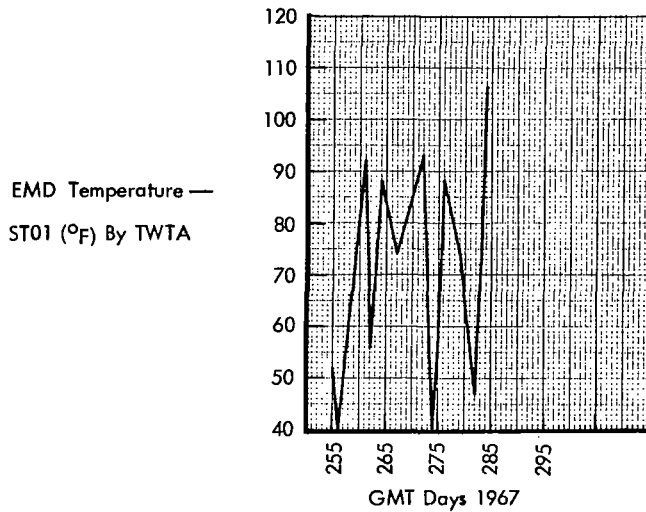
Figure 5-24: EMD Temperature History — TWTA

EMD Temperature —

ST02 (°F) By Transponder

1966 ←——→ 1967   GMT Days

EMD Temperature —

ST02 (°F) By Transponder

GMT Days 1967

EMD Temperature —

ST02 (°F) By Transponder

GMT Days 1967
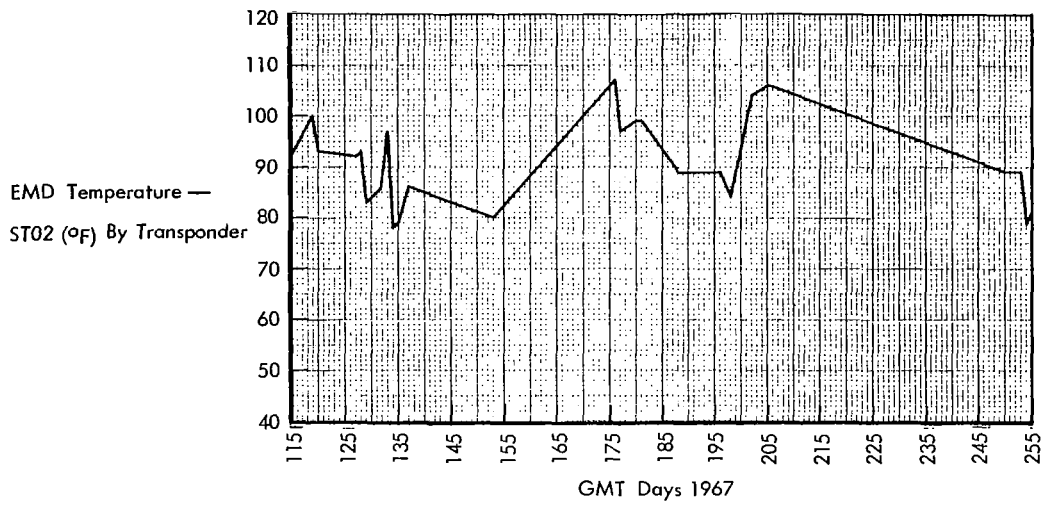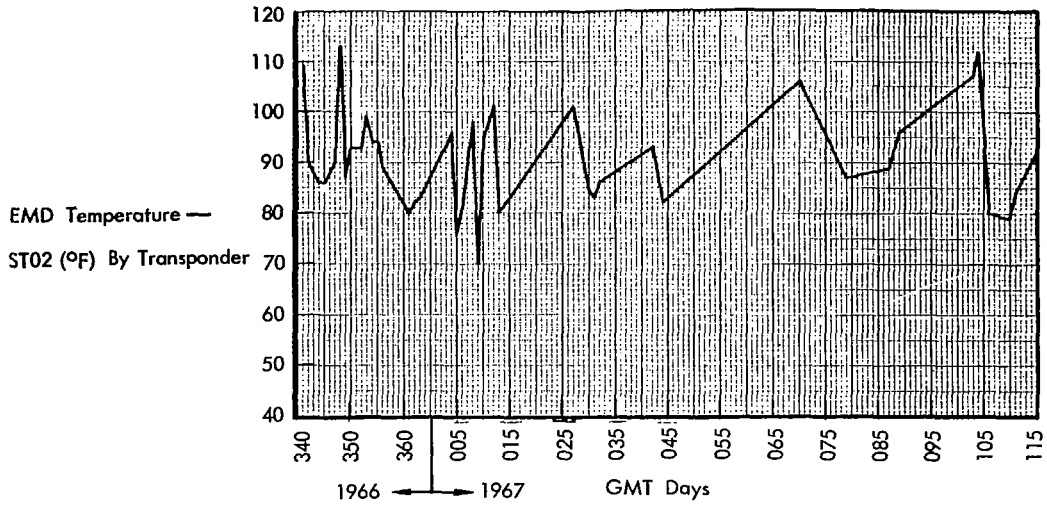
Figure 5-25: EMD Temperature History — Transponder

107

EMD Temperature —
ST03 (°F) By IRU

1966 ←——→ 1967   GMT Days

EMD Temperature —
ST03 (°F) By IRU

GMT Days 1967

EMD Temperature —
ST03 (°F) By IRU

GMT Days 1967
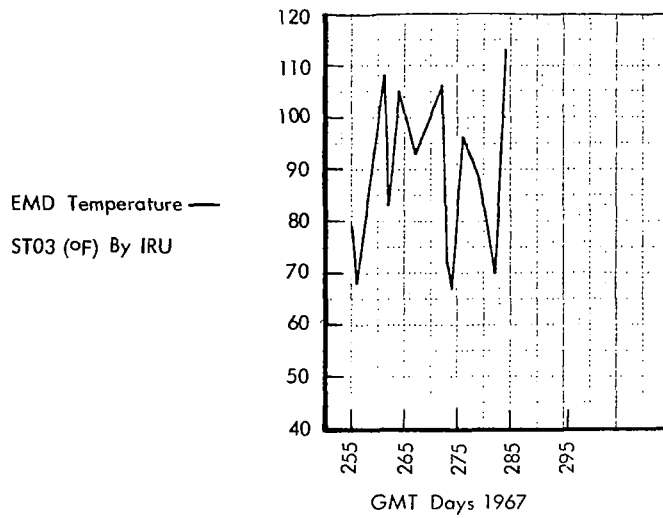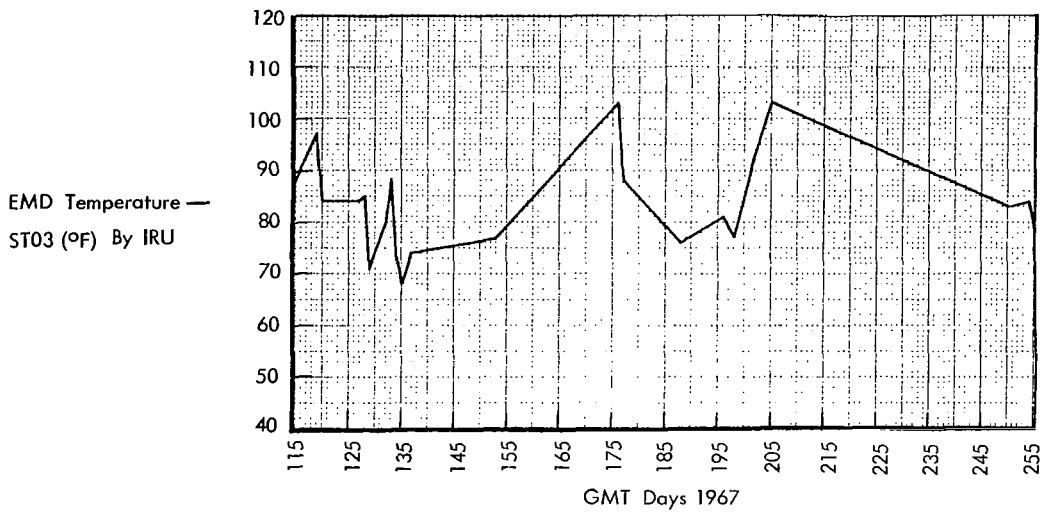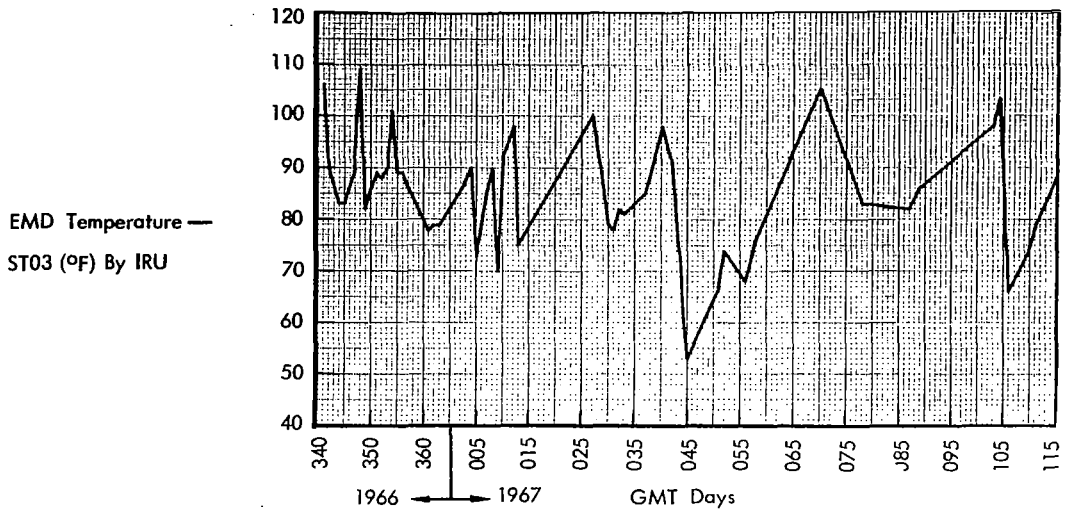
Figure 5-26: EMD Temperature History — IRU

pellant storage tanks and feed system, the bi-propellant rocket engine, and the thrust vector control (TVC) actuators. The reaction control subsystem includes the nitrogen storage tank (which is common to the velocity control system), thrusters and interconnecting plumbing, filter, and regulator. The reaction control subsystem provides the impulsive force to maintain attitude control and perform attitude maneuvers about the pitch, roll, and yaw axes of the spacecraft. The velocity and reaction control subsystem is shown schematically in Figure 5-27.
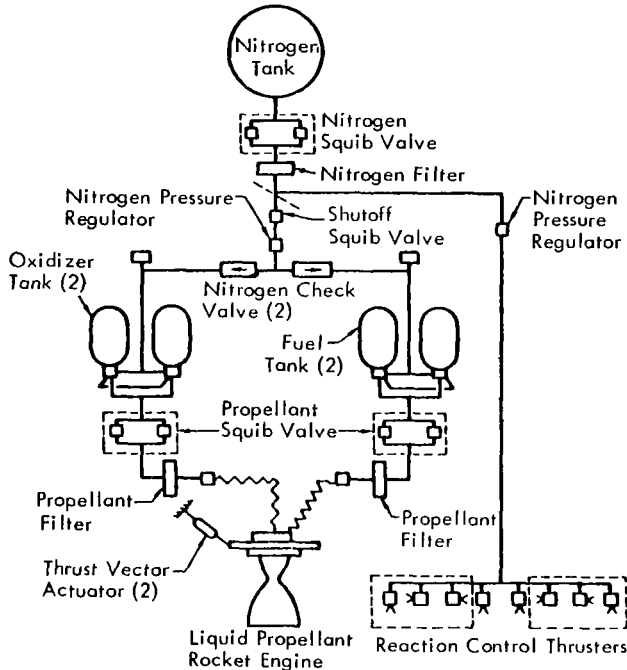
Figure 5-27:
Velocity and Reaction Control Subsystem

5.2.6.1 Reaction Control Subsystem Performance

The reaction control subsystem performed satisfactorily throughout the extended mission. The system maintained spacecraft attitude control in wide (2-degree) deadzone while on inertial hold in all three axes during the major part of the extended mission. Maneuvers were generally limited to those required for updating of the spacecraft pitch and yaw positions for thermal control and for special tests. To mini-

mize nitrogen consumption, most maneuvers were performed with the attitude control system operating in wide deadzone. The time histories of nitrogen tank pressure and temperature are shown in Figures 5-28 and 5-29, respectively.

Reaction control subsystem performance was evaluated on the basis of the nitrogen gas consumption for attitude control and thruster performance. It was concluded that the reaction control subsystem performance was nominal throughout the extended mission. There was no evidence of degradation in reaction control subsystem performance from that of the primary mission presented in Volume III of this report.

Typical orbital variations of the thermal environment during the extended mission are shown in Figure 5-30. The tank deck temperature is representative for the pressure regulation system components. The temperature environment for the thrusters would be from 5 to 10 degrees colder than the temperatures in the area surrounding the nitrogen storage tank.

Nitrogen Usage — Nitrogen usage is calculated, knowing the volume of the high-pressure system, by using the telemetered nitrogen storage bottle pressure and temperature. Predicted usage rate calculations are based on the maneuvers performed, the spacecraft moment of inertia about each axis, estimated limit cycle usage rates, and estimated disturbances. Minimum predicted nitrogen usage is based on minimum (single) pulsing of 12 milliseconds' duration of the thrusters during limit cycle operation. The maximum usage limit is based on pulse durations for limit cycle operation that result in 0.0025-degree-per-second angular rates in each axis. The equivalent pulse duration would be 35 milliseconds in pitch and yaw and 65 milliseconds in roll. Predicted usage rates for maneuvers (including Sun and Canopus acquisitions) and disturbances are the same for the minimum and maximum limits.

The actual nitrogen gas usage for the extended mission is shown in Figure 5-31. The major events that caused the higher usage rates are
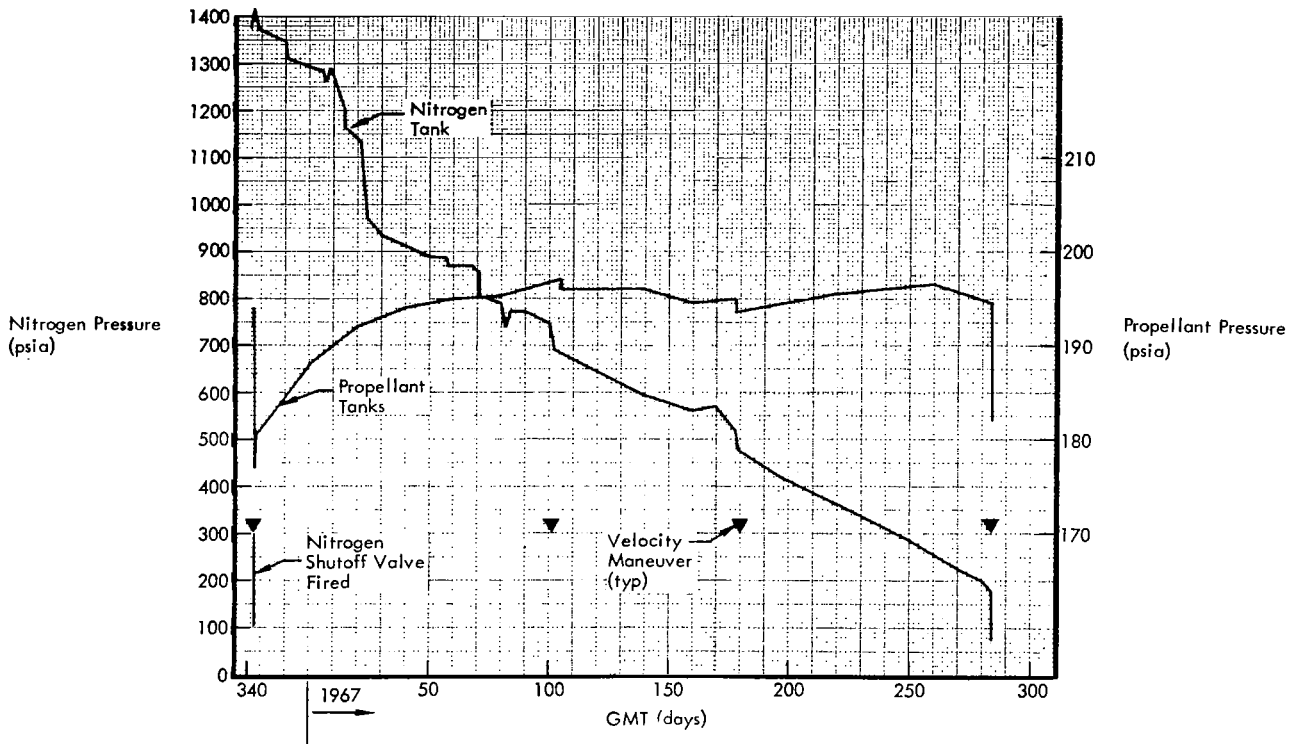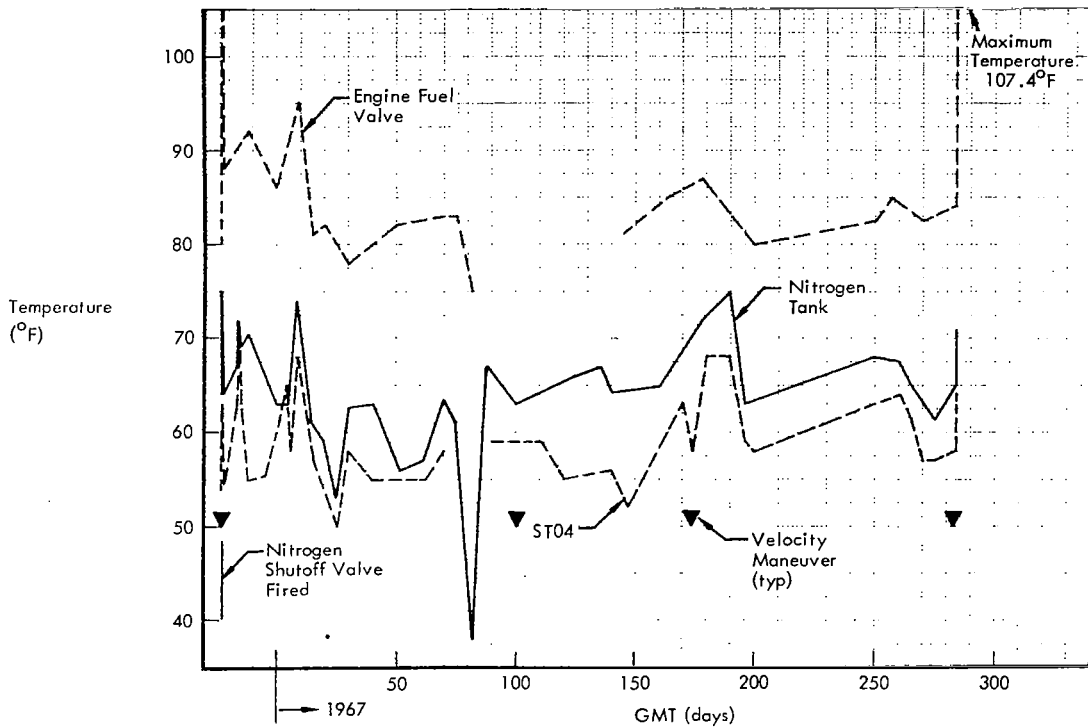
Figure 5-28: Nitrogen Tank Pressure History

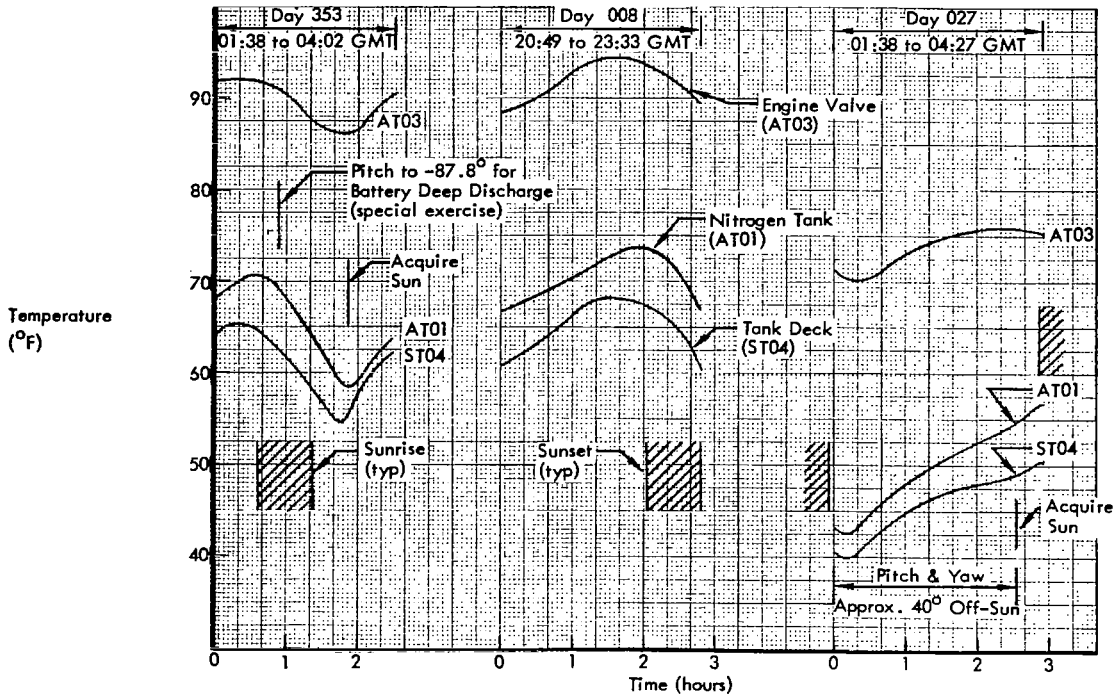Figure 5-29: Nitrogen Tank Temperature Profile

110

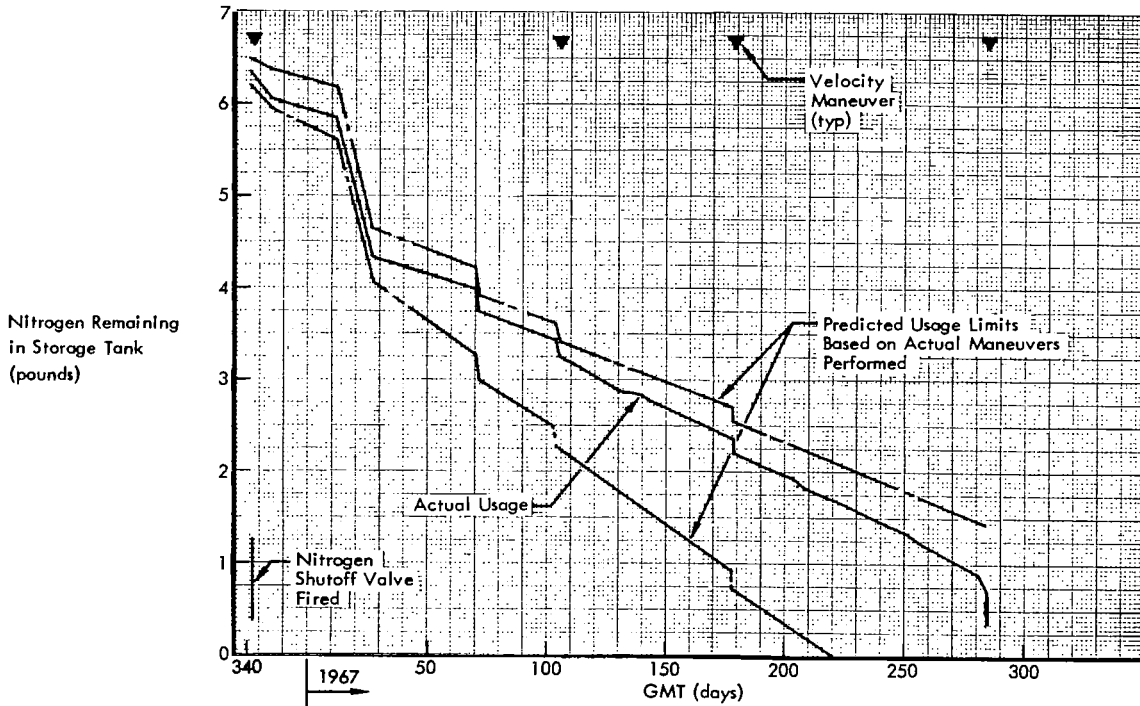Figure 5-30: Typical Orbital Thermal Variations

Figure 5-31: Nitrogen Supply Usage

111

summarized in Table 5-13. The nitrogen usage for the normal extended-mission mode of operation, which includes thermal maneuvers and ±2.0-degree limit cycling, ranged from 0.0125 to 0.0081 pound per day, with an average of 0.0104 pound per day. The maximum and minimum predicted rates are 0.018 and 0.010 pound per day, respectively.

5.2.6.2 *Thruster Performance*

Typical variations in spacecraft attitude during the extended-mission inertial hold mode of operation are shown in Figure 5-32. The effects of solar pressure and gravity gradient disturbances are particularly noticeable on the pitch and roll axes. Gravity gradient disturbances can be seen on the pitch and yaw axes after sunset. The pulse duration to accomplish each of the attitude reversals was analyzed and found to range from 15 to 53 milliseconds in roll, 19 to 34 milliseconds in pitch, and 10 to 36 milliseconds in yaw. All the pulse durations evaluated were within the predicted limits when the disturbances were taken into account

except for those occurring during tracker turn-on, which are shown in Figure 5-32. Triggering of the thrusters during the star tracker turn-on results from electrical noise peaks on the command signal line. The nitrogen required to take out the attitude rates resulting from this triggering is more than offset by the nitrogen saved due to the sensitive deadband control provided by the circuit for normal noise conditions. This condition is therefore not considered to be detrimental to the overall attitude control subsystem performance.

Although thruster performance cannot be directly determined from flight data, the compatibility between predicted and actual thruster operating modes and nitrogen usage verifies that the specific impulse in flight is very close to predicted values established from ground testing. The specific impulse used for predicting nitrogen usage was 68 seconds for limit cycle mode and 71 seconds for maneuvers.

Following the impact orbit transfer maneuver

Table 5-13: Major Events Using Nitrogen Gas

| Day (GMT)	Events	Day (GMT)	Events
342	Inclination change maneuver	028 to 070	Extended-mission mode of operation
348	Paint degradation test Solar degradation test Bright object sensor test	070	Canopus tracker glint tests
		071 to 104	Extended-mission mode of operation
353	Battery deep discharge test Gyro drift test Pitch and yaw maneuver Accuracy test	104	Orbit phasing maneuver
		105 to 178	Extended-mission mode of operation
354 to 010	Extended-mission mode of operation	178	Perilune increase maneuver
010	Star map	178 to 284	Extended-mission mode of operation
012	V/H survey - eastern limb V/H roll test	284	Impact orbit transfer maneuver
021 to 024	Mission III training exercises		
027	V/H survey - western limb V/H roll and pitch tests		
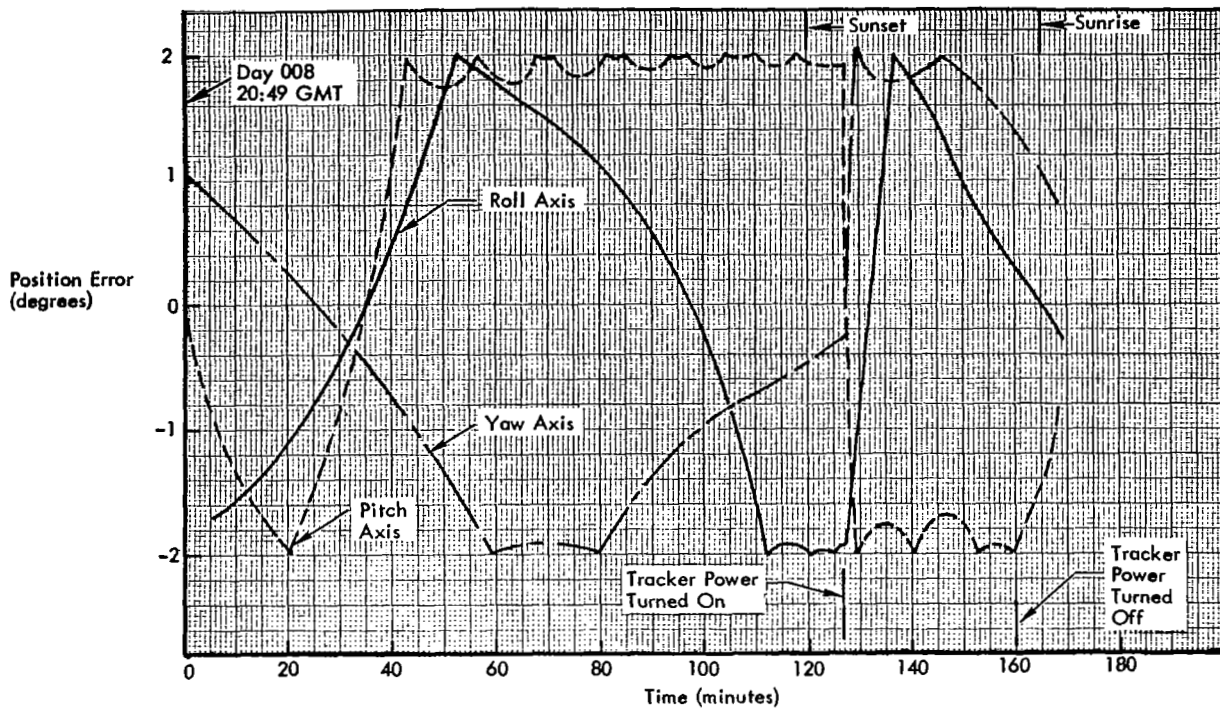
Figure 5-32: Reaction Control Subsystem Limit Cycle Operation in ±2.0-Degree Inertial Hold

(Day 284), a series of plus roll maneuvers was performed to determine the minimum storage bottle pressure at which the thrusters could maintain adequate control capability. As shown in Figure 5-28, on Day 284 the pressure in the nitrogen tank started at 180 psia and was reduced to 70 psia at the time data terminated as the spacecraft passed behind the Moon on its impact trajectory. An analysis of attitude control data confirmed that the spacecraft was maneuvering properly, with indicated nitrogen storage tank pressures as low as 70 psia. Ground tests performed on the system at low inlet pressures confirmed that rated thrust could be achieved in any one axis at inlet pressures as low as 77 psia.

5.2.6.3 Velocity Control Subsystem Performance

Velocity control subsystem performance was analyzed on the basis of telemetered propellant tank pressures, actuator position, and incremental velocity change. The velocity control subsystem was operated four times during the extended mission, each time successfully, with no evidence of degradation.

The propellant tank pressures and system temperatures during the extended mission are shown in Figures 5-28 and 5-29, respectively. Fuel and oxidizer tank pressures were at 195 psia prior to the orbit inclination velocity maneuver. The nitrogen shutoff squib valve which isolates the propellant tanks from the nitrogen storage bottle (Figure 5-27) was operated on Day 342 at 13:44 GMT, prior to the start of the orbit inclination maneuver. The propellant tank pressures dropped to 177 psia due to propellant expulsion during the engine burn and gradually increased to 195 psia during the next 60 days, which indicated a small internal leak in the shutoff squib valve. The initial pressure rise between Days 343 and 355 represents a leak rate of 140 standard cubic centimeters per hour. The pressure did not increase above the regulator lockup pressure of approximately 195 psia, however, indicating that the leak into the propellant tanks had virtually stopped. The reduction in leakage rate resulted from lockup of the pressure regulator which occurs at 195 psia, based on performance during the basic photographic mission. All other aspects of the velocity control subsystem

113

were normal throughout the extended mission. The details of each velocity maneuver performed during the extended mission are discussed in the following paragraphs.

Inclination Change Maneuver -- On Day 342, at 20:36 GMT, a velocity change maneuver was initiated to change the orbital inclination of Lunar Orbiter II from 12.0 degrees to 17.5 degrees. This inclination change was performed to provide data on an orbit with an inclination as close as practicable to the 21 degrees planned for Mission III. The maneuver provided a velocity change to the spacecraft of 100 meters per second, which is shown as a function of time in Figure 5-33. The average thrust during the burn was 99.6 pounds, as computed from acceleration and spacecraft weight. This value shows close agreement with the predicted thrust of 99.4 pounds based on the average propellant tank pressure, established from the data shown in Figure 5-34. The subsystem operated in the "blowdown" mode, since the shutoff valve had previously been actuated. The engine burn time established from telemetry data was 61.3 seconds. Engine fuel valve temperature during and after the burn, as presented in Figure 5-35, shows the typical effects of heat soak-back into the valves from the chamber.
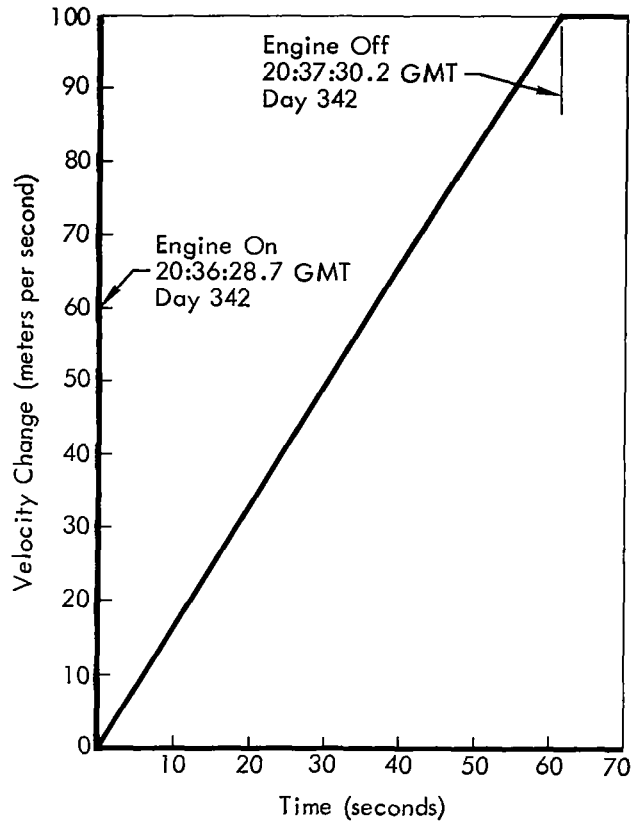
Figure 5-33:
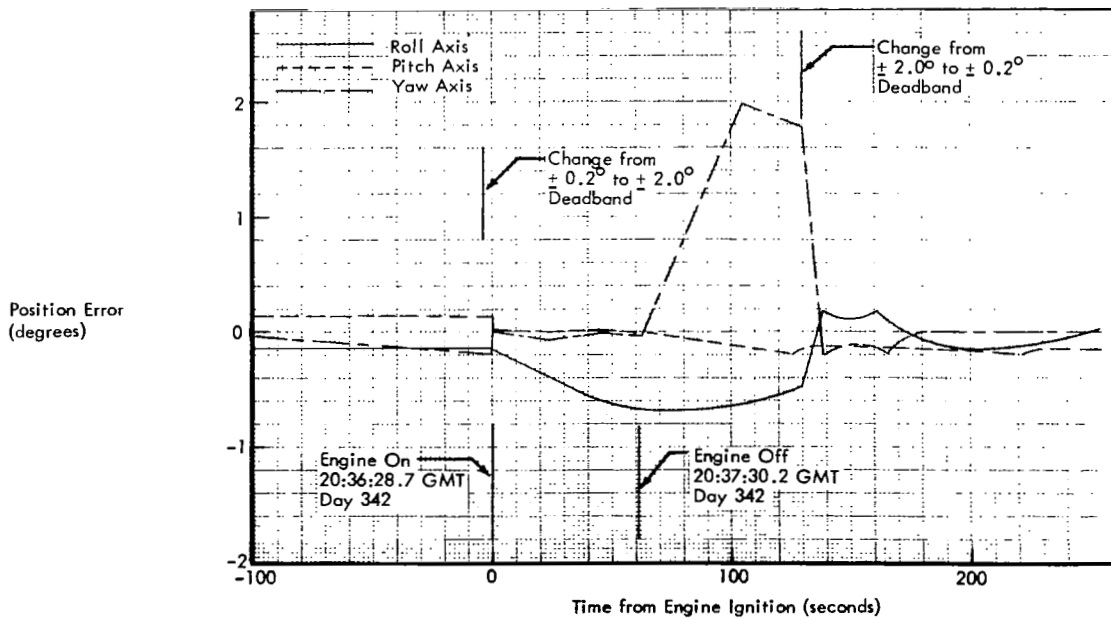**Engine Burn — Inclination Change Maneuver**
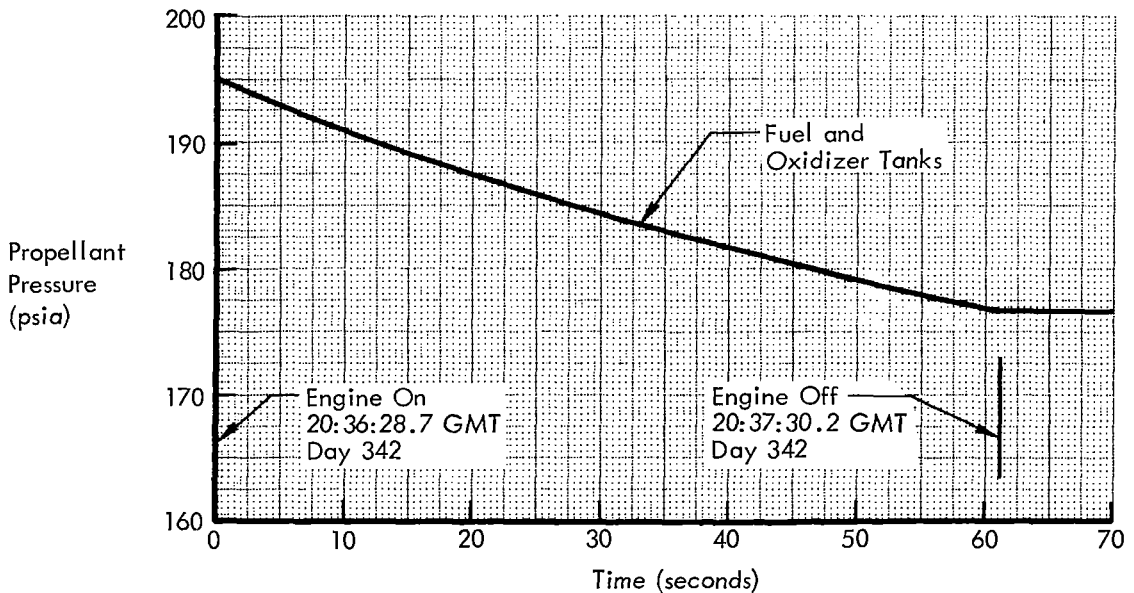
Figure 5-34: Propellant Tank Pressures — Inclination Change Maneuver
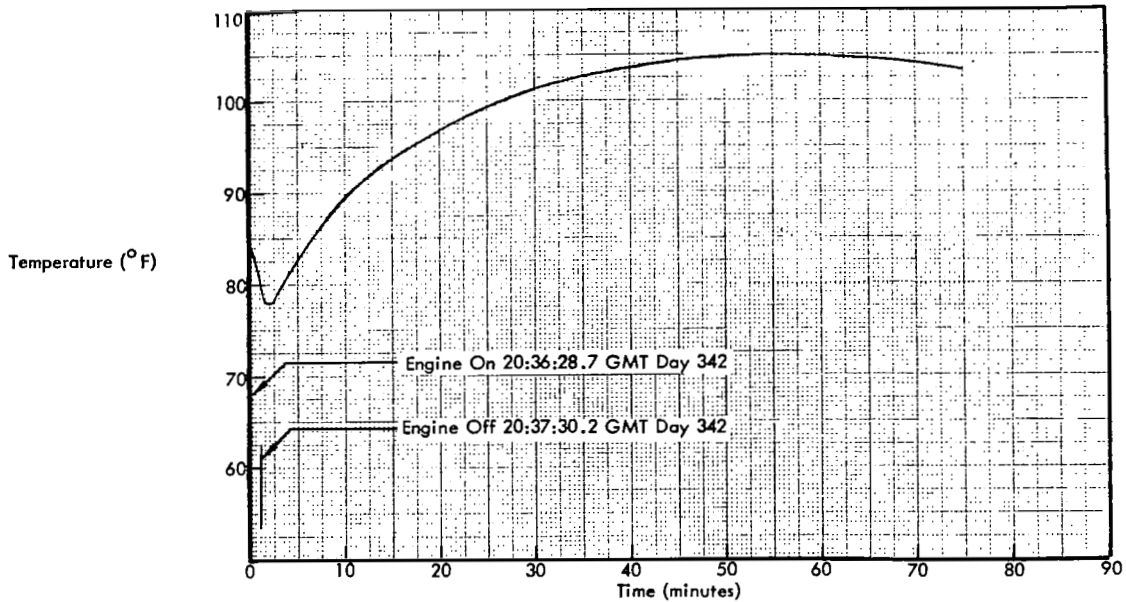
Figure 5-35: Temperature Soak-Back to Engine Fuel Valve — Inclination Change Maneuver

Performance of the thrust vector control system was satisfactory throughout the burn, as shown by Figure 5-36. No excursions in spacecraft attitude beyond ±0.1 degree were observed from telemetry data during the period the thrust vector control system had control capability.

The engine position data shown in Figure 5-37 confirm the stability of the system during the velocity maneuver. The engine position data also show that the spacecraft center of gravity location relative to the engine pointing angle has remained essentially constant throughout the mission.

Figure 5-36: Attitude Control — Inclination Change Maneuver
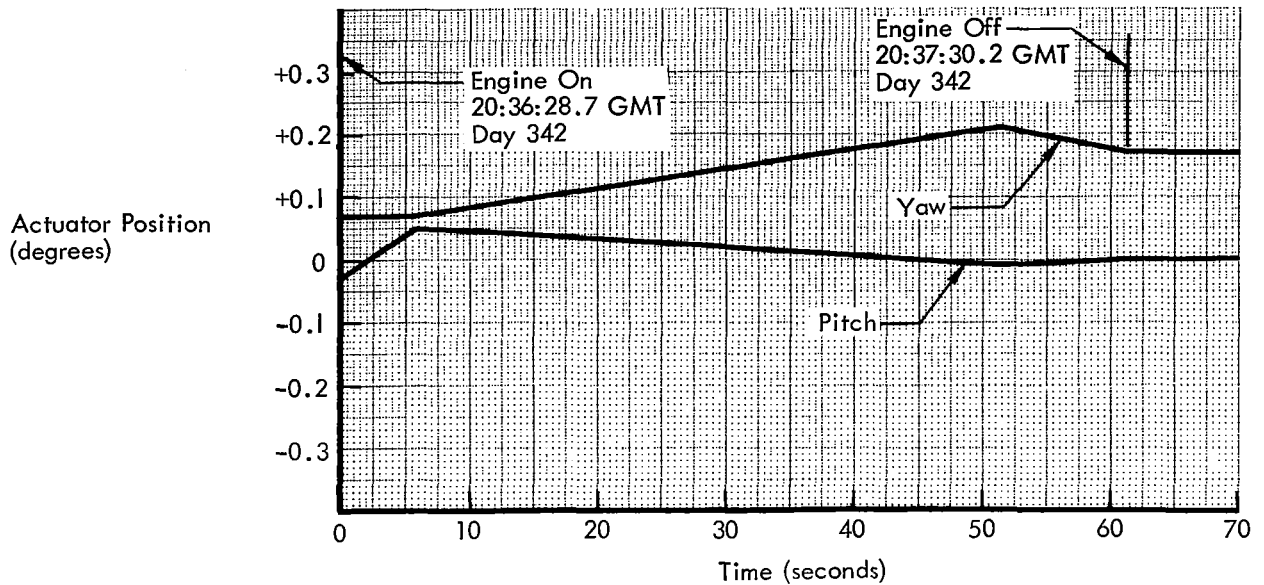
Figure 5-37: TVC Actuator Position — Inclination Change Maneuver

Orbit Phasing Maneuver -- On Day 104, at 09:01 GMT, a velocity change was performed to change the orbital phasing of the spacecraft to minimize the continuous time in the dark during the lunar eclipse of Day 114. The maneuver was required to impart to the spacecraft a velocity change of 5.5 meters per second, which was calculated to require a burn time of 3.2 seconds. Because of the short duration of the burn as compared to the data sampling rate it was not possible to confirm engine-burn time or thrust (estimated to be 103 pounds). The maneuver did terminate exactly as programmed, based on telemetered velocity data; in addition, the magnitude was verified by tracking data. The engine burn was short enough to preclude any extensive decay in propellant tank pressures which, although operating in the blowdown mode, decayed only 1.0 psi. The nitrogen gas supply pressure remained constant (the shutoff squib valve had been actuated).

Performance of the thrust vector control system was satisfactory, as shown in Figure 5-38.

Perilune Increase -- On Day 178, at 07:00 GMT, a velocity change maneuver was performed to raise the orbit perilune from approximately 67 kilometers to 113 kilometers to preclude lunar impact due to orbit decay. The maneuver

was required to impart to the spacecraft a velocity change of 8.0 meters per second, which would require a calculated burn time of 4.6 seconds. Because of the short duration of the burn as compared to the data sampling rate it was only possible to establish the engine-burn time (4.6 seconds) and the thrust level (103.3 pounds) by using the programmed time for engine ignition as a data point. The maneuver did terminate exactly as programmed, and the proper magnitude was verified by tracking data. The engine burn was short enough so that the propellant tanks, operating in the blowdown mode, experienced a pressure decay of only 2.0 psi. Again, the nitrogen gas supply pressure remained constant because of the previously actuated shutoff valve.

Performance of the thrust vector control system was satisfactory, as shown by Figure 5-39.

Terminal Transfer -- On Day 284, at 05:55 GMT, a velocity change maneuver was performed to place the spacecraft in an orbit which would impact the lunar surface. This maneuver was programmed to burn to oxidizer exhaustion, and then continue to hold the engine valves open to obtain the thrust that the expulsion of fuel alone would produce. Based on calculations derived from the spacecraft's weight and acceleration
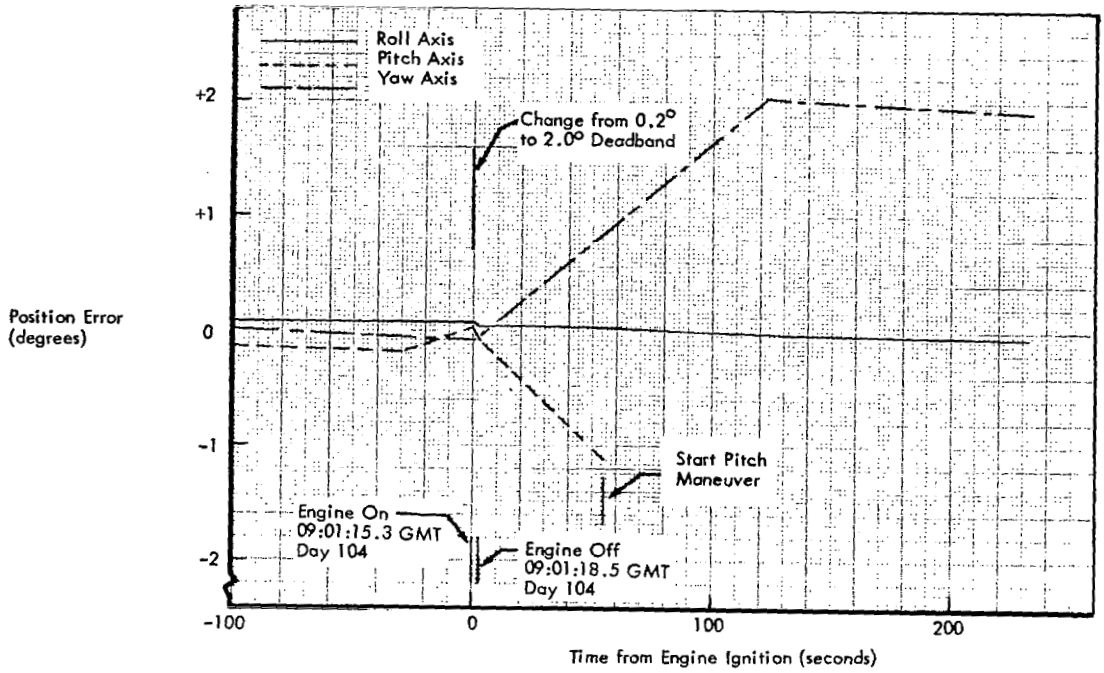
116

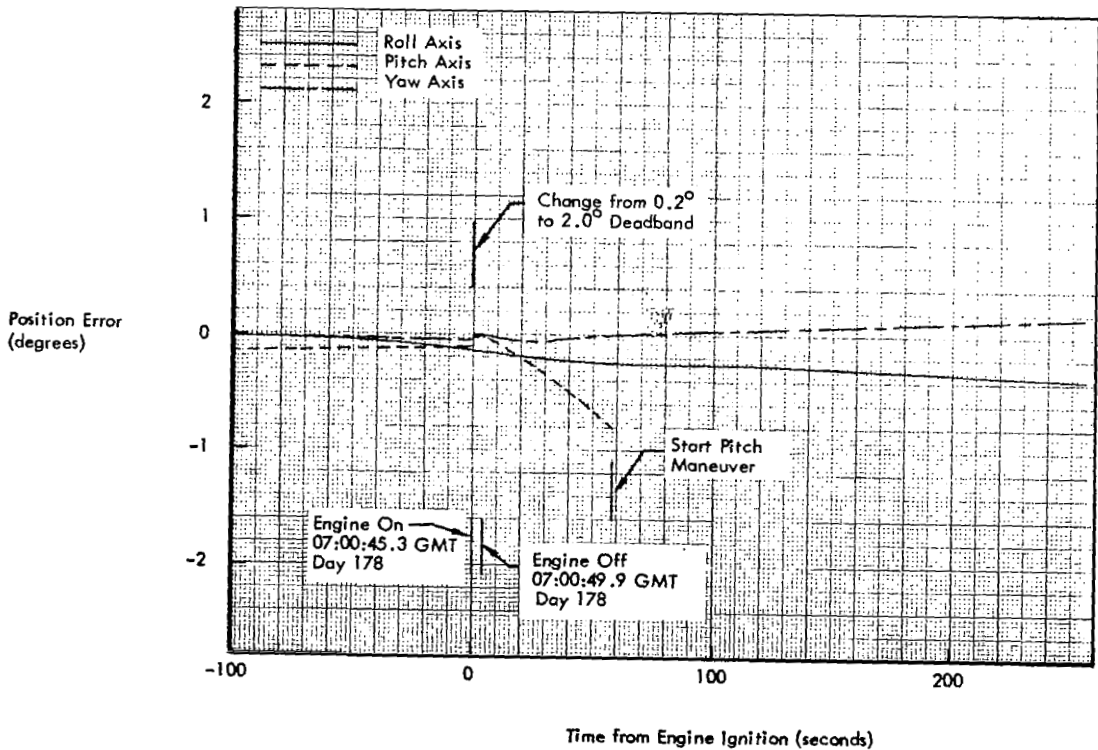**Figure 5-38: Attitude Control — Orbit Phasing Maneuver**

Figure 5-39: Attitude Control — Perilune Increase Maneuver

117

data, the velocity change obtained from bipropellant combustion was 61.5 meters per second, shown as a function of time in Figure 5-40. This burn lasted 35.5 seconds. The engine valves were held open for an additional 175.5 seconds, during which time an additional velocity change of 10.1 meters per second was imparted.

In the first 10 seconds after oxidizer exhaustion, a velocity change of approximately 8 meters per second was recorded. Using spacecraft weight, velocity data, flow, and pressure-drop characteristics of the engine injector, the thrust was calculated to be approximately 32.6 pounds with a specific impulse of 192 seconds for this period. The remaining 2 meters per second of velocity change took approximately 165 seconds and is considered to be provided in part by fuel vaporization. The velocity change as a function of time is shown in Figure 5-41 for the complete engine "on" time.

Propellant feed system pressures for the maneuver are shown in Figure 5-42. The fuel and oxidizer pressures were consistent with previous data obtained for the blowdown mode. The engine fuel valve temperature had virtually peaked out when data receipt ended (see Figure 5-43).

The engine position data shown in Figure 5-44 confirm the stability of the system during the period of bipropellant burning. During the succeeding 175 seconds that the thrust vector control system was functioning, the diverging actuator positions indicated a gradual lessening of control authority due to thrust decay as the residual fuel was expelled. This is confirmed by Figure 5-45, which shows the spacecraft position error changing from ± 0.05 at oxidizer exhaustion to ± 0.26 shortly before the engine "off" command was given.

Overall Subsystem Performance -- The overall subsystem performed satisfactorily throughout the entire 339 days of the photographic and extended missions. During this time, which represents the longest mission to date, seven velocity control maneuvers were performed. The longest elapsed time between maneuvers

was 127 days, which occurred between the inclination change maneuver (Day 342, 1966) and the orbit phasing maneuver (Day 104, 1967). Significant information pertaining to the seven velocity maneuvers is summarized in Table 5-14. An analysis of subsystem performance during each burn confirmed that the engine specific impulse averaged 278 seconds, which agrees with acceptance test data for the engine. The velocity control subsystem imparted to the spacecraft a total velocity change of 1,053.9 meters per second (including oxidizer exhaustion) using 273.3 pounds of propellant, based on an average engine specific impulse of 278 seconds.

Experience from ground tests and Mission I has indicated that the subsystem would impart a nominal velocity change of 1,037.3 meters per second to the spacecraft based on actual propellants loaded and a 99% expulsion efficiency. It is therefore concluded that the extra velocity change imparted to the spacecraft was primarily the result of a higher-than-predicted propellant expulsion efficiency, calculated to be 99.57% including fuel runout.

5.3 SPECIAL FLIGHT TESTS
Although the primary photographic mission of Lunar Orbiter II was successfully completed 32 days after launch, the spacecraft was capable of operating for periods up to 1 year after launch. In addition to obtaining scientific data about lunar size, shape, gravitational characteristics, and environment during the extended periods in lunar orbit, spacecraft subsystem performance was evaluated on the basis of special tests that involved maneuvering the spacecraft to various attitudes and orbital altitudes or inclinations.

Special tests performed during the extended mission fall into two categories: (1) experiments using the Lunar Orbiter spacecraft as a tool to obtain scientific and operational data, and (2) special exercises that are tests of the spacecraft or the equipment on board. The latter tests are reported herein; the experiments will generally be reported on by the particular agency requesting the experiment.
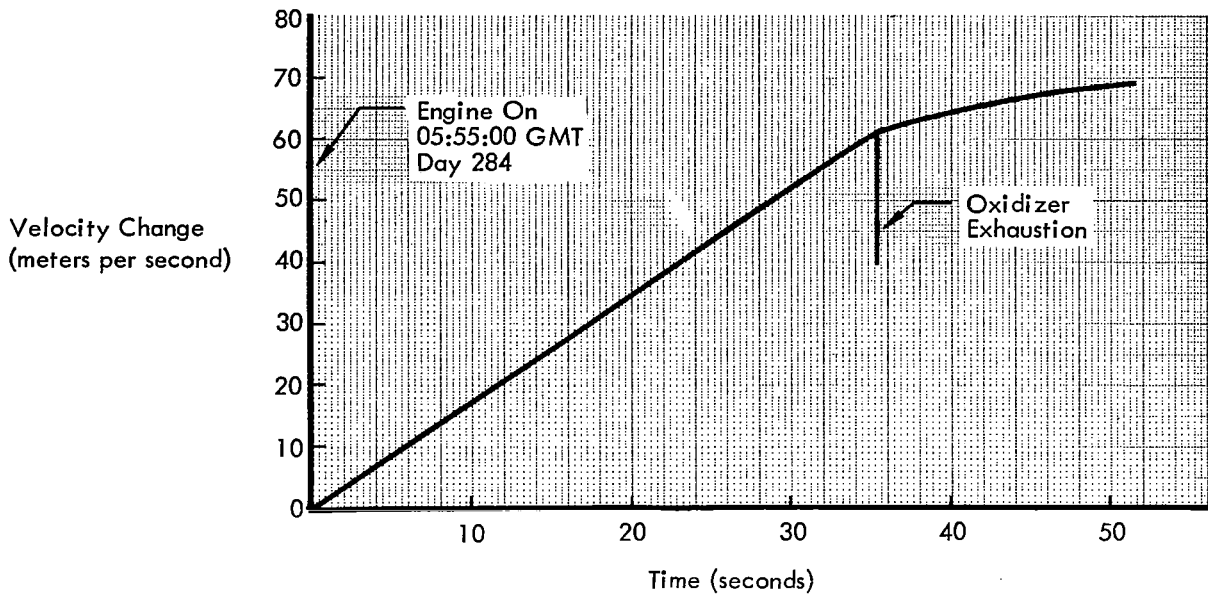
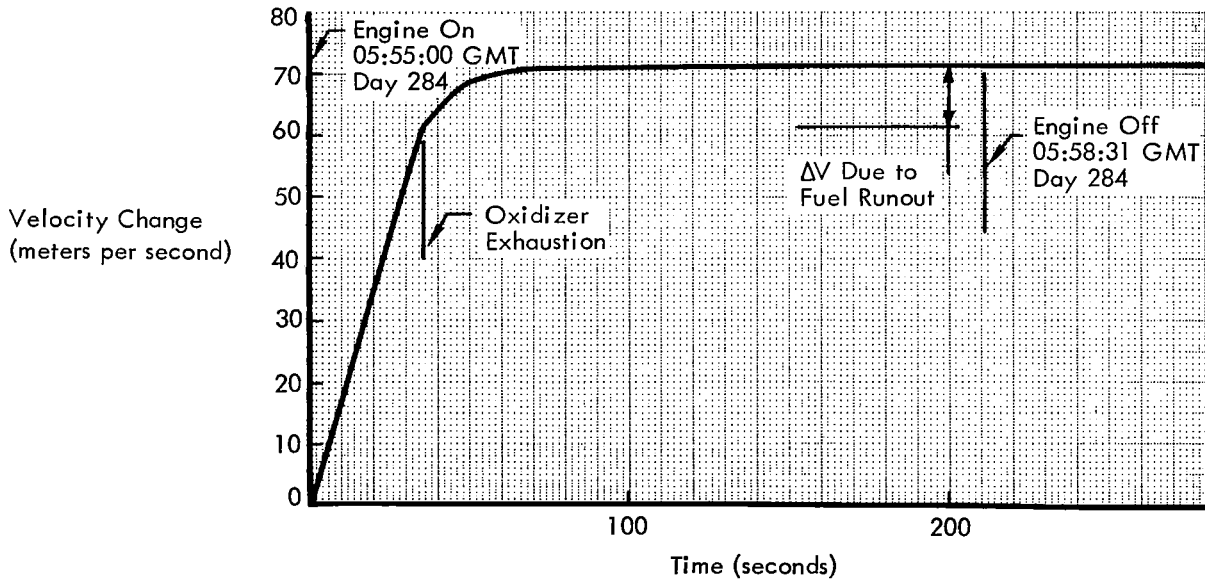**Figure 5-40: Velocity Change — Terminal Transfer Maneuver**

Figure 5-41: Velocity Change — Terminal Transfer Maneuver
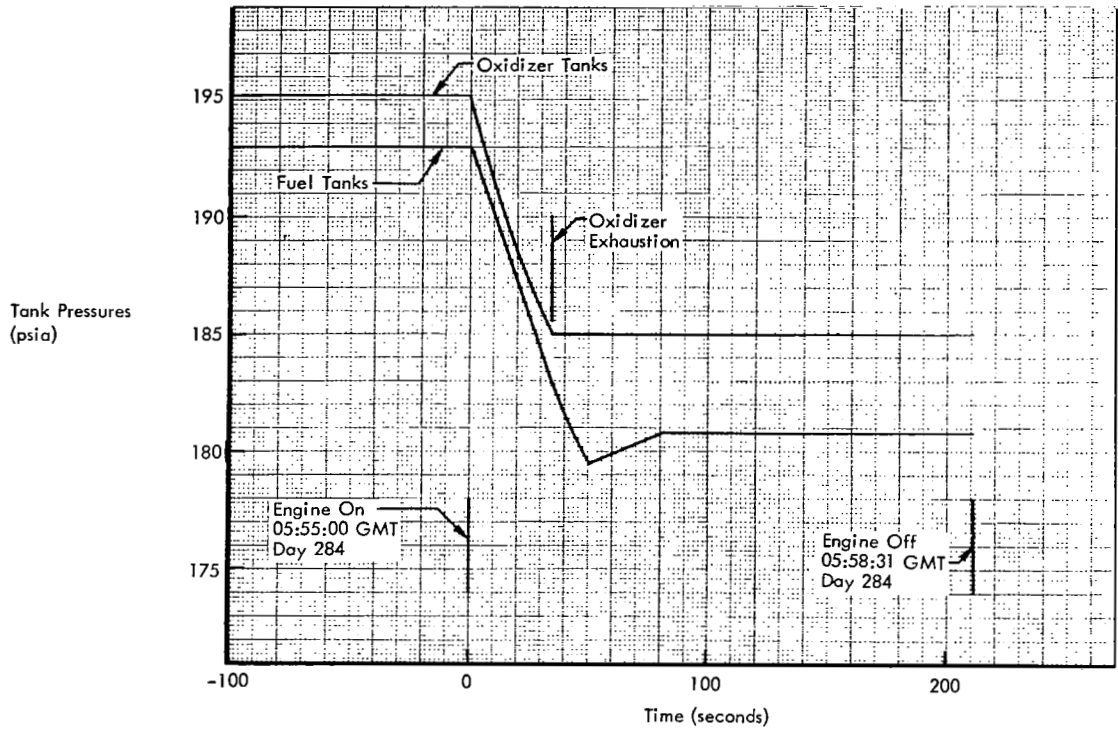
119

Figure 5-42: Propellant Tank Pressures — Terminal Transfer Maneuver
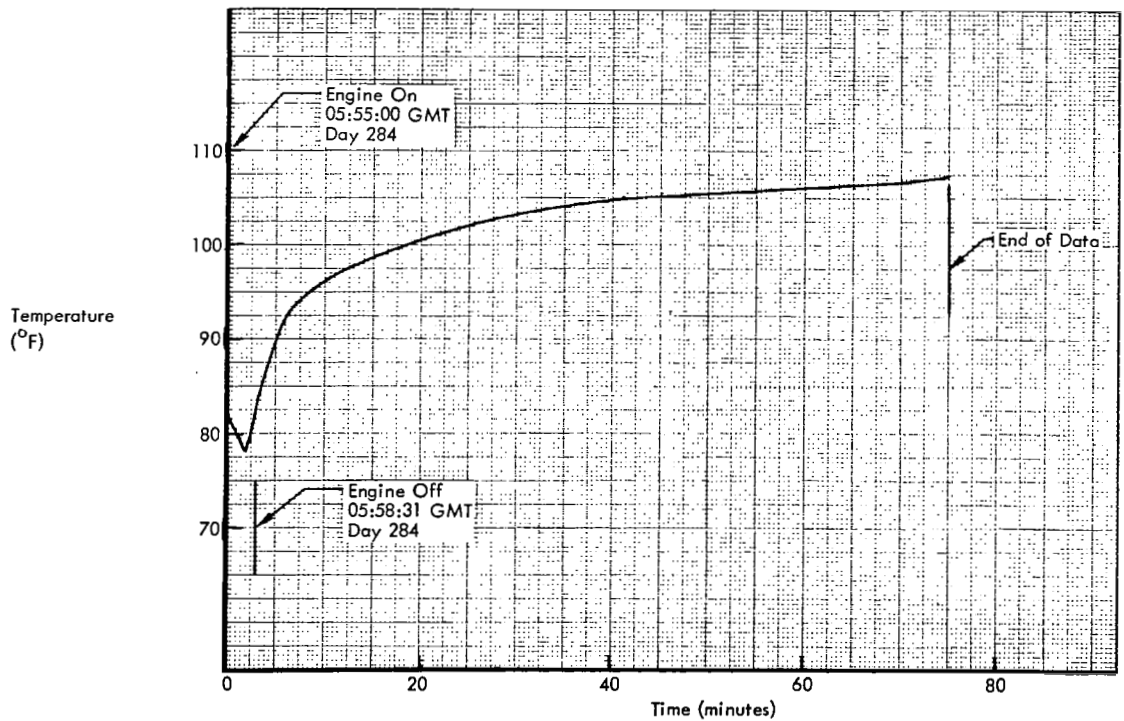

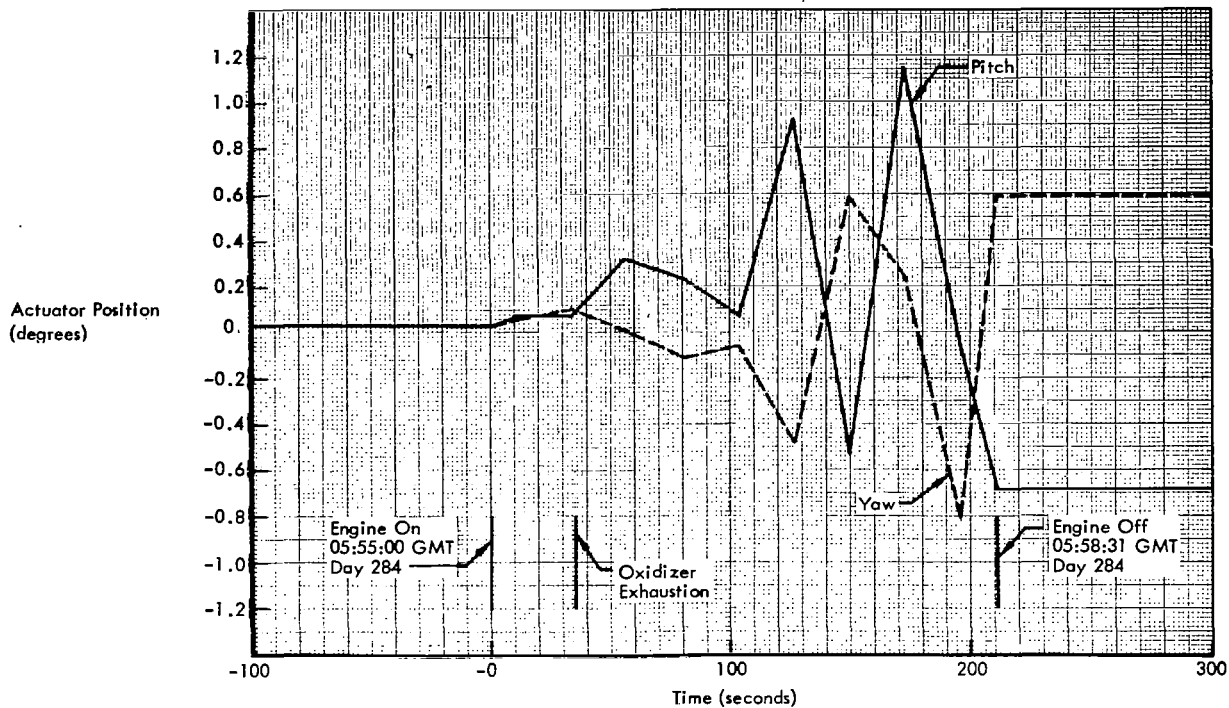**Figure 5-43: Temperature Soak-Back to Engine Fuel Valve — Terminal Transfer Maneuver**

120

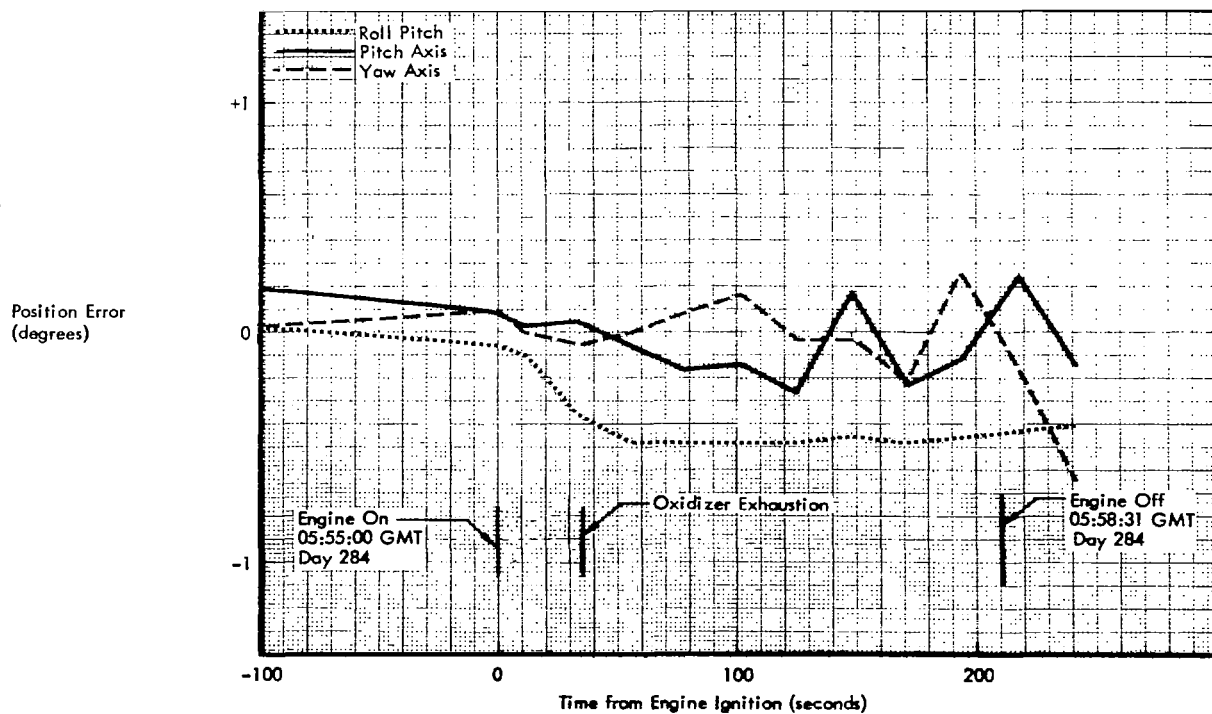Figure 5-44: TVC Actuator Position — Terminal Transfer Maneuver

Figure 5-45: Attitude Control — Terminal Transfer Maneuver

121

Table 5-14: Velocity Maneuver Summary

Event	GMT Time Day:Hr:Min	ΔV (M/Sec)	Burn Time (Sec)	Average Thrust (Lb)	Propellant Used (Lb)*
Launch	310:23:21 (1966)				**
Midcourse	312:19:30	21.1	18.1	101	6.6
Injection	314:20:26	829.7	611.6	101	222.4
Orbit transfer	315:22:58	28.1	17.4	102.5	6.4
Inclination change	342:20:36	100.0	61.3	99.6	22.0
Orbit phasing	104:09:01 (1967)	5.5	3.2	103	1.2
Perilune increase	178:07:00	8.0	4.6	103.3	1.7
Terminal transfer	284:05:55	61.5	35.5	100.5	13.0 2.5***
Total		1,053.9	751.7		275.8

*   Estimated by assuming a specific impulse of 278 sec
** 277.0 lbs propellant loaded at launch
*** Fuel expelled after oxidizer exhaustion provided an additional 10.1 meters per second ΔV

5.3.1 Command Address Test

Objective -- The objective of this test was to verify that the spacecraft would not accept a command transmitted to another spacecraft at normal signal strengths. This test also determined the command threshold signal strength. It further verified that a command received by the spacecraft at a signal strength below command threshold although garbled may be accepted.

Description -- The command to rotate the high-gain antenna 1 degree left was used so that an accidental execution of the command would not adversely affect the spacecraft.

The experiment consisted of three basic parts:
● At normal signal strength (−90dbm), three commands were transmitted with three different incorrect address codes.
● The command threshold signal strength was determined by increasing the signal strength from below threshold in 1-decibel increments until the command was verified three consecutive times (the correct address code was used).
● At the threshold signal strength, three commands were transmitted with three different incorrect address codes.

Data and Discussion -- Table 5-15 lists the experimental results, from which it can be seen that:
● The spacecraft would not accept an incorrect address code at normal signal strength.
● Command threshold signal strength was determined to be approximately −123 dbm.
● The spacecraft would not accept an incorrect code at threshold signal strength.

Conclusions -- At command signal strengths above threshold, the spacecraft would not accept a command with an improper address code. A command with an incorrect address code was not transmitted below command threshold level. Incorrect commands were registered below threshold level using the

Time (Day 342)	DSS-12 Power	Transponder AGC	Command Address	Command Verified	S/C Command Register Bit Pattern
16:14	2.6 KW	- 90 dbm	S/C 3	No	Register empty pattern
16:18			6	No	" " "
16:20			7	No	" " "
16:25	1.0 Watts	-124.9 dbm			
16:29			S/C 5	No	1, 3, 6, 7, 10, 25
16:32				No	Register empty pattern
16:35				No	" " "
16:38	1.3 Watts	-123.9 dbm			
16:40			S/C 5	No	1, 3, 6, 7, 10, 23, 26
16:44				No	1, 3, 6, 7, 10, 25
16:46				No	1, 3, 5, 6, 9, 24
16:53	1.6 Watts	-122.6 dbm			
16:54			S/C 5	Yes	1, 3, 6, 7, 10, 24
16:55				Yes	1, 3, 6, 7, 10, 24
16:58				Yes	1, 3, 6, 7, 10, 24
17:01	1.6 Watts	-122.6 dbm	S/C 3	No	Register empty pattern
17:03			6	No	" " "
17:06			7	No	" " "

Table 5-15: Improper Spacecraft Address Experiment

correct address code. This would indicate that it is statistically possible to load a command with an incorrect address code when the signal strength is below threshold.

5.3.2 Transponder Oscillator Drift Test

Objective -- The purpose of the oscillator drift test was to establish the transponder best lock frequency as a function of temperature after exposure to space environment.

Description -- The test, conducted with DSS-12 on Day 007, consisted of setting the ground receiver at zero static phase error and then recording the SPE and receiver VCO frequency at 15-minute intervals throughout the orbit. The procedure was used on two successive orbits with the spacecraft in one-way lock. Transponder temperature was also recorded throughout the pass.

Data and Discussion — On this test, DSS-12 furnished VCO frequencies, static phase error data and doppler count necessary for analysis of oscillator drift. Transponder temperature was also recorded during the tracking pass. Orbital parameters and frequency calculations could not be generated because no coherent tracking data could be obtained in one way lock. Mapped frequency predictions from previous coherent data were used in the calculation of drift during the data interval.

Conclusions -- The test proved to be inconclusive because the one-way frequencies as derived from station predicts were not sufficiently accurate to allow oscillator drift to be separated from Doppler effects.

5.3.3 Solar Panel Degradation Test

Objective — The purpose of this test was to obtain data from which solar panel degradation could be determined.

Description — On GMT Day 348, 1966, the spacecraft was maneuvered to bring the solar panels normal to the sunline. The panel output voltage and current were monitored for 7.47 hours.

Data and Discussion — Repeating this test was unnecessary, since the required data were obtained during other tests which required on-Sun operation. Figure 5-46 is a plot of this degradation data both before and after being corrected for the changing solar constant.

Conclusions — Total array degradation by the end of the extended mission following 339 days of space exposure was 5.5%. Most of the degradation appeared between GMT Days 120 and 180. Degradation appeared to diminish thereafter.
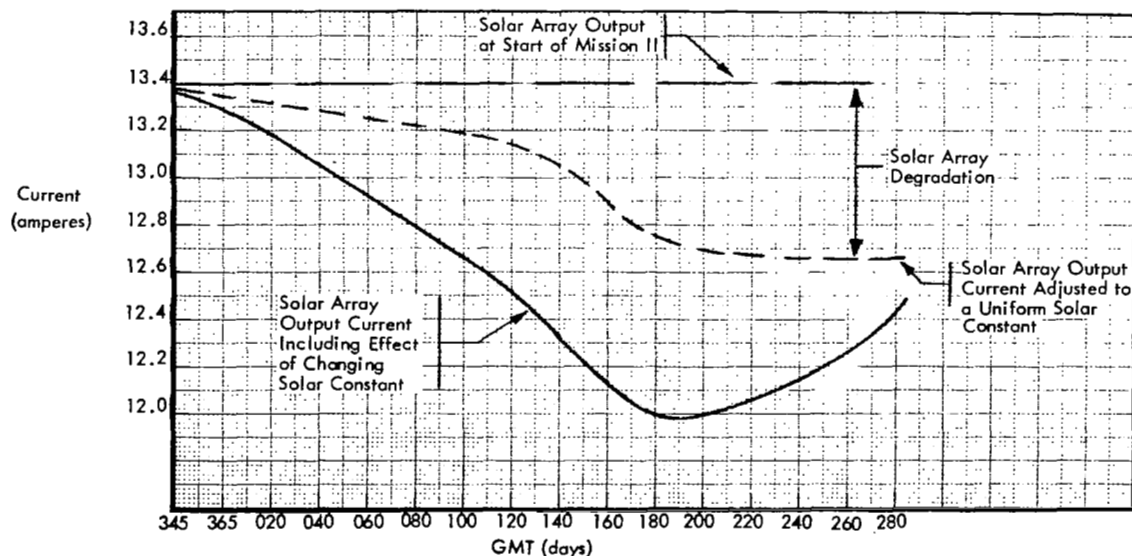

Figure 5-46: Solar Array Degradation

124

5.3.4 Battery Deep Discharge Tests

Objective -- Battery discharge tests were conducted in an attempt to erase the memory effect and thereby improve battery performance. In addition, the tests were designed to determine the operating characteristics under the energy demand anticipated during the lunar eclipse periods on April 24 and October 18, 1967.

Description -- The spacecraft was pitched off the sunline following a normal lunar night to obtain a greater depth of battery discharge.

Data and Discussion -- Complete correction of memory requires removal of all energy from the battery. Since this cannot be accomplished on a flying spacecraft, a partial erasure of memory was attempted using a deep discharge.

a) The first test, on Day 353, was primarily intended to erase the memory effect. The test was started at 03:22 GMT when the spacecraft was pitched +45 degrees from its current off-Sun position to 87.8 degrees off the sunline. This attitude, which was based on previous gyro drift characteristics, resulted in a solar array current of 0.5 amperes and a correspondingly slower battery discharge rate than was anticipated. To compensate for this slower discharge rate, the propellant tank heaters were commanded "on" for the last 5 minutes of the battery discharge. The battery was discharged for 66 minutes at an average rate of 3.99 amperes, and for 5 minutes at an average rate of 5.25 amperes, for a total discharge of 4.82 ampere-hours or 40% based on a 12-ampere-hour capacity.

b) The second test, on Day 110, was again intended to erase the memory effect in preparation for the lunar eclipse of Day 114 (April 24, 1967). The test was started at 13:34 GMT when the spacecraft was pitched an additional 45 degrees to take the spacecraft 100 degrees off the sunline. The battery discharge was continued through the normal lunar night and into the following lunar day, the Sun being reacquired at 14:51 GMT. The battery discharge current varied from 3.8 amperes at the start of the test to 4.34 amperes at the end, with an average discharge current of 4.0 amperes. Total discharge time was 77 minutes; thus, the total discharge was 5.13 ampere-hours, or a 42.8% depth of discharge based on a capacity of 12 ampere-hours.

c) The third test, on Days 272 and 273 (September 29 and 30) was conducted in two parts on two consecutive orbits. The intent was to erase any memory effect present, to evaluate the battery condition, and to ensure sufficient battery capacity to sustain the eclipse period as part of the preparation for the lunar eclipse. The first part was started at 20:35 GMT, after the battery had sustained 2,210 charge-discharge cycles. The battery discharge was continued through the normal nighttime period and into the following daytime, the Sun being reacquired at 21:18 GMT (see Figure 5-49). The battery discharge currents varied from 3.86 amperes at the start of the test to 4.31 amperes until the tank deck heaters were turned on approximately 44 minutes after the test began which increased discharge current from 4.31 to 5.67 amperes. These heaters were turned off after approximately 13 minutes, and the discharge current decreased from 5.81 to 4.46 amperes. The beginning battery voltage was 27.68 volts. The lowest voltage with the maximum load was 20.32 volts. Total discharge time was 63 minutes; thus, the estimated discharge was 4.47 ampere-hours or a 37.2% depth of discharge based on a capacity of 12 ampere-hours.

The second part was started at approximately 00:05 GMT. The battery discharge current varied from 5.597 amperes at approximately 10 minutes after the beginning of the test to a maximum of 5.75 amperes at 46 minutes. At this time, the tank deck heaters were turned off and the battery load decreased to 4.34 amperes. Battery and bus voltages reached 19.36 and 18.72 volts, respectively. The average discharge current was 4.85 amperes. Total discharge time was about 75 minutes; thus, the estimated total discharge was 6.05 ampere-hours, or a 50.4%

depth of discharge based on a 12 ampere-hour capacity.

Figure 5-19 in Paragraph 5.2.3.2 records the battery end-of-discharge parameters observed during the extended mission. Load and temperature variations caused by the spacecraft activities and the limited orbits monitored preclude obtaining a good battery end-of-discharge voltage trend. However, the dashed line in Figure 5-19 represents the best approximation of the end-of-discharge voltage decay, indicating that a small amount of memory effect may have been present.

A typical normal discharge curve is shown in Figure 5-47 and a typical deep discharge curve is shown in Figure 5-48. The normal discharge removed 2.23 ampere-hours; the deep discharge removed 5.13 ampere-hours of energy. Results of the last deep discharge test, performed on Days 272 and 273, are shown in Figure 5-49. The curve showing the battery voltage during the normal Sun occultation period is misleading, since the battery was not fully charged prior to this normal discharge period due to the extreme off-Sun operation of the spacecraft during the previous daylight period. Therefore, insufficient solar array power was available at this large off-Sun angle to permit a full rate of charge. The battery was fully charged, however, prior to each of the two deep discharge periods which followed. These deep discharge data were included in the review when the decision was made to crash the spacecraft prior to the eclipse.

Conclusions — Sufficient data were not available from orbits prior to and immediately following each deep discharge cycle to demonstrate the presence or correction of any memory effect. The data trend did indicate that memory, if present, was minimal. It can be concluded from the deep discharge tests performed on GMT Days 272 and 273 that, following 1 year in orbit, the battery had degraded to 50% of its initial capacity. The degradation was attributed to its higher-than-normal temperature environment.

5.3.5 Paint Degradation Test

Objective — The purpose of this test was to establish an equipment-mounting deck paint "degradation - time" profile.

Description — The spacecraft was maneuvered directly on-Sun in pitch and yaw and maintained for three consecutive orbits. The roll attitude was not critical. The spacecraft was operated in the normal standby mode, i.e., with the photo subsystem in standby mode, tank heaters off and the communications subsystem in Mode 3 (TWTA and ranging off). Specific data requirements included Measurement Numbers ST01 through ST09, AT01 and AT03. This experiment was to be performed at least once every 2 weeks. To conserve nitrogen, the on-Sun maneuver was to be performed during a planned Sun acquisition.

Data and Discussion — The thermal coating degradation test was performed on GMT Day 348. The spacecraft was to have been oriented "on-Sun" for three consecutive orbits to allow EMD temperatures to stabilize for determination of the thermal coating degradation. However, during the second orbit the spacecraft was maneuvered 40 degrees "off-Sun" for a period of 28 minutes, so that the EMD temperatures could not reach a stabilized value by the end of the third orbit. Prior to the spacecraft's reaching a stabilized temperature, the flight test coupon measurements (ST06 through ST09) became saturated at 106°F, and ST02 became saturated at 113.2°F. Measurements ST01 and ST03 would probably have become saturated had the spacecraft remained on-Sun for the full three orbits. Table 5-16 shows the EMD peak temperatures that were obtained just prior to sunset of the third orbit. While on-Sun, the battery temperature reached 125 degrees F. while charging and the charge controller went to trickle-charge, reducing the power dissipated in the battery by over 80 watts.

Conclusions — The data recorded, compared with the data obtained on Day 342, showed an increase in temperature of 2 to 3 degrees, thereby indicating that a thermal-coating degradation
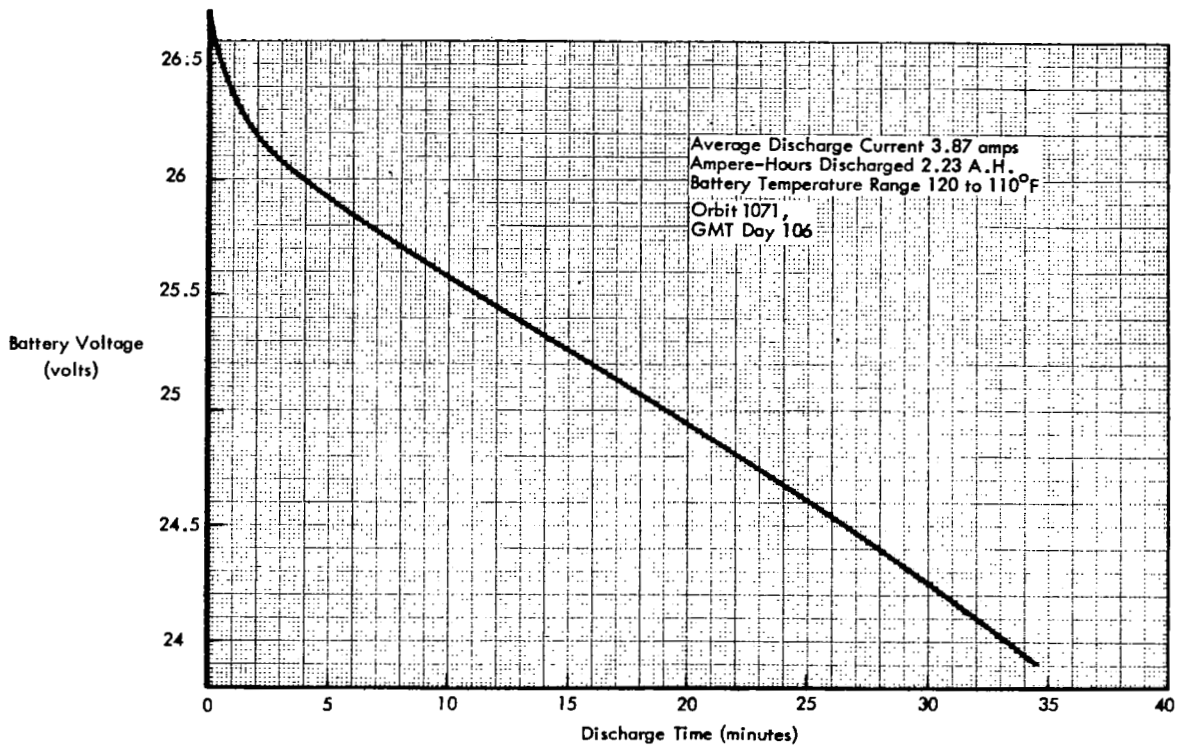
Average Discharge Current 3.87 amps
Ampere-Hours Discharged 2.23 A.H.
Battery Temperature Range 120 to 110°F
Orbit 1071,
GMT Day 106

Figure 5-47: Battery Normal Discharge Characteristics

Earth Occult

Average Discharge Current 4.0 Amperes
Ampere-Hours Discharged 5.13 A.H.
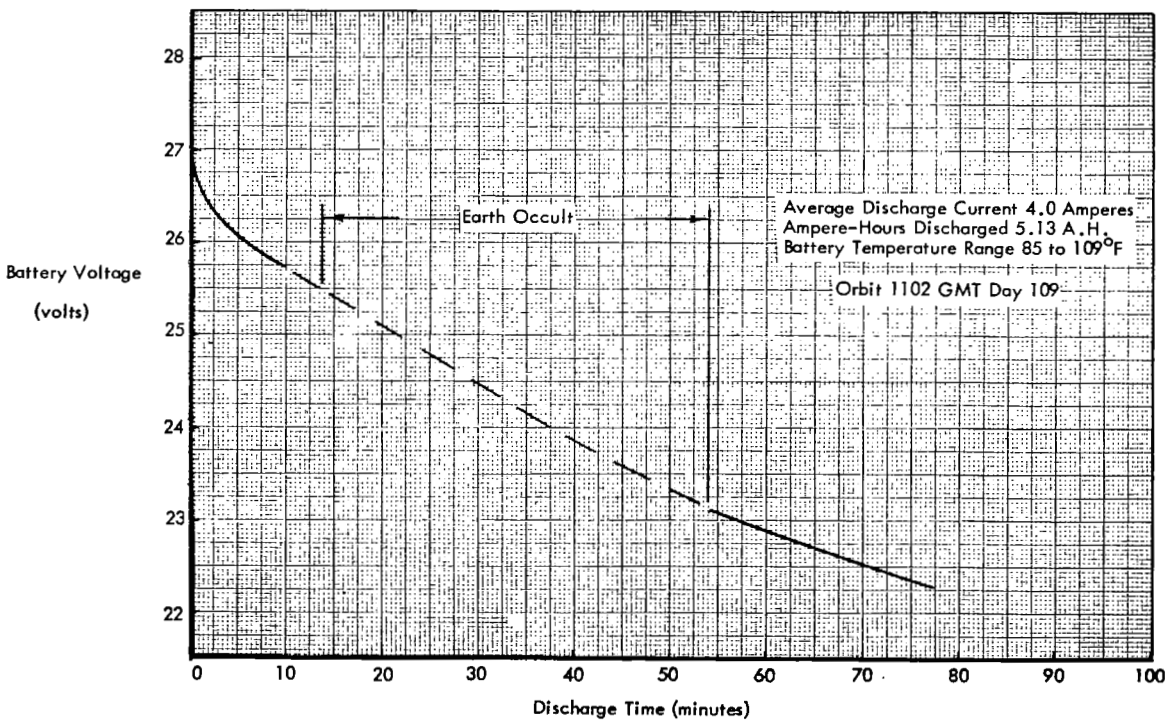Battery Temperature Range 85 to 109°F

Orbit 1102 GMT Day 109

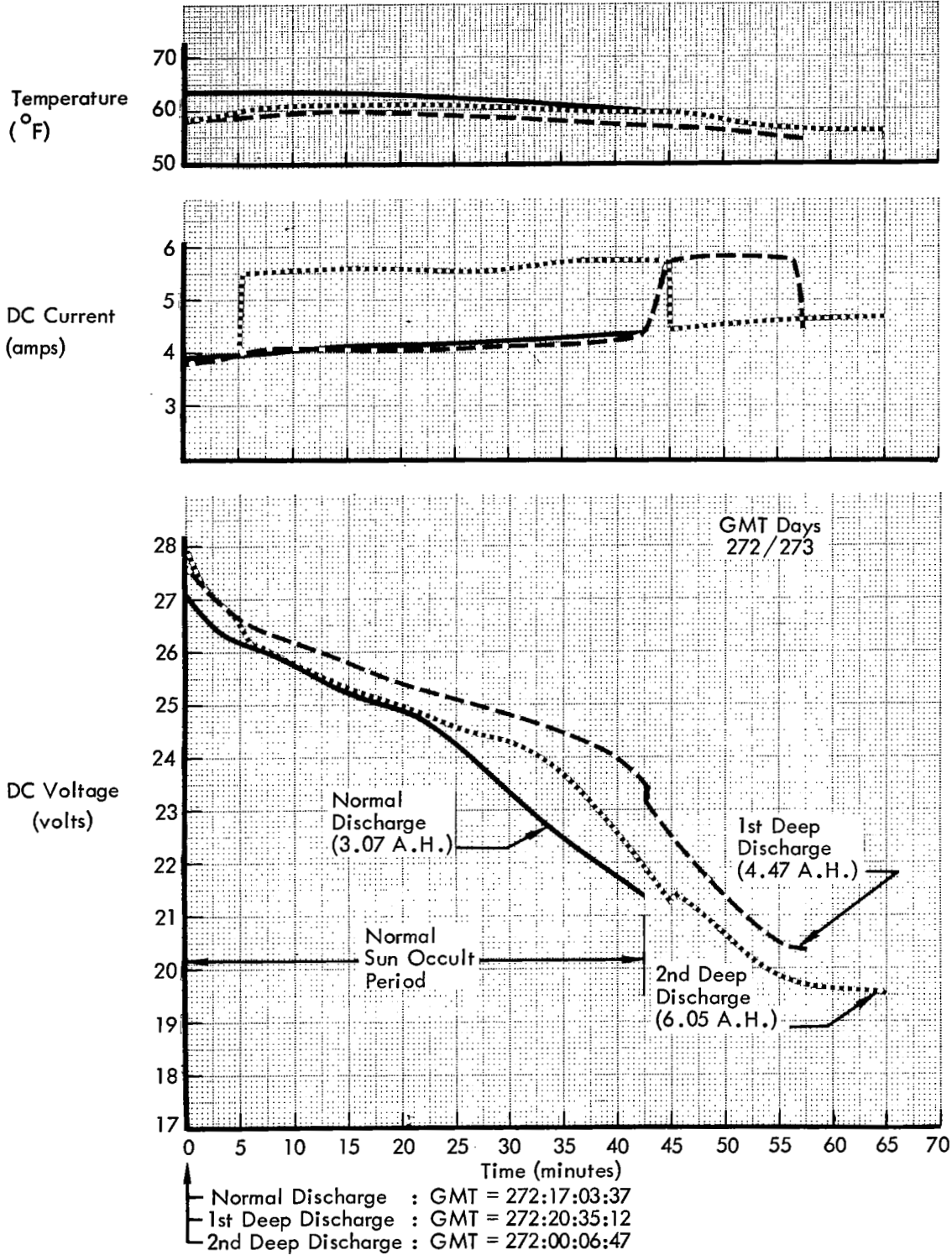Figure 5-48: Battery Deep Discharge Characteristics

127

Figure 5-49: Battery Discharge Performance During Sequential Deep Discharges

128

had already taken place. Also, many of the telemetry points had become saturated and no higher temperatures could be recorded. Since meaningful data could not be obtained, additional degradation tests were cancelled.

Table 5-16: Peak On-Sun Temperatures

Measurement Number	Location	Maximum Temperature
ST01	EMD at TWTA	97.9°F
ST02	EMD at Transponder	113.2
ST03	EMD at IRU	108.8
STO4	Tank deck temperature	71.5
ST05	Engine heat shield	52.2

5.3.6 Camera Thermal Door Open Test

Objective — The purpose of this test was to determine the thermal effects on the photo subsystem if the camera thermal door should fail in the "open" condition, and to determine the cooling characteristics during readout with the photo subsystem window exposed.

Procedure — Because the camera thermal door had already failed in the "open" position, a formal procedure was not prepared for this test.

Data and Discussion — Following detection of the camera thermal door failure the photo subsystem temperatures were normal, with the exception of the window temperature (PT03), which varied as expected with its exposure to deep space or sunlight.

Conclusions — Although the test was not formally performed, the following can be concluded.
1. Photo subsystem temperatures, except for window temperatures, vary in accordance with EMD temperature variations, based on

data obtained following CTD failure.
2. The rate of window temperature change cannot exceed the constraint of 7.5 degrees per hour without resulting in condensation on the inner surface of the window, based on data available from Mission IV.

5.3.7 V/H Pitch and Roll Tests

The following special tests using the photo subsystem V/H sensor were performed to determine the V/H tracking capability with the optical axis obliquely oriented relative to the local vertical. The results of these tests encouraged inclusion of oblique photography in the Mission III design.

5.3.7.1 V/H Roll Test (45 and 22.5 degrees)
Objective — The purpose of this test was to determine the capability of the V/H sensor to track during oblique photography at roll tilt angles up to 45 degrees.

Procedure — The test was conducted on Day 014 and consisted of orienting the spacecraft to roll tilt angles of 45 degrees and 22.5 degrees, and obtaining V/H sensor data. The following sequence of events and parameter values was used:

Sequence of Events	
GMT Day and Time	Event
014:21:59:59.8	0.2-degree deadzone
22:00:51.2	Acquire Sun
22:01:42.6	Sun sensor pitch, coarse off
22:21:59.8	Canopus sensor on
22:22:51.3	Roll -22.6 degrees
22:30:59.8	Cut Bimat
22:31:51.2	Solar eclipse off
22:33:33.8	Readout electronics on
22:33:59.6	Readout drive on
22:34:51.0	Second readout drive on
22:55:59.8	Readout drive off
22:57:42.4	Readout drive on
22:57:42.5	Canopus sensor off

Sequence of Events

GMT Day and Time	Event	GMT Day and Time	Event
014:22:58:34.0	Roll −11.92 degrees	23:15:40.9	Heater power on
22:59:49.3	Yaw +12.8 degrees		Solar eclipse on
23:01:06.3	Roll −65.7 degrees (Total roll +45 degrees)	23:15:47.5	Camera thermal door closed
		23:15:54.1	Camera thermal door control off
23:07:52.8	Readout drive on	23:16:45.6	Pitch +49.9 degrees
	Heater power off		
	Solar eclipse off		Orbit Parameters
23:07:52.9	Single frame camera sequence, slow rate		Day 014 23 Hours 10 Minutes 30 Seconds
	Camer thermal door open	1) Total V/H "on" time at 45 degrees = 4 Minutes	
23:07:59.5	Camera thermal door control off	2) Total V/H "on" time at 22.5 degrees = 2 Minutes	
	V/H on	3) Altitude at 45 degrees = approximately 115 kilometers	
23:10:59.8	Camera on	4) Phase angle at 45 degrees =approximately 82 degrees	
23:11:59.8	V/H off	5) Incidence angle at 45 degrees =approximately 74 degrees	
23:12:00.0	Roll −22.5 degrees (Total roll +22.5 degrees)	6) Altitude at 22.5 degrees =approximately 187 kilometers	
23:13:10.8	V/H on	7) Phase angle at 22.5 degrees =approximately 79 degrees	
	Camera thermal door control off	8) Incidence angle at 22.5 degrees =approximately 63 degrees	
23:15:40.8	V/H off	9) Single frame advanced normally	

Data and Discussion — The plot of the V/H roll test is shown in Figure 5-50, and indicates that the V/H ratio telemetry agreed very closely with that predicted, indicating the capability to photograph at angles up to 45 degrees. The film was moved by reading out (rewinding) to preclude possible scratching or wear of the film by the film clamp. Operation of the photo subsystem was normal during the exercise.

Conclusions — Examination of the data obtained on Day 014 indicates that oblique
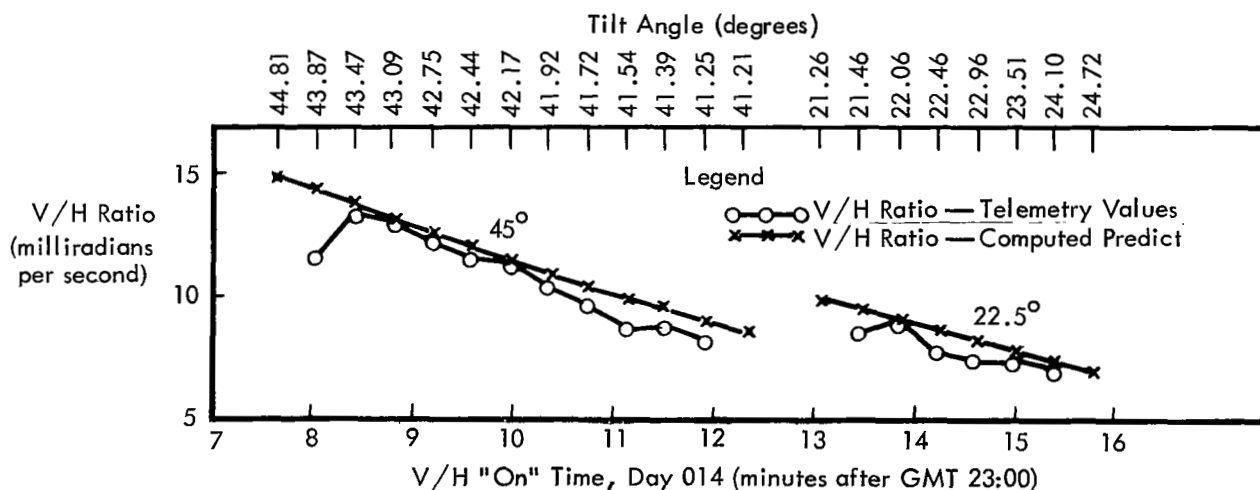
Figure 5-50: V/H Roll Test at 22.5 and 45 Degrees

130

photography at roll angles up to 45 degrees is feasible. Although the V/H sensor was used beyond its design limitations during these tests, satisfactory operation was obtained. The differences between V/H telemetry and the computed V/H - EVAL (slant range) indicated in the plot are to be expected. These may be attributed to the inaccuracies introduced in the computations by the assumptions of altitude, attitude, and irregularities in the lunar terrain.
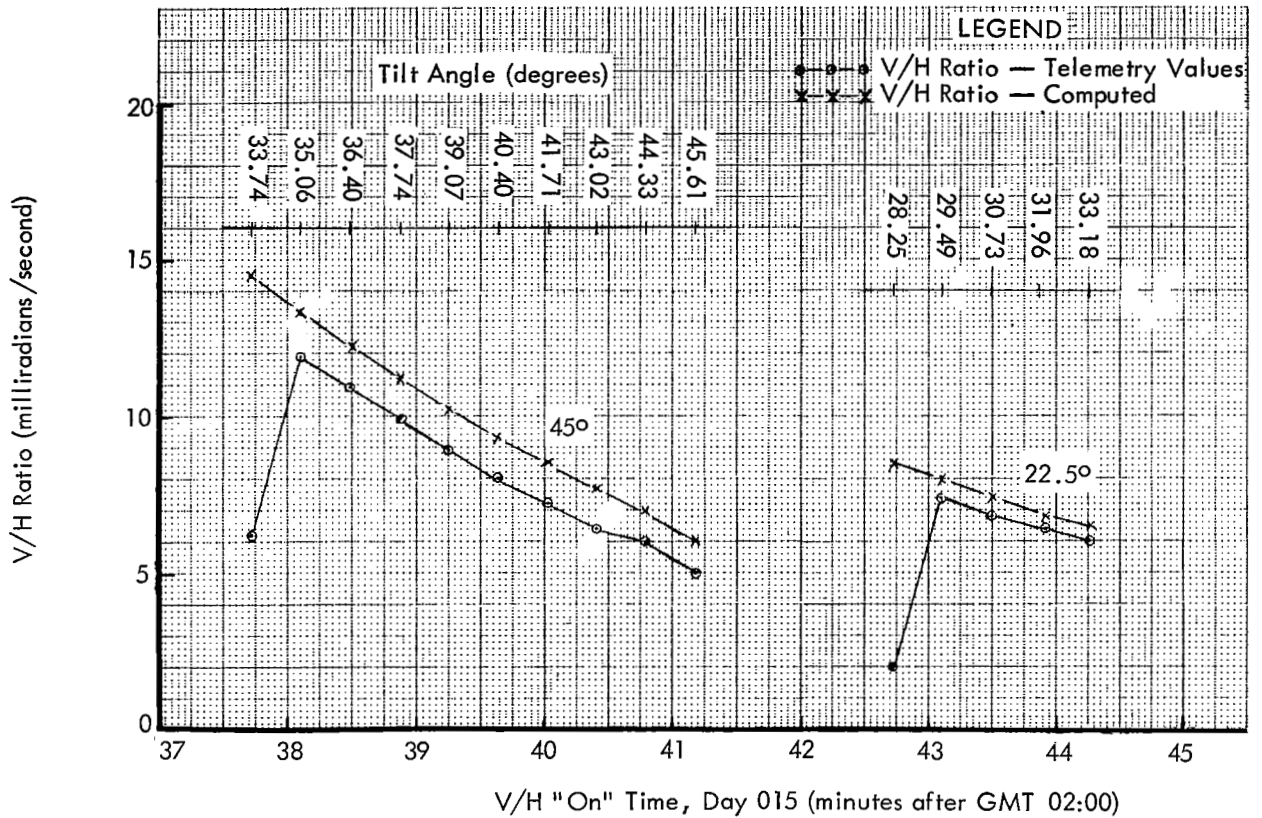
5.3.7.2 V/H Pitch Test (45 degrees and 22.5 degrees)

Objective — The purpose of this test was to determine the capability of the V/H sensor to track during oblique photography at pitch angles up to 45 degrees.

Sequence of Events

GMT Day and Time	Event	GMT Day and Time	Event
015:01:24:59.8	Sun sensor pitch, coarse on	02:43:34.8	Camera on
	Sun sensor yaw, coarse on	02:44:34.8	V/H off
01:25:51.2	Acquire Sun	02:44:34.9	Heater on
01:29:16.2	Sun sensor pitch, coarse off		Solar Eclipse on
	Sun sensor yaw, coarse off	02:44:41.5	Camera thermal door closed
01:53:59.8	Canopus sensor on	02:44:48.1	Camera thermal door control off
01:54:51.3	Roll −32.20 degrees	02:45:39.6	Yaw −12.00 degrees
02:25:59.8	Canopus sensor off	02:46:55.1	Pitch +27.90 degrees
02:26:51.3	Roll +9.2 degrees	02:48:42.3	2-degree deadzone
02:28:01.3	Yaw +11.96 degrees	02:49:33.7	Sun sensor yaw, coarse on
02:29:16.7	Pitch +49.60 degrees (Total pitch +45 degrees)		Sun sensor pitch, coarse on
02:34:59.8	Readout drive on		
	Heater power off		
	Solar eclipse off		Orbit 447 Parameters
02:34:59.9	Single frame camera sequence, slow rate		Day 015 02 Hours 40 Minutes 0 Seconds
	Camera thermal door open		1) Total V/H "on" time at 45 degrees =4 minutes
02:35:06.5	Camera thermal door control off		2) Total V/H "on" time at 22.5 degrees =2 minutes
02:37:26.5	Camera on		3) 2 single frames advanced to satisfy photo subsystem constraint
02:37:29.9	V/H on		4) Altitude at 45 degrees =134 km approximately
02:41:29.8	V/H off		5) Phase angle at 45 degrees =119 degrees approximately
02:41:30.0	Pitch −22.5 degrees (Total pitch +22.5 degrees)		6) Incidence angle at 45 degrees =70 degrees approximately
			7) Altitude at 22.5 degrees =170 km approximately
02:42:40.8	V/H on		8) Phase angle at 22.5 degrees =96 degrees approximately
	Camera thermal door control off		9) Incidence angle at 22.5 degrees =65 degrees approximately

Figure 5-51: V/H Pitch Test at 22.5 and 45 Degrees

Procedure — The exercise was conducted on Day 015 and consisted of orienting the spacecraft to pitch angles of 45 degrees and 22.5 degrees, and obtaining V/H sensor data. The following sequence of events and parameter values was used.

Data and Discussion — The plot of the V/H pitch test (Figure 5-51) shows that the V/H ratio telemetry agreed very closely with that predicted, indicating the capability to photograph at pitch angles up to 45 degrees. During the exercise, film was moving by reading out (rewinding) to preclude scratching or wear of the film by the film clamp. Operation of the photo subsystem was normal during the exercise.

Conclusions — Examination of the data obtained indicates that oblique photography at pitch angles up to 45 degrees is feasible. Although the V/H sensor was used beyond the design limitations during these tests, satisfactory

operation was indicated. The differences between V/H telemetry and the computed V/H-EVAL (slant range) indicated in the plot are to be expected. These may be attributed to the inaccuracies introduced in the computations by the assumptions of altitude, attitude, and irregularities in the lunar terrain.
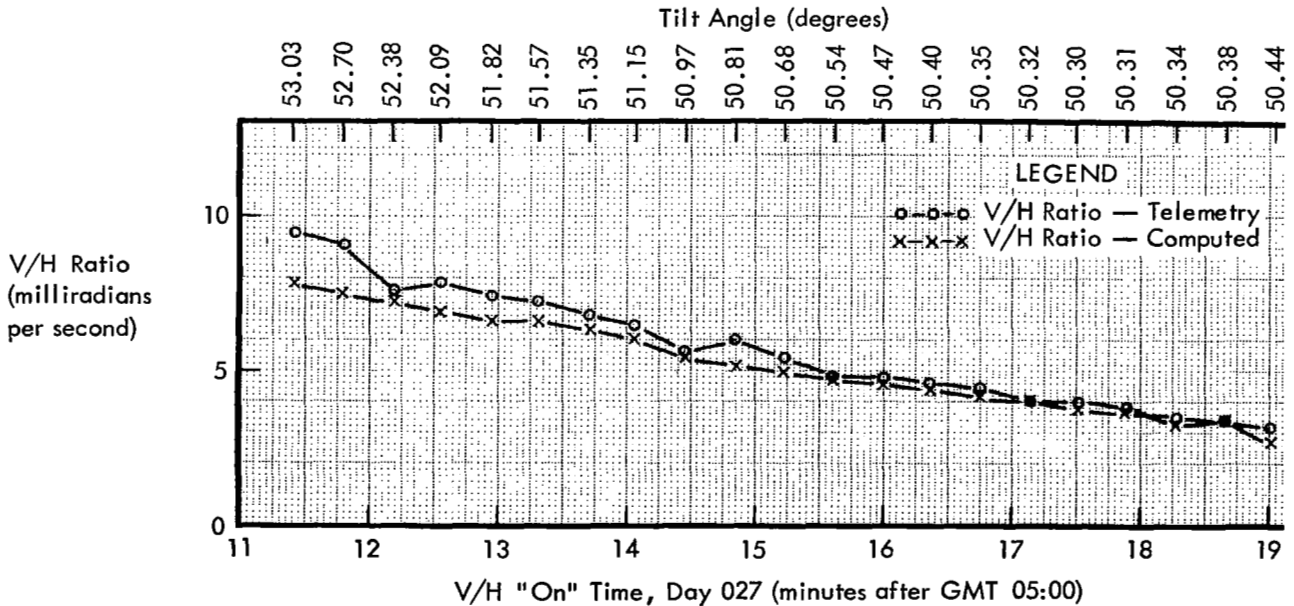
5.3.7.3 V/H High Roll Angle Test
Objective — The purpose of this test was to determine the capability of the V/H sensor to track during oblique photography at high roll angles.

Procedure — The test was conducted on Day 027 and consisted of orienting the spacecraft to roll angles approximating 53 degrees. The following sequence of events and parameter values was used.

Data and Discussion — The plot of this high roll angle test (Figure 5-52) shows that the V/H ratio telemetry agreed very closely with that

132

Sequence of Events

GMT Day and Time	Event	GMT Day and Time	Event
027:04:02:00.3	Acquire Sun	05:21:13.5	Roll −53.70 degrees
05:04:00.4	Roll −35.21 degrees	05:23:52.4	Pitch +55.0 degrees
05:06:02.3	Yaw +8.61 degrees	05:26:33.8	2.0-degree deadzone
05:07:11.0	Roll +88.90 degrees	05:26:33.9	Sun sensor yaw, fine off
05:10:53.3	Readout drive on		Sun sensor pitch, fine off
	Heater power off	05:35:00.3	Sun sensor yaw, fine on
	Solar eclipse off		Sun sensor pitch, fine on
05:10:53.4	Single frame camera sequence, slow rate	05:40:00.3	Sun sensor pitch, coarse off
	Camera thermal door open		Sun sensor yaw, coarse off
05:11:00.0	V/H on	05:45:00.3	Sun sensor yaw, coarse on
	Camera thermal door control off		Sun sensor pitch, coarse on
05:15:00.0	Camera on		
05:19:00.0	V/H off		Orbit 531 Parameters
05:19:00.1	Heater power on	1) Altitude = 167 kilometers	
	Solar eclipse on	2) Sun angle = 75 degrees	
05:19:06.7	Camera thermal door closed	3) Roll angle = 55 degrees (constrained by horizon)	
05:19:13.3	Camera thermal door control off	4) V/H ratio = 6.0 milliradians per second	
05:20:04.8	Yaw −8.61 degrees	5) V/H "on" time 8 minutes	

Figure 5-52: V/H High Roll Angle Test

133

predicted, indicating the capability to photograph at angles up to 53 degrees. Operation of the photo subsystem was normal during the exercise.

Conclusions — Examination of the data obtained indicates that oblique photography at roll angles up to 53 degrees is feasible. Although the V/H sensor was used beyond the design limits during this test, satisfactory operation was indicated. The differences between V/H telemetry and the computed V/H - EVAL (slant range) indicated in the plot are to be expected. These may be attributed to the inaccuracies introduced in the computations by the assumptions of altitude, attitude, and irregularities in the lunar terrain.

5.3.8 V/H High Sun Angle Test
Objective — The purpose of this test was to determine the V/H sensor operating character-

istics at high Sun angles near the terminator.

Procedure — The test was conducted on Day 013. The V/H sensor was commanded on approximately 2 minutes prior to the morning terminator and off 4 minutes after the morning terminator. The following sequence of events and parameter values was used.

Data and Discussion — The plot of this Sun angle test (Figure 5-53) shows that the V/H ratio telemetry agreed very closely with that predicted after sunrise (passage over the morning terminator). Examination of the telemetry data indicates that the required maneuvers were performed as planned and the V/H sensor performance was nominal.

Conclusions — This test indicates that the V/H sensor can successfully track at Sun angles as high as approximately 98 degrees.

| Sequence of Events		
GMT Day and Time	Event	Orbit 433 Parameters
013:01:30:50.7	Pitch −35.0 degrees	Time of passage over the terminator = Day 013:01:36:37 (All data apply to the above time)
01:34:31.1	Readout drive on	
	Heater power off	1) Total V/H "on" time = 6.0 minutes
	Solar eclipse off	2) V/H on 2 minutes prior to passage over the terminator
01:34:31.2	Single frame camera sequence, slow rate	3) Single-frame advance 4.0 minutes after V/H on
01:34:37.8	V/H on	4) Longitude = 66.2 degrees
	Camera thermal control door off	5) Latitude = 11.2 degrees
01:38:37.8	Camera on	6) Altitude = 84.3 kilometers
01:40:37.8	V/H off	7) True anomaly = 16.4 degrees
	Camera thermal door closed	8) Time from periapsis = 272.9 seconds
01:40:37.9	Heater power on	9) V/H ratio = 0.0223 radians per second
	Solar eclipse on	10) Sun angle = 90.0 degrees
01:40:44.5	Camera thermal door control off	11) Sun azimuth = 91.5 degrees
01:45:37.8	Sun sensor pitch, coarse on	12) Altitude rate = 0.134 kilometers per second
	Sun sensor yaw, coarse on	
01:45:37.9	2.0-degree deadzone	
01:46:29.4	Pitch +35.0 degrees	
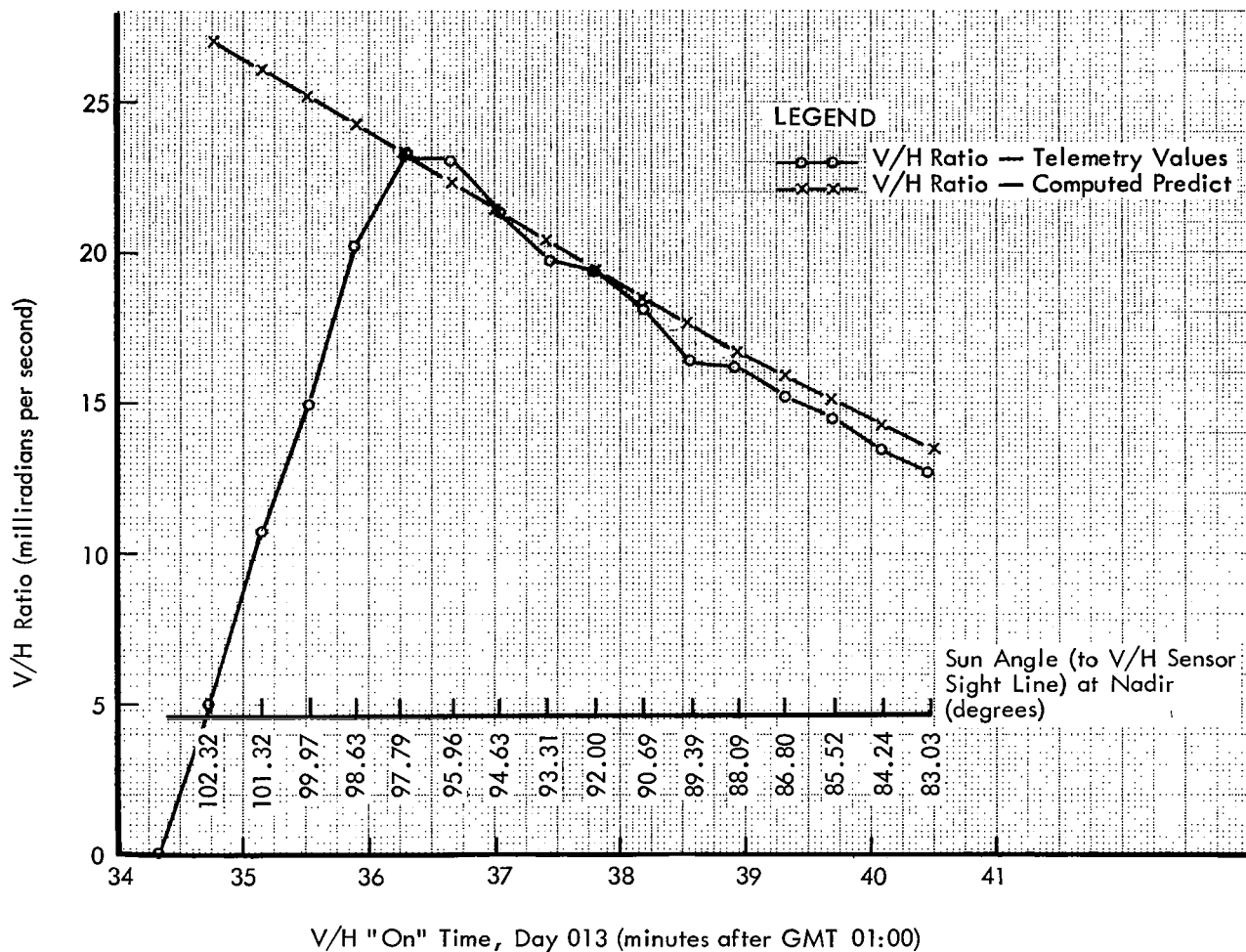
Figure 5-53: V/H High Sun Angle (Terminator) Test

Although the V/H sensor was used beyond its design limitation of 75 degrees, the differences between V/H telemetry and the computed V/H - EVAL (slant range) are to be expected. These differences can be attributed to the inaccuracies introduced in the computations by the assumptions of altitude, attitude, and irregularities in the lunar terrain.

5.3.9 V/H Sensor Temperature Test
Objective — The purpose of this test was to determine operating characteristics of the V/H sensor at maximum temperature and to determine maximum "on" time.

Procedure — This test was conducted on Day 027, in conjunction with the survey of the western limb, to conserve attitude control nitgrogen and to obtain more extensive data. The survey experiment is described in paragraph 4.2.1. The following sequence of events and parameters was used for these concurrent tests.

Data and Discussion — During the test the V/H sensor was operated for a total of 13.2 minutes. The V/H ratio decreased as expected during the test, from 14.8 to 2.6 milliradians per second, with a resulting increase in V/H sensor temperature of 1°F.

135

Sequence of Events

GMT Day and Time	Event	GMT Day and Time	Event
027:00:28:20.6	Sun sensor pitch, coarse on	01:48:30.0	Camera on
	Sun sensor yaw, coarse on	01:52:30.0	Camera on
00:29:12.0	0.2 −degree deadzone	01:53:42.0	V/H off
00:30:03.4	Acquire Sun	01:53:42.1	Heater on
00:33:28.5	Roll −70.0 degrees		Solar eclipse on
00:58:00.2	Canopus sensor on	01:53:48.7	Camera thermal door closed
00:58:51.6	Acquire Canopus plus	01:53:55.3	Camera thermal door control off
01:03:51.6	Acquire Canopus	01:54:46.8	Pitch +48.50
01:32:42.0	Canopus sensor off	01:57:15.3	Yaw −7.28
01:33:33.5	Roll +9.81		

Orbit 530 Parameters

01:34:44.6	Yaw +7.28

Time of passage over limb	= Day 027:01:43:21
01:35:50.7	Pitch +6.51 degrees

1) Sun angle	= 76.50 degrees
01:40:23.3	Readout drive on Heater power off Solar eclipse off

2) V/H ratio	= 11.45 milliradians per second

3) Altitude	= 157.8 kilometers
01:40:23.4	Single frame camera sequence, slow rate Camera thermal door open

4) True anomaly	= 38.6 degrees
01:40:30.0	V/H on Camera thermal door control off

5) Longitude	= 90 degrees

6) Latitude	= 16.67 degrees
01:44:30.0	Camera on

7) V/H "on" time	= .13.2 minutes

Conclusion — Examination of the data indicates that the V/H sensor operating temperature constraint of 6.6 minutes maximum "on" time, followed by at least 152 minutes "off," may be too conservative.

5.3.10 Star Map Tests

Objectives — The purposes of these tests were:
- To obtain the relative outputs of stars not observed on previous star maps;
- To locate Canopus in preparation for V/H experiments;
- To train for Mission III;
- To reestablish a roll reference after the roll gyro gimbal hangup.

*Description* — A star map exercise was conducted on GMT Days 010 at 20:30, 021 at 15:44 and 023 at 13:27. In each case, the exercise consisted of rolling the spacecraft through 360 degrees with the pitch and yaw axes fixed, and observed the readings of the star tracker.

Data and Discussion — One star map was developed on GMT Day 010, 1967 to locate Canopus in preparation for the V/H experiments. The orbit geometry at the time of this map was such that the tracker did not sweep the earthlit lunar surface. The results of this test are detailed in Table 5-17. Figure 5-54 shows the star map produced. The star map voltage recorded is generally larger than the Canopus ratio would indicate, and the ratio between the stars is not consistent. These conditions are due to a general background noise increasing the map voltage, and the fact that the star map voltage for each star is derived from different sections of the photomultiplier tube and the gain is not uniform over the face of the tube.

136

Table 5-17: Objects Observed During Star Map on Day 010, 1967, at 20:30

Telemetry Object No.	Catalog No.	Name	Clock Angle A Priori	Clock Angle Actual	Canopus Ratio	Map Voltage A Priori	Map Voltage Actual
1	194	β Umi, Kochab	187	189	0.05	— *	0.82
2	55	ζ Uma, Mizar	209	211	0.06	— *	0.76
	27	η Uma, Alkaid	213		0.09	— *	
3	501	Mars	267	275	0.1	— *	1.10
	66	γ Cru, Gienah	284		0.04	— *	
4	61	ι Car	337	340	0.06	— *	1.00
	40	δ Vel	339		0.08	— *	
	23	γ Vel	342		0.10	— *	
	131	ε Car, Avior	343		0.05	— *	
5	2	α Car, Canopus	0	"0"	1.0	3.30	3.12
6	160	α Cas, Bohedor	138	142	0.05	— *	0.82
	37	γ Cas, Cih	141		0.04	— *	
	81	β Cas, Caph	142		0.07	— *	

*Data not available
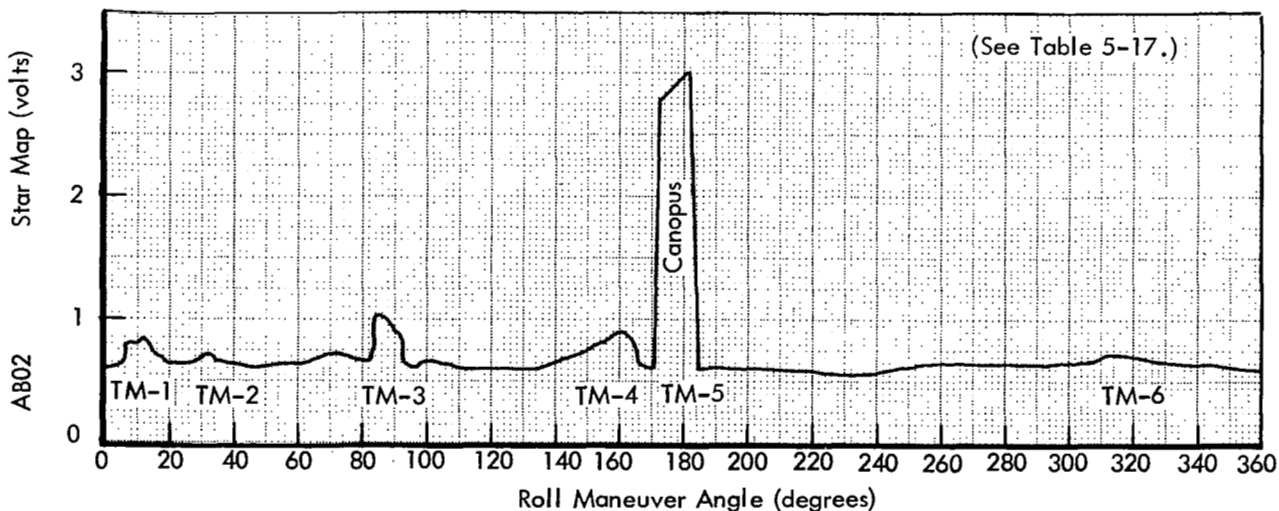
Figure 5-54: Star Map — Day 010, 1967

Table 5-18 details the results of a star map exercise conducted on GMT Day 021, 1967. Figure 5-55 shows the star map produced. The orbit geometry at this time was such that the tracker swept the lunar surface and resulted in a high brightness signal (TM-8) due to reflected earthlight. The other results were similar to those encountered on Day 010. This star map was prepared as a Mission III training exercise.

Table 5-19 details the results of the star map exercise conducted on Day 023 to relocate Canopus after the loss of roll reference due to roll gyro gimbal hangup. Figure 5-56 shows the star map produced. Again, the star tracker swept the earthlit lunar surface and the effect is seen between 85 degrees and 150 degrees of roll on the star map. At about 230 degrees in the maneuver, sunrise occurred with no glint resulting. One minute after the end of the maneuver, the spacecraft crossed over the sunlight terminator and, because the spacecraft was rolled about +25 degrees from Canopus, the star tracker apparently looked at or near the sunlit lunar surface, with resulting saturation of the star map signal and operation of the bright object sensor.

Conclusions — Additional star map data showing relative brightness between various stars were satisfactorily obtained with the Lunar Orbiter star tracker. These data were obtained during preparation of star maps for other purposes, as indicated in the preceding discussion.

			Clock Angle			
Telemetry Object No.	Catalog No.	Name	*A Priori*	Actual	Canopus Ratio	AB 02 Star Map Voltage (Actual)
Table 5-18: Objects Observed During Star Map on Day 021, 1967						

Telemetry Object No.	Catalog No.	Name	A Priori	Actual	Canopus Ratio	AB 02 Star Map Voltage (Actual)
TM-1	37	γCAS, Cih	136°	130°	0.07	0.84
	81	βCAS, Caph	138°	136°	0.04	0.86
TM-2	14	αBOO (Arcturus)	235°	233°	0.33	1.58
TM-3	501	MARS	264°	264°	-	1.20
TM-4	9	αVIR Spica	268°	270°	0.35	1.22
TM-5	63	δCEN	311°	310°	0.04	-
	74	θCAR	328°	to	0.04	
	56	κVEL	333°	336°	0.05	
	61	ιCAR Scutulum	335°		0.06	
TM-6	28	βCAR Miaplacidus	338°	341°	0.09	-
TM-7	2	αCAR Canopus	0°	0°	1	3.26
TM-8	602	Moon (illuminated by earthlight)	-	27° to 47°	-	3.94 peak
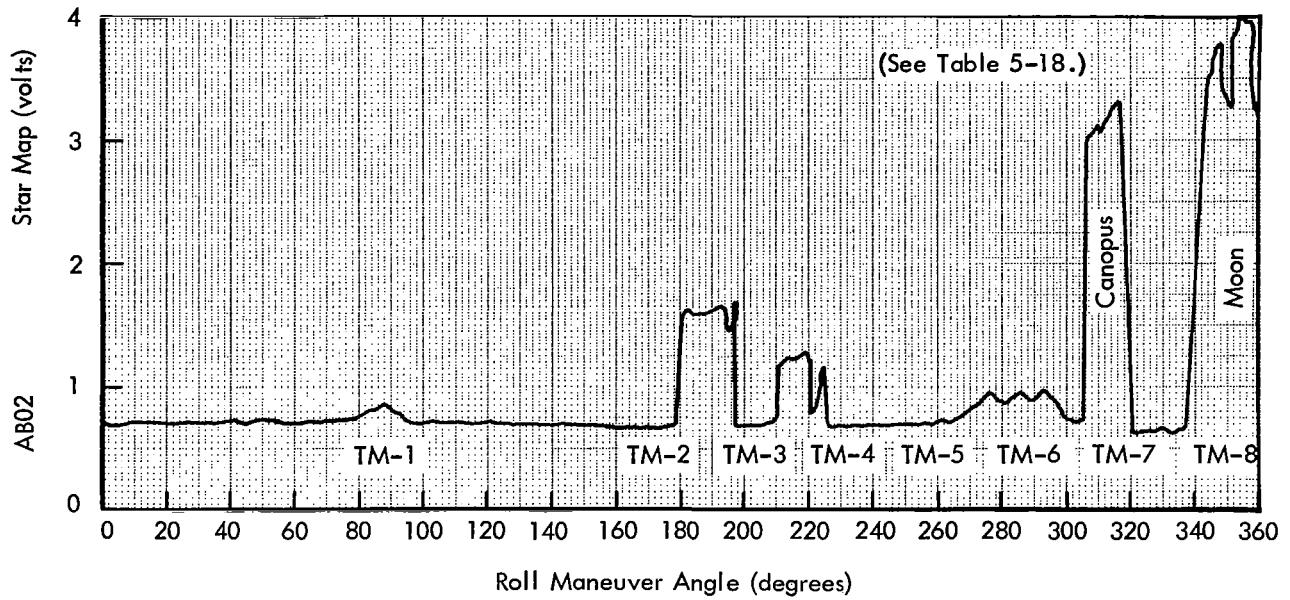
Figure 5-55: Star Map — Day 021, 1967

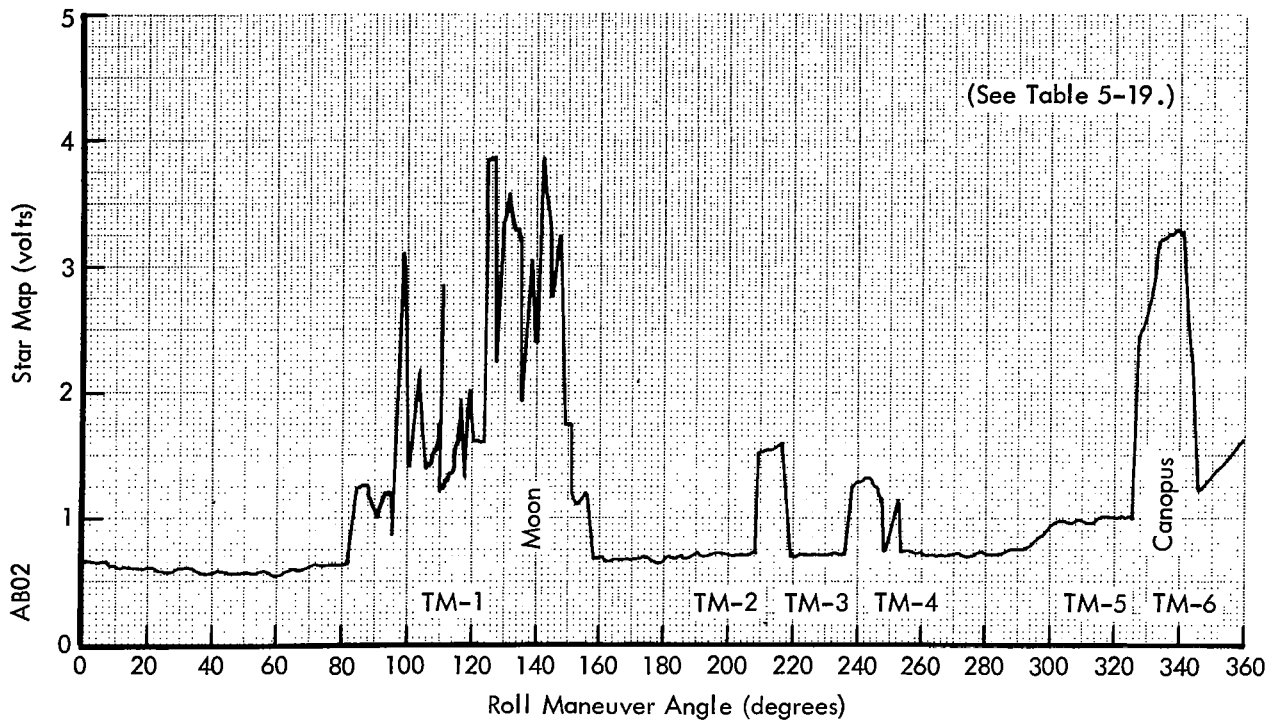| Telemetry Object No. | Catalog No. | Name | Clock Angle | | Canopus Ratio | AB 02 Star Map Voltage (Actual) |
			A Priori	Actual		
		Table 5-19: Objects Observed During Star Map on Day 023, 1967				
TM-1	601	Moon (illuminated by earthlight)	90°	100°-175°	-	3.9 peak
TM-2	14	αBOO, Arcturus	234°	237°	0.33	1.6
TM-3	501	Mars	263°	268°	-	1.3
TM-4	9	αVIR, Spica	267°	270°	0.35	1.3
TM-5	74	θCAR	327°	325°	0.04	0.9
	56	ϰVEL	333°		0.05	
	61	ιCAR	335°	to	0.06	to
	28	βCAR, Miaplacidus	338°		0.09	
	23	γVEL	345°	350°	0.10	1.05
TM-6	2	ναCAR, Canopus	360°	360° (reference)	1.0	3.3

139

Figure 5-56: Star Map — Day 023, 1967

5.3.11 Star Tracker Glint Mapping Test

Objective — Star map tests on Day 070 were performed to determine (a) whether or not mapping and tracking of Canopus at the South Pole during a Mission IV polar orbit was possible, and (b) that earthlight did not contribute noticeably to glint.

Description — Preparation for the test required location and tracking of Canopus. At 12:12:00 after sunset a star map was performed. The *a priori* star map is provided in Figure 5-57, and the star map data from telemetry are shown in Figure 5-58. No glint was observed in this star map since it was after sunset, but the star map established the operability of the tracker prior to performing tests in sunlight. A roll maneuver was performed over the PM terminator, followed by a pitch maneuver.

Data and Discussion — At 12:31:35 GMT the spacecraft was rolled +163 degrees to acquire Canopus. This maneuver was performed in the dark; hence, 163 degrees of the star map data of Figure 5-57 were repeated in orienting the tracker toward Canopus. Sunrise occurred at 12:44:07 GMT.

At 14:46 GMT the tracker was turned on. At 14:48:32 GMT Canopus was lost due to glint. The star map voltage then fluctuated between 3.12 and 4.32 volts, and the tracker's roll error output went hard over to −4.1 degrees. At 14:57:45 GMT the tracker was turned off. At 14:59:8.4 it was turned on again and acquired Canopus with no difficulty. Figure 5-59 shows the spacecraft Moon-Sun-Earth orientation that existed when Canopus was lost. At 15:02:21 GMT a + 360 degree roll maneuver was performed in sunlight. At 15:05, during the maneuver, the spacecraft altitude was 1,428.95 kilometers. The roll maneuver over the PM terminator was completed at 15:15:25 GMT, with the tracker then oriented toward Canopus. Figure 5-60 shows the telemetry data for this star map. From 232 to 291 degrees in the roll maneuver, the tracker looked at the Moon, causing the bright object sensor to operate. Glint was noted from 300 to 350 degrees in the maneuver. The recognition of Canopus at 360 degrees was nevertheless achieved.

At 18:13:26 GMT the tracker was maneuvered in sunlight away from Canopus with a +91.2-degree roll command, pointing the tracker line of
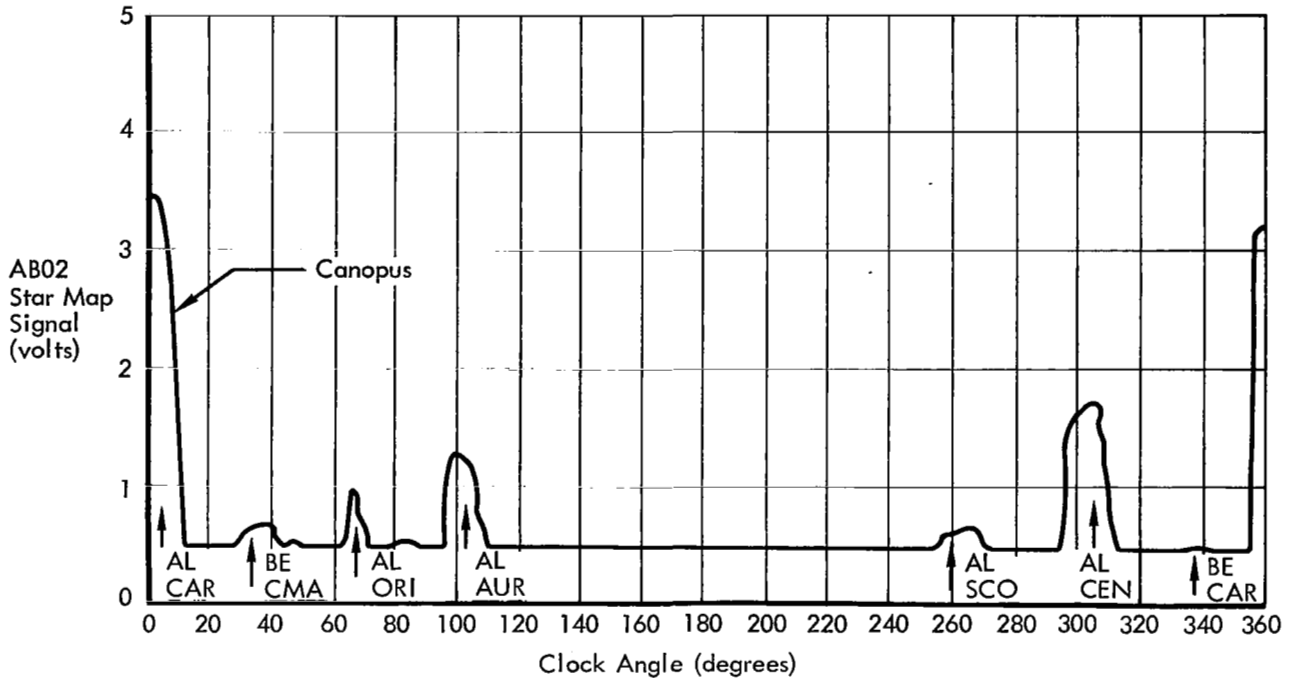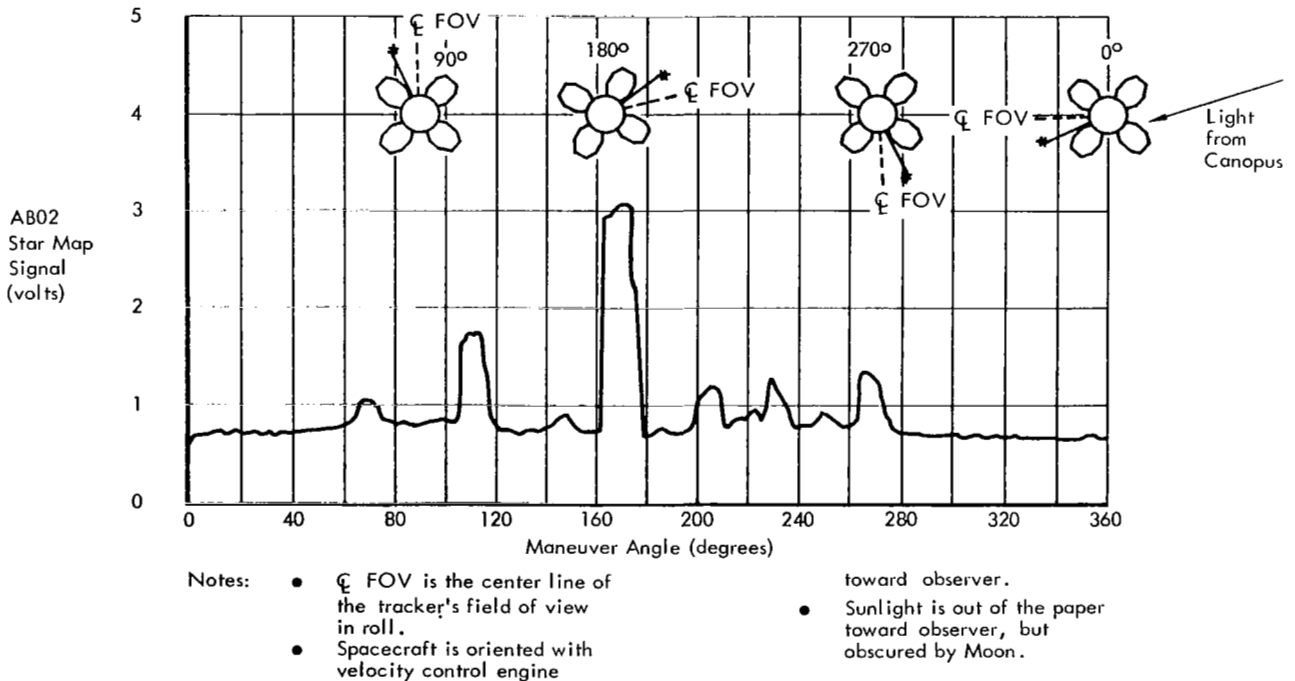
Figure 5-57: *A Priori* Star Map, Day 070, 1967 — 12:12:0

Notes:
- ₡ FOV is the center line of the tracker's field of view in roll.
- Spacecraft is oriented with velocity control engine toward observer.
- Sunlight is out of the paper toward observer, but obscured by Moon.

Figure 5-58: Telemetry Data Star Map, Day 070, 1967 — 12:10:56.8

Canopus

±104.3

-100   100

-90   90

-80   80

Sun

-70   70

March 11, 1967 (Day 070)
14:48:32 GMT
Lost Canopus

-60   60

1429 km

-50   50

-40   Moon   40

-30   30

-20   20

Moon's Shadow

-10   10

-5   0   5

Minutes
before
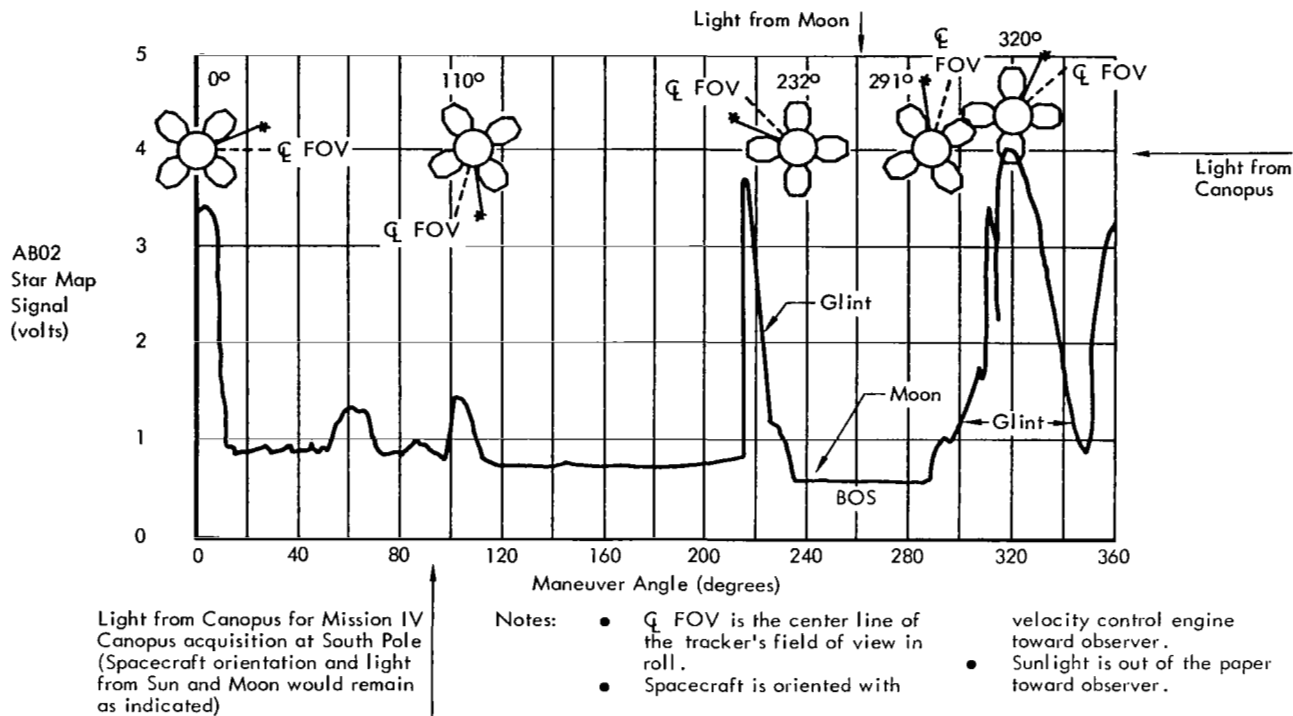Perilune

Minutes
after
Perilune
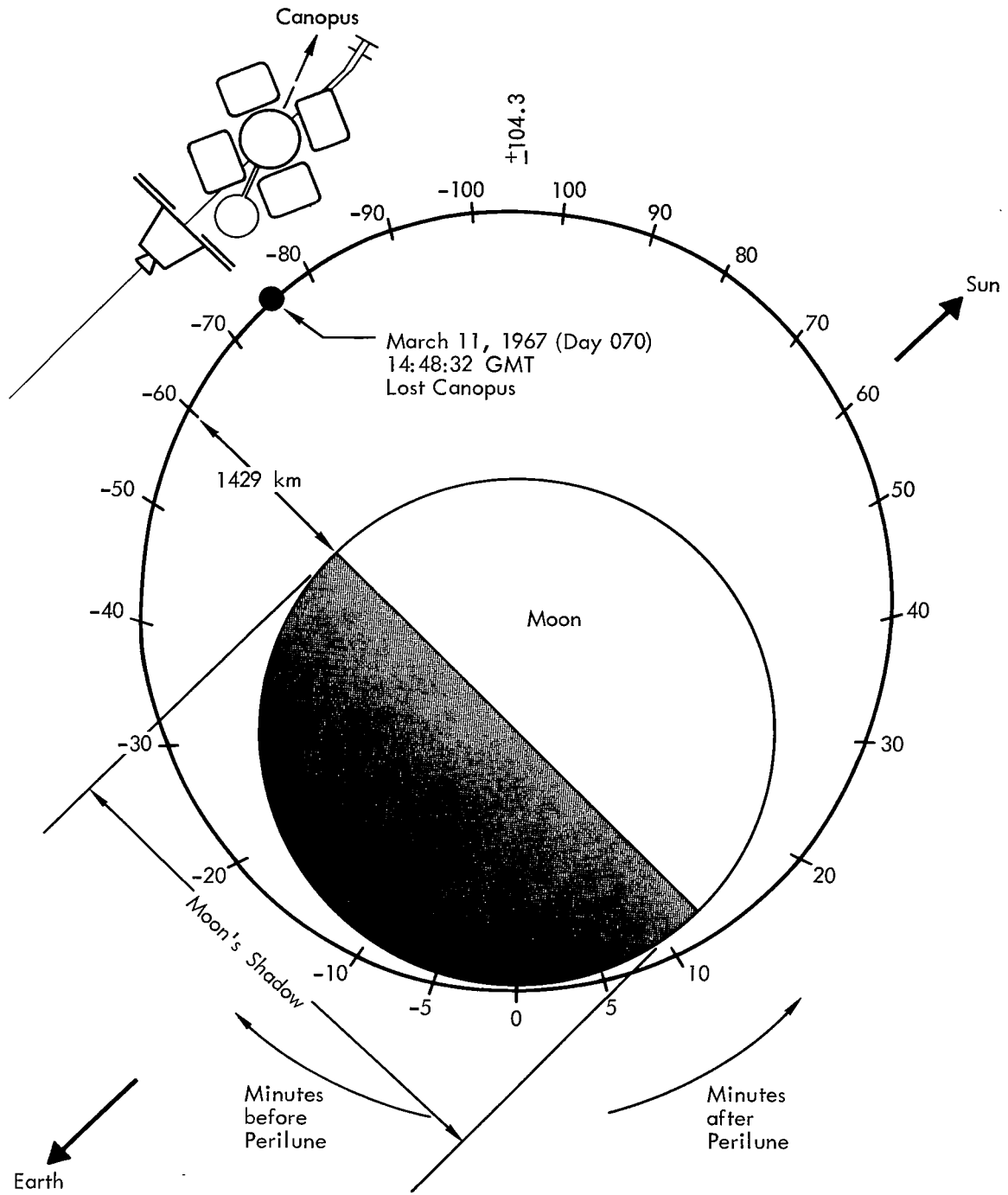
Earth

Figure 5-59: Spacecraft Moon-Sun-Earth-Canopus Orientation

Figure 5-60: Telemetry Data Star Map, Day 070, 1967 — 15:02:21

sight away from the Moon at an angle of 20 degrees before the PM terminator was to be crossed. Figure 5-61 shows the star map output for this maneuver. This roll attitude resulted in the tracker's receiving low-level (about 1.1 volts) glint. The tracker was turned off at 18:23:57 to break lock on the glint and was turned back on at 18:25:29. The star map output then dropped to 0.82 to 0.86 volts. The tracker then was tracking the star BE TAU at a Canopus ratio of 0.11. The altitude at 18:35 GMT was 1,429.86 kilometers. However, the crossing of the PM terminator occurred approximately 3.5 minutes prematurely.

With the tracker still oriented to + 91.2 degrees in roll, away from the Moon, the spacecraft was commanded to pitch + 360 degrees in sunlight at 21:59:23 GMT. The telemetry star map data for this maneuver appear in Figure 5-62. At 22:05 the altitude was 1,430.79 kilometers. Glint appeared from 93 to 233 degrees in the pitch maneuver, with the star map fluctuating between 2.3 and 3.92 volts. The bright object sensor operated from 233.2 to 249 degrees when the light interference increased. Upon completion of the pitch maneuver, the tracker was locked on glint at 1.14 volts star map, then cycled once from off to on, with no glint showing up following tracker turn-on.

Conclusion — From these tests on Lunar Orbiter II under simulated Mission IV conditions, it was concluded that glint was not a serious problem, although it did cause loss of lock on Canopus for a short period of time at 14:48:32 GMT on Day 070. In general, acquisition of Canopus was achieved whenever it was attempted under the simulated Mission IV conditions, and the glint problem during Mission IV can easily be overcome by operational adjustments.
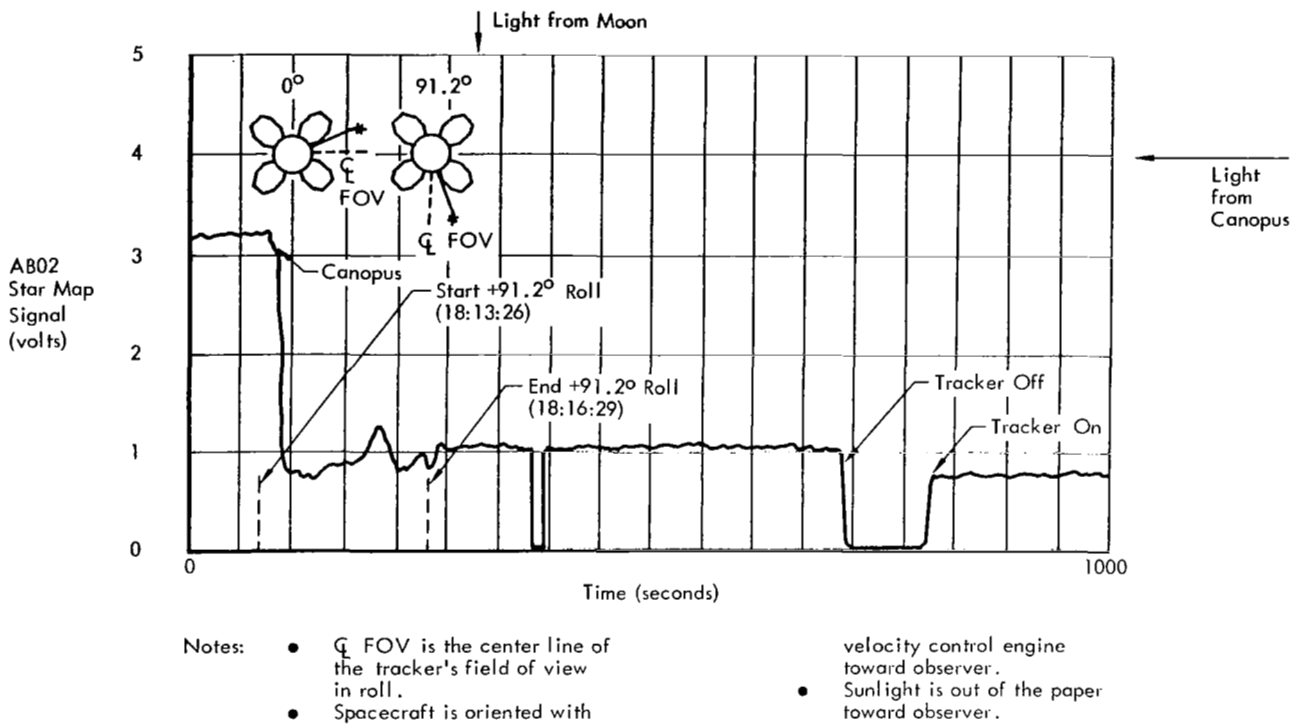
143

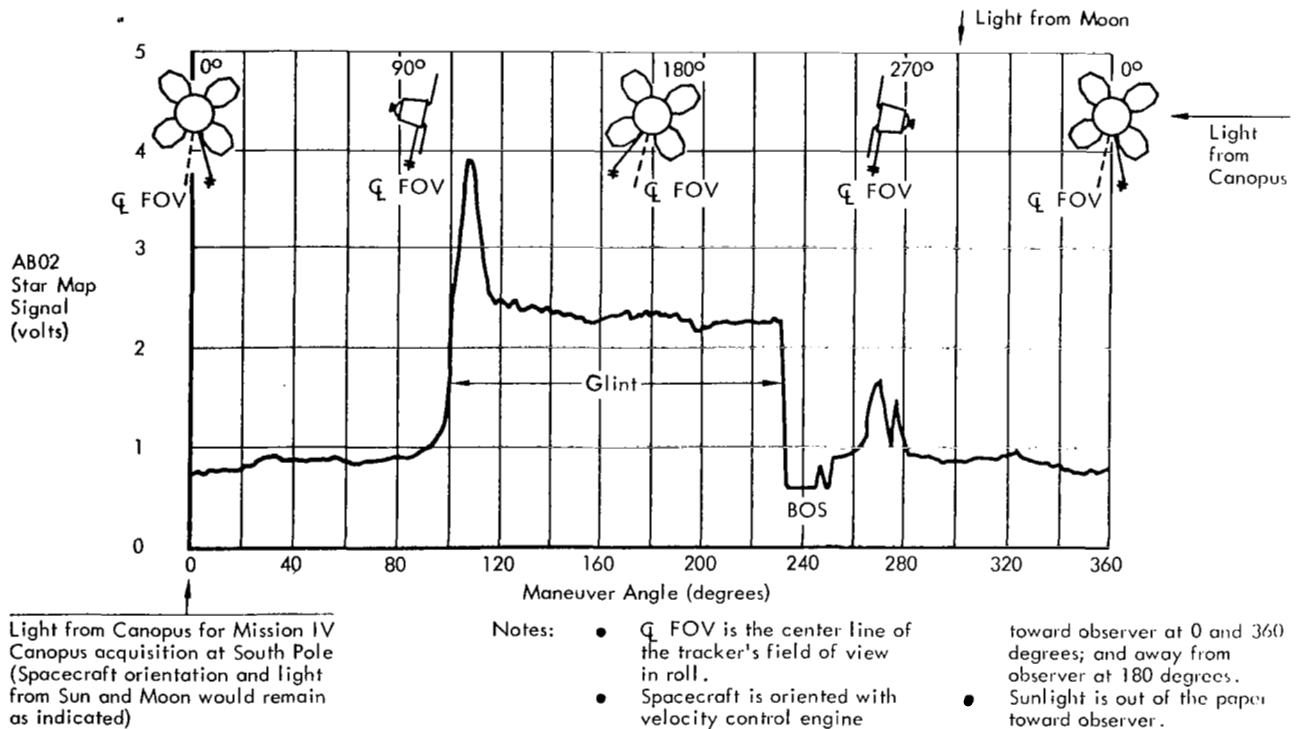**Figure 5-61: Telemetry Data Star Map, Day 070, 1967 — 18:12:0**

Notes:
- ₵ FOV is the center line of the tracker's field of view in roll.
- Spacecraft is oriented with velocity control engine toward observer.
- Sunlight is out of the paper toward observer.

Light from Canopus for Mission IV Canopus acquisition at South Pole (Spacecraft orientation and light from Sun and Moon would remain as indicated)

Notes:
- ₵ FOV is the center line of the tracker's field of view in roll.
- Spacecraft is oriented with velocity control engine toward observer at 0 and 360 degrees; and away from observer at 180 degrees.
- Sunlight is out of the paper toward observer.

Figure 5-62: Telemetry Data Star Map, Day 070, 1967 — 21:49:45

144

5.3.12 Star Tracker Bright Object Sensor Test

Objective — The purpose of this test was to determine the angles with respect to the Sun at which the bright object sensor of the star tracker closed and reopened the Sun shutter.

Description — The test proceeded as follows.

348:05:09:00 Start pass; Spacecraft on Sun

348:05:59:25 Roll 0.01 degree to place roll axis in inertial hold

348:06:00:11 Tracker on

348:06:02:06 Start yaw −40-degree maneuver

348:06:18:10 End yaw maneuver

348:06:19:46 Start yaw +40-degree maneuver

348:06:26:42 End yaw maneuver

The test consisted of a −40-degree yaw maneuver from an on-Sun attitude to swing the star tracker toward the Sun, causing the bright object sensor shutter to close over the tracker lens. During this test the centerline of the tracker's optical path was at an angle of +40 degrees from the line to Canopus. This 40-degree angle is the total drift accumulated in the roll axis since the last time the star tracker had been used to obtain a roll-axis attitude "fix" on Canopus.

Data and Discussion — From Figure 5-63 it can been seen that before initiation of the yaw maneuver the star map output was low, at approximately 0.85 volt. As the yaw maneuver proceeded, a glint suddenly became evident, causing the star map output to reach 3.2 volts. The angle in yaw between the star tracker's centerline and the sunline at which glint from the Sun first became significant was 89 degrees. After the shutter reopened and the angle in yaw between the tracker's centerline and the Sunline was 90.5, the star map output dropped to 0.85 volt.

The bright object sensor closed during the −40-degree yaw maneuver when the angle

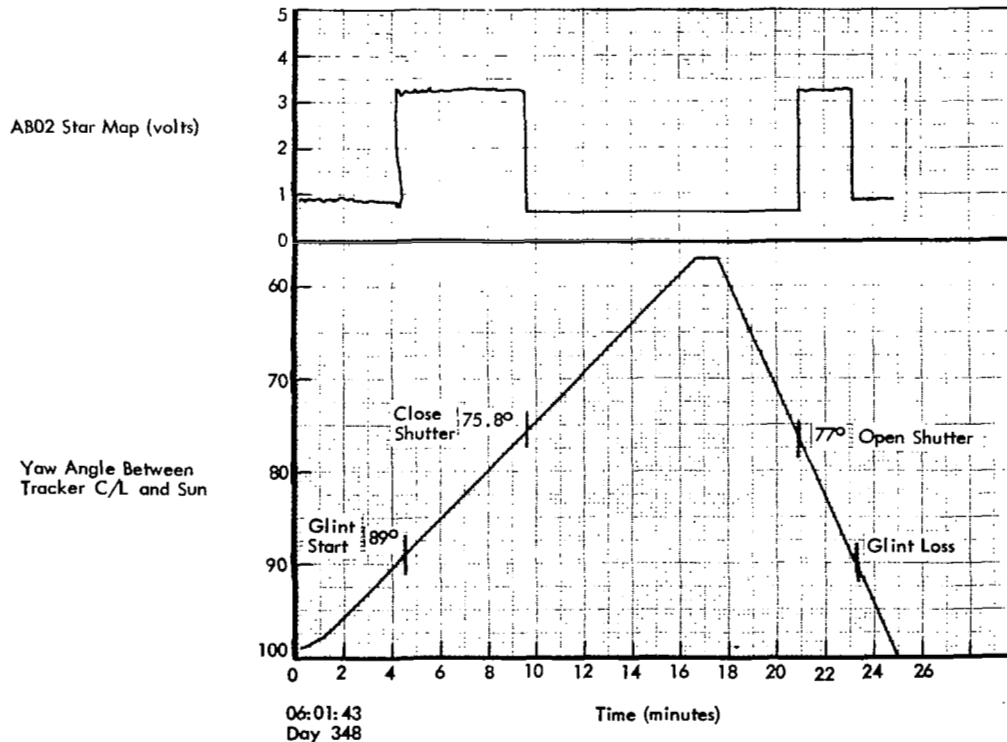**Figure 5-63: Bright Object Sensor Characteristics**

145

between the tracker centerline and the Sun was 75.8 degrees (see Figure 5-63) and reopened during the +40-degree yaw maneuver when the angle was 77 degrees. Immediately before closure, and again after reopening, the tracker brightness signal was 3.2 volts.

Conclusion — Spacecraft orientation, as shown in Figure 5-64, indicates that the star tracker did not look at the Moon during this test. Based on the results discussed herein, operation of the bright object sensor was normal.

5.3.13 Pitch and Yaw Maneuver Accuracy Test

Objective — The object of this test was to determine pitch and yaw maneuver accuracies to see if the errors would be significant in locating photo sites, as well as to provide data for subststem performance evaluation.
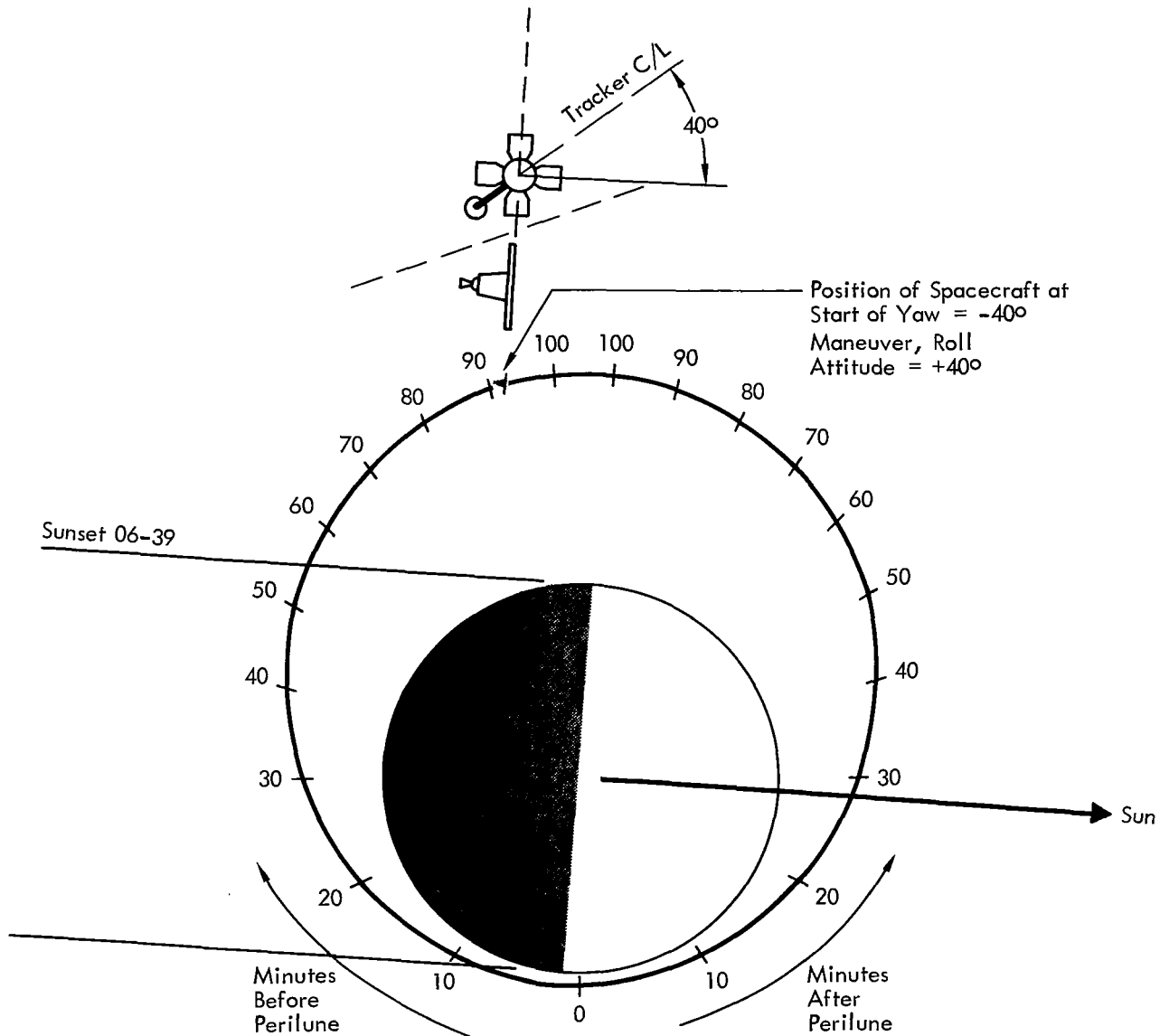
Figure 5-64: Spacecraft Orientation During Check of Star Tracker Bright Object Sensor Operation

146

Description — The sequence of events on Day 353, 1966 for this special test appears below.

353:06:27:03 Sunrise

353:06:55:28 Acquire Sun; fine sun sensors only

353:07:00:26 Pitch +360 degrees

353:07:12:10.4 End of pitch maneuver

353:07:13:54.9 Yaw +360 degrees

353:07:25:39.3 End of yaw maneuver

The test consisted of 360-degree maneuvers starting from sun lock. The maneuver error was determined from the initial and final sun sensor readings. The initial sun sensor reading is equal to the last sun sensor position reading (AGO7F or AGO8F) taken at the start of the maneuver, plus the product of spacecraft pitch or yaw rate (AGO5 or AGO6), times the time between the last sun sensor position reading and the start of the maneuver. The final sun sensor reading is equal to the first sun sensor reading after completion of the maneuver, minus the gyro position reading interpolated to the same time period.

Data and Discussion — The results of the tests were published in an interim report; however, the results shown below are a refinement of the previous numbers.

Conclusion — It is evident from the data below that the maneuver functions on the spacecraft are performing well within the design requirement of 0.3 %.

5.3.14 IRU Turn Off-Turn On Test
Objective — A test to observe the effects of inflight IRU turn-off and turn-on was conducted after the impact burn on Day 284.

Description — The spacecraft was oriented on-Sun (Sun acquired) in wide deadband with all sensors on, when the following sequence was employed to turn the IRU off and on.

1. Canopus recognition simulator on
2. Acquire Canopus, tracker off
3. 0.2-degree deadband
4. Sun sensors off
5. IRU off (284:06:24) — After the IRU went off, the solar array current indicated that the spacecraft was drifting off the Sun at the rate of 0.043 degrees per second.
6. IRU on (284:06:38) Note: EMD temperature (STO3) was 95°F
7. Sun sensors on (284:06:45)

Data and Discussion — The gyro wheel currents, bus voltage, and load current are shown in Figure 5-65. It may be noted that immediately after turn-on, the spacecraft started back to the sunline at 0.27 degree per second, went by the sunline, as shown by a maximum array current of 12.4 amps, and continued to drift off in the opposite direction. Pitch and yaw rates were saturated positive, roll rate was saturated positive until 06:41, at which time it crossed the deadband at 1.2×10^{-4} deg/sec^2 to minus saturation at 06:46.

When the sun sensors were turned back on, the pitch and yaw rates immediately went from positive saturation to negative saturation and the spacecraft began acquiring the Sun at 0.29 degree per second. The Sun acquisition was completed at 06:50. To verify that the IRU was

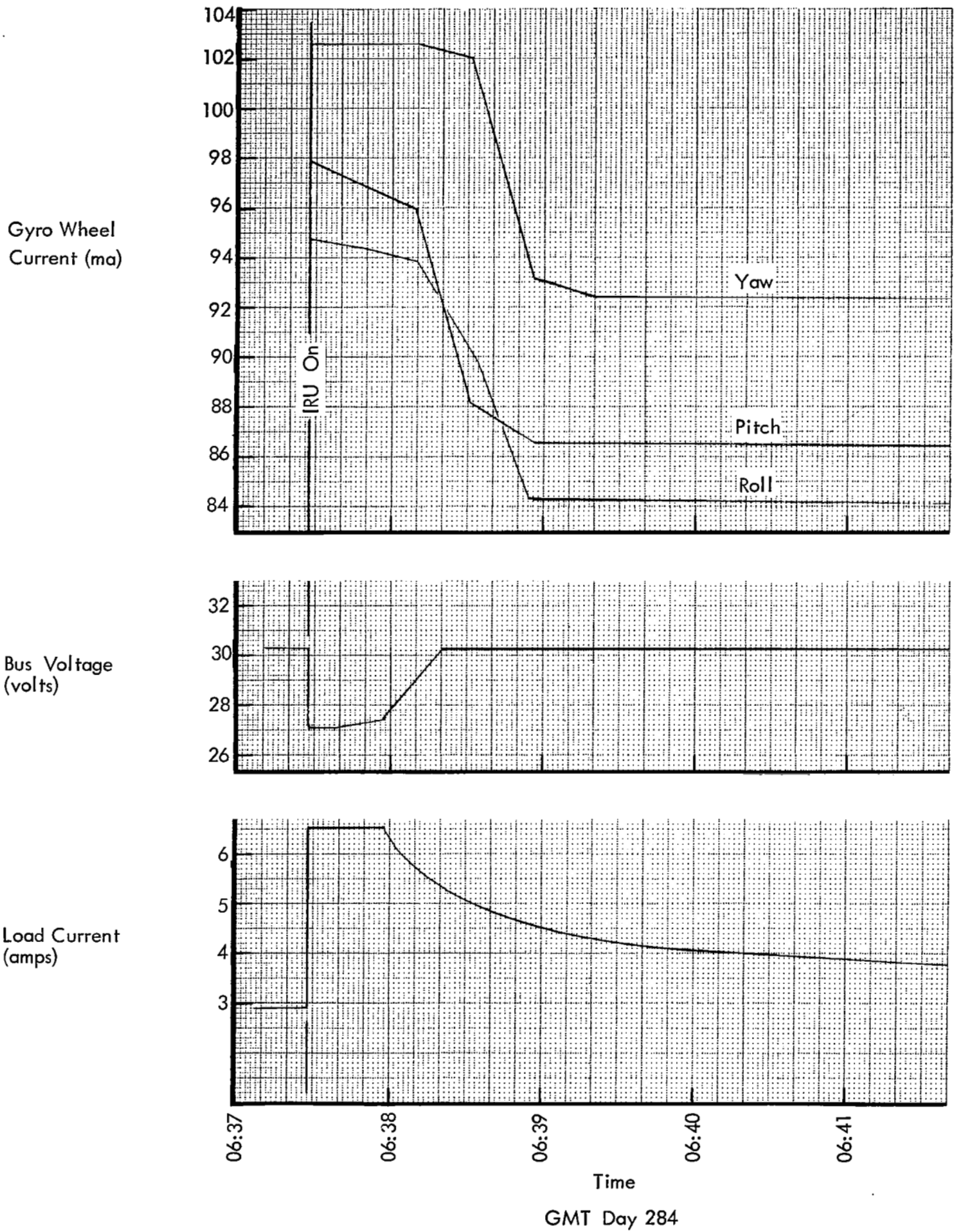| Commanded Maneuver	Initial Sun Sensor Reading	Final Sun Sensor Reading	Actual Maneuver	Maneuver Error	Percent Error
Pitch +360	+0.152	+0.101	359.949	−0.051	−0.014
Yaw +360	−0.146	+0.215	360.361	+0.361	+0.100

Figure 5-65: Gyro Wheel Currents After IRU Turn-On

148

operating properly, and also to determine whether maneuver control could be maintained at low tank pressures, a series of 29 consecutive roll maneuvers was performed starting at 06:51. All axes appeared to be operating normally. Proper maneuver control in roll was observed until the moment the spacecraft impacted the Moon. The last data received indicated a nitrogen supply pressure of only 70 psia at a temperature of 66.5° F (0.35 pounds of nitrogen).

Conclusion — A small amount of gas was consumed during the IRU turn-off and turn-on, as evidenced by the rate changes observed. However, gas consumption was less than calculated since no change was noted in the tank pressure. After IRU turn-on, proper spacecraft attitude control was attained.

"The aeronautical and space activities of the United States shall be conducted so as to contribute . . . to the expansion of human knowledge of phenomena in the atmosphere and space. The Administration shall provide for the widest practicable and appropriate dissemination of information concerning its activities and the results thereof."

— NATIONAL AERONAUTICS AND SPACE ACT OF 1958

NASA SCIENTIFIC AND TECHNICAL PUBLICATIONS

TECHNICAL REPORTS: Scientific and technical information considered important, complete, and a lasting contribution to existing knowledge.

TECHNICAL NOTES: Information less broad in scope but nevertheless of importance as a contribution to existing knowledge.

TECHNICAL MEMORANDUMS: Information receiving limited distribution because of preliminary data, security classification, or other reasons.

CONTRACTOR REPORTS: Scientific and technical information generated under a NASA contract or grant and considered an important contribution to existing knowledge.

TECHNICAL TRANSLATIONS: Information published in a foreign language considered to merit NASA distribution in English.

SPECIAL PUBLICATIONS: Information derived from or of value to NASA activities. Publications include conference proceedings, monographs, data compilations, handbooks, sourcebooks, and special bibliographies.

TECHNOLOGY UTILIZATION PUBLICATIONS: Information on technology used by NASA that may be of particular interest in commercial and other non-aerospace applications. Publications include Tech Briefs, Technology Utilization Reports and Notes, and Technology Surveys.

Details on the availability of these publications may be obtained from:

SCIENTIFIC AND TECHNICAL INFORMATION DIVISION

NATIONAL AERONAUTICS AND SPACE ADMINISTRATION
Washington, D.C. 20546